HYDROCARBON ENRICHED BIOFUEL PRODUCTION FROM LIQUEFACTION OF SORGHUM BIOMASS

by

Yang Yue

(Under the Direction of Sudhagar Mani)

ABSTRACT

Hydrocarbons enriched biofuels has received great attention to replace fossil based hydrocarbons due to its potential to reduce greenhouse gas (GHG) emissions. Energy crops such as sweet sorghum and energy sorghum produced from marginal lands can be converted into hydrocarbon rich biofuels. This study has developed a two-stage hydrothermal liquefaction (HTL) technology followed by hydrodeoxygenation (HDO) from sweet sorghum bagasse to produce 12 wt. % of hydrocarbons and 27 wt. % of sugar streams with an overall carbon conversion efficiency of 38%. Alternatively, the effect of torrefaction pretreatment on the catalytic fast pyrolysis of energy sorghum using red mud was investigated. The catalytic pyrolysis of sorghum favored the improved ketone yield (5 wt. %), while the combined torrefaction pretreatment with catalytic fast pyrolysis favored the hydrocarbon yield (0.78 wt.%). Techno-economic assessment study concluded that the minimum selling price of biofuels from 2-stage HTL pathway was 52.3 % less expensive than that of combined torrefaction and catalytic fast pyrolysis pathway.

INDEX WORDS: hydrocarbon, pyrolysis, torrefaction, liquefaction, techno-economic analysis

# HYDROCARBON ENRICHED BIOFUEL PRODUCTION FROM LIQUEFACTION OF SORGHUM BIOMASS

by

YANG YUE

B.S., Beijing University of Chemical Technology, China, 2005.

M.S., Virginia Polytechnic Institute and State University, U.S., 2011.

A Dissertation Submitted to the Graduate Faculty of the University of Georgia in Partial Fulfillment of the Requirements for the Degree

DOCTOR OF PHILOSOPHY

ATHENS, GEORGIA

2016

# HYDROCARBON ENRICHED BIOFUEL PRODUCTION FROM LIQUEFACTION OF SORGHUM BIOMASS

by

YANG YUE

Major Professor: Sudhagar Mani

Committee: Jim Kastner
K.C. Das
Yajun Yan

Electronic Version Approved:

Suzanne Barbour
Dean of the Graduate School
The University of Georgia
December 2016

## ACKNOWLEDGEMENT

Firstly, I would like to appreciate my advisor, Dr. Sudhagar Mani, who guided me and supported me for my Ph.D. studies. His academic insight and scientific attitude will impact me all my life. I also would like to thank Dr. Kastner for providing facilities and valuable guidance on my research. I would like to thank Dr. Das and Dr. Yan for serving as my graduate advisory committee and provided me supportive comments.

I also must thank Dr. Hari P. Singh at Fort Valley State University for his financial support of my torrefaction studies and provided me the feedstock of sorghum biomass.

I would like to acknowledge my fellow lab members: Maryam Manouchehrinejad, and Thomas Brett Beery for their help on techno-economic analysis and fast pyrolysis. It will be a cherish memories to spend nearly three with them. I am also grateful to Joby Miller, who trained me and analyzed many samples for my study.

I also dedicated my appreciating to my parents, who, from the first day of my life to the future, are always supporting and encouraging me as best as they can. Every progress I ever made is all from your selfless love.

Last but not least, I am also thankful to my wife Yue Ma. Without your accompany and encouragement, I am not able to step this far. Your love will be with me forever. Thank you to my son, you are the motivation for my every effort.

# Table of Contents

Page

List of Tables

Page

List of Figures

Page

# I. Introduction

The contradiction between dwindling reservation of fossil fuels and increasing world-widely energy demand is a primary challenge for hydrocarbon fuels supply. Additionally, the environmental issue of excess greenhouse emission, plus economic conflicts and national security resulted from unbalancing distribution of fossil fuels resource also promptly motivated researchers and positive policies for exploring sustainable and renewable energy sources. This essential requirement promotes the US government to alleviate energy issue through the development of biofuels, which serve as a crucial alternative to petroleum.

The current biofuel production approaches involve two main technologies: thermo-chemical and biochemical, as well as mechanical extraction (esterification). Among which, fast pyrolysis, hydrothermal liquefaction (HTL), fermentation and mechanical extraction aim to produce liquid biofuels with following advantages and limitations. Although, bioethanol and various valued added chemicals were commercialized with biochemical approach, fermentation is considered more suitable for alcohol based fuels production, but inadaptable to synthesize longer carbon chain biofuels. Thermal chemical approach (pyrolysis and liquefaction) provide multiple hydrocarbons with C7-C16 but limited by various highly oxygenated compounds by-products and considered less economic feasibility on industrial scale. Hydroprocessing is mandatory to improve the undesirable physicochemical properties of bio-oils, such as acidity, corrosion, thermal instability, oil products before engine combustion. Actually, although some above technologies satisfy a portion of the requirements of economic feasibility, conversion efficiency, manageable procedure and environmental conservation, but few could satisfy simultaneously to reach our

expecting. Typically, almost neither approach currently is competitive to fossil fuel process due to the limitations of preparation process, cost and product quality, but with comprehensive research and promising policies, those restrains will be hurdled

Lignocellulosic biomass is sustainably available worldwide and considered as a promising resource for fossil fuel alternation with neutral $CO_2$ emission. Sorghums are a C4 plant, characterized by high photosynthetic efficiency and have been widely planted in central and southwest of the States. The properties of high yield, drought tolerance, nitrogen independent and non-arable land competition make sorghum attractive for lignocellulose biomass supply. Sweet sorghum bagasse was the residue after juice extraction, the high moisture content and affluent availability make sweet sorghum bagasse an appropriate feedstock for HTL. Energy sorghum, with much less moisture content was adaptable for pyrolysis.

It was proposed to develop a promising thermal approach with considerable hydrocarbon conversion efficiency and practical economic feasibility to produce bio-oil as drop-in fuels through either HTL or catalytic fast pyrolysis (CFP). However, with lignocellulose biomass, one of HTL current issues was that supported by limited data and discrete trails, chemical and physical conversions involved in the whole process of HTL lack comprehensive understanding and essential principle mastery. Specifically, for lignocellulosic biomass feedstock, the decomposed mixed soluble sugars and benzene-type intermediates from lignocellulose macromolecular compositions (cellulose, hemicellulose and lignin) were apt to form solid residues through cross reaction and repolymerization, thus impaired the hydrocarbon yield during upgrading into drop-in-biofuels and also intrigued refinery catalysts deactivation and poisoning. Additionally, hemicellulose from lignocellulosic biomass was reported not as suitable as lignin for biocrude production with unsatisfying yield and high content of oxygenated compounds, such as carboxylic

acids. Therefore, a strategy of a mild temperature HTL pretreatment was proposed to convert hemicellulose into sugar co-product; followed by a combination of severe temperature HTL and HDO process to enhance the hydrocarbon content in upgraded bio-oil.

For fast pyrolysis process, coke was formed with the repolymerization and cross reaction between small molecular intermediates from hemicellulose and phenols from lignin, which poisoned the active sites and dramatically impaired the life span of catalyst during upgrading. This meant a frequent regeneration of used catalyst and resulted in an increase on total cost of pyrolysis-hydrocracking process. Therefore, it was essential to promptly develop a coking resistance and economic catalyst to satisfy hydrocarbon production through CFP. Meanwhile, torrefaction pretreatment was reported to uniform biomass structure and components; remove half of coke precursors and oxygenated compounds, typically carboxylic acid, by thermal decomposition of hemicellulose. The concentrated lignin in torrefied lignocellulosic biomass also provided higher phenols content, which were the precursor of hydrocarbon after upgrading.

In this study, two-stage HTL-HDO process and torrefaction-CFP process were respectively proposed and conducted with sorghum biomass as feedstock. In two-stage HTL-HDO process, mild temperature was applied in the 1$^{st}$ stage HTL to hydrolyze as much as hemicellulose into sugars; the 2$^{nd}$ stage HTL was combined with HDO with severe reaction conditions to produce hydrocarbon enriched upgraded bio-crude. In the torrefaction-CFP process, torrefaction pretreatment was applied to remove hemicellulose firstly. An economic, coke-resistant, sacrificial catalyst of red mud was following employed for CFP after torrefaction. Process optimization, biofuel compositional analysis, and major compounds identification were conducted to aid in the systematic understanding of potential reaction pathways and improve the hydrocarbon conversion efficiency. Finally, techno-economic analysis (TEA) was implemented to estimate the economic

feasibility of above two approaches. With above studies, it was proposed to achieve the following objectives:

(i) Implement the combination of two-stage HTL and HDO process to produce C5 and C6 sugars stream and hydrocarbon enriched upgraded biocrudel from sweet sorghum bagasse

(ii) Investigate the impacts of torrefaction and red mud on bio-oil composition and study the possibility to produce hydrocarbon from energy sorghum through the combination of torrefaction-CFP process

(iii) Estimate the economic feasibility of above processes (two stage HTL and torrefaction-CFP)

With above objectives, the results and conclusions were aimed to provide a foundation for future study to overcome current limitations on biofuel production through thermal chemical technologies.

In this dissertation, previous research results were firstly summarized in Chapter 2 as background and literature review to provide a foundation for this study. The two-stage HTL-HDO process was described in Chapter 3 and Chapter 4; among which, Chapter 3 focused on the 1$^{st}$ stage HTL pretreatment and Chapter 4 was related to 2$^{nd}$ stage HTL-HDO. Conventional HTL-HDO was also used for comparison and described in Chapter 4. Chapter 5 described the torrefaction pretreatment and analyzed the properties of solid and liquid products from sorghum torrefaction. The impacts of torrefaction and red mud on pyrolytic product were estimated in Chapter 6 with pyro-GC/MS. According to the results of pyro-GC/MS, the fluidized bed reactor was applied to analyze the yields and compositional of CFP bio-oil, which was described in Chapter 7. Finally, the economic feasibility of above two processes were estimated in Chapter 8 with techno-economic analysis.

## II. Background and Literature Review

### 2.1 Fossil energy current status and biofuel development

#### 2.1.1 Fossil energy crisis

Abundant energy is the guarantee of economic and social development. Currently, fossil fuels support around 85% of global energy supplies, but with a rapidly dwindling reservation. Based on International Energy Outlook, the daily world liquid fuel consumption will reach 113 million barrels in 2030. The predictive primary energy demand in the United States will reach 2240 Mtoe in 2035. Currently, the global consumption reaches 31 billion barrels of transportation fuels annually; among which, the United States consumes 25% with the reserves of 2.4% (http://planetforlife.com/). With this consumption speed, the reservation fossil oil could only supply the development of US for approximate 49 years. Thus, it is obvious that with the depletion of fossil fuel and the increasing world-scale energy demand, US will definitely confront enormous economic decline if without new energy supply. Therefore, US promptly requires a sustainable and environmental conservational petroleum alternative to satisfy industrial and transportation requirement.

#### 2.1.2 Fossil oil limitation and issue

The modern prosperous society essentially relays on the application of fossil fuels energy. Meanwhile, current global issues involving environmental impacts and national security are the main reflections of fossil fuels application and reserves.

The utilization of fossil fuels associates with negative environmental impact, represented by the excess greenhouse gas emission. Fossil fuel combustion results in 98% of carbon emission

into the atmosphere, coupling with deleterious nitrogen oxides and sulfur oxides gasses and particle pollutions. Released carbon dioxide is the significant and major fraction of greenhouse gas, and was reported to raise from 29.0 billion metric tons in 2006 to 33.1 billion metric tons in 2015 and 40.4 billion metric tons in 2030. The transportation sector is responsible for about 25% of worldwide CO2 emissions and it will increase to nearly 50% of the total emissions by 2030.

Additionally, limited reservation and unbalance distribution of fossil oil cause national security issues. The World crude oil reserves were estimated at 1,342 billion barrels, among which, 61% store in the Middle East. 70% of US oil supply depends on import; this restriction influences greatly on the local economics and policies, also dramatically promote the exploration of domestic energy resource.

2.1.3 Renewal energy and bioenergy

Renewal energy is regarded as the most sensible alternative to fossil fuels for its sustainable development and zero greenhouse gasses emission. Renewal energies include solar, wind, falling water, biomass, gravitational forces, and geothermal energy. Geographical distribution diversity, time-depend supplies and relevant low conversion efficiency are the typical restrictions for most renewable energy become world scale application. Currently, approximately 16% of global total energy consumption comes from renewable resources. Based on European Renewable Energy Council, it was proposed that renewable energy would satisfy half of the global energy demand in 2040.

In the narrow sense, bioenergy refers to the combustible biofuels converted from biomass, which contributes 10-14% of the world's energy supply (Mckendry, 2002). A typical and attractive character of bioenergy is carbon neutral, which represents biofuels release as much carbon as biomass taken up during growth; thus causes no additional greenhouse gas emission.

Biofuel has experienced three generations of development. The first generation biofuel is derived from sugar-rich crops, such as corn and sugar cane. In 2008, around 18 billion gallons bio-ethanol and 4 billion gallons bio-diesel were respectively produced globally (IEA, 2009) through corn fermentation and oils or fats transesterification (Naik et.al., 2010). However, the competition with food makes the first generation biofuel less appealing. The second generation biofuel - bio-ethanol is fermented form lignocellulose biomass, but limited with low energy recovery efficiency, additionally, the short carbon alcohol is not a desirable fuel for combustion. Microalgae fuel was developed as the third generation biofuel mainly characterized by its high lipid content. This property of microalgae also essentially advocates to produce biodiesel.

Two main technologies implemented the conversion of biomass to biofuels: thermo-chemical and bio-chemical/biological processes. Thermo-chemical conversion includes combustion, gasification, pyrolysis and hydrothermal liquefaction. Power, heat and biofuel are major products from thermal chemical conversion obtained with severe reaction conditions; while Bio-chemical conversion aims to produce biofuel and value-added bioproducts. The common used biochemical technology encompasses digestion and fermentation. Digestion aims to produce biogas, mainly methane and carbon dioxide through bacterial anaerobic digestion with an energy recovery efficiency around 20-40%. Fermentation is wide-scale industrialized for bio-ethanol and other value added chemicals production (mostly alcohols) from organisms. Combination with metabolic engineering, fermentation visions an extensive application for biofuel as well as a diversity of industrial and medical production.

2.2 Lignocellulosic biomass

It has been widely acknowledged that starch and triglycerides are no longer considered priority and sufficiency for the demand of biofuel preparation currently due to the food

competition. Lignocellulose biomass is extremely appealing as a primary and appropriate alternative of carbon source due to its carbon neutrality, relative abundance, renewability and nonfood competition (Bridgwater et al., 1999; David and Ragauskas 2010). It was reported that 1.6 billion tons of lignocellulose could be sustainably available annually from the US which, if effective conversion, could offset 43% of total domestic petroleum consumption and easily achieve the target of Energy Independence and Security Act (Bond et al., 2014) mentioned above.

Lignocellulosic biomass is extremely appealing as a primary and appropriate alternative of carbon source for biofuel conversion due to its carbon neutrality, relative abundance, renewability and nonfood competition (David and Ragauskas, 2010; Sannigrahi et al., 2010).The three main routes are cataloged by the target products: syngas production by gasification, bio-oils production by pyrolysis or liquefaction, and aqueous sugar by hydrolysis. However, no matter what process applied, the products upgrading and separation is often more extensive than the primary conversions of biomass.

2.2.1 Sorghum biomass

Emerging as an excellent C4 energy crop, sorghum is characterized by high photosynthetic efficiency and has been obtained more attentions recently for its lignocellulose biomass supply which indicated potential capability for above goals. Its plantation features of drought tolerance and nitrogen use efficiently avoided the excess use of water and nitrogen as well as arable land competition, which both represented economic input cost. Additionally, the multiple life cycles annually and stem sugar production qualified sorghum biomass with desirable yield and sugars platform. Above advantages provided sorghum a sustainable biomass for lignocellulose feedstock with wide-region adaptable plantation. Although of tropical origin, sorghum can be grown successfully between the latitudes of 450 °N to 520 °S. It is an annual plant of short life cycle (3-

5 months time to maturity) and, therefore, in tropical and sub-tropical climates can yield more than one crop a year.

Moreover, the diploid genomes of sorghum have been sequenced and the compositional characterization was eligible to be modified and improved artificially (Calviño and Messing, 2012). This enabled sorghums to be a model system and the study of sorghum also accelerated the development pace of other Panicoideae subfamily energy crops including maize, sugarcane, Miscanthus and switchgrass (Lanzatella et al., 2010; Swaminathan et al., 2010; Wang et al., 2010). With the consideration of its practical strength on seed production, agronomic practices, and infrastructure establishment (Stefaniak, et al., 2012), sorghum has been identified by USDOE as one of the best potential crops to develop into biofuels and value-added chemicals (USDOE, 2011)

2.2.2 Sweet sorghum and energy sorghum

Sweet sorghum and energy sorghum are two typical perennial cultivated varieties, well compatible with current agricultural systems and widely planted in the south regions of the States. Sweet sorghum is noted for its high fermentable sugars content. The average yield of sweet sorghum was reported of 15.7 metric dry tons of biomass hectare$^{-1}$ year$^{-1}$ with ranging from 10 to 20 metric dry tons hectare$^{-1}$ year$^{-1}$ (Daystar et al., 2014) depending on regions, climate, and fertilization. Its stalk contains up to 75% juice, with sugar content of 12 to 23 wt. % (http://agronomy.unl.edu/sweetsorghum. Ismail Dweikat). It was reported holocellulose accounted for 22.6 – 47.8 wt.% in dried sweet sorghum stalk; monomeric sugars took up for 43.6 – 58.2 wt.% (Antonopoulou et al., 2008). The dominant sugar component is sucrose, followed by glucose and fructose, which constituted an excellent feedstock for ethanol fermentation or syrup preparation with minimal pretreatment (Prasad et al. 2007; Almodares and Hadi 2009). After extracting the juice, the remaining biomass named bagasse is rich in lignocellulose with affluent availability but

ineffective utilization. This character makes sweet sorghum bagasse extremely appealing as a low-cost source for biofuel conversion.

Rather than sugar in stalk, energy sorghum is currently bred for high biomass yield and commonly utilized as silage due to high fiber content. The average yield of energy sorghum was reported to be 13.7 metric dry tons hectare$^{-1}$ year$^{-1}$ (USDA National Agricultural Statistics Service, 2008) with most distribution in southern Great Plains (Kansas, Nebraska, and Texas) (Shoemaker and Bransby, book chapter). Currently, energy sorghum has expanded utilization for biomass production for energy conversion, such as in the field of biofuels fermentation, especially after introduction of the traits such as brown midrib (*bmr*) and photoperiod-sensitivity varieties (Shoemaker and Bransby, book chapter).

2.3 Thermal chemical conversion of bio-oil production

Since last 80s, bioenergy has been widely studied and developed to reduce the dependency on conventional fossil fuels. It has been confirmed environmental sustainability as it is converted from plants or plant-derived materials. Besides biochemical strategies, plant biomass can be converted into bioenergy through thermochemical conversion routes, which currently includes four major technologies: combustion, gasification, pyrolysis and liquefaction based on the catalytic reaction condition and target products. Although above thermochemical approaches have achieved the usable bioenergy, the reaction conditions, mechanisms, products, and utilizations alter remarkably depending on thermochemical processes. With above four thermochemical conversion technologies, bioenergy is obtained in two formations: heat/electricity and biofuels. The latter is more attractive for its easier transport and high energy density; therefore, has been widely appealing as a promising alternative for energy crisis globally. In this section, the processes of

combustion and gasification were general introduced; hydrothermal liquefaction and pyrolysis were separately described with a little more details in next sections.

The current biomass combustion commonly applies co-firing approach. Plant biomass and coal mixing as feedstock has been proved to be a cost-effective process with the advantages of lower greenhouse gas emission and higher combustion efficiency (higher H/C in feedstock). Therefore, it is widely employed for producing electricity in commercialization. Woody biomass is more desirable than herbaceous biomass, as the latter contains a higher ash content and has a higher risk of slagging and fouling. The current scale of combustion plant ranged up to 4000 MW (Zhang et al., 2010). The combustion efficiency also generally increased with scale.

Biomass gasification is one of the most crucial routes for energy generation with wide application all over the world. Gasification is a thermal process that converts biomass into combustion gas ($H_2$, CO and $CH_4$) in the presence of a partial oxygen or oxidants such as $CO_2$, air or steam. These gasifying medium could help to rearrange the molecular structure of the biomass feedstock and also add hydrogen to the decomposition; thus improve the gaseous fuels with higher H/C ratio. The significant difference between gasification and combustion is the release manner of the stored chemical energy in biomass composition. In combustion, the energy releases directly in the form of heat; while in gasification, energy is transferred into conveniently deliverable gaseous products (McKendry, 2012). The gaseous product is so-called synthesis gas (syngas), which is mainly used for electricity generation or used as an intermediate for synthetic petroleum production. There are typical four processes in biomass gasification: drying, pyrolysis, oxidation (combustion) and reduction (char gasification) (Baruah, 2014). Although these steps occur successively with temperature, there is no strict boundary between any adjacent steps, and actually, some of the steps eventually overlap in gasification. The drying process occurs between 100-200

°C, with the function of removing the moisture in biomass; pyrolysis process was described above and the condensable vapor is produced in pyrolysis with temperature range of 150–700 °C; during 700-1500 °C, oxidation and char gasification occur simultaneously, rearrangement between hydrocarbon and gasifying agents is the dominant reaction in this stage. In biomass gasification, gasifying agents is one of the most significant factors which determines the final gaseous product. Air is the most used gasifying agent with the advantage of the affluent availability and zero cost; however, the nitrogen in air increases the power demand and decreases the total heating value of the syngas. Pure oxygen is a better gasifying agent but with higher costs. Steam, as the most attractive agent, increases both heating valve and hydrogen content of syngas. It is generated from water heated by the excess heat in plant, and therefore nearly costs zero.

### 2.3.1 Hydrothermal liquefaction

Hydrothermal liquefaction (HTL) is a currently rapid developing technology motivated by the origin of petroleum and derived from hydrothermal catalytic conversion to produce biocrude oil from various biomass in the presence of subcritical water at moderate temperature (280-370 °C) and high pressure (10-25 Mpa). High energy reward, low oxygen and moisture content, various available biomass resources, and no de-moisture pretreatment required are remarkable advantages for HTL biocrude oil. Generally, during the HTL process, being decomposed and reformed, biomass macromolecular are cleaved at C-C bonds and oxygen is removed in the form of water and carbon dioxide through carbonization reaction. The mechanism of HTL involves a comprehensive process of hydrolysis, fragmentation and repolymerization reactions. Hydrolysis occurs first; soluble sugars, acids, aldehydes, ketones and furfurals are consequently produced through dehydration, deoxygenation, decarboxylation and other fragmentation reactions. Accompanying with carbonization, these small molecular compounds can be further rearranged

*intra* or internally through condensation, cyclization and repolymerization reactions, producing solid residues with holding time (Demirbaş, 2010). The remove of oxygen from biomass is achieved mainly through the decarboxylation and dehydration reaction. Super/subcritical water is commonly utilized as an attractive media in above reactions for its extraordinary properties of ionic product, dielectric constant and density (Rogalinski et al., 2008)

The primary target product of HTC is an oily organic liquid called biocrude oil, which mainly consists of fuel-like epoxides chemicals and benzene derivate chemicals, with byproducts of gas fraction, aqueous products and solid residues. Biocrude could not be directly utilized as transport fuels before refinery due to deleterious characters of high moisture content, acidity and O/C ratio.

Biomass composition and HTL conditions are two dominant factors that determine the yield and quality of biocrude oil. For different types of lignocellulosic biomass, the compositional diversity and structural divergence (Bhaskar et al., 2008) result in discretely optimal yield. Extensive research has been performed on the liquefaction of various lignocellulosic biomass and demonstrated the variances in biocrude oil yield from different lignocellulosic biomass ranging from 8% to 47% under 200-410 °C,15-60 min. For woody biomass, Liu used pinewood as the feedstock for HTL at 200 °C, 1 M Pa for 20 min with acetone as solvent. The biocrude yield was 26.5 wt.% with 4-methyl-1,2-benzenediol as the dominant product; while ethanol was used as solvent, the major product was (E)-2-methoxy-4-(1-propenyl)-phenol (Liu and Zhang, 2008). Yang studied birch powder HTL and reported with 5% $K_2CO_3$ as catalyst, methanol as solvent, biocrude yield was 30 wt.% at 300 °C for 60 min (Yang et al., 2009). Li applied higher temperature of 340 °C, the biocrude yield reached 46.9% from Salix psammophile (SP) branch residues under 2 M Pa for 20 min. The major products were lactones, acids, ketones, alcohols, phenolics,

furan, and long-chain alkane (Li et al., 2013). Tymchyshyn employed 10 wt. % $Rb_2CO_3$ and $Ba(OH)_2$ as catalyst to liquefied sawdust from 250 °C to 350 °C under 2 M Pa $H_2$ for 60 min. The phenolic/neutral oil yield arrived 32% with phenolic compounds such as 2-methoxy-phenol, 4-ethyl-2-methoxy-phenol, and 2,6-dimethoxy-phenol as dormant compounds (Tymchyshyn and Xu, 2010).

As to herbaceous biomass, rice husk was used for HTL at 280 °C for 15 min, the obtained biocrude was 8.3 wt.% of feedstock with main compounds in biocrude of 2-methoxy-phenol, 4-methyl phenol, hexadecanoic acid and 1, 2-benzenediol derivatives (Karagöz et al., 2005). Zhang and Song respectively applied 300 °C and 410 °C as the HTL temperature with $Na_2CO_3$ as catalyst. The biocrude yield from stalks (Indonesia stalk and cornstalk) were respectively 36% (Zhang et al., 2008) and 47.2% (Song et al., 2004). It was indicated from above experimental results that alkaline catalyst and higher temperature (330-350 °C) benefited the yield and oil components with more phenols.

2.3.2 Pyrolysis

Pyrolysis is a thermal chemical technology to convert biomass into transportable energy and chemical production under high temperature (500-600°C) in the absence of oxygen. Pyrolysis feedstock is widely available from agricultural waste to paper slurry, but woody biomass is mostly focused due to its consistency and comparability.

During the pyrolysis, complex reactions occurred simultaneously and successively, which involving decompositions and cross reactions between the compounds in plant biomass. Typically, there are three stages during the pyrolysis process. The first stage occurs between 120 C and 200 C with a slight biomass weight loss. The dominant reactions in this stage are internal rearrangements, including bond breakage, the appearance of free radicals, and the formation of

carbonyl groups. Water, carbon monoxide, and carbon dioxide are the products. The second-stage is the main pyrolysis process with a dramatical decrease of biomass, in which solid pre-pyrolyzed biomass decomposes into volatile fraction and further condenses into liquid products. The last stage is the continuous char devolatilization. The products are gasses, which mainly composed of CO2 and CO; condensable vapors (liquid), which contained bio oil and moisture, as well as short chain acids; and charcoal (solid residues).

Similar as hydrothermal liquefaction, products of pyrolysis includes bio-oil, which is the main products of pyrolysis condensed from vapors, gas fraction and bio-char. With different pyrolysis operation condition, there is essential difference on products components and proportions: high temperatures with longer residence time are adaptable for gas conversion from biomass, which is considered more approximate to gasification and not commonly employed in pyrolysis; moderate temperatures with short vapour residence time are optimum for preparing liquid fraction, for instance, biocrude; while, moderate temperatures with longer temperature are desirable for biochar products. Therefore, due to the different heating rate from low to high, pyrolysis can be classified into slow pyrolysis for bio-char conversion, fast pyrolysis (flash pyrolysis) for biocrude conversion.

Fast pyrolysis was an efficient and feasible process to selectively convert lignocellulose into a liquid fuel. Extremely high heating rate is the essential feature of fast pyrolysis, which reached its desirable temperature 500C within seconds, thus promotes the biomass decompose very quickly to vapors and aerosols and some charcoal and gas. Other features of fast pyrolysis include that (i) a finely ground biomass feedstock is required for better thermal conductivity to reach the high heat transfer rate; (ii) extremely short hot vapour residence times with cooling rate

is also demanded for minimizing secondary reactions; (iii) rapid removal of char to minimize cracking of vapours.

As the target product of fast pyrolysis, the fuels are produced mainly through primary pyrolytic reactions, while secondary reactions occur simultaneously producing tar, as well as multiple thermal decompositions. (Mohan, 2006). Therefore, the condensed phase contains various complicated compounds as well as moisture, and some of which negatively influence the bio-oil characters for combustion. Except water, those compounds are commonly high-oxygen content organic chemicals and required to be removed or converted through catalytic deoxygenation reaction after biocrude oil upgrading. For solid residues, chars are preferred product of slow pyrolysis, while fast pyrolysis declines char yield with more valued biocrude oils.

Pyrolysis feedstock is widely available from agricultural waste to paper slurry, but most current studies focus on the lignocellulose biomass feedstock due to its affluent availability and ineffective utilization. These plant biomass could be divided into two groups: wood and woody residues; and herbaceous biomass.

Oasmaa et al. employed pinewood as feedstock in a circulated fluidized bed pilot plant at 520 °C, the bio-oil yield reached 74.4%, with elemental components of 43.5 – 46.7% carbon, 7% hydrogen, and 46 – 49% of oxygen as well as moisture content of 16 – 21% (Oasmaa, 2003). Agblevor applied similar bench-scale bubbling bed reactor to produce bio-oils from poplar wood, switchgrass and corn stover with respectively bio-oil yields of 62.2%, 61.5%, and 59.9% at 500°C (Agblevor et al., 2005). The elemental components of above bio-oils were also quite similar: 55.8 – 57.4% of carbon, 6.6 – 6.9% of hydrogen, and 34.2 – 36.3% of oxygen. This elemental distribution in above bio-oils was in a good accordance with that from oak, pine, and switchgrass obtained in a vortex reactor by Czernik (Czernik et al., 2005). Azeez obtained higher bio-oil yields

from beech and spruce wood (62.7 wt %) than those from iroke and albizia (50.6 – 54.7 wt%) with a bench-scale bubbling bed reactor. They proposed the lower bio-oil yields from tropical woods due to higher ash content, especially potassium and calcium. They also found the difference in the wood lignin component (the different percentage of G, S, H lignin) resulted in a difference in bio-oil components. 3 wt % of the beech, iroke, and albizia bio-oils were composed of syringols, while no syringols found in spruce bio-oil (Azeez et al., 2010). Hassan studied the influences of lignin and holocellulose on the quality and yield of pyrolysis bio-oil from cotton and pinewood at 450 °C. They reported that higher holocellulose content favored the bio-oil yield while it aggravated the viscosity but ameliorated acidity (Hassan, 2009).

Herbaceous biomass especially the agricultural residues has also been widely investigated for pyrolysis; however, the yields and qualities from herbaceous biomass are commonly uncompetitive to wood bio-oil.

Yanik et al. investigated the pyrolysis oils from corncob, straw, and oreganum stalks at 500 °C with fluidized bed reactor. The bio-oil yields ranged from 35 to 41%, much less than wood biomass; however, the moisture content in oil was relevant low, less than 15% of the total liquid. Carboxylic acids, non-aromatic ketones, methanol, and phenols were the dominant compound in aqueous phase (Yanik et al., 2007). The bio-oil from sugar cane bagasse indicated a higher yield than wood bio-oil. Piskorz et.al, found the yield from sugar cane bagasse could reach 66 – 73 wt% with a significant increase content of hydroxyacetaldehyde in bio-oil (Piskorz and Scott, 2006). They also studied other agricultural residues including sorghum bagasse, wheat chaff, and sunflower hulls with respective bio-oil yields of 69.4%, 66.7%, and 56.1% (Piskorz et al., 1998). Oasmaa (Oasmaa et al., 2010a) studied various woods, grasses, and agricultural residues at 480 – 520 °C with bench-scale bubbling bed reactor and found the bio-oil yields from canary grass was

highest of 75 wt%, followed by pine and eucalyptus wood pyrolysis bio-oil, with the yields of 70 – 72 wt%. But the bio-oil yields from hay, rape straw, and barley straw were significantly less, ranging 52 – 60 wt%.

Based on above results, it is obvious that the biomass specie is the most significant factor, which determines the bio-oil yield as well as quality due to the distribution of hemicellulose, cellulose and lignin content. Reactor configurations are also regarded as remarkable. The most common used reactors in bench scale pyrolysis involve bubbling fluidized bed, circulating fluidized bed, rotating cone, ablative and entrained flow reactor (Mohammad, 2012). Among which, fluidizing bed reactor is most adaptable due to its convenient operation, high stability and high bio-oil yield. Temperature, is also important, but usually employed around 500-600C for plant biomass. Higher temperature may cause gasification. This significantly decreases the oil yield.

2.3.2.1 Catalytic fast pyrolysis

Catalytic fast pyrolysis is processed to simultaneously combine the fast pyrolysis with the catalytic transformation. During CFP, primary pyrolysis vapors experienced catalytical decarboxylation or dehydration before condensed into liquid product. These less oxygenated liquid fuels were obtained from catalytic cracking under 300–500°C, atmospheric pressure without the requirement of hydrogen. Soluble inorganics, metal oxides, micro-porous materials, mesoporous materials, and supported metal catalysts were widely studied and applied for CFP, typically, including but more than “zeolites, silica–alumina, silicalite, FCC catalysts, alumina, molecular sieves, metal oxides such as zinc oxide, zirconia, ceria, and copper chromite, metal chlorides, phosphates, sulfates, and alkali” (Liu et al., 2014).

## 2.4 Hydrotreatment

The properties of HTL bio-oil were listed and compared with petroleum (Table 2.1). Obviously, liquefaction bio-oil has more moisture content and higher O/C ratio than crude oil, thus impairs the bio-oil quality on two aspects: relatively low heating values and corrosion against combustor. Sourcing from the free and physical bond water in biomass and subcritical water solvent, moisture still accounts for 5 wt. % of the liquefaction oil after extraction. Although this satisfies the minimum requirement of maintaining combustion (Mortensen et al., 2011), bio-oil is still considered an inappropriate fuel for combustion directly due to undesirable combustion property mainly from high oxygen content compounds, such as acids and ketones. Corrosion of combustor is another issue from carboxylic acids. The oxygen content in liquefaction bio-oil reaches around 10%, which is twenty times more than that in crude oil.

For comparison, the properties of bio-oil produced from another thermal process, fast pyrolysis, are also investigated. Bio-oil from fast pyrolysis is yielded at higher temperature (about 500 °C) and atmospheric pressure. Rather than a product of thermodynamic equilibrium, fast pyrolysis bio-oil is generated within seconds of residue time at pyrolysis temperatures, followed by a rapid quenching process. The component difference between fast pyrolysis bio-oil and liquefaction bio-oil is a larger amount of polar organic compounds existing in the former after extraction (Balat et al., 2009; Oasmaa et al., 2010b). This difference is mainly caused by conversion process, since in HTL, solvent water dissolves most polar organic compounds, especially carboxylic acids, and could be separated as aqueous phase byproduct.

Compared to crude oil, bio-oil, derived from biomass, is a renewable and sustainable fuel. It is also regarded as a clean fuel for its zero contents of sulphur and nitrogen if obtained from lignocellulose, which avoids the emissions of $SO_x$ and $NO_x$ gasses and achieves zero net emission

of $CO_2$. These advantages of bio-oil are so attractive that prompts an upgrading process to remove oxygen content, in order to satisfy bio-oil combustion. Current upgrading techniques include hydrotreatment (hydrodeoxygenation (HDO)), catalytic cracking, and emulsification process.

2.4.1 HDO process

HDO is a deoxygenation reaction to produce upgrade bio-oil (hydrocarbons) in the presence of hydrogen and heterologous catalyst at moderate temperature (250-450 °C) with high pressure (75-300 bar). Theoretically, oxygen in bio-oil is possible to remove completely in the form of water, which predicts the maximum hydrocarbon yield of 56–58 wt%. However, as to the selectivity of HDO reaction, the practical reaction is described by Venderbosch as:

$$CH_{1.47}O_{0.56} + 0.39H_2 \longrightarrow 0.74CH_{1.47}O_{0.11} + 0.19CH_{3.02}O_{1.09} + 0.29H_2O,$$

where, $CH_{1.47}O_{0.11}$ represents HDO products in oil phase; $CH_{3.02}O_{1.09}$ is the aqueous phase product (Wildschut et al., 2009a). On the basis of Venderbosch's formula, although 19% carbon is potentially transferred into aqueous phase, a considerable improvement of oxygen content from 12 wt % in liquefaction bio-oil to less than 5% is possible to achieve, with an increasing high heating valve from 32-36 MJ/kg to 42-45 MJ/kg, which quite approaches to that of crude oil of 44 MJ/kg (Wildschut et al., 2009b).

Upgraded bio-oil yield ($m_{oil}/m_{feed}$) and degree of HDO (1-wt $\%_{\text{ O in product}}$/wt $\%_{\text{ O in feed}}$) are two significant factors to estimate HDO conversion efficiency. The former describes the recovery quantity and the latter indicates the product quality. Higher degree of HDO always reflects more water and $CO_2$ removal from oil fraction, therefore, upgraded bio-oil yield has a negative correlation and determined by the degree of HDO. Generally, the degree of HDO depends on the catalysts and reaction conditions.

Heterologous catalysts involve metal oxide or sulphide catalysts and transition metal catalysts. For metal oxide or sulphide, Co-$MoS_2$ and Ni-$MoS_2$ are conventional hydrotreatment catalysts and also widely used in bio-oil HDO. Co and Ni serve as promoters and provide electrons to Molybdenum. After accepting the electron, molybdenum is active and the bond between molybdenum and sulfur is weakened; this results in a sulfur vacancy site. This vacancy site absorbs and removes oxygen atom from the molecular of bio-oil compounds in HDO process. $MoS_2$ can be replaced by $MoO_3$, but with a lower activity. Moberg et al. studied the several alternative oxides and founds the activities trends follow: $WO_3$ >$MoO_3$ >$V_2O_5$ >$Nb_2O_5$ (Moberg et al., 2010). Transition metal catalysts include noble metals of Ru, Pt and Pd on the support of active carbon or $ZrO_2$. Wildschut et al studied the efficiency of Ru/C, Pd/C, Pt/C, Co-$MoS_2/Al_2O_3$, Ni-$MoS_2/Al_2O_3$ at 350 °C 200 bar over 4 h. Ru/C and Pd/C showed promising catalysis efficiency on oil yield (52% and 63% respectively) and the degree of HDO (86% and 85%) (Wildschut et al., 2009b). However, the high price of noble metal limits its application. Basic metal catalyst is proposed as a possible alternation of noble metal catalyst, but a more extensive study is still required for its properties and utilization. Except for catalyst, carrier material can also be improved. Relevant inert property and high surface area qualify carbon a suitable support and more stable than $Al_2O_3$, which may convert to boehmite (AlO(OH)) during the HDO of bio-oil. Similarly, $ZrO_2$ is also a promising carrier for its neural nature.

Deactivation is an inevitable issue of heterologous catalysts. In HDO, deactivation is mainly caused by the formation of coke through polymerization reaction on the surface of catalyst. Furimsky and Massoth indicated that catalyst properties, bio-oil component and HDO reaction conditions were significant factors leading the formation of coke. Generally, catalysts are deactivated after around 200 h HDO reaction, but with higher hydrogen pressure, the deactivation

could be slowed down (Gualda et al., 1996). This causes a dilemma between the additional cost of hydrogen and the extension of catalyst activity.

2.4.2 Catalytic cracking process

Hydrogen is not required during catalytic cracking process, which occurs at atmospheric pressure, usually with heterologous zeolites catalysts at temperatures of 300 to 600 °C. Aromatic hydrocarbons are majority product of upgraded bio-oil fraction. Benzene, toluene, xylene, and naphthalene were reported as dominant components (Adjaye and Bakhshi,1995a ; Adjaye and Bakhshi,1995b) with an increasing yield of acetic acid, furfural and furans (Adam et al., 2005).

In the catalytic cracking process, decarbonylation, decarboxylation and dehydration reactions occur associating with oxygen elimination, but C-C bond cracking is the dominant reaction to convert large hydrocarbons molecular into smaller ones. Adjaye and Bakhshi postulated reaction pathway mechanism: thermal effects occurred firstly to separate light and heavy fractions from bio-oil; followed by thermal catalytic effects produced the desired organic distillate fraction with coke and gasses. During above reactions, higher temperature accelerates cracking rate, which is crucial to remove oxygen. However, meanwhile, increasing cracking temperature was reported to decrease upgraded bio-oil yield due to the rapid formation of various smaller volatile compounds. Therefore, a balance between oxygen elimination and oil yield is a significant consideration to optimize the reaction temperature. Similarly, extended cracking time improves the degree of deoxygenation, but increases the formation of coke, thus shorten catalyst lifetime. This compromise between deoxygenation and catalyst activity is another prerequisite for optimizing cracking reaction.

Zeolites are commonly utilized as heterologous catalysts for cracking reaction. Adjaye et al. investigated HZSM-5, H-mordenite, H-Y, silica-alumina, and silicalite in bio-oil cracking

upgrade at 330 to 410 ℃ and found the activity followed the order of HZSM-5 > H-mordenite > H–Y > silica-alumina > silicalite (Adjaye and Bakhshi, 1995a; Adjaye and Bakhshi, 1995b). They proposed the acid sites determined the activities of zeolites and further affected the deoxygenating efficiency; meanwhile, those acid sites were also susceptible to coke and led deactivate. Basically, compared with HDO, several obvious drawbacks of catalytic cracking including a large amount of coke formation, rapid catalysts deactivation and lower energy recovery (Balat et al., 2009) are the limitations of catalytic cracking application in bio-oil upgrading.

2.5 Techno-economic assessment of bio-oil production

Techno-economic analysis (TEA) is a method to estimate the application of technology and its economic feasibility on the management of product and process developments. With the process simulation and modeling, it helps to make decisions on investment and profit. In order to serve as a supplement or substitute of market fuel, the bio-oil obtained through the processes of either HTL or fast pyrolysis are required to be investigated its economic feasibility before the commercialization, including capital investment, operating cost and the final product value.

For TEA, the $n^{th}$ plant is commonly assumed to conduct the economic analysis. The capital investment could be estimated based on the dollar of the current year. For the equipment cost,

$$Current\ equipment\ cost = cost\ at\ original\ scale \times \left(\frac{Current\ capability}{original\ capability}\right)^{n} \times \frac{current\ year\ index}{quote\ cost\ year\ index}$$

(NREL,2011 ), Where, 'n' is the scale factor, typically, 0.6 to 0.7.

The energy and materials balance are stimulated with software such as CHEMCAD or Aspen Plus. The total capital cost is multiplied with installation factor. The operating costs contain various items such as raw materials, chemicals, wastes, and utilities. The fixed operating costs include maintenance and labor costs. The estimated result is provided with minimum fuel selling price (MFSP), which is under the specific discounted cash flow rate and plant life, the selling price

of the fuel can make the net present value of the process equal to zero. As different fuels vary on characterization, gallon gasoline-equivalent is used as a reference to standard the price of biofuel product, which is gasoline-equivalent price at $/GGE. It was calculated by comparing the higher heating value (HHV) of final product of biofuel with that of generic commercial gasoline,

$$MFSP\ (\$/\text{GGE}) = \frac{MFSP\ of\ final\ product \times gasoline\ HHV}{Final\ product\ HHV}$$

2.5.1 TEA of biofuel production through pyrolysis and upgrading process

Pyrolysis is an appealing technology to convert various biomass into biofuel through a series of processes including grinding, dry, pyrolysis, hydrotreating, hydrocracking and distillation. The economic feasibility of producing biofuel through pyrolysis with industrial scale was currently estimated with the accumulation of results from labs and pilots. Shemfe investigated the impact of electric power generation on bio-oil production, and concluded the minimum fuel selling price (MFSP) of $8.29/gge with the plant capacity of 72 MT/day pine wood (Shemfe et al., 2005). However, because of the high cost of pinewood in British, approximate $120/ton, the final MFSP was uncompetitive to that from US reported from NREL. NREL provided two reports on TEA of pyrolysis; one was aiming to estimate the influence of building hydrogen plant on MFSP (NREL 2010); the other was to combine the process of pyrolysis and hydroprocessing (hydrotreating and hydrocracking) (PNNL 2013). Both applied the capacity of 2000 dry ton pinewood per day. Form the former report, it was drawn that with hydrogen plant increased the cost of MFSP from $2.11/gal to $3.09/gal; The capital cost of hydroprocessing was around 1.7 folds of that of pyrolysis and 2.41 times of pretreatment (drying and grind). From the latter report, the MFSP was found approximately $3.39/gge. Onarheim studied different feedstocks (Onarheim et.al., 2015) with plant capacity of 0.5 ton/day and found forest residual was more appropriate for bio-oil production with the MFSP of $2.2/gge, which was lower than pinewood of 3.1$/gge.

### 2.5.2 TEA of biofuel production through HTL and upgrading process

HTL is current starting thermal chemical technology with limited data collected from pilot. Few reports have been published on the assessment of HTL economics. The two available estimations were conducted from NREL and PNNL. It was reported from NREL report that MFSP of final algae biofuel was 4.49 $/gge with the plant capacity of 1034 ton/day. The processes included algae culture, pretreatment, HTL, upgrading processes, as well as nutrition recycle from HTL aqueous waste. $H_2$ generation was produced on site. The carbon conversion efficiency of final biofuels product from algae was 65%. The cost of algae was the limitation of MFSP, which estimated price was 430 $/ton. (NREL, 2014). PNNL employed pinewood for biofuel production with the feedstock price of 70 $/ton. The reported MFSP was slightly decreased at 4.44 $/gge. (PNNL, 2014) with the plant capacity of 2000 ton/day. This was caused the carbon conversion efficiency of the final product from pinewood was 35%, 46.2% lower than that from algae.

References

Adam, J., Blazso,´ M., Me´sza´ros, E. Pyrolysis of biomass in the presence of Al-MCM-41 type catalysts. Fuel 2005;84(12–13): 1494–502.

Agblevor, F., Besler, S. and Wiselogel, A. Fast Pyrolysis of Stored Biomass Feedstocks. Energy Fuels, 1995,9, 635 – 640.

Adjaye, J.D., Bakhshi, N.N. Production of hydrocarbons by catalytic upgrading of a fast pyrolysis bio-oil. part I: Conversion over various catalysts. Fuel Processing Technology 1995a;45(3):161–83.

Adjaye, J.D., Bakhshi, N.N. Production of hydrocarbons by catalytic upgrading of a fast pyrolysis bio-oil. Part II: Comparative catalyst performance and reaction pathways. Fuel Processing Technology 1995b;45(3):185–202.

Antonopoulou, G., Gavala, H.N., Skiadas, I.V., Angelopoulos, K., Lyberatos, G. Biofuels generation from sweet sorghum: fermentative hydrogen production and anaerobic digestion of the remaining biomass. Bioresources Technology 2008. 99,110–119.

Azeez, A.M., Meier, D., Odermatt, J. and Willner, T. Fast pyrolysis of African and European lignocellulosic biomasses using Py-GC/MS and fluidized bed reactor. Energy Fuels, 2010, 24, 2078 – 2085.

Balat, M., Balat, M., Kirtay, E., Balat, H. Main routes for the thermo-conversion of biomass into fuels and chemicals. Part 1: Pyrolysis systems. Energy Convers. Manage 2009; 50:3147–57

Baruah, D. and Baruah, D. C. Modeling of biomass gasification: A review. Renewable and Sustainable Energy Reviews 2014, 39(0): 806-815.

Bhaskar, T., Sera, A., Muto, A., and Sakata, Y. Hydrothermal upgrading of wood biomass: Influence of the addition of $K_2CO_3$ and cellulose/lignin ratio. Fuel. 2008, 87(10-11), 2236-2242

Bridgwater, A.V., Meier, D., Radlein, D. An overview of fast pyrolysis of biomass. Organic Geochemistry 1999;30(12):1479-93.

Calviño, M. and Messing, J. Sweet sorghum as a model system for bioenergy crops. Current Opinion in Biotechnology. 2010,23(3): 323-329.

Czernik, S., Scahill, J. and Diebold, J. The production of liquid fuel by fast pyrolysis of biomass. J. Sol. Energy Eng.,2005, 117, 2 – 6.

David, K. and Ragauskas, A.J. Switchgrass as an energy crop for biofuel production: a review of its ligno-cellulosic chemical properties. Energy Environmental Science 2010;3:1182–9

Demirbaş, A. Mechanisms of liquefaction and pyrolysis reactions of biomass. Energy Conversion and Management 2000;41(6):633-46

Daystar, J., Gonzalez, R., Reeb, C., Venditti, R., Treasure, T., Abt, R., and Kelley, S. Economics, Environmental Impacts, and Supply Chain Analysis of Cellulosic Biomass for Biofuels in the Southern US: Pine, Eucalyptus, Unmanaged Hardwoods, Forest Residues, Switchgrass, and Sweet Sorghum, BioResources 2014, 9(1), 393-444.

Hassan, E.M., Yu, F., Ingram, L. and Steele, P.H. The potential use of whole-tree biomass for bio-oil fuels Energy Sources, Part A, 2009, 31, 1829 – 1839.

International Energy Agency. World Energy Outlook 2009, OECD/IEA, Paris, 2009.

Jahirul, M.I., Rasul, M.G., Chowdhury, A.A., Ashwath, N. Biofuels Production through Biomass Pyrolysis —A Technological Review. Energies 2012, 5, 4952-5001

Jones, S., Davis, R., Zhu, Y., Kinchin, C., Anderson, D., Hallen, R., Elliott, D., Schmidt, A., Albrecht, K., Hart, T., Butcher, M., Drennan, C., Snowden-Swan, L. Process Design and Economics for the Conversion of Algal Biomass to Hydrocarbons: Whole Algae Hydrothermal Liquefaction and Upgrading. 2014 a, NREL report.

Jones, S., Tan, E., Jacobson, J., Meyer, P., Dutta, A., Cafferty, K., Snowden-Swan, L., Padmaperuma, A. Process Design and Economics for the Conversion of Lignocellulosic Biomass to Hydrocarbon Fuels. 2013. PNNL report

Karagöz, S., Bhaskar, T,, Muto, A., Sakata, Y. Comparative studies of oil compositions produced from sawdust, rice husk, lignin and cellulose by hydrothermal treatment. Fuel 2005;84(7-8):875-84.

Li, C., Yang, X., Zhang, Z., Zhou, D., Zhang, L., Zhang, S., Chen, J. Hydrothermal liquefaction of desert shrub salix psammophila to high value-added chemicals and hydrochar with recycled processing water. BioResources 2013;8(2):2981-97

Liu, C., Wang, H., Karim, A.M., Sun, J., Wang, Y. Catalytic fast pyrolysis of lignocellulosic biomass. Chemical Society Reviews. 2014, 43(22): 7594-7623

Liu, Z. and Zhang, F.S. Effects of various solvents on the liquefaction of biomass to produce fuels and chemical feedstocks. Energy Conversion and Management 2008;49(12):3498-504.

Mckendry, P. Energy production from biomass (part 2): conversion technologies. Bioresource Technology. 2002; 86: 47-54

Ming, R., Green, P.J., Meyers, B.C. Genomic and small RNA sequencing of Miscanthus giganteus shows the utility of sorghum as reference genome sequence for Andropogoneae grasses. Genome Biol. 2010,11: R12.

Moberg, D.R., Thibodeau, T.J., Amar, F.G., Frederick, B.G. Mechanism of hydrodeoxygenation of acrolein on a cluster model of $MoO_3$.The Journal of Physical Chemistry C 2010;114(32):13782-95.

Mortensen, P.M., Grunwaldt, J.D., Jensen, P.A., Knudsen, K.G., Jensen, A.D. A review of catalytic upgrading of bio-oil to engine fuels. Applied Catalysis A: General 2011;407(1–2):1-19.

Naik, S.N., Goud, V.V., Rout, P.K., and Dalai, A.K. Production of first and second generation biofuels: A comprehensive review. Renewable and Sustainable Energy Reviews. 2010,14(2): 578-597.

Oasmaa, A., Kuoppala, E. and Solantausta, Y. Fast Pyrolysis of Forestry Residue. 1. Effect of Extractives on Phase Separation of Pyrolysis Liquids Energy Fuels, 2003, 17, 433 – 443.

Oasmaa, A., Solantausta, Y., Arpiainen, V., Kuoppala, E. and Sipila, K., Fast pyrolysis bio-oils from wood and agricultural residues Energy Fuels, 2010a, 24, 1380 – 1388.

Oasmaa, A., Kuoppala, E., Ardiyanti, A. Characterization of hydrotreated fast pyrolysis liquids, Energy and Fuels 2010b:24(9); 5264-72.

Okada, M., Lanzatella, C., Saha, M.C., Bouton, J., Wu, R., Tobias, C.M. Complete switchgrass genetic maps reveal subgenome collinearity, preferential pairing and multilocus interactions. Genetics, 2010, 185:745-760.

Onarheim, K., Lehto, J., and Solantausta, Y. Technoeconomic Assessment of a Fast Pyrolysis Bio-oil Production Process Integrated to a Fluidized Bed Boiler. Energy Fuels, 2015, 29 (9), 5885–5893

Piskorz, J., Majerski, P., Radlein, D., and Scott, D. Fast pyrolysis of sweet sorghum and sweet sorghum bagasse. J. Anal. Appl. Pyrolysis, 1998, 46, 15 – 29.

Piskorz, J. and Scott, D. in Science in Thermal and Chemical Biomass Conversion, ed.

V. Bridgwater and D. G. B. Boococke, CPL Press, 2006, 1273 – 1281.

Rogalinski, T., Liu, K.Y., Albrecht, T. Hydrolysis kinetics of biopolymers in subcritical water. The Journal of Supercritical Fluids 2008;46(3):335-41

Sannigrahi, P., Ragauskas, A.J., Tuskan, G.A. Poplar as a feedstock for biofuels: a review of compositional characteristics, biofuels. Biofuels, Bioproducts Biorefining 2010; 4:209–26.

Song, C., Hu, H., Zhu, S., Wang, G., Chen, G. Nonisothermal catalytic liquefaction of corn stalk in subcritical and supercritical water. Energy and Fuels 2004;18(1):90-96.

Shemfe, M.B., Gu, S., Ranganathan,P. Techno-economic performance analysis of biofuel production and miniature electric power generation from biomass fast pyrolysis and bio-oil upgrading. Fuel 2015, 143: 361-372.

Swaminathan, K., Alabady, M.S., Varala, K., De Paoli, E., Ho, I., Rokhsar, D.S., Arumuganathan, A.K., Wang, J., Roe, B., Macmil, S., Yu, Q., Murray, J.E., Tang, H., Chen, C., Najar, F., Wiley, G., Bowers, J. Genomic and small RNA sequencing of Miscanthus giganteus shows the utility of sorghum as reference genome sequence for Andropogoneae grasses. Genome Biol. 2010,11: R12.

U.S. Department of Energy (USDOE). 2011. U.S. billion-ton update: Biomass supply for a bioenergy and bioproducts industry. ORNL/TM-2011/224. Oak Ridge National Laboratory, Oak Ridge, TN.

Thilakaratne, R., Brown, T., Li, Y., Hu, G., Brown, R. Mild catalytic pyrolysis of biomass for production of transportation fuels: a techno-economic analysis. Green Chem., 2014, 16 , 627–636

Tymchyshyn, M., Xu, C. Liquefaction of bio-mass in hot-compressed water for the production of phenolic compounds. Bioresource Technology 2010;101(7):2483–90.

United States Department of Agriculture. (2008), Data and Statistics. Available from: http://www.usda.gov/wps/portal/!ut/p/_s.7_0_A/7_0_1OB?navid=DATA_STATISTICS&parentnav=AGRICULTURE&navtype=RT.

Wildschut, J., Mahfud, F.H., Venderbosch, R.H., Heeres, H.J. Hydrotreatment of fast pyrolysis oil using heterogeneous noble-metal catalysts. Industry and Engineering Chemistry Research 2009a;48(23):10324–34

Wildschut, J., Arentz, J., Rasrendra, C.B., Venderbosch R.H., Heeres, H.J.Catalytic hydrotreatment of fast pyrolysis oil: Model studies on reaction pathways for the carbohydrate fraction. Environmental Progress and Sustainable Energy 2009b;28(3):450-60.

Xiu, S. and Shahbazi, A. Bio-oil production and upgrading research: A review. Renewable and Sustainable Energy Reviews 2012;16(7): 4406-14.

Yang, Y., Allan, G., Chunbao, X. Production of bio-crude from forestry waste by hydro-liquefaction in sub-/super-critical methanol [electronic resource]. AIChE Journal 2009;55(3): 807-19.

Yanik, J., Kornmayer, C., Saglam, M. and Yüksel, M. Fast pyrolysis of agricultural wastes: Characterization of pyrolysis products. Fuel Process. Technol., 2007, 88, 942 – 947.

Zhang, B., Huang, H.J., Ramaswamy, S. Reaction kinetics of the hydrothermal treatment of lignin. Applied Biochemistry Biotechnology 2008;147(1-3):119-31.

Zhang, L., Xu, C., Champagne, P. Overview of recent advances in thermos chemical conversion of biomass. Energy conversion and management 2010, 51: 969-982.

Zhu, Y., Biddy, M.J., Jones, S.B., Elliott, D.C., Schmidt, A.J. Techno-economic analysis of liquid fuel production from woody biomass via hydrothermal liquefaction (HTL) and upgrading. Applied Energy 2014,129:384–394.

Table 2.1 Summary of fuel properties from biomass liquefaction and conventional crude oil

| Fuel Properties | Liquefaction biocrude | Pyrolysis bio-oil | Petroleum |
|---|---|---|---|
| C [wt %] | 73 | 55-65 | 83-86 |
| O [wt %] | 13 | 28-40 | <1 |
| H [wt %] | 10 | 5-7 | 11-14 |
| S [wt %] | n/a | <0.05 | <4 |
| N [wt %] | 4 | <0.4 | <1 |
| Water [wt %] | 2-5 | 15-30 | 0.1 |
| Ash [wt %] | 0.78 | <0.2 | 0.1 |
| HHV [MJ/kg] | 32-36 | 16-19 | 44 |
| pH | n/a | 2.8-3.8 | n/a |
| ρ [kg/L] | 1.0 | 1.05-1.25 | 0.86 |
| μ [cP] [50 °C] | 843 | 40-100 | 180 |
| O/C | 0.1 | 0.3-0.5 | ≈0 |
| H/C | 1.6 | 1.5-1.9 | 1.5-2.0 |

Data cited from (Mortensen et al., 2011)

## III. The Initialization of Two Stage Hydrothermal Liquefaction (HTL) and Its Application on upgraded biocrude Production from Sweet Sorghum Bagasse. Part I: 1st stage HTL pretreatment[1]


### Abstract

A two-stage hydrothermal liquefaction (HTL) was initialized and conducted in this study to (i) enhance carbon conversion efficiency of lignocellulose into biofuels; (ii) avoid repolymerization reaction between furfural decompositions from hemicellulose and phenol-type intermediates from lignin, which impairs the yield of HTL biocrude and the quality of downstream hydrodeoxygenation (HDO) upgraded biocrude. 1st stage HTL (1stSH) was implemented at lower temperature with the purpose of hydrolyzing as much hemicellulose as possible into C5 sugar stream. 2nd stage HTL (2ndSH) was sequentially conducted for biocrude production with the solid product of 1stSH as feedstock. HDO was designed to combine with 2ndSH to produce hydrocarbons concentrated upgraded bio-oil from HTL liquid products. In this first fraction of two stage HTL-HDO (TSHH) study, 1stSH was carried out and the products were analyzed. Under the optimal 1stSH condition of 170 °C and 60 min, 94.1 % of hemicellulose and 49.2 % cellulose were respectively hydrolyzed into C5 and C6 sugars with the maximum yield of 28.52 g/L. This sugars stream is a desirable feedstock for value-add chemicals or alcohol-base biofuel conversion, such as bioethanol fermentation. The most adaptable 1stSH solid product was obtained at 170 °C for 90 min, consisting of 46.0 wt % lignin, 42.7 wt % cellulose and negligible amount of hemicellulose.


[1] Yang Yue, Sudhagar Mani and Jim Kastner. To be submitted to Energy & Fuel

This solid product was proposed to be used as substrate for upgraded biocrude conversion with 2nd stage HTL-HDO, which will be described in the next fraction of our study.

***Keywords***: liquefaction, sweet sorghum bagasse, hemicellulose, two-stage HTL

## 3.1 Introduction

The contradiction between dwindling reservation of fossil fuels and increasing world-wide energy demand is a primary challenge for hydrocarbon fuels supply. Additionally, the environmental issue of excess green-house emission, plus economic conflicts and national security resulted from unbalance distribution of fossil fuels resource also promptly motivate researches and positive policies for exploring sustainable and renewable energy sources. This essential requirement promotes the US government to alleviate energy issue through the development of biofuels, which serves as a crucial alternative of petroleum. It was proposed from Energy Independence and Security Act that by 2022, 36 billion gallons (857 million barrels) of biofuels would have been mandatorily provided as blending fuel annually (U.S. Energy Independence and Security Act, 2007). Lignocellulosic biomass is an attractive feedstock for biofuel conversion with affluent availability but ineffective utilization. It was reported that 1.6 billion tons of lignocellulose could be sustainably available annually over the US, which if effective conversion, could offset 43% of total domestic petroleum consumption and easily achieve the target of Energy Independence and Security Act (Bond et al., 2014).

HTL is a current startup technology to directly converse a diversity of biomasses into renewable biofuels in the presence of subcritical water at high temperature (280-370 °C) and high pressure (10-25 M Pa). De-moisture pretreatment is not necessary and cheap cost water is employed as solvent at subcritical phase for biocrude production (Mortensen et. al., 2011). However, one of the current issues of lignocellulosic biomass HTL is that the complexity of

structural carbohydrates hinders biocrude yield and impairs upgraded biocrode quality after downstream hydrodeoxygenation (HDO) process. Specially, for herbaceous biomass, hemicellulose constituted around 20-40 wt. %; however, it only contributed to 5.3 wt. % of biocrude, and the majority products were aqueous components (42 wt. %), among which, carboxylic acids accounted for 45% (Yoshida and Saka, 2006). Additionally, cross reactions occurred between the furfural derivate compounds decomposed from hemicellulose and phenol-type intermediates from lignin, and formed solid residues through repolymerization (Liu et. al., 2013). This further damaged the biocrude yield and increased the difficulty of HDO process. Therefore, it was proposed that hemicellulose is a less efficient feedstock for HTL-HDO upgraded biorude conversion (Pinkowska et.al., 2011).

Sweet sorghum is a typical C4 energy crop and wild planted in the south regions of the States. Its juice is rich in sucrose and can be fermented into alcohol-based biofuels with minimal pretreatment (Daystar et al., 2014). After extracting the juice, the rest named bagasse is rich in moisture (60-80%), which makes sweet sorghum bagasse extremely appropriate as a wet lignocellulosic biomass for HTL reaction.

The objective of this study is to enhance carbon conversion efficiency from lignocellulose to hydrocarbons concentrated upgraded biocrude through a combination of gradient-temperature two-stage HTL and HDO processes (Fig.3.1). The 1$^{st}$SH aims to convert as much hemicellulose as possible into C5 sugar stream. During this process, a fraction of amorphous cellulose was also hydrolyzed into glucose. The obtained mixture of xylose and glucose was an ideal sugar stream for bioethanol co-fermentation, which, depending on strains and operating conditions, increased 13.8%-1.24 folds on ethanol yield than xylose and was reported as a promising strategy for bioethanol commercialization. (Fu and Peiris, 2008; Krishnan et al., 1999). The solid product, rich

in lignin and cellulose, from 1st stage HTL was employed for upgraded bio-oil conversion through 2nd stage HTL-HDO. The carbon conversion efficiency of lignocellulose could be significantly increased by two considerations: (i) compared to biocrude, hemicellulose-derived C5 sugar stream was more efficient for alcohol-based biofuel fermentation; (ii) the interaction between furfural intermediates from hemicellulose and lignin units could be essentially avoided, thus further reduced byproducts formation during lignocellulosic biomass HTL. To the best of our knowledge, there has been no research to apply such a multifaceted outreach of HTL technology into upgraded biocrude and sugar platform conversion simultaneously. This paper focused on the 1st stage of TSHH with sweet sorghum bagasse as feedstock; the optimal yield of sugars stream and components of solid products were analyzed. As a thermal pretreatment, this work process provided a foundation for high quality upgraded biocrude production, which described in followed 2nd stage HTL-HDO section.

3.2 Materials and Methods

Sweet sorghum bagasse used in this study was obtained from Fort Valley State University, Fort Valley, Georgia, USA. Sulfuric acid was purchased from Sigma-Aldrich with analytical reagent. Deionized water used in the experiments was prepared by our lab. Helium was obtained from Airgas Company (U.S.).

The stainless steel reactors utilized for 1st SH reaction were Parr 5000 multi-reactor heater & stirrer system with Parr 4871 process controller. The maximum temperature and permissible pressure for the vessel were respectively 300 °C and 3000 psi with the capability of 75 ml. Teflon gasket was used to avoid pressured gas leakage during the reaction. Agitation of 300 rpm was provided by magnetic stirrer with the maximum speed of 750 rpm. The average heating rate was 10.2 °C /min and the cooling rate was 34.4 °C/min with water bath.

3.2.1 Design of 1st SH

At the 1stSH, lower temperature (160-200°C) was applied to hydrolyze hemicellulose and partial cellulose from grinded dried sweet sorghum bagasse. The conditions for 1stSH were designed on the basis of severity factor (logR0), which was currently used to estimate and interpret the effects of reaction conditions:

$$R_0 = \int_0^t \exp\left({}^{T_{(t)} - T_{(ref)}}/_{14.75}\right) dt$$ (Overend et al,, 1987)

Where, temperature (T /°C) is a function of time (t /min); $T_{ref}$ is the reference temperature ($T_{ref}$ =100 °C); 14.75 is an empirical parameter.

Five different severity factors ranging from 3.43 to 4.02 were estimated on hemicellulose hydrolysis and the yield of C5 and C6 sugars stream. The conditions of 1stSH were described in table 3.1.

3.2.2 Biomass pretreatment and analysis

Sweet sorghum bagasse was grinded with knife mill into fine powder with average size of 0.3 mm and oven-dried at 105 °C in air overnight. This grinded material was kept in desiccator until use. The compositional characterization of pretreated sweet sorghum bagasse was measured with ultimate analysis and proximate analysis; lignin component was determined with pyro-GC/MS described in 2.4; higher heating valve (HHV) was analyzed with oxygen bomb calorimeter; the contents of structural carbohydrates and lignin were determined with wet chemical analysis according to NREL standard protocol (Selig et al., 2008).

3.2.3 1st SH procedure and products separation

In a typical experiment, 5.0 g of pretreated sweet sorghum bagasse powder was placed into the vessel followed by the addition of 50 ml DI water. The suspension was well-mixed before loading. After weighting the total weight of vessel and reactants, the reactor was assembly loaded

and securely sealed. The air inside the reactor was purged and displaced with helium three times and the headspace of the vessel was pressurized with high purity helium to 300 psi. The suspension was continuously stirred at 300 rpm during the reaction. The 1$^{st}$SH process was monitored through Parr Specview program. After the reaction, the vessel was removed from heater system and immediately vertically placed into water bath until room temperature. The gas sample was extracted from headspace through a Swagelok stainless steel blowdown needle valve into a sealed air sample bag for GC-TCD analysis. The vessel was then unloaded after pressure releasing through the blowdown valve. The liquid and solid products were weighted with the vessel and physically completely collected.

The mixture products were filtered with vacuum filtration through Whatmann #4 90mm filter paper. Additional 25 ml DI water was used to rinse the solid product to collect all residual liquid product. The rinsing solution was merged with the filtrate. Post acid treatment of filtrate was implemented if necessary by adding $H_2SO_4$ solution into liquid product until the final concentration of 4% and hydrolyzing at 121℃ for 1hr. The liquid samples were stored in refrigerator before analysis, and solid samples were dried in oven at 105 ℃ overnight.

3.2.4 HTL products instrumental analysis

The collected gas sample from 1$^{st}$ SH was analyzed with GC-TCD using Carboxen 1000 60/80 SS Packed Column (15ft x 1/8 in), which was specifically for $H_2$, $O_2$, $N_2$, CO, $CH_4$ and $CO_2$ identification. The inlet and detector temperatures were respectively set at 100 ℃ and 140 ℃. The temperature was initialized at 35 ℃ for 5 min and ramped up to 200 ℃ with the heating rate of 20 ℃ /min, and held constant for 5.75 min. The gas sample injected was 50 μl and Helium was used as carrier gas.

In the liquid product, monosaccharides (xylose and glucose), carboxylic acids and furan derivate were determined with HPLC using Coragel 94 column. The oven temperature was 60°C and 4 mN sulfuric acid was used for mobile phase. The flow rate was constant at 0.6 ml/min. The sample volume injected was 5 µl.

The elemental components of solid product were determined with ultimate analysis; the operation method was the same as that of sweet sorghum bagasse characterization analysis. Wet chemical analysis was also operated on solid product to measure the remaining structural carbohydrates and lignin contents on the basis of NREL standard protocol (Selig et al., 2008).

The lignin compositions were analyzed with pyro-GC/MS. Around 2.0 mg of each sample was weighted with three replications and single-shot pyrolyzed at 500 °C for 12 sec with Frontier lab pyrolyzer (PY-2020 iD). The volatile compounds were separated with HP-5ms Capillary Column (30m x 0.25um x 0.25mm) (Agilent Technologies Inc) which combined with a 6890N GC system. The oven temperature program was initially set at 50 °C for 2 min; then ramped to 280 °C with the heating rate of 5 °C /min and kept constantly for 53 min. Helium was employed as the carrier gas with the flow rate of 1 ml/min and the split ratio was set at 50:1. The lignin components were identified with NIST11 mass spectral library.

The calculation of products conversions were defined as follows:

$$\text{Hemicellulose conversion} = \left(1 - \frac{\text{mass of hemicellulose in } 1^{st}\text{SH solid product}}{\text{mass of hemicellulsoe in feedstock}}\right) \times 100\%$$

$$\text{Cellulose conversion} = \left(1 - \frac{\text{mass of cellulose in } 1^{st}\text{SH solid product}}{\text{mass of cellulsoe in feedstock}}\right) \times 100\%$$

$$\text{C5 sugar conversion from hemicellulose} = \left(\frac{\text{mass of C5 sugar in } 1^{st}\text{SH liquid product}}{\text{mass of hemicellulsoe in feedstock}}\right) \times 100\%$$

$$\text{C5 sugar conversion from biomass } = \left(\frac{\text{mass of C5 sugar in } 1^{st}\text{SH liquid product}}{\text{mass of biomass feedstock}}\right) \times 100\%$$

3.3 Results and Discussions

3.3.1 Characterization of sweet sorghum bagasse

Sweet sorghum bagasse was mainly constituted with moisture, ash, starch, hemicellulose, cellulose and lignin. The compositional characterization and higher heating valve of sweet sorghum bagasse were listed in table 3.2. Structural carbohydrates analysis indicated, after juice extraction, the residual soluble sugars accounted for 11.55 wt. %, in which glucose accounted for 49.4%, sucrose 16.1%, and fructose 34.6%. Lignin accounted for 17.66 wt. % of total biomass; most lignin was formed from p-hydroxyl phenol (H lignin) unit. The proportions of hemicellulose and cellulose were respectively 19.68 wt. % and 36.17 wt. % in sweet sorghum bagasse. The O/C and H/C ratios were 0.94 and 1.57; both indicated fairly low energy density of sweet sorghum bagasse. This measured H/C ratio was close to the report of 1.52 (Meryemoğlu et al., 2014), where whole sorghum was used as the feedstock for HTL; the determined O/C ratio of 0.94 was between the O/C ratios of whole sorghum (0.69) and sorghum hydrolysate (1.34) (Meryemoğlu et al., 2014).

3.3.2 Chemical analyses of 1$^{st}$SH products

Under the designed conditions in table 3.1, the yields of each fraction after 1$^{st}$SH were showed in table 3.3. Gas product was only detected with higher temperature (>190 °C) or higher severity factor (>3.85). $CO_2$ was the only identified component in gas product from 1$^{st}$ SH.

It was also found at the same level of severity factor, a combination of lower temperature and longer holding time was more desirable for hemicellulose hydrolysis except two conditions (190°C for 10 min and 200 °C for 5 min) at $\log R_0$=3.70 (table 3.4). However, when reaction temperature reached 180 °C, C5 sugar yield reduced dramatically (Fig.3.3a) resulted from the decomposition of C5 sugar into furan derivate and carboxylic acids.

Accompanying with hemicellulose hydrolysis, amorphous cellulose was, to some extent, hydrolyzed into C6 oligomer and monomer sugars. The composition analysis of solid residues indicated that the simultaneous hydrolysis of hemicellulose and amorphous cellulose occurred from 160 °C to 200 °C (table 3.4). Fig.3.2 displayed the hydrolysis conversions of hemicellulose and cellulose under designed conditions.

The C5 sugar conversions were respectively described in Fig.3.3c and Fig.3.3d on the basis of hemicellulose and sweet sorghum bagasse. Compared with the hemicellulose content of 19.68% in raw sweet sorghum bagasse, the highest hemicellulose decomposition of 95.2% occurred at 200 °C for 5 min, followed by 94.1% at 170 °C for 90 min. However, the C5 sugar conversion at 200 °C, 5 min was as low as 1.72% on the basis of total biomass. Most hemicellulose hydrolysis products at this temperature were further decomposed into furfural, acetate and formate. The maximum conversion of C5 sugar of 17.65% was obtained at 170 °C for 60 min with post acid treatment on the basis of the dried biomass weight. After 60 min, although the hemicellulose continued decomposing, less C5 sugar was obtained. This was because the degradation rate of C5 sugar to furfural was higher than its yield rate from hemicellulose hydrolysis. Similar trends were observed at other temperatures. We also found that within the beginning several minutes of the reaction, a great amount of hemicellulose were hydrolyzed. The hemicellulose hydrolysis rate remarkably decreased with time until reaching the balance, where the hydrolysis rate of hemicellulose or oligomer xylose equaled to the degradation rate of monomer xylose. Rather than the inhabitation effect of the decomposed products, we proposed that fast hydrolysis of hemicellulose occurred simultaneously with slow hydrolysis at lower temperature. A fraction of hemicellulose, which was less tolerance to temperature, could be directly hydrolyzed into xylose rapidly rather through oligomer xylose; the remaining hemicellulose was supposed to be more

stable and gradually hydrolyzed into oligomer xylose with a much lower reaction constant. The observed hemicellulose hydrolysis results and above proposition were in accordance with Shen's kinetics study (Shen and Wyman, 2011). However, limited by the reactor and cooling system, the kinetical constant of hemicellulose hydrolysis was not able to be determined.

Besides hemicellulose, a fraction of cellulose was also hydrolyzed. At each reaction temperature, cellulose content decreased in solid product with time. However, the maximum hydrolysis of cellulose stopped at around 50%, where it was considered the amorphous cellulose was completely hydrolyzed. With the same severity factor, lower temperature with longer holding time was also considered more favorable for amorphous cellulose hydrolysis. For instance, at the severity factor of 3.85, 170 ℃ for 60 min was able to accomplish all the amorphous cellulose hydrolysis, while 88% amorphous cellulose was converted at 180 ℃ for 30 min and 74% at 190 ℃ for 15 min.

The C5 and C6 sugars were obtained in the forms of oligomers and monomers. Post-acid hydrolysis treatment further hydrolyzed oligomer saccharides into monomers. Unlike Shen's report (Shen and Wyman, 2011), about 10 folds enhancement on glucose and xylose yields after post acid treatment, we found monomer sugars yields increased from 45% to 70%. This difference might be because of the different structural and tolerance of holocellulose between sweet sorghum bagasse and corn stover. The maximum yields of C5 sugars and glucose were respectively 17.04 g/L at 170 ℃ for 60 min and 12.32 g/L at 170 ℃ for 90 min. The optimal condition for C5 and C6 sugars yield was 170 ℃ for 60 min with total sugar yield of 28.52 g/L. Higher temperature with longer holding time increased conversion rates of furfural and 5-HMF and impaired the total sugar yield. However, considering the residual hemicellulose in solid, the condition of 170 ℃ for

90 min was more appropriate and employed for 1$^{st}$SH, where 94% hemicellulose was hydrolyzed with the yield of sugar mixture at 28.14 g/L.

The yields of other dominant aqueous components in liquid product were also analyzed with HPLC and described in Fig.3.4. 5-hydroxymethyfurural (5-HMF), furfural, acetate and formate showed similar yield trends as C5 and C6 sugars, increasing with holding time at each operating temperature. The maximum yields of 5-HMF, furfural, acetate and formate were obtained at 170 °C for 90 min, respectively 3.43g/L, 1.89 g/L, 3.89 g/L and 5.46 g/L. Under above concentrations of furans and carboxylic acids, *S. cerevisiae*, an industrial yeast strain to ferment ethanol from C5 and C6 sugars, was reported to be adaptable and active (Palmqvist and Hahn-Hägerdal, 2000). It was also observed post acid hydrolysis treatment harvested more furfural and carboxylic acids except 5-HMF. Yin proposed that this probably due to under diluted acidic condition, 5-HMF was degraded into formate and 1, 2, 4-benzenetriol (Yin and Tan, 2012). However, 1, 2, 4-benzenetriol were neither detected with GC-MS nor HPLC. It was deductible that other unidentified pathways may involve 5-HMF degradation.

As described above, although hemicellulose in lignocellulosic biomass could be completely removed through 1$^{st}$SH with severe reaction conditions, the expense of impairing C5 and C6 sugars yield during this process significantly damaged potential carbon resource and was considered uneconomical. Actually, solid product from 1$^{st}$SH at 170 °C for 90 min was appropriate as a result of optimization, which consisted of 46.0 wt % lignin, 42.7 wt % cellulose, 2.7 wt % hemicellulose and 3.6 wt % water insoluble ash. Compared to the initial sweet sorghum bagasse, there were enhancements of 28.3% on lignin and 6.5% on cellulose; declines of 16.9 % on hemicellulose and 11.6 % on water soluble sugars. This lignin and cellulose concentrated solid product would be effectively utilized in 2$^{nd}$ stage HTL-HDO process for upgrading biocrude

conversion. The liquid co-product of C5 and C6 sugars stream from hemicellulose could be used as another significant carbon resource.

### 3.4 Conclusion

TSHH approach was initialized and 1$^{st}$SH was conducted successfully in this paper. 57.9% carbon of lignocellulosic biomass was converted into sugar stream from hemicellulose and partial cellulose at 170 °C for 60 min with the maximum yield of 28.52 g/L. This C5 and C6 mixed sugar stream was appropriate for bio-ethanol and other value-added chemicals conversion. The optimal 1$^{st}$SH condition for solid product was 170 °C for 90 min. The component of 1$^{st}$SH solid product was 46.0 wt % lignin and 42.7 wt % cellulose with negligible amount of hemicellulose. This solid product was considered a more adaptable feedstock for upgraded bio-oil production through 2$^{nd}$ stage HTL-HDO process.

References

Bond JQ, Upadhye AA, Olcay H, Tompsett JA, Jae J, Xing R, Alonso DM, Wang D, Zhang T, Kumar R, Foster A, Sen SM, Maravelias CT, Malina R, Barrett SRH, Lobo R, Wyman CE, Dumesic JA, Huber GW. 2014. Production of renewable jet fuel range alkanes and commodity chemicals from integrated catalytic processing of biomass. Energy Environ. Sci. 7, 1500-1523.

Daystar J, Gonzalez R, Reeb C, Venditti RA, Treasure T, Abt R, Kelley S. 2014. Economics, Environmental Impacts, and Supply Chain Analysis of Cellulosic Biomass for Biofuels in the Southern US: Pine, Eucalyptus, Unmanaged Hardwoods, Forest Residues, Switchgrass, and Sweet Sorghum. BioResources. 9, 393-444.

Fu N, Peiris P. 2008. Co-fermentation of a mixture of glucose and xylose to ethanol by Zymomonas mobilis and Pachysolen tannophilus. World J Microbiol Biotechnol.24. 1091–1097.

Krishnan MS, Ho NW, Tsao GT. 1999. Fermentation kinetics of ethanol production from glucose and xylose by recombinant Saccharomyces 1400 (pLNH33). Appl Biochem Biotechnol, 77–79, 373–88.

Liu H, Li M, Yang S, Sun R. 2013. Understanding the Mechanism of Cypress Liquefaction in Hot-Compressed Water through Characterization of Solid Residues. Energies.6, 1590-1603.

Meryemoğlu B, Hasanoğlu A, Irmak S, Erbatur O.2014. Biofuel production by liquefaction of kenaf (Hibiscus cannabinus L.) biomass. BioResources. 151, 278-283.

Mortensen PM, Grunwaldt JD, Jensen PA, KG Knudsen, Jensen AD. 2011. A review of catalytic upgrading of bio-oil to engine fuels. Appl. Catal. A- Gen. 407, 1-19.

Overend RP, Chornet E. 1987. Fractionation of lignocellulosics by steam-aqueous pretreatments. Philos. Trans. R. Soc. Lond. 321,523–536.

Palmqvist E, Hahn-Hägerdal B. 2000. Fermentation of lignocellulosic hydrolysates. II: inhibitors and mechanisms of inhibition. BioResources. 74, 25-33

Pinkowska, H., Wolak, P., Z1ocinska A. 2011. Hydrothermal decomposition of xylan as a model substance for plant biomass waste -Hydrothermolysis in subcritical water. Biomass Bioenergy. 35, 3902-3912

Selig M, Weiss N, Ji Y. 2008. In: Laboratory Analytical Procedure No. TP-510-42629. National Renewable Energy Laboratory, Golden, CO.

Shen J, Wyman CE. 2011. A novel mechanism and kinetic model to explain enhanced xylose yields from dilute sulfuric acid compared to hydrothermal pretreatment of corn stover. BioResources. 102, 9111-9120.

U.S. Energy Independence and Security Act, 2007

Yin S, Tan Z. 2012. Hydrothermal liquefaction of cellulose to bio-oil under acidic, neutral and alkaline conditions. Appl. Energy. 92, 234-9.

Yoshida K, Saka S. Organic acid production from Japanese beech by supercritical water treatment. In: The 2nd Joint International Conference on Sustainable Energy and Environment. C-032, Thailand; 2006. p. 1–6, 22.02.2010.

Table 3.1. The conditions of 1st SH *

| Temperature /°C | Time /min | Catalyst | Gas** | Modified severity factor ($logR_0$) |
|---|---|---|---|---|
| 1st stage HTL | | | | |
| 160 | 60 | n/a | He | 3.55 |
| 160 | 90 | n/a | He | 3.73 |
| 170 | 30 | n/a | He | 3.55 |
| 170 | 45 | n/a | He | 3.72 |
| 170 | 60 | n/a | He | 3.85 |
| 170 | 90 | n/a | He | 4.02 |
| 180 | 15 | n/a | He | 3.56 |
| 180 | 20 | n/a | He | 3.68 |
| 180 | 30 | n/a | He | 3.85 |
| 180 | 45 | n/a | He | 4.02 |
| 190 | 10 | n/a | He | 3.69 |
| 190 | 15 | n/a | He | 3.86 |
| 200 | 2 | n/a | He | 3.43 |
| 200 | 5 | n/a | He | 3.73 |

*DI water was used as the solvent for above HTL reactions. The biomass loading rates were constant with 10% (w/w). The headspace was pressured with helium to 300 psi.

Table 3.2. Composition analysis of sweet sorghum bagasse sample

| Sweet sorghum bagasse compositions | | | |
|---|---|---|---|
| Ultimate analysis | C (%, dry) | 41.30 (0.11) | |
| | H (%, dry) | 5.39 (0.04) | |
| | N (%, dry) | 1.32 (0.14) | |
| | O (%, dry) | 51.98 (0.21) | |
| | O/C | 0.94 | |
| | H/C | 1.57 | |
| Proximate analysis | Moisture (%, wt.) | 7.36 (0.03) | |
| | Volatile carbon(%, dry) | 77.03 (0.12) | |
| | Ash (%, dry) | 4.59 (0.03) | |
| | | Soluble ash (%, dry) | 66.2 |
| | | Insoluble ash (%, dry) | 33.8 |
| | Fixed Carbon (%, dry) | 18.38 (0.12) | |
| Heating value | High Heating value (MJ/kg) | 16.30 (0.25) | |
| Carbohydrate and lignin compositions analysis | Lignin (%, wt) | 17.66 (2.38) | |
| | | Syringyl (%, wt) | 9.54 |
| | | Guaiacyl (%, wt) | 34.58 |
| | | p-Hydroxyl phenol (%, wt) | 55.97 |
| | Hemicellulose (%, wt) | 19.68 (0.36) | |
| | Cellulose (%, wt) | 36.17 (0.63) | |
| | | 11.55 (2.72) | |

| | | | |
|---|---|---|---|
| Sweet sorghum bagasse compositions | | | |
| | Soluble residue sugars (%, wt) | Sucrose (%, wt) | 16.05 |
| | | Glucose (%, wt) | 49.37 |
| | | Fructose (%, wt) | 34.58 |

Table 3.3. The yields of 1st stage HTL

| Reaction condition | | | Yield wt. % | | |
|---|---|---|---|---|---|
| Modified severity factor ($logR_0$) | Temperature /°C | Time /min | Gas | Solid | Aqueous |
| 3.40 ± 0.3 | 200 | 2 | 4.04 | 44.85 | 51.11 |
| 3.55 ± 0.3 | 160 | 60 | 0.00 | 46.33 | 53.67 |
| | 170 | 30 | 0.00 | 41.33 | 58.67 |
| | 180 | 15 | 0.00 | 45.00 | 55.00 |
| 3.70 ± 0.3 | 160 | 90 | 0.00 | 41.67 | 58.33 |
| | 170 | 45 | 0.00 | 43.33 | 56.67 |
| | 180 | 20 | 0.00 | 42.83 | 57.17 |
| | 190 | 10 | 4.04 | 45.25 | 50.71 |
| | 200 | 5 | 4.04 | 48.08 | 47.88 |
| 3.85 ± 0.3 | 170 | 60 | 3.33 | 43.33 | 53.33 |
| | 180 | 30 | 3.33 | 39.00 | 57.67 |
| | 190 | 15 | 3.33 | 41.33 | 55.33 |
| 4.00 ± 0.3 | 170 | 90 | 3.33 | 43.00 | 53.67 |
| | 180 | 45 | 6.67 | 36.33 | 57.00 |

Table 3.4. The composition of 1[st]SH solid products

| Reaction condition | | | Remaining contents of lignin and structural carbohydrates in 1[st]SH solid products, wt. % | | |
|---|---|---|---|---|---|
| Modified severity factor ($logR_0$) | Temperature, °C | Time, min | lignin | hemicellulose | cellulose |
| 3.40 ± 0.3 | 200 | 2 | 38.92 | 8.09 | 55.59 |
| 3.55 ± 0.3 | 160 | 60 | 28.03 | 12.34 | 51.42 |
| | 170 | 30 | 27.85 | 12.69 | 52.23 |
| | 180 | 15 | 27.86 | 13.51 | 58.03 |
| 3.70 ± 0.3 | 160 | 90 | 30.55 | 11.45 | 52.12 |
| | 170 | 45 | 30.56 | 10.61 | 45.36 |
| | 180 | 20 | 35.00 | 12.23 | 56.78 |
| | 190 | 10 | 36.90 | 8.40 | 53.07 |
| | 200 | 5 | 51.11 | 2.36 | 45.41 |
| 3.85 ± 0.3 | 170 | 60 | 42.75 | 4.99 | 41.67 |
| | 180 | 30 | 39.94 | 6.45 | 51.73 |
| | 190 | 15 | 31.38 | 6.35 | 55.29 |
| 4.00 ± 0.3 | 170 | 90 | 45.97 | 2.74 | 42.70 |
| | 180 | 45 | 35.02 | 5.03 | 48.58 |

*Insoluble ash content was constant of 3.6 wt. % after 1[st] SH

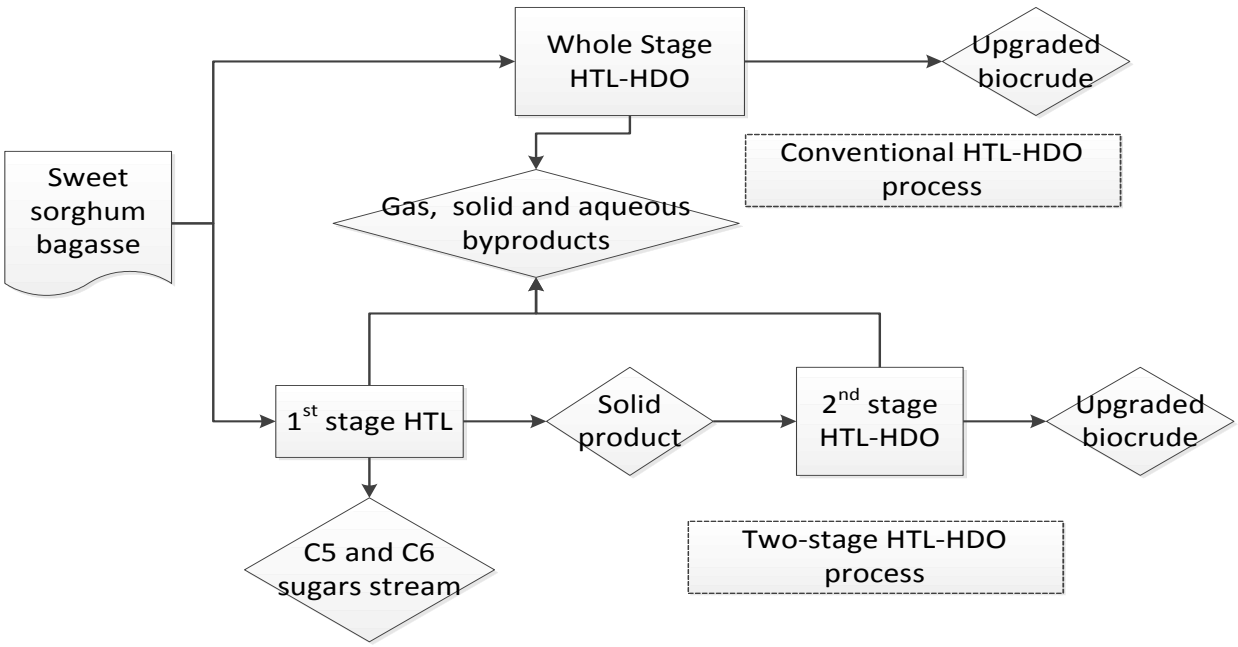


Fig.3.1 The scheme of conventional HTL-HDO and two-stage HTL-HDO processes

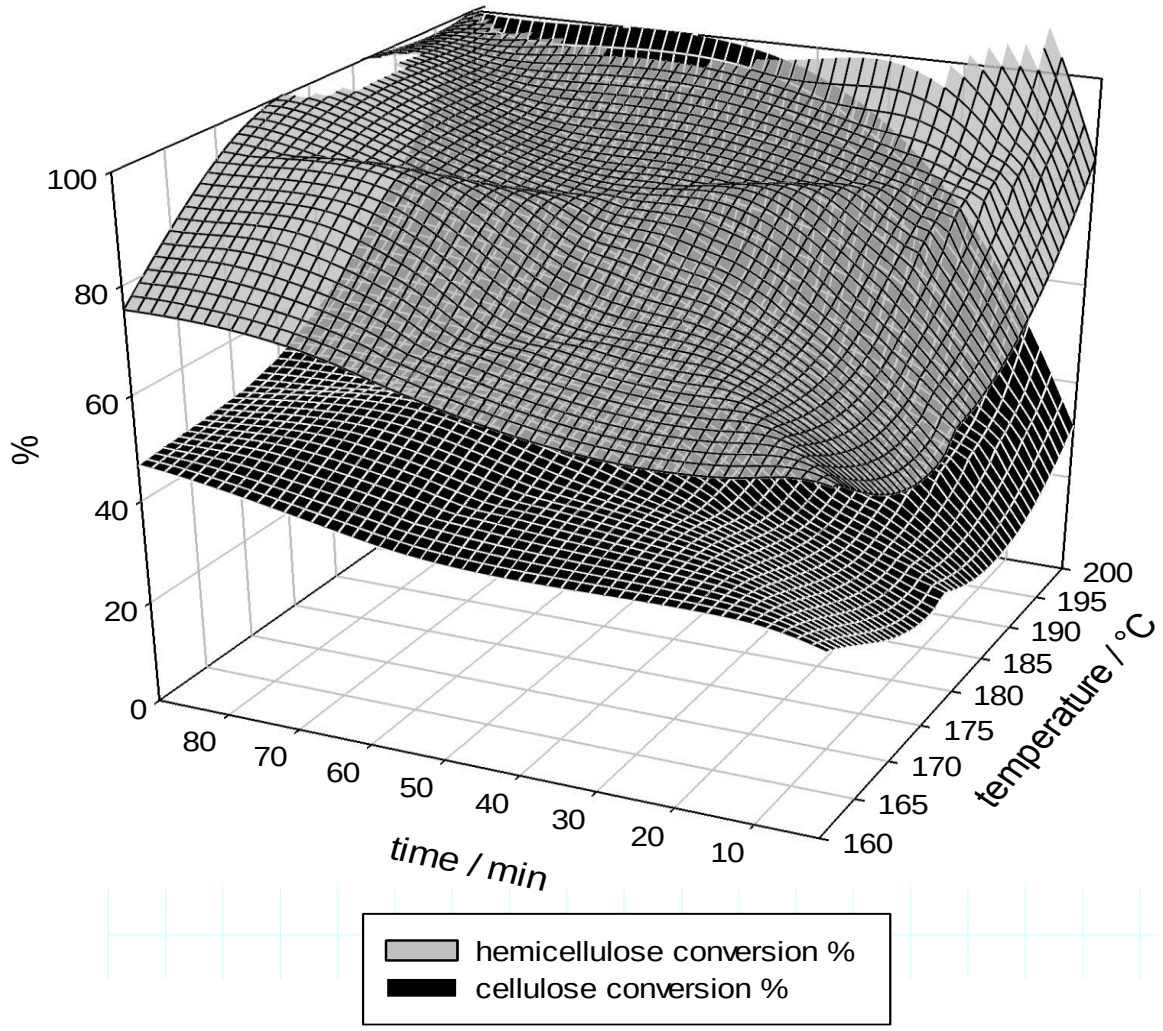


Fig.3.2 Hemicellulose and cellulose decomposition under different conditions of 1st SH

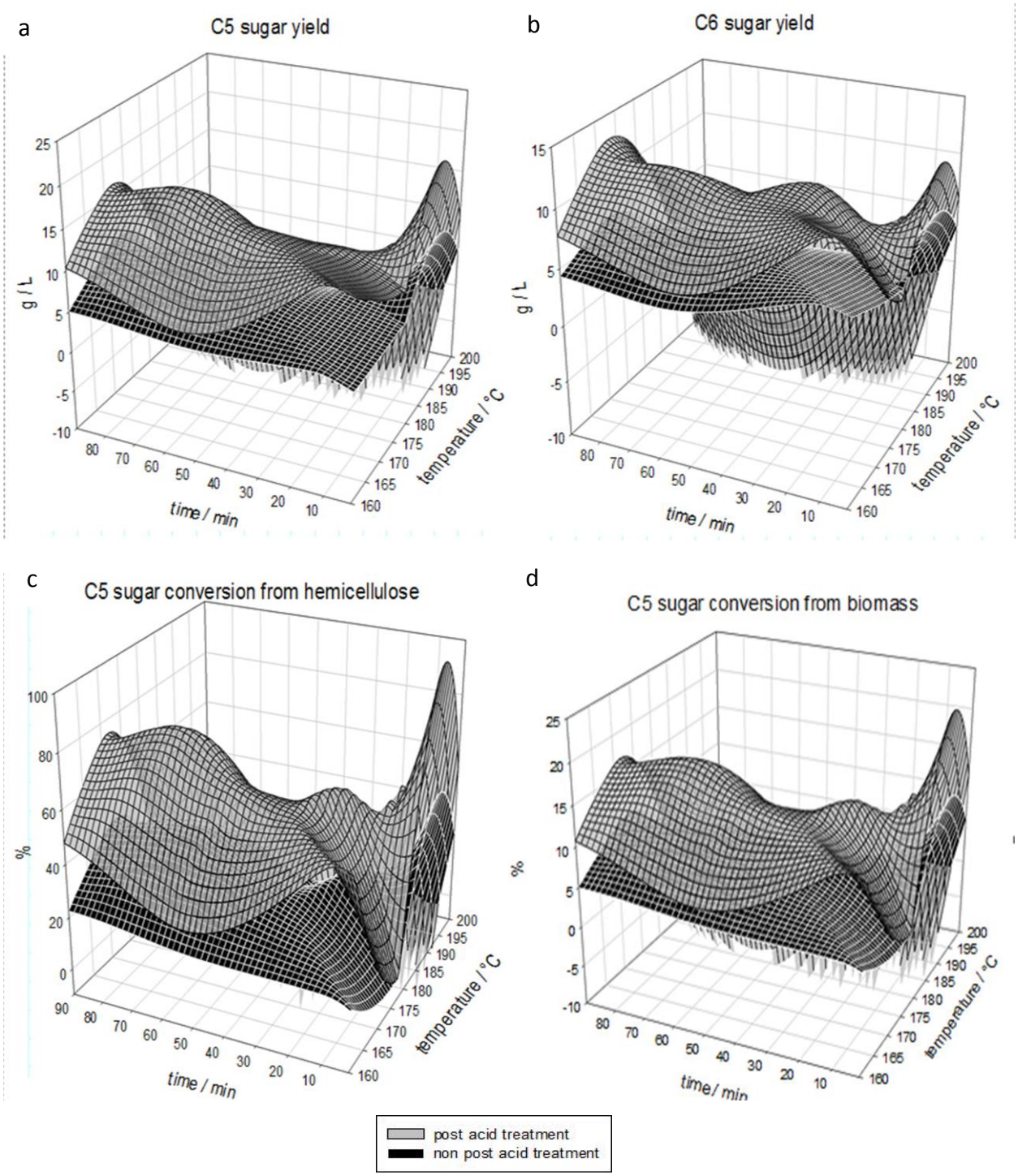


Fig.3.3 Sugar conversion and yield from hemicellulose and cellulose.

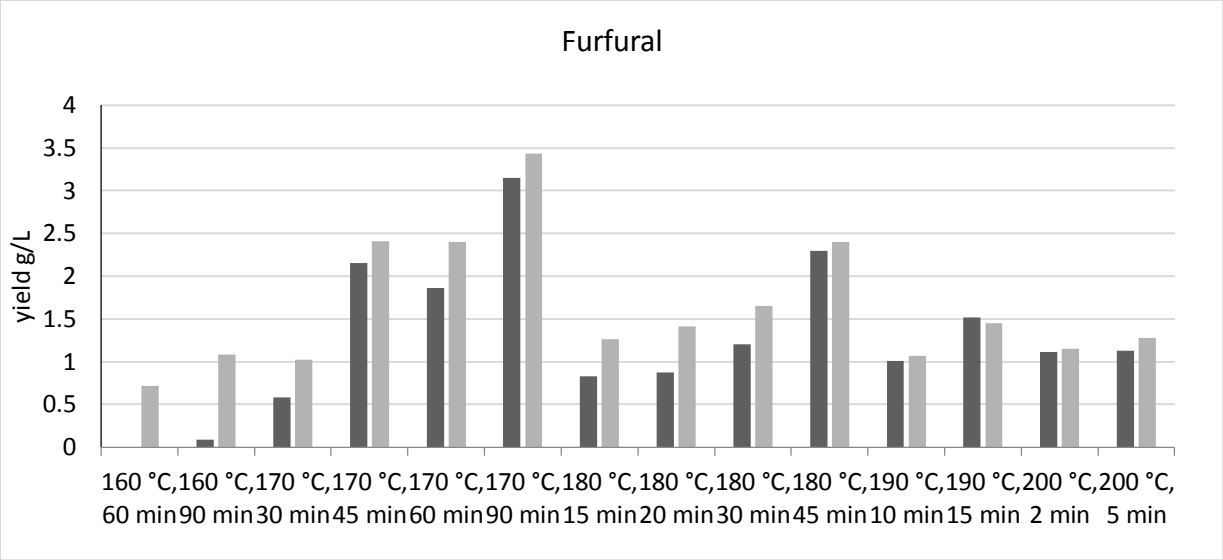
Furfural
yield g/L
4
3.5
3
2.5
2
1.5
1
0.5
0
160 °C, 60 min
160 °C, 90 min
170 °C, 30 min
170 °C, 45 min
170 °C, 60 min
170 °C, 90 min
180 °C, 15 min
180 °C, 20 min
180 °C, 30 min
180 °C, 45 min
190 °C, 10 min
190 °C, 15 min
200 °C, 2 min
200 °C, 5 min

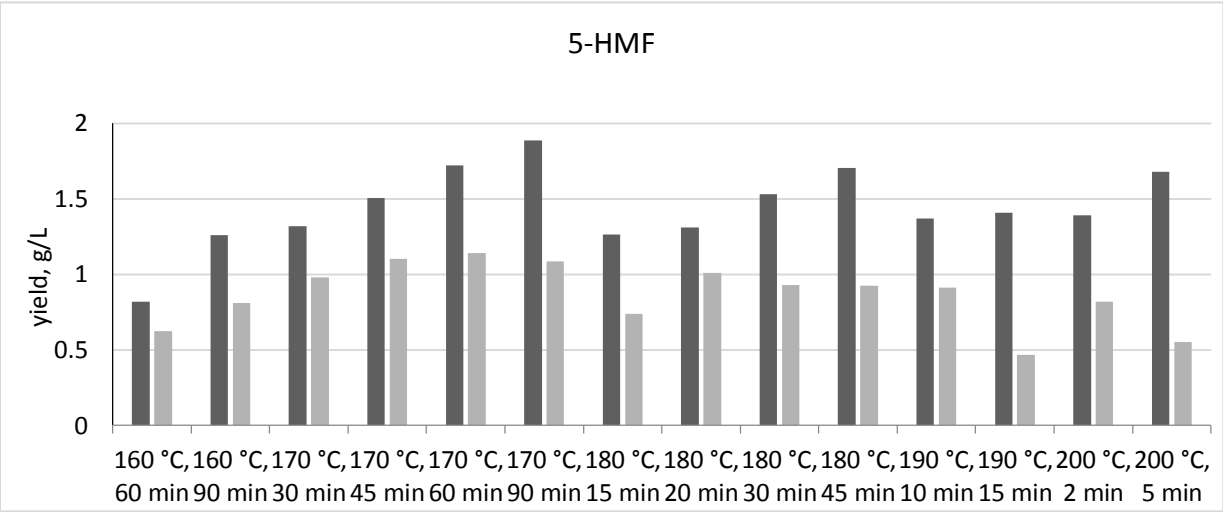
5-HMF
yield, g/L
2
1.5
1
0.5
0
160 °C, 60 min
160 °C, 90 min
170 °C, 30 min
170 °C, 45 min
170 °C, 60 min
170 °C, 90 min
180 °C, 15 min
180 °C, 20 min
180 °C, 30 min
180 °C, 45 min
190 °C, 10 min
190 °C, 15 min
200 °C, 2 min
200 °C, 5 min

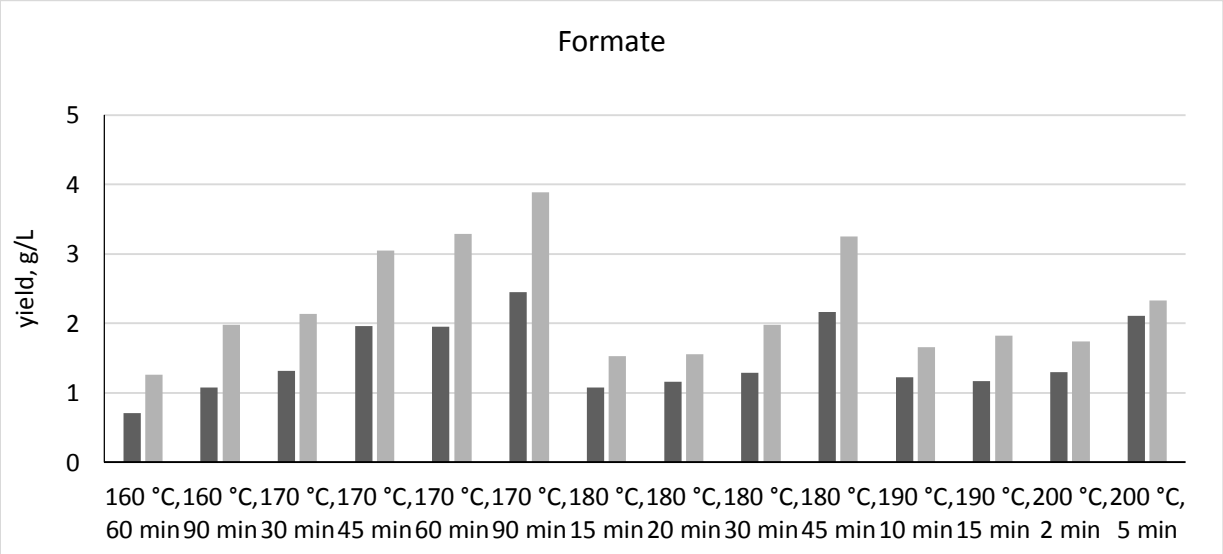
Formate
yield, g/L
5
4
3
2
1
0
160 °C, 60 min
160 °C, 90 min
170 °C, 30 min
170 °C, 45 min
170 °C, 60 min
170 °C, 90 min
180 °C, 15 min
180 °C, 20 min
180 °C, 30 min
180 °C, 45 min
190 °C, 10 min
190 °C, 15 min
200 °C, 2 min
200 °C, 5 min

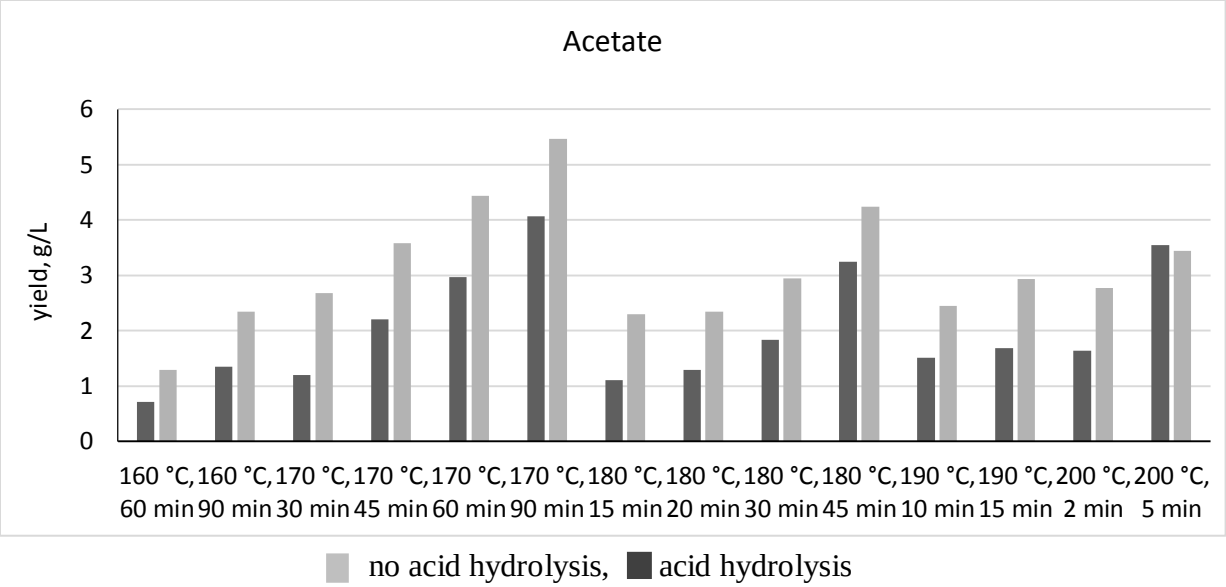


Fig.3.4 The yield of dominant liquid byproducts of 1$^{st}$SH. a, furfural; b,5-HMF; c, formate; d, acetate.

## IV. The Initialization of Two-Stage Hydrothermal Liquefaction and Its Application on upgraded biocrude oil Production from Sweet Sorghum Bagasse. Part II: 2nd stage Hydrothermal Liquefaction (HTL) and Hydrodeoxygenation (HDO)[2]


### Abstract

A temperature-gradient two-stage HTL was designed and combined with HDO process to improve both upgraded biocrude quality and carbon conversion efficiency from lignocellulosic biomass into biofuels. The 1st stage HTL (1stSH) process and result analysis were described in Part I. In this paper, WSHH process was used as control, through which HTL condition was optimized for 2nd stage HTL (2ndSH). The biocrude yield of 2ndSH from hemicellulose free sweet sorghum bagasse was 37.83 wt. %, increasing 49.53% than that with whole stage HTL (WSH) from initial sweet sorghum bagasse. After HDO, the upgraded biocrude yield from TSHH reached 41.70 wt. %, among which 95.75 wt. % was composed of hydrocarbons; 1.79 folds higher than hydrocarbon content from WSHHUB. 1-Ethenyl-3-ethyl-benzene, 2,3-dihydro-1,6-dimethyl-1H-Indene, eicosane and heptacosane were were the dominant compounds, accounting for 28% of yielded hydrocarbons. Form unit sweet sorghum bagasse, the carbon conversion of TSHH achieved 37.95%, which was 16.96% higher than WSHH. The recovered energy of TSHH was 50.67% in the form of upgraded biocrude, 19.79% higher than that from WSHH.



***Keywords***: two-stage HTL HDO, hydrocarbons, upgraded biocrude, sweet sorghum bagasse


[2] Yang Yue, Sudhagar Mani and Jim Kastner. To be submitted to Energy & Fuel

## 4.1 Introduction

Lignocellulosic biomass is a sustainable and renewable resource, well-utilized for biofuels conversion with the advantages of abundant availability and carbon neutral emission. It was estimated 10 billion tons lignocellulosic biomass harvested annually all over the world, 70% of which was from agricultural straw (Sanchez and Cardona, 2008). Sweet sorghum as a typical C4 energy crop was widely scattered in south regions of the States for syrup preparation. It has excellent characters, such as arable land uncompetitive, short growth cycle, high biomass production, wide adaptability, drought resistance, low fertilizing rates and extraordinary sugar yield (Reddy, et. al., 2005; Tesso et. al., 2005; Vasilakogou et. al., 2011). Its bagasse residue after juice extraction was rich in lignocellulose but utilized inefficiently.

HTL is a promising energy efficient thermal chemical approach, adaptable for biocrude conversion from a diversity of biomasses. Compatibility with wet biomass is one of the most obvious advantages of HTL. Sweet sorghum bagasse, which has 60-80% of moisture could be directly utilized as an appropriate herbaceous feedstock for HTL. Hydrolysis, fragmentation and repolymerization reactions occurred sequentially during HTL. The reported biocrude yield from lignocellulosic biomass was approximate 30-40 wt. % (Tymchyshyn and Xu, 2010; Song et.al., 2004; Xu and Etcheverry, 2008; Liu and Zhang, 2008; Yang et.al., 2009), which was synthetic influenced by HTL operational parameters. It was advised the most adaptable HTL temperature ranged from 300 °C to 350 °C, either below or excess above range impaired biocrude yield (Zhou et. al., 2010; , Yin et. al.,2010; Qu et. al., 2003; Sugano et.al., 2008). The utilization of alkaline catalyst could significantly suppress the formation of solid product and enhance the biocrude yield (Song et. al., 2004). Karagöze et al. employed 0.94 M $K_2CO_3$ on wood HTL and found that the biocrude yield increased from 17.8 wt. % to 33.7 wt. %, meanwhile, solid residues reduced from

42 wt. % to 4 wt. % (Karagöz et.al., 2005 (a); Karagöz et. al., 2006). Boocock (Boocock and Sherman, 2009) and Qu (Qu et al., 2003) indicated prolonged retention time suppressed biocrude yield, which was caused by the cracking of biocrude or its precursors to gasses and chars through condensation and repolymerization (Li et al., 2009). This conclusion was also confirmed by National Collaborative Research Infrastructure Strategy (NCRIS, University of Sydney, Australia) through continuous HTL process that shorter residence time with higher heating rate benefited biocrude yield (Jazrawia et. al., 2013).

Currently, one of issues on lignocellulose HTL is hemicellulose component limits biocrude yield and impairs HDO upgraded biocrude oil quality. Hemicellulose constituted around 20-40 wt. % of total biomass in agricultural residuals, but only contributed to 5.3 wt. % of biocrude; the majority HTL product of hemicellulose was aqueous compounds (42%) (Yoshida and Saka, 2006). Liu also reported cross reactions occurred between hemicellulose decomposed intermediates and lignin units, which caused solid residues through repolymerization (Liu et.al., 2013). However, few research has been reported to address above issue. In this paper, a combination of gradient-temperature two-stage HTL and HDO processes was initialized with the purposes of (i) increasing carbon conversion efficiency of biofuels from sweet sorghum bagasse; (ii) improving the quality (hydrocarbon content) of upgraded biocrude. The detailed process and result analysis of 1$^{st}$SH was introduced in Part I. This section focused on 2$^{nd}$ stage HTL HDO process, WSHH was used as control. The carbon conversion efficiency and compositional distribution of upgraded biocrude from above processes were analyzed and compared.

## 4.2 Materials and Methods

Sweet sorghum bagasse used in this study was obtained from Fort Valley State University, Fort Valley, Georgia, USA. Dichloromethane with analytical reagent, magnesium perchlorate, and

5 wt. % ruthenium on carbon (Ru/C) were all purchased from Sigma-Aldrich. Deionized water used in the experiments was prepared by our laboratory. Helium and hydrogen were obtained from Airgas Company (U.S.). The feedstock for 2$^{nd}$SH was the solid product from 1$^{st}$SH, the preparation process of which was described in Part I. This feedstock contained 46.0 wt % lignin and 42.7 wt % cellulose with negligible hemicellulose.

The stainless steel reactors utilized for both HTL and HDO reactions were Parr 4598 batch micro-stirred reactors system with maximum temperature of 500 °C and pressure of 5000 psi. The vessel capability was 100 ml. A consumable Parr Grafoil graphite gasket was used to avoid pressured gas leakage during reaction. A 4-blade impeller (0.81 dia.) powered by a magnetic stirrer (model no. A1120HC6, 1/8 hp variable speed) provided agitation with the maximum speed of 750 rpm. The vessel was heated through a ceramic fiber external jacket (700 watts), and the processes of HTL and HDO reaction were monitored with Parr Specview program. The average heating rate was 14 °C /min while the average cooling rate was 34.5 °C/min with water bath.

4.2.1 HTL and HDO procedures

In a typical HTL reaction, 5 g of dried biomass was placed into the vessel followed by the addition of 50 ml 0.94M potassium carbonate solution if necessary. Helium was used to purge and displace the air in headspace until 500 psi. The reaction was operated at the temperature of 350 °C. Whole stage HTL (WSH) was implemented firstly with dried sweet sorghum bagasse powder as feedstock to study the effects of holding time, catalyst and reducing gas on biocrude yield and components. With this propose, holding times from 15 to 60 min were estimated; hydrogen as reducing gas was also attempted; 0.94M potassium carbonate was employed. The optimum condition of WSH was applied for 2$^{nd}$SH. The operational procedures of WSH and 2$^{nd}$SH were the same as 1$^{st}$SH, described in Part I of TSHH study.

HDO reaction was immediately implemented with WSH (or 2$^{nd}$SH) liquid and solid products as substrate. HDO yield was thereby calculated based on the amount of HTL liquid and solid products. 1.5 g Ru/C was added into the vessel before HDO as catalyst for upgraded biocrude conversion. Hydrogen was used to purge the headspace under the pressure of 50 psi for 30 sec for three times and finally pressurized until 500 psi. The HDO reaction was operated at 350 °C for 4 hr with the agitation of 500 rpm. After HDO reaction, the operation procedure of products collection was the same as 1$^{st}$SH described in Part I. The collected solid and liquid samples were stored in refrigerator before separation.

4.2.2 Separation and extraction procedures

40 ml methylene chloride (DCM) solvent was added into the mixture of HTL or HTL-HDO liquid and solid products to extract solid-attached biocrude. The mixture was then filtered with vacuum filtration through Whatmann #4 90mm filter paper. The solid residue was rinsed with additional 15 ml DCM to collect residual biocrude. The rinsing solution was merged with the filtrate. The oil fraction in liquid products was extracted with DCM and decanted off from aqueous phase using a separatory funnel. 1.0 g anhydrone (magnesium perchlorate) was added into the DCM-soluble fraction to remove residual moisture. This anhydrone-biocrude oil mixture was filtered again, the harvested de-moisture oil fraction was further transferred into a round-bottomed flask for rotary evaporation in water bath of 36 °C for 60 min under the vacuum degree of 2 mm Hg. The DCM free biocrude or upgraded biocrude was then collected and weighted before storing in refrigerator.

4.2.3 HTL-HDO products instrumental analysis

The components of gas products from above HTL and HDO reactions were analyzed with GC-TCD. Major compounds in aqueous product were determined with HPLC. The elemental

composition of biocrude was measured with ultimate analysis after dichloromethane evaporation. Above analysis instruments and operation were described in Part I of this work. Moisture content was analyzed with Karl Fisher Titration.

The compositions of biocrude were analyzed with GC-MS using HP-5ms Capillary Column (30m x 0.25um x 0.25mm). The oven temperature program was initially set to 40 ℃ for 4 min; then increased to 275 ℃ with the heating rate of 5 ℃ /min and hold constantly for 5 min. The Mass Spec interface was set at 280 ℃. The inlet temperature was 260 ℃. Helium was used as carrier gas with flow rate of 0.8 mL/min and the split ratio of 50:1. Major compounds identified with GC-MS from biocrude and upgraded biocrude were quantitatively analyzed with internal standard method. Neat compounds of toluene, trimethyl benzene, pentadecane, 2-methoxy phenol and 2-cyclopenten-1-one were respectively used to estimate the mass percentage of aromatic hydrocarbons, benzenes, alkanes, phenols and cyclic ketones. DCM was used as solvent to mix the internal standard, 1-hexanol, at the concentration of 1.04 g/L and above neat compounds to calibrate standard curves with three replications. For biocrude and upgraded biocrude compositional analysis, standard stock solution was prepared immediately before GC-MS operation by adding 10 μl 1-hexanol into 800 μl DCM. After vortex, 35 μl standard stock solution was mixed with 302 μl biocrude or upgraded biocrude sample. 1 μl mixed sample solution was injected into GC-MS after filtration with 0.45 μm filter. The solvent delay was setup for 3 min for DCM. The compositions were identified by matching fragmentation patterns with NIST mass spectral library.

4.2.4 Statistical analysis

The yields and products analysis of whole stage HTL (HDO) and two stage HTL (HDO) were measured with three replications. The average data were reported as the results.

## 4.3 Results and Discussions

The operation processes of WSH-HDO and 2nd stage HTL –HDO was indicated in Fig.4.1 with mass balance as a summary and a comparison of the yields

### 4.3.1 Effects of HTL conditions on biocrude conversion

The temperature from 300 °C to 350 °C was commonly reported and considered appropriately for HTL biocrude conversion with various biomasses, including forest residues, agricultural wastes and aquatic plant (Zhou et al., 2010; Yin et al., 2010). Because of related higher cellulose and lignin contents from both sweet sorghum bagasse and 1stSH solid product, which respectively used as the feedstocks of WSH and 2ndSH, the reaction temperature of 350°C was applied for WSH and 2ndSH in this study.

Reaction time, catalyst and reducing gas were respectively estimated to study the optimum condition for biocrude conversion from sweet sorghum bagasse with WSH. Combining with reaction temperature of 350 °C, holding time from 15 to 60 min was employed to adjust WSH reaction severity. It was found alkaline salt catalysts effectively suppressed the repolymerization reaction and reduced the solid byproduct during HTL. The order of alkaline salt catalytic effect followed the sequences of $K_2CO_3 \approx Na_2CO_3 > CsCO_3 > RbCO_3$ (David and Ragauskas, 2010; Sannigrahi et al., 2010). In this study, 0.94 M $K_2CO_3$ was employed; non-catalytic WSH was used as control. The yield of catalytic WSH biocrude was listed in table 4.1. It was showed the biocrude yield notably increased 1.44 folds in the presence of $K_2CO_3$ from non-catalytic WSH. On the basis of mass balance, the increased biocrude was considered to be obtained from aqueous products, which decreased 49.0 %. This result was in according with Toor's report (Toor et al., 2011). Additionally, similar to Sugano's report (Sugano et al., 2008), a significant decrease of 58.4 % on solid product and a 2.5-fold enhancement on gas product were also observed. The remarkable

enhancement on gas yield with alkaline catalyst was resulted from alkali carbonate effect proposed by Appell (Appell et al., 1971). The dominant component of WSH gas product was $CO_2$ (table 4.2). Hydrogen repressed the formation of gas (22.5%) and solid (49.9%) products; however, from where, those unconsumed carbon in lignocellulosic biomass mainly contributed to aqueous products rather than converted into biocrude. Actually, the biocrude yield with hydrogen only increased 18.6%, much less than double, which was expected by Tymchyshyn (Tymchyshyn and Xu, 2010).

Various holding times were also estimated under helium or hydrogen atmosphere. The biocrude yield increased 46. 2% with time from 15 min to 30 min and then decreased 15.7% after 60 min. The maximum biocrude yield of 25.30% was obtained at 30 min. A prolonged retention time suppressing biocrude yield has been reported by Boocock (Boocock and Sherman, 2009) and Qu (Qu et al., 2003). The decline of biocrude with time was proposed that either biocrude or its precursors cracked into gas and char through condensation and repolymerization reactions (Li et al., 2009). Although the detailed mechanism of biocrude decomposition was still unclear, this study, to some extent, confirmed an enhancement on gas yield was caused by the extended reaction time. However, enhancements on yields of solid byproducts were not observed with time in this study. Karagöz indicated longer holding time also affected the compositions of biocrude (Karagöz et al., 2004); however, from the GC-MS analysis, the dominant compounds in biocrude were similar from 15 min to 60 min, but with some difference on quantity (table 4.4).

The elemental composition of biocrude (table 4.3) and solid product (table A1) were measured with ultimate analysis. It was indicated after 30 min, 42.6% carbon in sweet sorghum bagasse feedstock was converted into biocrude in the presence of 0.94 M $K_2CO_3$. This carbon conversion efficiency was 1.45 times higher than non-catalytic biocrude. Either shorter (15 min)

or longer (60 min) holding time impaired the carbon conversion, respectively declined 28.57% and 10.54%, mainly resulted from the reduction of biocrude yield. Those unutilized carbons were mainly converted into aqueous products, typically carboxylic acids. The higher heating value (HHV) of biocrude could be calculated based on the elemental composition by the Dulong Formula, that

$$HHV(\mathrm{MJ/kg}) = 0.3383\mathrm{C} + 1.422\,(\mathrm{H} - \mathrm{O}/8)$$

After WSH, HHVs of biocrudes ranged from 29.10 MJ/kg to 32.99 MJ/kg (table 4.3), nearly double of the sweet sorghum bagasse feedstock of 16.30 MJ/kg.

In the presence of $K_2CO_3$, O/C ratio was 0.23 from biocrude at 350 °C for 30 min and decreased with time to 0.17 after 60 min. The accumulation of carboxylic acids in aqueous phase and $CO_2$ in gas fraction was proposed to lead O/C ratio decline. However, this deoxygenation process accompanied with carbon loss and damaged the carbon conversion efficiency. The H/C ratio was almost keeping constantly from 15 min to 60 min, approximate to 1.24. Hydrogen inlet did not improve O/C and H/C ratios, which, to some extent, indicated hydrogen atmosphere alone could not effectively provide reducing power for biocrude deoxygenation.

The biocrude component of catalytic WSH was quantitatively analyzed with GC-MS. There were more than two hundred compounds identified. Cyclic ketones, phenols and hydrocarbons composed the majority, taking up to more than 90 % of total area from chromatogram. The distributions of these major compounds were quantitatively estimated and listed in table 4.4. As the dominated component, cyclic ketones accounted for 56.8~74.6 wt. % of the catalytic biocrude, mainly in the form of methylated cyclopenten-1-one. These cyclopenten-1-one derivate were primarily generated from the decomposition of hemicellulose and cellulose through one of the cardinal intermediates, 5-hydroxymethyl furfural (5-HMF), which was

dehydrated from cellulose and hemicellulose units, xylose and fructose, and further convert into cyclopenten-1-one through benzenetriol (Pińkowska et. al., 2011; Antal et. al.,1990 (a); Bonn et. al.,1985). Another minor resource of cyclopenten-1-one was reported from the decomposition of lignin unit, catechol (Sasaki and Goto, 2008). With the extension of reaction time from 15 min to 30 min, the yield of methylated cyclopenten-1-one compounds declined first; then slightly increased at 60 min. Hydrogen promoted the formation of methylated cyclohexanone derivate, probably through the reduction and re-cyclization of cyclopenten-1-one derivate compounds. However, the inlet of hydrogen was not able to reduce the yield of cyclic ketones in WSH biocrude. Phenols derivate, as the second dominated component, mostly existed in the form of alkylation, from the decomposition of both structural carbohydrates and lignin through two separated pathways. For structural carbohydrates decomposition route, similar to cyclopenten-1-one derivate compounds described above, the formation of alkylated phenols was another important branch from 5-HMF and benzenetriol (Pińkowska et. al., 2011; Antal et. al.,1990 (a); Bonn et. al.,1985). For lignin decomposition pathway, alkylated phenols could be either converted from lignin unit modification or formed through addition reaction of lignin decomposition compounds, hydroxylated phenols with C2-C6 oxides (Kang et. al., 2013). It was also observed that the yield of phenols increased with reaction time. Additional hydrogen reduced a small amount of phenols into benzenes, mainly in the form of alkylated benzene methanol. Hydrocarbons as the desirable products, however, harvested with low yield in WSH biocrude from 4.78 wt. % to 7.43 wt. %. Hydrogen did not increase the conversion of hydrocarbons. The maximum yield of hydrocarbons was 1.88 % on the basis of sweet sorghum bagasse feedstock, obtained at 30 min with 0.94 M $K_2CO_3$ as catalyst. A negligible amount of alkanes were identified at this condition. Actually, more than 68% identified hydrocarbons were in the form of aromatics in WSH biocrude. The identified

alkanes of pentadecane and heptadecane were only converted at either 15 min or 60 min with $K_2CO_3$. Fatty acids were the main compositional difference between whole stage catalytic biorude and non-catalytic biocrude. n-hexadecanoic acid and 13-octadecenoic acid were the typically dominant fatty acids only observed in non-catalytic biocrude. It was proposed that the formation of fatty acids was suppressed at high pH with the presence of $K_2CO_3$. However, due to the lack of standard fatty acid compound, the mass percentages of fatty acids in non-catalytic biocrude were not able to provide.

The major compounds yields of WSH aqueous phase were analyzed with HPLC (Fig.4.2). The pH value was one of the most significant factors that influenced the finial yields of most water soluble compounds. Generally, with the process of HTL, the C5 and C6 monomer sugars from cellulose and hemicellulose hydrolysis decomposed into short chain carboxylic acids, typically lactic acid, formic acid and acetic acid. The accumulation of carboxylic acids gradually promoted the reaction atmosphere from weak alkaline ($K_2CO_3$ added) or neutral (non-catalyst added) into weak acidic. This acidic condition inhibited the formation of lactate from pyruvaldehyde through glyceraldehyde and dihydroxyacetone, from fructose decomposition under alkaline or neutral condition (Yin and Tan, 2012). The maximum yield of lactate was 7.53 g/L, obtained at 15 min in the presence of $K_2CO_3$. This yield decreased 2.8 folds after 60 min. When $K_2CO_3$ was not added, the lactate yield reduced 11.6 times compared to catalytic yield at 30 min. The inlet of hydrogen did not show influence on lactate yield. The yield of acetate was found increasing with reaction time; the maximum yield of 13.54 g/L was measured after 60 min without $H_2$. Acetate was mainly formed from levoglucosan decomposition, which dehydrated from glucose (Kabyemela et.al., 1999; Antal et. al., 1990 (b)). The yield of acetate decreased 30% at 30 min from $K_2CO_3$ added to non-catalytic WSH. This might be caused by less carboxylic acids accumulated under neutral

condition, especially lactic acid and formic acid. The formation of formate was primarily controlled by two routes. One was 5-HMF decomposed into formic acid and levulinic acid at acidic condition; the other was glucose decomposed into erythrose, which further decomposed into formic acid through glycolaldehyde under alkaline condition (Yin and Tan, 2012). In the presence of $K_2CO_3$, above two pathways sequentially occurred with pH dropping. The formate yield, generally, indicated a trend of enhancement from 5.39 g/L to 6.43 g/L with reaction time, 2.55 folds higher than $K_2CO_3$ absence condition. Hydrogen improved the formation of formic acid, increased its yield of 23.2% after 60 min. The yields of glucose, C5 sugars (xylose and arabinose) and succinate were relevantly stable, respectively with the average yield of around 0.24 g/L, 0.16 g/L and 2.2 g/L. These low yields indicated approximately 99.4% C6 sugar from cellulose and 99.3% C5 sugars from hemicellulose were decomposed during WSH. Additionally, there was no furfural and 5-HMF detected from above reaction conditions. This was because the intermediates of furfurals and 5-HMF were reported unstable, and rapidly decomposed into carboxylic acids, humus and benzenetriols at 350 °C (Yin and Tan, 2012; Bonn et al., 1985).

4.3.2 Chemical analysis of 2$^{nd}$SH products

Based on above description, the HTL condition of 350 °C, 30 min with 0.94 M $k_2CO_3$ were considered most adaptable and applied for 2$^{nd}$SH to liquefy hemicellulose free sweet sorghum bagasse. As described in Part I, 1$^{st}$SH solid product consisted of 46.0 wt % lignin, 42.7 wt % cellulose, 2.7 wt % hemicellulose and 3.6 wt % water insoluble ash. Compared to the initial sweet sorghum bagasse sample, there were an enhancement of 18.1 % on cellulose, 1.61 folds on lignin; a decline of 86.3% on hemicellulose and no residual water soluble sugars.

The yields of 2$^{nd}$SH products were also showed in table 4.1. Compared with WSH at 350 °C for 30 min, a dramatic increase of 49.4% on biocrude indicated the hemicellulose free sorghum

was more appropriate for biocrude production with the final yield of 37.8 wt. %. This yield was higher than most of reports from pine wood (Karagöz et al., 2005 (a)), birth wood (Yang et al., 2009), sawdust (Tymchyshyn and Xu, 2010; Karagöz et al., 2005 (b)) and cornstalks (Tymchyshyn and Xu, 2010). The 2$^{nd}$SH biocrude yield increased accompanying with less aqueous byproducts, which reduced 44.3 % from WSH. Additionally, the observation of slight enhancement on solid yield of 2$^{nd}$SH from WSH indicated the employment of 0.94 M $K_2CO_3$ had successfully prevented the repolymerization reaction between hemicellulose decomposition intermediates and lignin unit derivate.

The elemental analysis of 2$^{nd}$SH biocrude was listed in table 4.3. According to Dulong Formula above, the HHV of 2$^{nd}$SH biocrude was 35.80 MJ/kg, which respectively increased 19.45 % from the WSH biocrude, and 1.20 folds from the initial sweet sorghum bagasse. The O/C and H/C ratios of 2$^{nd}$SH biocrude were respectively 0.11 and 1.27. Compared to the O/C and H/C ratios of 0.23 and 1.25 from WSH biocrude, hemicellulose free sorghum feedstock benefited the biocrude deoxygenation on 52.2%, but with a slight improvement on H/C ratio.

The components of 2$^{nd}$SH biocrude were analyzed with GC-MS and also compared with WSH biocrude under the same reaction condition (table 4.5). Ketones and phenols compounds constituted the majority of 2$^{nd}$SH biocrude, respectively accounted for 44.3 wt. % and 46.5 wt. %. The cyclic ketones content reduced 48.6% compared to WSH biocrude due to the 1$^{st}$SH pretreatment, in which process, 94.1% hemicellulose and 49.3% cellulose were removed in the form of C5 and C6 sugars stream (Part I). Methylated 2-Cyclopenten-1-one was still the representational ketone compound; its formation pathway was described above in 3.3. The content of phenols increased 29.9% from WSH biocrude, which could benefit downstream upgraded process. 82.9% of phenols were in the form of alkylation, and its distribution was quite similar

with WSH biocrude. Hydrocarbons content slightly increased; small fractions of benzenes were detected. Basically, there is no remarkable difference on biocrude distribution after hemicellulose removal, which indicated hemicellulose did not influence much on biocrude composition.

From table 4.1, a remarkable decline of 44.3 % occurred on the yield of 2$^{nd}$SH aqueous products. The HPLC analysis of 2$^{nd}$SH aqueous compounds indicated this decline was resulted from the reduction of carboxylic acids, typically succinate, lactate, formate and acetate, which respectively decreased 97.9%, 55.2%, 30.6% and 41.8% (Fig.4.3). The removal of hemicellulose crucially suppressed the formation of carboxylic acids with the total difference of 11.72 g/L.

4.3.3 Chemical analysis of products from WSHH and TSHH

The yields of WSHH and TSHH products were listed in table 4.1. Compared to WSHH, TSHH indicated remarkable enhancement of 49.9% on upgraded biocrude; meanwhile, aqueous fraction decreased 46.2%. The gas yields from both HDO processes were comparative. It was also observed TSHH solid product increased 85.0% in the form of coke and tar, attaching on the surface of Ru/C, which mainly formed through polymerization during the reduction process of ketones and phenols into hydrocarbons in upgraded biocrude.

The gas components analysis of HDO were implemented with GC-TCD and listed in table 4.2. There was 34.2% initial hydrogen consumed as hydrogen donor in TSHH process, 17.8% higher than whole stage HTL HDO. $CH_4$ contents were notably increased after HDO reactions because of the hydrogenation of cracked branched carbon from methylated phenols and cyclopentens (Furimsky 2000); respective increased 15.23 and 8.36 times compared to WSH and 2$^{nd}$SH. However, ethane, a minor phenols catalytic HDO product, formed from branch on alkylated benzenes (Furimsky 2000), was not identified with GC-TCD.

The elemental compositions of HDO upgraded biocrude (table 4.3) indicated oxygen content respectively reduced 29.0% from WSH biocrude and 2.74% from 2$^{nd}$SH biocrude. The O/C and H/C ratios of both upgraded bio-oils were approximate to petroleum, in accordance with Mortensen's report (Mortensen, et al. 2011). The HHVs of upgraded biocrudes were calculated with Dulong Formula of 38.76 MJ/kg (WSHHB) and 38.90 MJ/kg (TSHHUB), which were nearly 7.4% lower than Mortensen's report (Mortensen, et al. 2011). Analysis with Karl Fischer titration, the moisture contents of upgraded bio-oil were 0.48% after WSHH and 0.41% after TSHH, respectively reduced 84% and 73% from WSH biocrude and TSH biocrude.

The major compounds of upgraded biocrude were indicated in table 4.6. After HDO, the desirable product of hydrocarbons respectively accounted for 34.3% and 95.8% of the whole stage and two stage HDO upgraded biocrudes, which separately increased 3.62 and 10.68 folds of their proportions in HTL biocrude. Aromatic hydrocarbon was the dominant component, around twice as much as alkanes. It was also successfully confirmed that after removal of hemicellulose, the 2$^{nd}$SH biocrude was more favored for hydrocarbon conversion because phenols were concentrated 1.26 folds and ketones content declined 21.9%. Almost all ketones and phenols in two stage HTL biocrude were converted into hydrocarbons. Theoretically, with sufficient reducing donor, straight ketones such as 2-butanone and 2-pentanone could firstly form into alcohols through hydrogenation and further removed oxygen into saturated alkanes. Methylated 2-cyclopenten-1-one compounds, which accounted for around 50% of HTL biocrude, could either be deoxygenated firstly into cyclopentene, or hydrogenated into cyclopentanone and further reduced into cyclopentane. However, on the basis of GC-MS results, only 1,2,3-trimethyl-cyclopentene, and ethylidenecyclobutane were identified from TSHHUB with the contents of 0.39% and 2.15% respectively. Therefore, it was indicated majority 2-cyclopenten-1-one derivate underwent an

addition reaction route; through reduction, cyclization with phenols and finally converted into polycyclic aromatic hydrocarbons, which accounted for 49.3 % of aromatic hydrocarbons. As to the WSHH, 31.1 % methylated 2-cyclopenten-1-one derivate were hydrogenated from WSH biocrude in the form of cyclopentanone. The alkylated phenols derivate could experience dehydroxylation, demethylation and saturation to form aromatic hydrocarbons during HDO (Furimsky 2000). 1-Ethenyl-3-ethyl-benzene was the represented compound in TSHHUB, accounting for 7.38%. Around 10.9 % of WSHHUP and 28.7 % of TSHHUB were composed of long chain alkanes, ranging from C12 to C27. Rather than formed from fatty acids decarboxylation, which was not detected from catalytic WSH biocrude, it was proposed those long chain alkanes were formed from ring crack of aromatic hydrocarbons.

The major compounds in HDO aqueous products were indicated in Fig.4.4. Sugars and their primary intermediates (5-HMF and furfural) were detected with small amounts, ranging from 0.14 to 0.26 g/L. Carboxylic acids were still the dominant compounds. The yields of succinate, lactate, formate and acetate from TSHH were respectively 1.23 g/L, 1.32 g/L, 6.48 g/L and 8.03 g/L, reduced 15.1% ~48.3% compared to WSHH. This was not only because less carboxylic acid produced in 2$^{nd}$SH aqueous phase, but also resulted from less alkylated cyclopenten compounds formation from hemicellulose free feedstock, which reduced into aromatic hydrocarbons and carboxylic acids through decarbonylation during catalytic HDO. It was also indicated after HDO process, the formate concentrations respectively increased 1.08 and 0.55 folds from whole stage and two stage HTL, whereas, acetate concentrations did not show remarkable enhancement. This was proposed that the radical carboxyl from deoxygenation crack were more likely to form formate in aqueous phase rather than polymeric carbon carboxylic acids.

## 4.4 Conclusion

The combination of gradient-temperature two-stage HTL and HDO processes was successfully initialized and conducted in this study. The carbon conversion efficiency and upgraded biocrude quality were both improved. From unit sweet sorghum bagasse, the carbon conversion efficiency of WSHHUB was 32.14% with the energy recovery of 42.30%. Although it appeared the carbon conversion efficiency of TSHHUB only achieved 21.63% with the energy recovery of 27.02% from 42.1% of carbon in initial unit sweet sorghum bagasse; the remaining 57.9% of carbon contributed on the formation of C5 and C6 sugars stream with the yield of 28.14 g/L during 1$^{st}$SH. If this sugar stream was co-fermented into bioethanol, the estimated bioethanol practical yield was 45.9 % (Krishnan et al., 1999), which equaled to another 16.32% of carbon from unit sweet sorghum bagasse converting into biofuels. Therefore, the total carbon conversion of TSHH process could achieve 37.95%, 16.96% higher than WSHH. The recovered energy of TSHH was also estimated to be 50.67% (HHVs of ethanol was 29.85 MJ/kg (http://cta.ornl.gov/bedb/appendix_a/Lower_and_Higher_Heating_Values_of_Gas_Liquid_and_Solid_Fuels.pdf)), 19.79% higher than that from WSHH. On the aspect of biocrude quality, 95.75 wt. % of TSHHUB was composed of hydrocarbons, 1.79 folds higher than hydrocarbon content in WSHHUB. Above results confirmed hemicellulose was more adaptable for C5 sugar hydrolysis rather than biocrude conversion through HTL. The application of TSHH process benefited biofuels conversion from lignocellulosic biomass and laid a foundation for future HTL- HDO research.

References

Antal MJJ, Mok WSL, Richards GN. 1990 (a). Mechanism of formation of 5-(hydroxymethyl)-2-furaldehyde from D–fructose and sucrose. Carbohydr. Res. 199, 91–109.

Antal MJJ, Mok WSL, Richards GN. 1990 (b). Four-carbon model compounds for the reactions of sugars in water at high temperature. Carbohydr. Res. 199, 111–15.

Appell, HR, Fu YC, Friedman S, Yavorsky PM, Wender, I. 1971. Converting organic wastes to oil: replenishable energy source; Report No. 203669, Pittsburgh Energy Research Center, U.S. Bureau of Mines; U.S. Government Printing Office: Washington, DC.

Bonn G, Rinderer M, Bobleter O. 1985. Hydrothermal degradation and kinetic studies of 1, 3-dihydroxy-2-propanone and 2, 3-dihydroxypropanal. J. Carbohydr. Chem. 4, 67–77.

Boocock DGB, Sherman KM. 2009. Further aspects of powdered poplar wood liquefaction by aqueous pyrolysis. Can. J. Chem. Eng. 63, 627–33.

David K, Ragauskas AJ. 2010. Switchgrass as an energy crop for biofuel production: a review of its lignocellulosic chemical properties. Engr. Environ. Sci. 3, 1182–90.

Furimsky, E. 2000. Catalytic hydrodeoxygenation. Appl. Catal., A 199, 147-190.

Jazrawia C., Billerb P., Rossb A.B., Montoyaa A., Maschmeyerc T., Haynes B.S. 2013. Pilot plant testing of continuous hydrothermal liquefaction of microalgae. Algal Res. 2, 268-277.

Kabyemela B, Adschiri T, Malaluan R, Arai K. 1999. Glucose and fructose decomposition in subcritical and supercritical water: Detailed reaction pathway, mechanisms, and kinetics. Ind. Eng. Chem. Res. 38, 2888–95.

Kang S, et al. 2013. Hydrothermal conversion of lignin: A review. Renew. Sust. Energ. Rev. 27, 546-58.

Karagöz S, Bhaskar T, Muto A, Sakata Y, Uddin MA. 2004. Low-temperature hydrothermal treatment of biomass: effect of reaction parameters on products and boiling point distributions. Energy Fuels. 18, 234–41.

Karagöz S, Bhaskar T, Muto A, Sakata Y, Oshiki T, Kishimoto, T. 2005 (a). Low-temperature catalytic hydrothermal treatment of wood biomass: analysis of liquid products. Chem. Eng. J. 108,127–37.

Karagöz S, Bhaskar T, Muto A, Sakata Y. 2005 (b). Comparative studies of oil compositions produced from sawdust, rice husk, lignin and cellulose by hydrothermal treatment. Fuel. 84, 875-84.

Karagöz S, Bhaskar T, Muto A, Sakata Y. 2006. Hydrothermal upgrading of biomass: Effect of $K_2CO_3$ concentration and biomass/water ratio on products distribution. Bioresour. Technol. 97, 90–98.

Krishnan MS, Ho NW, Tsao GT. 1999. Fermentation kinetics of ethanol production from glucose and xylose by recombinant Saccharomyces 1400 (pLNH33). Appl Biochem Biotechnol, 77–79, 373–88.

Li H, Yuan X, Zeng G. 2009. Liquefaction of rice straw in sub- and supercritical 1, 4-dioxane-water mixture. Fuel Process. Technol. 90, 657-63.

Liu HM, Li MF, Yang S, Sun RC. 2013. Understanding the Mechanism of Cypress Liquefaction in Hot-Compressed Water through Characterization of Solid Residues. Energies.6, 1590-1603.

Liu Z, Zhang FS. 2008. Effects of various solvents on the liquefaction of biomass to produce fuels and chemical feedstocks. Energy Convers. Manage. 49, 3498-504

Mortensen PM, et al. 2011. A review of catalytic upgrading of bio-oil to engine fuels. Appl. Catal. A- Gen. 407, 1-19.

Qu Y, Wei X, Zhong C. 2003. Experimental study on the direct liquefaction of Cunninghamia lanceolata in water. Energy. 28, 597–606.

Reddy, B.V.S., et al. 2005. Sweet sorghum: A potential alternate raw material for bio-ethanol and bio-energy. Intl. Sorghum and Millets Newsletter 46:79-86.

Sanchez, O.J. and Cardona, C.A. 2008. Trends in biotechnological production of fuel ethanol from different feedstocks. Bioresour. Technol., 99, 5270–5295.

Sannigrahi P, Ragauskas AJ, Tuskan GA. 2010. Poplar as a feedstock for biofuels: a review of compositional characteristics, biofuels. Biofuels, Bioprod. Bioref. 4, 209–26.

Sasaki W.M. and Goto M. 2008. Recovery of phenolic compounds through the decomposition of lignin in near, and supercritical water. Chem Eng Process. 47, 1609–1619

Song C., Hu H., Zhu S., Wang G., Chen G. 2004. Nonisothermal catalytic liquefaction of corn stalk in subcritical and supercritical water. Energ. Fuel. 18, 90-96.

Sugano M, Takagi H, Hirano K, Mashimo K. 2008. Hydrothermal liquefaction of plantation biomass with two kinds of wastewater from paper industry. J. Mater. Sci. 43, 2476–86.

Tesso, T.T, Claflin, L.E., Tuinstra, M.R. 2005. Analysis of stalk rot resistance and genetic diversity among drought-tolerant sorghum genotypes. Crop Sci.45, 645-652.

Toor, S. S., et al. 2011. Hydrothermal liquefaction of biomass: A review of subcritical water technologies. Energy. 36, 2328-2342.

Tymchyshyn M, Xu C. 2010. Liquefaction of bio-mass in hot-compressed water for the production of phenolic compounds. BioResources. 101, 2483–90

Vasilakogou, I., Dhiam, K., Karagiannidis, N., Gatsis, T. 2011. Sweet sorghum productivity for biofuel under increased soil salinity and reduced irrigation. Field Crop Res. 120, 38-46.

Xu C., Etcheverry T. 2008. Hydro-liquefaction of woody biomass in sub- and super-critical ethanol with iron-based catalysts. Fuel. 87, 335-45.

Yang Y, et al. 2009. Production of bio-crude from forestry waste by hydro-liquefaction in sub-/super-critical methanol [electronic resource]. AIChE J. 55, 807-19.

Yin S, Dolan R, Harris M, Tan Z. 2010. Subcritical hydrothermal liquefaction of cattle manure to bio-oil: effect of conversion parameters on bio-oil yield and characterization of bio-oil. Bioresour. Technol. 101, 3657–64.

Yin S, Tan Z. 2012. Hydrothermal liquefaction of cellulose to bio-oil under acidic, neutral and alkaline conditions. Appl. Energy. 92, 234-9.

Yoshida K, Saka S. Organic acid production from Japanese beech by supercritical water treatment. In: The 2nd Joint International Conference on Sustainable Energy and Environment. C-032, Thailand; 2006. p. 1–6, 22.02.2010.

Zhou D, Zhang L, Zhang S, Fu H, Chen J. 2010. Hydrothermal liquefaction of Macroalgae Enteromorpha prolifera to bio-oil. Energy Fuels. 24, 4054–61.

Table 4.1. Reaction conditions and yields of HTL and HDO

| Reaction conditions | | | | | | | | |
|---|---|---|---|---|---|---|---|---|
| WSH[a] | | | | | | 2[nd]SH[b] | WSHH[c] | TSHH[d] |
| Catalyst | 0.94M $K_2CO_3$ | | | | Non-catalyst | 0.94M $K_2CO_3$ | 5% Ru/C | 5% Ru/C |
| Gas inlet[**] | He | | | $H_2$ | He | He | $H_2$ | $H_2$ |
| Time /min | 15 | 30 | 60 | 60 | 30 | 30 | 240 | 240 |
| Agitation /rpm | 300 | 300 | 300 | 500 | 300 | 300 | 500 | 500 |
| Yields / wt. % | | | | | | | | |
| Gas | 9.33 | 36.03 | 41.30 | 32.00 | 11.00 | 36.90 | 34.76 | 32.91 |
| Solid | 8.03 | 6.67 | 5.33 | 2.67 | 15.89 | 7.47 | 4.01 | 7.42 |
| (Upgraded) | 17.30 | 25.30 | 21.33 | 25.30 | 10.38 | 37.83 | 27.81 | 41.70 |
| Bio-oil | | | | | | | | |
| Aqueous | 65.34 | 32.00 | 32.04 | 40.03 | 62.80 | 17.83 | 33.42 | 17.97 |

Note: a, yield of WSH was calculated on the basis of dried sweet sorghum bagasse powder; b, yield of 2[nd]SH was calculated on the basis of 1[st]SH solid product; c, yield of WSHH was calculated on the basis of solid and liquid products from WSH; d, yield of TSHH was calculated on the basis of solid and liquid products from 2[nd]SH.

Table 4.2. Gas product components of HTL and HDO reactions

| Reactions | WSH | | | | | 2nd SH | WSHH | TSHH |
|---|---|---|---|---|---|---|---|---|
| catalyst | 0.94 M $K_2CO_3$ | | | | Non-catalyst | 0.94 M $K_2CO_3$ | 5 % Ru/C | 5 % Ru/C |
| Gas inlet** | He | | | $H_2$ | He | He | $H_2$ | $H_2$ |
| Time /min | 15 | 30 | 60 | 60 | 30 | 30 | 240 | 240 |
| | Gas product components % (v/v) | | | | | | | |
| $CO_2$ | 98.22 (3.71) | 98.53 (2.09) | 98.61 (3.33) | 98.60 (6.01) | 94.14 (4.01) | 96.67 (0.24) | 77.61 (0.87) | 72.15 (1.03) |
| CO | 0.56 (0.03) | - | - | - | 5.43 (0.16) | - | - | - |
| $CH_4$ | 1.22 (0.01) | 1.47 (0.13) | 1.39 1(0.29) | 1.40 (0.27) | 0.43 (0.01) | 3.33 (0.24) | 22.39 (0.24) | 27.85 (0.81) |
| $H_2$ consumption | | | | - | | | 29.05 (3.20) | 34.22 (2.54) |

Table 4.3. Ultimate analysis and HHVs of biocrude and upgraded biocrude

| | WSH | | | | | 2nd SH | WSHH | TSHH | Benchmark |
|---|---|---|---|---|---|---|---|---|---|
| Catalyst | 0.94M $K_2CO_3$ | | | | Non-catalyst | 0.94 M $K_2CO_3$ | 5 % Ru/C | 5 % Ru/C | Petroleum (Mortensen et al., 2011) |
| Gas inlet** | He | | | $H_2$ | He | He | $H_2$ | $H_2$ | |
| Time /min | 15 | 30 | 60 | 60 | 30 | 30 | 240 | 240 | |
| C [wt.%] | 72.81 (0.25) | 69.62 (0.34) | 73.96 (0.41) | 74.52 (0.10) | 69.13 (0.29) | 79.30 (0.53) | 74.62 (2.12) | 78.93 (2.48) | 83~86 |
| H [wt.%] | 7.46 (0.02) | 7.24 (0.01) | 7.66 (0.08) | 7.57 (0.01) | 6.86 (0.06) | 8.37 (0.06) | 9.06 (0.31) | 9.11 (0.20) | 11~14 |
| N [wt.%] | 1.36 (0.06) | 1.35 (0.02) | 1.30 (0.02) | 1.12 (0.01) | 1.24 (0.02) | 0.63 (0.03) | 0.84 (0.02) | 0.58 (0.03) | <1 |
| O [wt.%] | 18.38 (0.24) | 21.79 (0.33) | 17.08 (0.49) | 16.79 (0.11) | 22.73 (0.33) | 11.70 (0.54) | 15.48 (1.91) | 11.38 (2.71) | <1 |
| O/C | 0.19 | 0.23 | 0.17 | 0.17 | 0.25 | 0.11 | 0.16 | 0.11 | ≈0 |
| H/C | 1.23 | 1.25 | 1.24 | 1.22 | 1.19 | 1.27 | 1.46 | 1.38 | 1.5-2.0 |
| HHVs [MJ/kg] | 31.97 | 29.97 | 32.88 | 32.99 | 29.10 | 35.80 | 38.76 | 38.90 | 44 |

Table 4.4. Major compounds distribution in biocrude from WSH

| Catalytic whole stage HTL condition | | | | |
|---|---|---|---|---|
| Gas inlet** | He | | | $H_2$ |
| Time /min | 15 | 30 | 60 | 60 |
| Compounds | Mass % | | | |
| *Cyclic ketones* | *74.57* | *56.75* | *58.48* | *60.29* |
| Cyclopentanone, 2,5-dimethyl- | 4.23 | 2.78 | 4.72 | 6.00 |
| 2-Cyclopenten-1-one, 2,3-dimethyl- | 5.11 | 2.51 | 1.64 | 1.37 |
| 2-Cyclopenten-1-one, 2,3,4-trimethyl- | 31.57 | 21.95 | 15.72 | 17.03 |
| 2-Cyclopenten-1-one, 2,3,4,5-tetramethyl- | 33.66 | 29.51 | 36.40 | 32.44 |
| Cyclohexanone derivate | | | | 3.44 |
| *Phenols* | *18.62* | *35.83* | *35.30* | *32.35* |
| Phenol | 0.88 | 1.66 | | |
| Phenol, 2-methyl- | 0.00 | 2.43 | 0.99 | |
| Phenol, 4-methyl- | 3.21 | 5.21 | 3.06 | 3.12 |
| Phenol, 2,4-dimethyl- | | | 13.59 | 12.22 |
| Phenol, 3,5-dimethyl- | 8.54 | 10.65 | | 1.65 |
| Phenol, 2-ethyl-4-methyl- | 1.84 | 1.46 | 2.16 | 2.44 |
| Phenol, 2-ethyl-5-methyl- | | 3.38 | | 4.55 |
| Phenol, 4-ethyl-3-methyl- | | | 4.05 | 1.40 |
| Phenol, 2-methyl-5-(1-methylethyl)- | 1.29 | 2.52 | | |
| Thymol | | | 3.67 | |

| | | | | |
|---|---|---|---|---|
| Methoxy phenols | | 8.51 | 7.78 | 6.97 |
| | 2.86 | | | |
| | *6.81* | *7.43* | *6.22* | *4.78* |
| *Hydrocarbons* | | | | |
| *Aromatic hydrocarbons* | | 7.43 | 5.07 | 4.78 |
| | 4.61 | | | |
| | 0.93 | | | |
| 1,3-Dimethyl-1-cyclohexene | | | | |
| | 0.65 | 1.21 | 0.55 | |
| Toluene | | | | |
| | 2.22 | 1.32 | 2.24 | 0.76 |
| 1H-Indene, 2,3-dimethyl- | | | | |
| | | 4.05 | 1.56 | |
| 1H-Indene, 2,3-dihydro-1,6-dimethyl- | | | | |
| | | | | 1.43 |
| Naphthalene, 1,2-dihydro-2-methyl- | | | | |
| | | | | 0.74 |
| Benzene, 1-methyl-4-(1-methyl-2-propenyl)- | | | | |
| Cyclopropane, 1,1,2-trimethyl-3-(2-methyl-1- | | | | |
| propenyl)- | | | | 0.79 |
| | | | | 0.74 |
| Benzene, 1-methyl-4-(1-methyl-2-propenyl)- | | | | |
| | | 0.85 | 0.71 | 1.06 |
| Other aromatic hydrocarbons | 0.81 | | | |
| *Alkanes* | *2.20* | | *1.15* | |
| | 1.20 | | 0.72 | |
| Pentadecane | | | | |
| | 1.00 | | 0.43 | |
| Heptadecane | | | | |
| | | | | 2.58 |
| *Benzenes* | | | | |
| | | | | 1.66 |
| Benzenemethanol, 4-(1,1-dimethylethyl)- | | | | |
| | | | | 0.92 |
| Other benzenes | | | | |

Table 4.5. The comparison of major compounds in biocrudes from WSH and 2ndSH

| Compounds | WSH | 2ndSH |
|---|---|---|
| | Mass % | |
| *Straight ketones* | | *6.11* |
| 2-Butanone | | 4.82 |
| 2-Pentanone | | 1.29 |
| *Cyclic ketones* | *56.75* | *38.19* |
| Cyclopentanone, 2-methyl- | | 2.74 |
| Cyclopentanone, 2,5-dimethyl- | | 3.70 |
| 2-Cyclopenten-1-one, 2,3-dimethyl- | 2.78<br>2.51 | 4.33 |
| 2-Cyclopenten-1-one, 2,3,4-trimethyl- | 21.95 | 10.59 |
| 2-Cyclopenten-1-one, 3,4,4-trimethyl- | | 7.20 |
| 2-Cyclopenten-1-one, 2,3,4,5-tetramethyl- | 29.51 | 9.64 |
| *phenols* | *35.83* | *46.53* |
| Phenol | 1.66 | 3.03 |
| Phenol, 2-methyl- | 2.43 | 2.97 |
| Phenol, 4-methyl- | 5.21 | 5.00 |
| Phenol, 4-ethyl- | 0.98 | 2.77 |
| Phenol, 2,4-dimethyl- | 10.65 | 10.09 |
| Phenol, 2,4,6-trimethyl- | | 5.34 |
| Phenol, 2-ethyl-5-methyl- | 3.38 | 2.61 |
| Phenol, 2-methyl-5-(1-methylethyl)- | 2.52 | |
| 1,3-Benzenediol, 4,5-dimethyl- | 3.64 | 1.01 |

| | | |
|---|---|---|
| 1,4-Benzenediol, 2,3,5-trimethyl- | 1.46 | 2.49 |
| Others phenols | 4.87 | 11.22 |
| *hydrocarbons* | *7.43* | *8.20* |
| Toluene | 1.21 | |
| Cyclohexene | | 1.15 |
| 1H-Indene, 1,3-dimethyl- | 1.32 | 0.86 |
| 1H-Indene, 2,3-dimethyl- | | 1.96 |
| 1H-Indene, 2,3-dihydro-1,6-dimethyl- | 4.05 | 0.37 |
| 1H-Indene,2,3-dihydro-2,2-dimethyl- | | 1.15 |
| Other hydrocarbons | 0.85 | 2.71 |
| *Benzenes* | *0* | *0.97* |

Table 4.6. The comparison of major compounds in upgraded biocrudes from WSHH and TSHH

| Compounds | WSHH | TSHH |
|---|---|---|
| | Mass % | |
| *Ketones* | *25.50* | *0* |
| 2-Butanone | 10.22 | |
| Cyclopentanone, 2-methyl | 8.09 | |
| Cyclopentanone, 1-ethyl-2-methyl | 7.19 | |
| *Phenols* | *40.17* | *4.25* |
| phenol | 3.52 | |
| Phenol, 2-methyl | 4.81 | |
| Phenol, 3-methyl | 7.57 | 0.51 |
| Phenol, 2,5-dimethyl | 8.75 | 2.35 |
| Phenol, 2-ethyl-5-methyl | 4.25 | |
| Phenol, 4-ethyl | 7.73 | |
| Phenol, 2-propyl | 3.54 | |
| Phenol, 2,3,5-trimethyl- | | 1.38 |
| *Hydrocarbons* | *34.33* | *95.75* |
| *Aromatic hydrocarbons* | *23.43* | *61.53* |
| Toluene | 4.69 | 2.50 |
| Xylene | 2.35 | 1.94 |
| Ethylbenzene | 4.71 | 1.75 |
| Cyclohexene | | 2.97 |

| | | |
|---|---|---|
| Benzene, 1-ethenyl-3-ethyl | 4.17 | 7.38 |
| Benzene, 2-butenyl | 3.74 | 0.60 |
| Indane | 3.77 | |
| Benzene, 1-ethenyl-4-ethyl- | | 3.25 |
| Naphthalene | | 3.83 |
| Benzene, (2-methyl-1-butenyl)- | | 3.80 |
| 1H-Indene, 2,3-dihydro-1,6-dimethyl- | | 7.31 |
| 1H-Indene,2,3-dihydro-2,2-dimethyl- | | 3.84 |
| Naphthalene, 2-methyl- | | 3.95 |
| Other aromatic hydrocarbons | | 23.93 |
| *Alkanes* | *10.90* | *34.22* |
| Pentadecane | 2.93 | 2.30 |
| Heptadecane | 3.41 | 1.39 |
| Eicosane | | 6.50 |
| Heptacosane | | 5.30 |
| Octadecane | | 2.40 |
| Tetracosane | 2.63 | 2.02 |
| 9-octyl-heptadecane | 1.93 | |
| Tridecane | | 1.84 |
| Other alkanes | | 6.95 |

a.

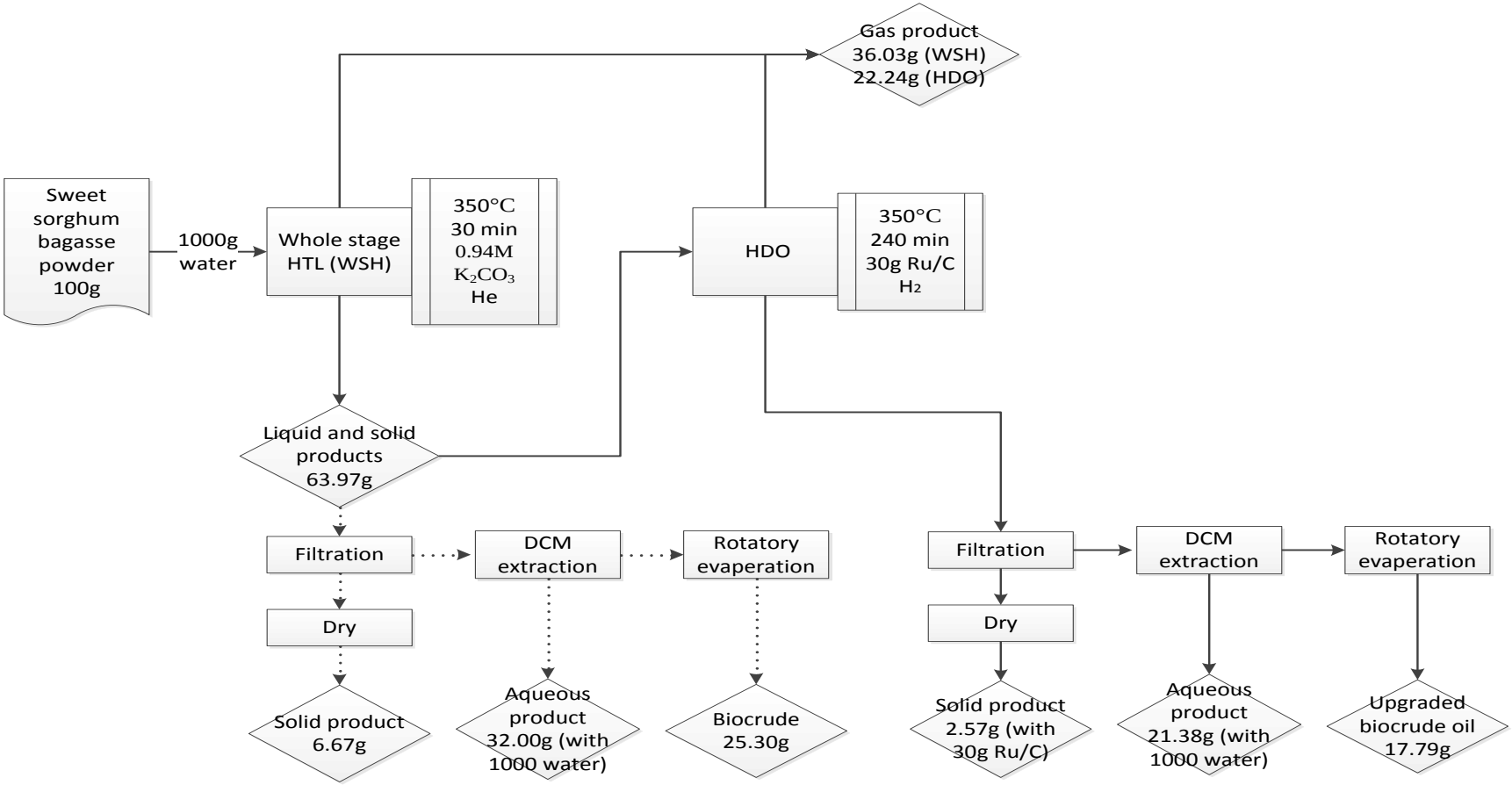
Gas product
36.03g (WSH)
22.24g (HDO)
Sweet sorghum bagasse powder 100g
1000g water
Whole stage HTL (WSH)
350°C
30 min
0.94M
$K_2CO_3$
He
HDO
350°C
240 min
30g Ru/C
$H_2$
Liquid and solid products 63.97g
Filtration
DCM extraction
Rotatory evaperation
Dry
Solid product 6.67g
Aqueous product 32.00g (with 1000 water)
Biocrude 25.30g
Filtration
DCM extraction
Rotatory evaperation
Dry
Solid product 2.57g (with 30g Ru/C)
Aqueous product 21.38g (with 1000 water)
Upgraded biocrude oil 17.79g

b.

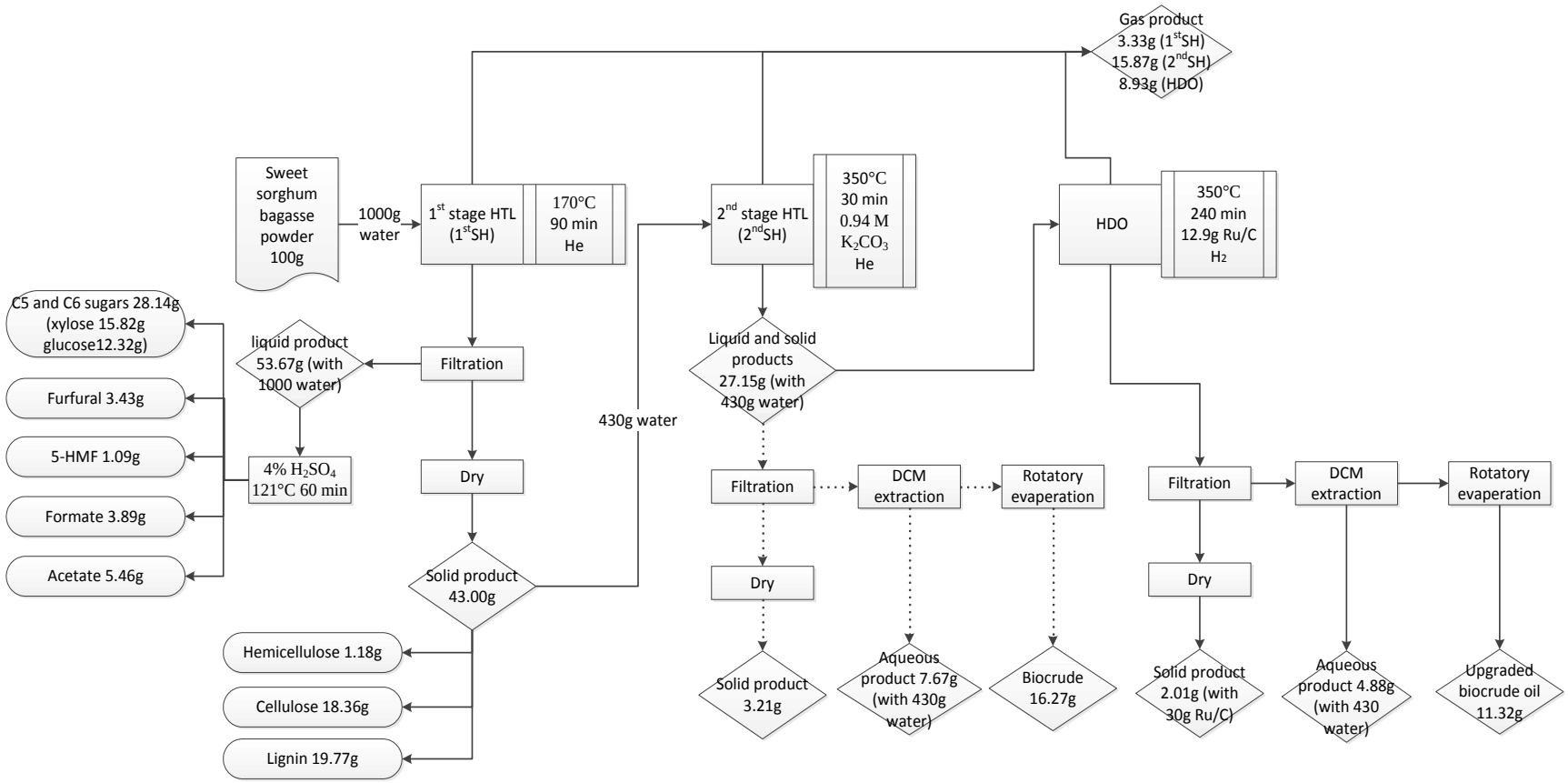


Fig.4.1 Scheme of whole stage HTL-HDO and two stage HTL-HDO processes. a, whole stage HTL HDO process; b, two stage HTL HDO process

Note: dash line indicated the separation and analysis processes of whole stage HTL, if HDO was implemented after HTL, the dash line fraction was not operated

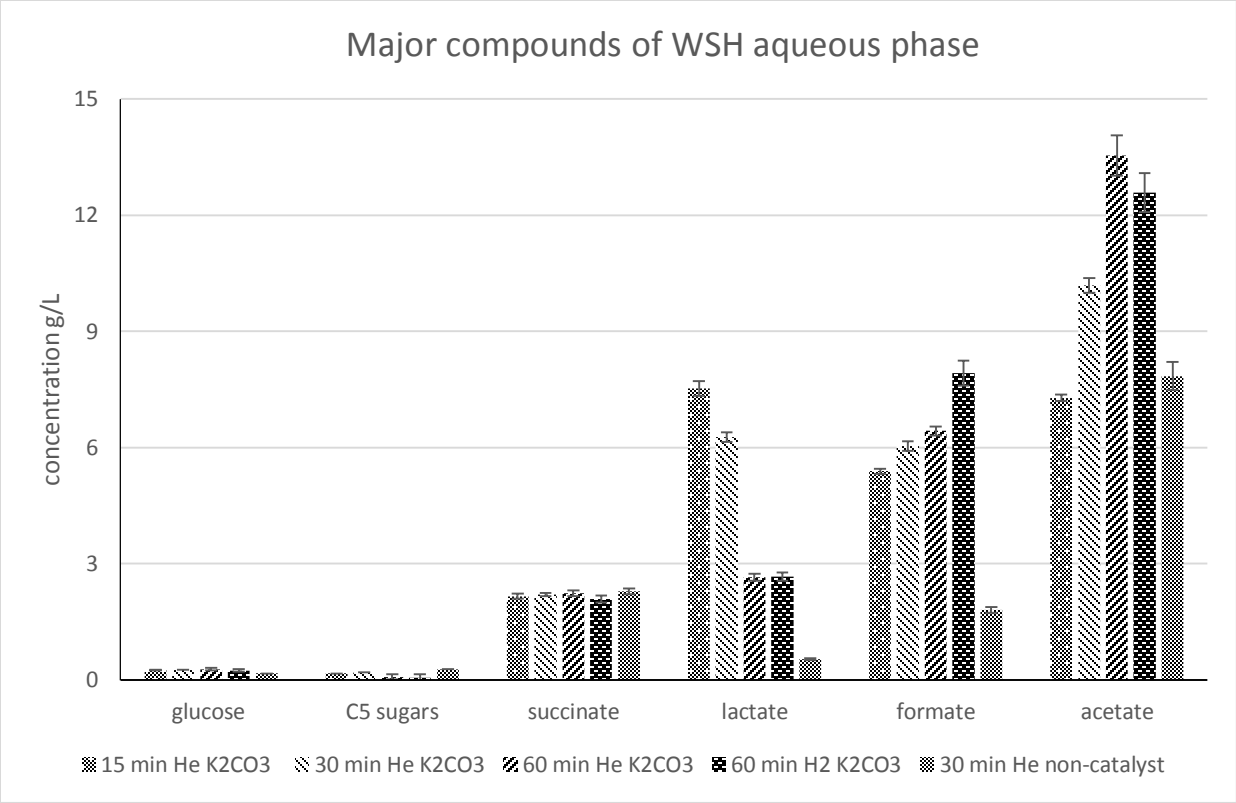


Fig.4.2 Major compounds of WSH aqueous phase

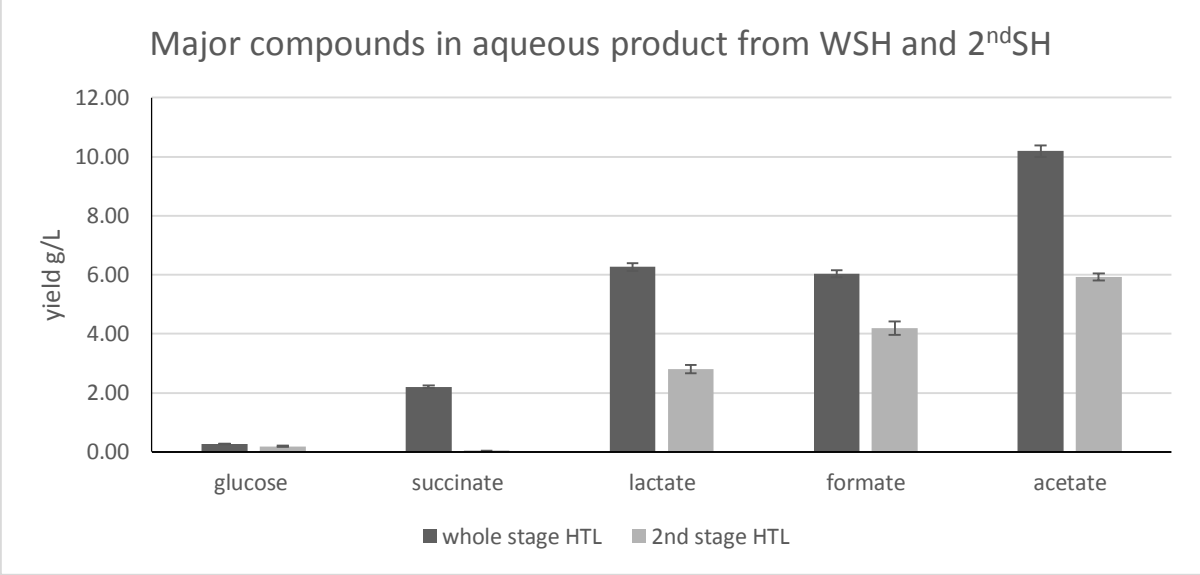


Fig.4.3 Major compounds in aqueous phase from WSH and 2ndSH

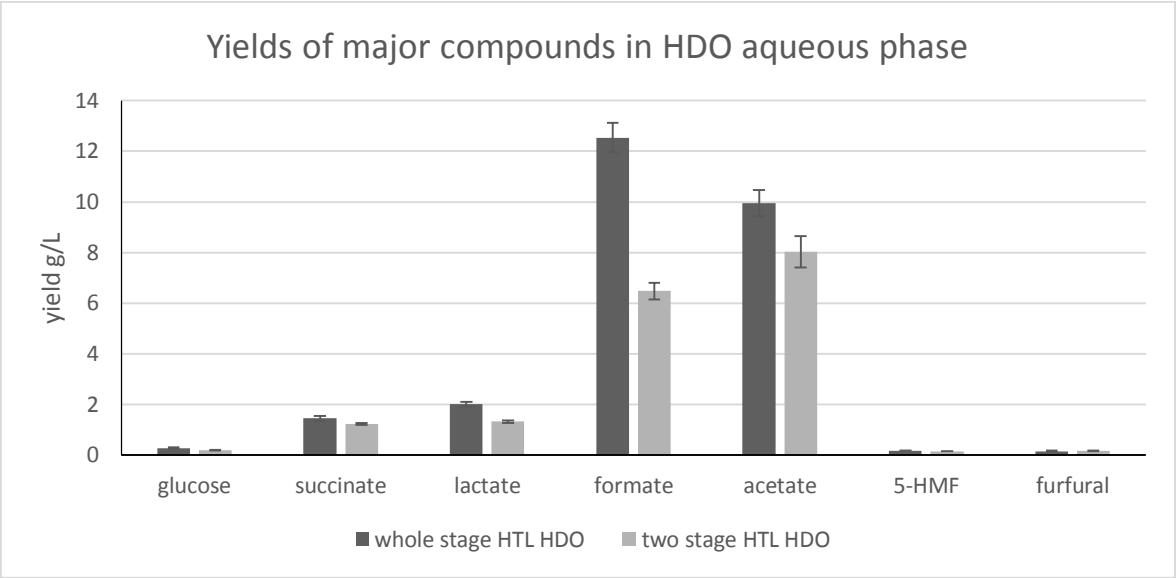


Fig.4.4 Major compounds of WSHH and TSHH aqueous phase

## V. Thermal Pretreatment of Sorghum Biomass to Improve Fuel Properties[3]


### Abstract

Torrefaction is a low temperature (240-320°C) pyrolysis process under anoxic condition that produces energy dense solid fuel (similar to coal), condensable liquids and non-condensable gasses derived from hemicellulose and lignin. In this study, energy sorghum and sweet sorghum bagasse were employed as feedstock for torrefaction at three different temperatures for 30 min. The yields of torrefied biomass were ranged from 43-65% for sweet sorghum bagasse and 51-70% for energy sorghum respectively. An overall increase in energy density (1.61 and 1.39 folds) and decrease in moisture content (2.13 and 2.49 times) were observed from both torrefied sorghums. Besides water, the most dominant compounds in both condensable liquids were acetic acid, with maximum yield of 101.90 g $L^{-1}$ from sweet sorghum bagasse torrefaction. Phenolic type chemicals and furan derivate were the other major components in oil fraction of liquid product, accounted up to 58 wt %. Furfural and furan carboxyl aldehydes were the leading compounds in the aqueous fraction of torrefied liquid product from sweet sorghum bagasse. Whereas, ketones and alcohols were the dominant components in the aqueous fraction from energy sorghum. The condensable liquids products can be further upgraded into high-value platform chemicals, while the solid fuel can be directly co-fired with coal.


[3] Yang Yue, Sudhagar Mani, Hari Singh and Bharat Singh. To be submit to Bioresource Technology

***Keywords***: torrefaction, sorghum biomass, energy yield, torrefied liquid products, components analysis

## 5.1 Introduction

Biomass is the widest available and largest renewable resource for biofuels conversion to address the diminishing fossil energy reserves and mitigate the environmental issues from petroleum-based economy (Zhang et al., 2012). Lignocellulose biomass, especially energy crop, has attracted extensive attention for its affluent availability and non-food competition. It was reported by the United States Department of Energy (DOE) that around $1.2 \times 10^9$ dry Mg of lignocellulose biomass could be obtained annually in the States for biofuels production (Perlack et al., 2005) through thermochemical and biochemical conversion.

Sorghum is a unique plant feedstock in that all its aboveground growth components (stem sap sugar, biomass or grain) can be converted into biofuel. It has traditional usage in fodder, syrup and grain and has been selected and bred accordingly for these purposes. It is a C4 crop characterized by a high photosynthetic efficiency. Although of tropical origin, sorghum can be grown successfully between the latitudes of 450 °N to 520 °S. It is an annual plant of short life cycle (3-5 months time to maturity) and, therefore, in tropical and sub-tropical climates can yield more than one crop a year. Furthermore, sorghum is tolerant to many stresses including drought, heat, and salinity (Almodares and Hadi, 2009; Prasad et al., 2008).

Forage varieties including those with photoperiod sensitive types and high in biomass content are categorized into high biomass or energy sorghums. These are typically taller,

leafier and later maturing than grain varieties. Biomass yields vary from 15 to 25 Mt $ha^{-1}$, but yields as high as 40 Mt $ha^{-1}$ has been reported (Packer and Rooney, 2014). Sweet sorghum provides another source of substantial biomass. Plant stalk is rich in fermentable sugars (70-80% as sucrose and the remaining as glucose and fructose) for syrup or ethanol production (Rooney et al., 2007; Murray et al., 2008). The combined sugar content of the juice varies between 9-15% and sugar yields vary from 3.6 to 15.5 Mt $ha^{-1}$. The bagasse is the byproduct of stalk crushing and represents approximately two-third of the dry biomass (Vermerris et al., 2008).

Torrefaction is a low temperature (240-320°C) pyrolysis process under anoxic condition that produces terrified solid biomass and condensable liquids and non-condensable gasses. During torrefaction, the fibrous structure and tenacity of biomass are destructed (Stelt et al., 2011); oxygen and water are removed from lignocellulose through carboxylation and dehydration reactions; thus nearly doubled the energy density of the terrified solid biomass, which could be further used as the feedstock for gasification and co-firing. The torrefied condensable liquid products were derived from volatile components in holocellulose and partial lignin; and could be extracted into oil and aqueous fraction, and be further upgraded into high-value platform chemicals.

For biofuels production from lignocellulose biomass, the structural and componential heterogeneity, low energy density and non-uniformed physical characters impair the efficiency of economic logistics, grindability pretreatment and energy yield of biofuels. Torrefaction as a promising thermal pretreatment, has been widely reported on various applications for biofuel production to improve low-quality biomass into physically consistent feedstock with higher energy density and lower moisture. Phanphanich investigated the

impact of grindability on torrefied woodchips and indicated the fuel characteristics of ground torrefied biomass was significantly improved. The higher heating values of torrefied pinewood chips increased 8.8-37.5% ranging from 250 to 300 °C with the energy yield of 71-90% (Phanphanich and Mani, 2011). Zhang and Hilten respectively studied the effects of torrefaction on bio-oil production with non-catalytic and catalytic upgrading fast pyrolysis. They found that pyrolysis bio-oil quality, to some extent, was improved with elevated torrefaction temperature; however, the cross-reaction between lignin and cellulose defragments were proposed to impair the yield of aromatic hydrocarbons (Zhang et al., 2012; Hilten et al., 2013). Deng evaluated the torrefaction pretreatment of agriculture wastes on co-gasification with coal (Deng et al., 2009) and indicated the integration of torrefaction and gasification significantly increased energy efficiency. Couhert certified the improvement on syngas quality with terrified feedstock and reported that approximately the same quantities of $CO_2$, 7% more $H_2$ and 20% more CO were obtained from terrefied beechwood after gasification for 2 s at 1400 °C (Couhert et al., 2009). Most current research concentrated on the characterization analysis and the application speculation of torrefied biomass. However, as far to our knowledge, the liquid product of torrefaction was lack of study. Actually, there were scarce reports on the utilization of torrefaction liquid product, which was mainly composed of acetic acid and phenol derivate compounds and could be upgraded into high-value platform chemicals.

To comprehensively utilize the torrefaction products, sorghum was employed as the feedstock due to its wide availability, drought tolerence, non-arable land competition and less N fertilizer dependent. The energy density of sorghum was around 16 MJ kg-1 with the moisture content of 7-9 wt. %. In this study, energy sorghum and sweet sorghum bagasse

were used as the torrefaction feedstock; the characterization of torrefied sorghums and condensable liquid products were measured and analyzed with two objectives: (i) investigate the impact of torrefaction temperature on the mass yield and energy density from sorghum biomass; (ii) analyze the components of torrefaction products for its potential to produce value-added platform chemicals.

## 5.2 Materials and Methods

Energy sorghum and sweet sorghum bagasse were obtained from the ongoing experiments at the Fort Valley State University, Fort Valley, Georgia, USA. The experimental site was located at 32° 30' N and 83° 52' W, with elevation of 155 m above mean sea level. The soil is classified as Orangeburg loamy fine sand (fine loamy, kaolinitic, themic Typic Kandiudults), with 2 to 5% slope (USDA, NCRS, 2015). The soil was composed of 650 g $kg^{-1}$ sand, 250 g $kg^{-1}$ silt, 100 g $kg^{-1}$ clay, and 5.9 g C $kg^{-1}$ organic content at the 0-30 cm depth. Average (40-yr) air temperature at the site ranges from 8$^{o}$C in January to 27$^{o}$C in July and total annual precipitation is 1215 mm. The field for sowing was prepared by disc harrowing to a depth of 15 to 20 cm, and leveling with an S-tine harrow to a depth of 10 cm. A basal fertilization of 0-20-20 NPK at the rate of 50 kg $ha^{-1}$ was applied. Sorghum varieties EJ7281 (sweet sorghum) and ES5200 (biomass sorghum) (Ceres Inc., Thousand Oaks, California) were planted in late May at the rate of 123,500 and 197,600 seeds $ha^{-1}$, respectively, in plots of four 12 m long rows spaced 0.76 m apart. Plots were fertilized with N at the rate of 90 kg $ha^{-1}$ in split doses, first when the plant reached 5$^{th}$ leaf stage and the second 3 weeks later. Sweet sorghum plots were harvested at dough stage and biomass

sorghum in mid-October. Sweet sorghum stalk was squeezed for sugar. Both energy sorghum and bagasse biomass were firstly field dried and subsequently open air dried in shade.

Energy sorghum and sweet sorghum bagasse sorghums were chopped into 10 mm to 240 mm in length and pre-dried before torrefaction. Two continuously annual samples (2012 and 2013) of above two sorghum biomasses were employed for the compositional analysis with three replications. The average moistures of energy sorghum and sweet sorghum bagasse were 9.29 wt. % and 7.83 wt. % respectively. The ultimate analysis, proximate analysis, higher heating values (HHVs) and holocellulose content were measured and listed in Table 5.1.

Solvents of dichloromethane (DCM) and sulfuric acid used in this study were obtained from Sigma-Aldrich with chemical pure. Calcium carbonate used for wet chemical analysis was also purchased from Sigma-Aldrich. Deionized water used in the experiments was prepared by our lab. Nitrogen used for torrefaction were purchased from Airgas.

5.2.1 Torrefaction experiment

Energy sorghum and sweet sorghum bagasse were torrefied in a steel batch torrefaction reactor ($30\text{cm} \times 30\text{cm} \times 15\text{cm}$), which was located inside a heated electric furnace. For each run, approximate 600 g sorghum sample was added into the reactor. The reactor was sealed with steel gasket to avoid gas product leaking during torrefaction. Three temperatures (250, 275 and 300 °C) were implemented for 30 min. The residence time of 30 min was testified to be optimal for torrefaction based on our previous studies (Phanphanich and Mani, 2011). The reaction temperature was monitored and controlled with a thermocouple, which was inserted through a 15cm fillister into the center of the reactor. The

temperature was recorded with an average heating rate of 1.15 °C $min^{-1}$ until the desired temperature. The air inside the reactor was purged and displaced with nitrogen before heating and nitrogen was continuously passed through the reactor with the influx rate of 2 ppl to avoid ignition and oxidation throughout the torrefaction process. The evaporated gas product from sorghum feedstock was condensed with a series of four metal condensers, cooled with ice-bath. The condensable gas was collected in the form of liquid product at the bottom of four condensers. Non-condensable gas was exhausted into the atmosphere through water bath. After the torrefaction reaction, the reactor was cooled with fans until room temperature. Nitrogen influx was stopped until the reactor temperature dropped below 50 °C. The torrified sorghum and the condensable liquid sample were collected and weighed respectively. The torrefied sorghum samples were sealed and stored at room temperature while the liquid samples were extracted with DCM into oil fraction and aqueous fraction before respective storage.

5.2.2 Separation and extraction

After the torrefaction reaction, 50 ml DCM was added into liquid samples in the four condensers and successively collected into a separatory funnel. The oil fraction in mixture was extracted and decanted off from aqueous phase with DCM. If the aqueous fraction appeared dark brown, there was residual oil and scattered tar remaining. Additional 10 ml DCM was applied to extract the organic components until the aqueous phase appeared clear. Both oil fraction and aqueous fraction were weighed and stored in refrigerator before analysis.

5.2.3 Analysis of torrefaction products

5.2.3.1 Analysis of solid torrefied sorghums

The torrefied sorghum samples were grinded with ball mill into fine powder and dried at 105 °C in oven overnight before analysis. The characterizations of both torrefied sorghums were analyzed with ultimate analysis and proximate analysis with three replications. The former measurement was conducted with elemental analyzer (LECO CHNS 932, LECO Corporation, St. Joseph, MI), where oxygen content was obtained by difference. The later determination was implemented with a micro thermos-gravimetric analyzer (TGA701, LECO Corporation, St. Joseph, MI), where the contents of ash, volatiles, and fixed carbon were given on dry basis.

The HHVs of torrefied sorghums were also estimated with adiabatic oxygen bomb calorimeter (IKAC 2000, IKA Works, Inc., NC). The contents of hemicellulose, cellulose and lignin were determined with wet chemical analysis according to National Renewable Energy Laboratory (NREL) standard protocol (Selig et al., 2008).

The lignin components of both raw sorghums and torrefied sorghums were analyzed with pyro-GC/MS. Around 2.0 mg of each sample was single-shot pyrolyzed at 500 °C with Frontier lab pyrolyzer (PY-2020 iD) with three replications. The volatile compounds were separated with HP-5ms Capillary Column (30m x 0.25um x 0.25mm) (Agilent Technologies Inc., CA) in a 6890N GC system. The oven temperature program was initially set at 50 °C for 2 min; then ramped to 280 °C with the heating rate of 5 °C $min^{-1}$ and kept constantly for 53 min. Helium was employed as the carrier gas with the flow rate of 1 ml $min^{-1}$ and the split ratio was set at 50:1. The lignin components were identified with NIST11 mass spectral

library.

5.2.3.2 Analysis of torrefaction liquids

The components of aqueous fraction and oil fraction from liquid product were respectively analyzed with GC-MS using HP-5ms Capillary Column (30m x 0.25um x 0.25mm). The oven temperature program was initially set to 40 °C for 4 min; then increased to 275 °C with the heating rate of 5 °C $min^{-1}$ and hold constantly for 5 min. The Mass Spec interface was set at 280°C. The inlet temperature was 260 °C. Helium was used as carrier gas with flow rate of 0.8 mL $min^{-1}$ and the split ratio of 50:1. The liquid sample volume injected was 1 μl. The solvent delay was setup for 3 min for DCM. The compositions of the samples were identified by matching fragmentation patterns with NIST mass spectral library.

The major compounds in aqueous fraction were determined with HPLC using Coragel 94 column. The oven temperature was constant at 60°C and 4mN sulfuric acid was used for mobile phase. The flow rate was constant at 0.6 ml $min^{-1}$. The sample volume injected was 5 μl.

5.2.4 Calculation of torrefaction yield

The torrefied products included solid torrefied sorghum, non-condensable gas, and condensable liquid, which further separated into aqueous and oil fraction. The yields of above products were calculated as follows:

$$\text{Yield of torrefied sorghum} = \frac{\text{mass of torrefied sorghum}}{\text{mass of sorghum feedstock}} \times 100\%$$

$$\text{Yield of condensable liquid} = \frac{\text{mass of liquid product}}{\text{mass of sorghum feedstock}} \times 100\%$$

$$\text{Yield of gas fraction} = 1 - \frac{\text{mass of torrefied sorghum}}{\text{mass of sorghum feedstock}} - \frac{\text{mass of liquid product}}{\text{mass of sorghum feedstock}} \times 100\%$$

$$\text{Yield of aqueous fraction} = \frac{\text{mass of aqueous product}}{\text{mass of sorghum feedstock}} \times 100\%$$

$$\text{Yield of oil fraction} = \frac{\text{mass of liquid product} - \text{mass of aqueous product}}{\text{mass of sorghum feedstock}} \times 100\%$$

5.2.5 Statistical analysis

The HHVs of torrefied sorghums were separately compared on the basis of above three torrefaction temperatures (250, 275 and 300 °C) with one-way ANOVA and Turkey multiple comparison test. SAS program (Version 9.4) was employed to implement above statistical analysis with the significant difference level at $P < 0.05$.

5.3 Results and Discussions

5.3.1 Characterization of sorghum biomass

Energy sorghum and sweet sorghum bagasse were mainly constituted with moisture, ash, holocellulose and lignin. The components of energy sorghum were 7.83% of moisture, 3.47% of ash, 21.44% of hemicellulose, 33.24% of cellulose and 19.94% of lignin. The components of sweet sorghum bagasse were similar to those of energy sorghum, moisture accounted for 9.29%, ash for 3.28%, hemicellulose for 18.50%, cellulose for 33.15%. The dominant structural unit was p-hydroxyl phenol (H lignin) for both sorghums. The HHVs of energy sorghum and sweet sorghum bagasse were respectively 17.33 MJ $kg^{-1}$ and 16.45 MJ $kg^{-1}$, which were comparable to rice straw (Deng et al., 2009) and birch (Pach et al., 2002). The O/C and H/C ratios were respectively 0.87 and 1.54 for energy sorghum; and 0.99 and

1.61 for sweet sorghum bagasse. The compositional properties of both sorghum biomasses were indicated in Table 5.1.

5.3.2 Yield analysis of torrefaction products

During torrefaction, free water and physically bound water were successively released from sorghum biomass when temperature reached 100 to 200 °C (Stelt et al., 2011). Most hemicellulose and a small amount of lignin started to decompose mainly through decarboxylation and dehydration reactions after 200 °C. Cellulose and most lignin were more tolerant and decomposed fractionally at torrefaction temperature; most unbinding cellulose and lignin were more brittle to breakdown and aggregate into acid insoluble components. This led the appearances of terrified sorghums darker (Fig.5.1) and the yields decreased with temperature due to the continuous formation of volatiles compounds. Their yields ranged from 53.1- 69.8% for torrefied energy sorghum and 41.3- 64.7% for torrefied sweet sorghum bagasse respectively (Fig.5.2). The yields of condensable liquid and non-condensable gas, which derived from sorghum volatiles, on the contrast, increased with temperature. There was no significant difference in non-condensable gas yields between two sorghums at each temperature, which mainly constituted with $CO_2$ and CO due to the decarboxylation of hemicellulose and partial cellulose. However, more condensable liquid product was produced from sweet sorghum bagasse than energy sorghum. Typically, with the temperature raised from 250 to 300 °C, the yield of aqueous fraction from energy sorghum torrefaction gradually increased from 9.44% to 15.29%; whereas, it increased from 15.27% to 23.33% from sweet sorghum bagasse (Fig.5.2). Such a difference in yields of torrefied sorghum and condensable liquid were produced because more holocellulose were decomposed from sweet sorghum

bagasse (90.7-100% hemicellulose and 43.8-93.0% cellulose from 250 to 300 ℃) than energy sorghum (68.8-93.7% hemicellulose and 24.8-66.8% cellulose from 250 to 300 ℃) due to their componential and structural heterogeneity.

5.3.3 Characterizations of torrefied sorghums

The characterizations of torrefied sorghum were indicated in Table 5.1. The oxygen was released with temperature through decarboxylation and dehydration reactions from hemicellulose and partial depolymerized cellulose. Its contents were respectively reduced by 10.95% for energy sorghum and 18.83% for sweet sorghum bagasse at 300 °C, which resulted in the decrease of O/C ratios. H/C ratios of two torrefied sorghums also reduced due to reduction of hydroxyl substitutes. The combination of O/C and H/C ratios indicated the elemental distribution of torrefied sorghums was approaching to lignite with temperature (Fig.5.3). Compared with our previous torrefaction study with pine chips, it was indicated that torrefied wood biomass displayed desirable H/C and O/C ratios than torrefied herbaceous biomass. However, this was mainly because of the difference on initial holocellulose and lignin content in raw biomass. The similar slopes during torrefaction process in Fig.5.3 illustrated their dominant decomposition reactions were alike but might occur at different temperature range.

The energy yields of torrefied sorghums also shared the same trend, respectively 84.64%, 73.21% and 69.96% of torrefied energy sorghum at 250, 275 and 300 °C. Considering the torrefied energy sorghum yield, energy densities respectively increased 21.23%, 37.33% and 36.30% at above three torrefaction temperatures. Similarly, after torrefaction, 78.99% to 70.36% of energy was stored in torrefied sweet sorghum bagasse, but

with energy density increased 22.13% to 63.40%. This energy reward was less desirable than torrefied wood biomass reported by (Bergman et al., 2005), which around 90% of the initial energy content was retained in torrefied solid product. However, on the contrast of Prins, who reported energy density decreased with torrefaction temperature from terrified willow because of the formation of acetate acid at higher temperature (300°C) (Prins et al., 2006), our study found most acetate acid was formed before 250°C, this was probably a crucial difference between wood torrefaction and herb torrefaction.

In accordance with Zhang's report (Zheng et al., 2012), it was also found that hemicellulose and cellulose were remarkably decomposed in both sorghums during torrefaction. The residual hemicellulose contents of torrefied energy sorghum were respectively 9.58% at 250 °C, 3.19% at 275 °C and 2.64% at 300 °C, which indicated that 68.9%, 92.1% and 93.7% of hemicellulose was decomposed from raw energy sorghum. For sweet sorghum bagasse, more hemicellulose was degraded at the same condition. The remaining hemicellulose content in torrefied sweet sorghum bagasse was 2.65% at 250 °C, 2.14% at 275 °C and 0% at 300 °C. Cellulose from sweet sorghum bagasse was also more susceptible to temperature. There was only 5.37 % cellulose to be intact at 300 °C from sweet sorghum bagasse while 21.5 % from energy sorghum. The holocellulose and lignin components of torrefied sorghums were indicated in Fig.5.4. It was also indicated that the aggregation of breakdown cellulose and lignin was the dominant component, ranging 60-80 % in torrefied sorghums after 275 °C, in which, around 99% was acid insoluble.

In lignocellulose biomass, p-hydroxyphenyl (H), guaiacyl (G), and syringyl (S) were phenylpropanoids lignin units respectively produced from the three lignin monolignols: p-coumaryl alcohol, coniferyl alcohol, and sinapyl alcohol (Boerjan et al., 2003). During

torrefaction, H lignin was dramatically degraded and became stable at 22-24% for both sorghums after 250°C. Correspondingly, the contents of S and G lignin increased and respectively retained 33-35% and 41-45% after 250°C (Fig.5.5). Although the lignin components distribution of raw sorghums were with more difference, their contents became uniform after torrefaction.

5.3.4 Characterizations of liquid products

The liquid products involved oil fraction and aqueous fraction after extraction with DCM. The oil fraction included the oil components and tars; the latter was a sticky heavy liquid and composed of large molecular compounds. These large molecular compounds were commonly formed during torrefaction and pyrolysis, and soluble to most organic solvent. The components of liquid products were determined with GC/MS. There were hundreds of compounds existed in either aqueous or oil fraction and it was hard to identify all of them. The major compounds were analyzed and listed in Table 5.2 and Table 5.3. HPLC was also implemented for quantitative analysis of main compounds in aqueous fraction and their yields were indicated in Fig.5.6. The sorghum componential and structural heterogeneity led to distinct decomposition intermediates and cross reactions, which influenced the final components distribution in torrefied liquids between energy sorghum and sweet sorghum bagasse.

5.3.4.1 Components of oil fraction

The oil fraction was mainly decomposed of organic acids, phenolic type chemicals, furan derivate and ketones. There was no significant difference in distribution of major identified organic components between sorghum liquid products from 250°C to 275°C.

However, remarkable cross reactions between holocellulose and lignin decompositions occurred from 275℃ to 300 ℃, typically influenced the distributions of phenol derivate and ketones. The former was mainly converted from hemicellulose and lignin, and could be further updated for biofuels. Multiple phenol derivates were formed after torrefaction. The simple structural phenol (phenol and its methyl-/ ethyl- derivate) was formed from hemicellulose decomposition due to the relevant simple unit structure of hemicellulose; while the phenol derivate with methoxy substitutes was considered to be converted form lignin decomposition (Boerjan et al., 2003). In spite of partial decomposition, it was also found that the lignin contributed more phenol derivate than hemicellulose. Actually, the major products from hemicellulose were acetic acids and $CO_2$, which intended to reduce oxygen content rather than produce oil compounds at torrefaction.

Furans derivate was identified with abundance as well, especially from sweet sorghum bagasse torrefaction. Furfural was the dominant compound of furans derivate, which was formed from the decomposition of holocellulose (Stefanidis et al., 2014). More furfural was observed from sweet sorghum bagasse torrefaction than that from energy sorghum. This was resulted from more holocellulose decomposition from sweet sorghum bagasse under the same torrefaction condition. Another important component in oil fraction was ketones. Cycle ketones were reported to be derived from secondary cellulose decompositions in oil fraction (Wang et al., 2011); however, in our study, only linear ketones were identified which were considered to be converted from hemicellulose decomposition (Horne and Williams, 1996). Although acetate acid was the dominant compound in both oil fraction from sorghum torrefaction, with contents of 11-38 wt %, it was considered that those remaining acetate acid oil fraction was the residue of aqueous acetate acid after extraction.

Additionally, depolymerization and defragment reactions also occurred on cellulose, which formed glucose derivate (1,6;2,3-dianhydro-4-O-acetyl-beta-d-gulopyranose) and other secondary intermediates.

5.3.4.2 Components of aqueous fraction

Definitely, water was the dominant component in aqueous fraction. Most condensed water was derived from free water and physically bound water in sorghums; while a small fraction was obtained from the dehydration reaction.

Acetic acid was the second dominant component in aqueous fraction. Its contents and yields from both sorghums increased with temperature (Table 5.3 and Fig. 5.6). The maximum yield of acetic acid from energy sorghum and sweet sorghum bagasse in aqueous fraction were respectively 92.61 g $L^{-1}$ and 101.90 g $L^{-1}$ at 300°C for 30 min. There were two main pathways to form acetic acid during torrefaction. The main route was through the cleavage of acetyl group on hemicellulose unit with the release of $CO_2$ (Shen et al., 2010); the other route was from the cellulose decomposition intermediate of 5-HMF (Wang et al., 2011). The formation routes of acetic acid supported that higher acetic acid yield was obtained from sweet sorghum bagasse due to its holocellulose was more susceptible to temperature.

Except acetic acids, alcohols and ketones were the major components in energy sorghum torrefaction aqueous fraction; while furan type chemicals were the major aqueous components from sweet sorghum torrefaction based on GC/MS (Table 5.3). The different distribution of major aqueous components was essentially resulted from the distinct sorghum components and their diverse decomposition routes, plus various cross reactions between

individual decomposition intermediates. It was proposed that furan intermediates were formed firstly from hemicellulose of both sorghums. As to energy sorghum, these furan intermediates were more apt to further defragment into C4 alcohols and ketones, which had relevant strong polarity and were easy to solve with water. For sweet sorghum bagasse, as the hemicellulose decomposition was more accessible, the furans intermediates were formed earlier and more apt to convert into relevant stable chemicals in the form of furfural and furancarboxaldehydes. Additionally, aldehydes type chemicals were also identified from sweet sorghum bagasse torrefaction aqueous fraction, and among which, hydroxyacetaldehyde was widely reported as a cellulose thermal decomposition product (Lin et al., 2009; Shen et al., 2009)

Most major compounds of sorghum torrefaction aqueous fraction increased with temperature. Hydroxyacetone and methanol had higher yields from energy sorghum, respectively reached 13.73 g $L^{-1}$ at 300°C and 12.43 g $L^{-1}$ at 275°C. For both sorghums, the methanol yield reached maximum at 275°C and then decreased at 300°C; the decomposition route of methanol was still unclear. 5-HMF was only formed from sweet sorghum bagasse cellulose with similar yield of 2.8-3.2 g $L^{-1}$ at each torrefaction temperature, through direct ring-opening or rearrangement reactions of glucose (Stefanidis et al., 2014). Furfural had a higher yield from sweet sorghum bagasse hemicellulose and the maximum yield reached 3.79 g $L^{-1}$ at 300°C. The major components in torrefaction aqueous fraction were quite similar with Stelt's report (Stelt et al., 2011), however, formic acid and lactic acid were not detected with HPLC because of different biomass feedstock.

## 5.4 Conclusions

Torrefaction was commonly performed to improve biomass energy density and physiochemical characters. In this study, sorghums torrefied products were analyzed for comprehensive utilization. The energy yields of torrefied sorghums reached 70% -85% with energy densities increased by 21% -63%. The characterizations of torrefied sorghums were approximate to lignite and more adaptable for co-firing. Various valuable co-products were obtained from liquid products, which could be further upgraded into platform chemicals. The different distributions of major components in oil and aqueous fractions were resulted from the componential and structural heterogeneity of biomass, which led distinct decomposition intermediates and cross reactions.

**Acknowledgement**

The project was financially supported by the USDA-NIFA sustainable bioenergy research grant number GEOX-2010-03868 via Fort Valley State University.

References

Almodares, A. and Hadi, M.R., 2009. Production of bioethanol from sweet sorghum: A review. Afr. J. Agric. Res. 4,772-780.

Bergman, P.C.A., Boersma, A.R., Zwart, R.W.R., Kiel, J.H.A., 2005. Torrefaction for biomass co-firing in existing coal-fired power stations "biocoal". Report ECN-C-05-013. Petten, The Netherlands: ECN

Boerjan, W., Ralph, J., Baucher, M., 2003. Lignin biosynthesis. Annu. Rev. Plant. Biol., 54, 519–549

Couhert, C., Salvador, S., Commandre´ J- M., 2009. Impact of torrefaction on syngas production from wood. Fuel. 88, 2286-2290.

Deng, J., Wang, G.J., Kuang, J.H., Zhang, Y.L., Luo Y.H., 2009. Pretreatment of agricultural residues for co-gasification via torrefaction. J. Anal. Appl. Pyrolysis. 86, 331-337.

Horne, P. A., Williams, P. T, 1996. Reaction of oxygenated biomass pyrolysis model compounds over a ZSM-5 catalyst. Renew. Energ. 7, 131–144.

Lin, Y.C., Cho, J., Tompsett, G.A., Westmoreland P.R., Huber G.W., 2009. Kinetics and mechanism of cellulose pyrolysis, J. Phy. Chem. C. 113, 20097–20107.

Murray, S.C., Rooney, W.L., Hamblin, M.T., Mitchell, S.E., Kresovich, S., 2009. Sweet sorghum genetic diversity and association mapping for brix and height. Plant Genome. 2, 48-62.

Pach, M., Zanzi, R., Bjornbom, E., 2002. Torrefied biomass a substitute for wood and char coal. In: 6th Asia-pacific international symposium on combustion and energy utilization.

Packer, D. J., Rooney, W.L., 2014. High-parent heterosis for biomass yield in photoperiod-sensitive sorghum hybrids, Field Crops Res. 167, 153-158.

Perlack, R.D., L.L. Wright, A.F. Turhollow, et al. Biomass as feedstock for a bioenergy and bioproduct industry: the technical feasibility of a billion ton annual supply. Reported prepared for DOE under contract DE-AC05-000R22725. 59. P. 2005

Phanphanich, M. and Mani, S., 2011. Impact of torrefaction on the grindability and fuel characteristics of forest biomass. Bioresour. Technol. 102, 1246-1253.

Prasad, P.V.V., Pisipati, S.R., Mutava, R.N., Tuinstra, M.R., 2008. Sensitivity of grain sorghum to high temperature stress during reproductive development. Crop Sci. 48, 1911–1917.

Prins, M.J., Ptasinski, K.J., Janssen, F.J.J.G., 2006. More efficient biomass gasification via torrefaction. Energy. 31, 3458-3470.

Roger N. Hilten, Richard A. Speir, James R. Kastner, Sudhagar Mani, and K. C. Das, 2013. Effect of Torrefaction on Bio-oil Upgrading over HZSM-5. Part 1: Product Yield, Product Quality, and Catalyst Effectiveness for Benzene, Toluene, Ethylbenzene, and Xylene Production. Energy Fuels. 27, 830-843

Rooney, W.L., Blumenthal, J., Bean, B., Mullet, J.E., 2007. Designing sorghum as a dedicated bioenergy feedstock. Biofuel Bioprod. Bior. 1920, 147-157.

Selig, M., Weiss, N., Ji, Y., 2008. In: Laboratory Analytical Procedure No. TP-510-42629. National Renewable Energy Laboratory, Golden, CO.

Shen, D., Gu, S., 2009. The mechanism for thermal decomposition of cellulose and it main products. Bioresour. Technol. 100, 6496–6504.

Shen, D.K., Gu, S., Bridgwater, A.V., 2010. Study on the pyrolytic behavior of xylan based hemicellulose using TG-FTIR and Py-GC-FTIR, J. Anal. Appl. Pyrol. 87, 199–206.

Stefanidis, S. D., Kalogiannis, K. G., Iliopoulou, E. F., Michailof, C. M., Pilavachi, P. A., Lappas, A. A., 2014. A study of lignocellulosic biomass pyrolysis via the pyrolysis of cellulose, hemicellulose and lignin. J. Anal. Appl. Pyrol. 105,143-150.

US Department of Agriculture (USDA), Natural Resources Conservation Service (NCRS). Custom Soil Resource Report. Accessed on 3/ 2/2015.

Van der Stelt, M. J. C., Gerhauser, H., Kiel, J. H. A., Ptasinski, K. J., 2011. Biomass upgrading by torrefaction for the production of biofuels: A review. Biomass Bioenerg. 35, 3748-3762.

Vermerris, W., Rainbolt, C., Wright, D., Newman, Y., 2008. Production of biofuel crops in Florida: Sweet sorghum. University of Florida IFAS extension publication #SS AGR 293, pp. 1-7.

Wang, S., Guo, X., Liang, T., Zhou, Y., Luo, Z., 2011. Mechanism research on cellulose pyrolysis by Py-GC/MS and subsequent density functional theory studies. Bioresour. Technol. 104, 722–728.

Zheng, A., Zhao, Z., Chang, S., Huang, Z., He, F., L, H., 2012. Effect of Torrefaction Temperature on Product Distribution from Two-Staged Pyrolysis of Biomass. Energ. Fuel. 26, 2968-297

Table 5.1. Characterizations of torrefied sorghums

| Torrefied Sorghum | Temperature | Moisture (%) | Fixed Carbon (%) | Volatiles Dry (%) | Ash Dry (%) | C (wt.%) | H (wt.%) | N (wt.%) | O* (wt.%) | HHV (MJ $kg^{-1}$) |
|---|---|---|---|---|---|---|---|---|---|---|
| Energy sorghum | raw | 7.83 (0.24) | 17.01 (0.63) | 79.39 (1.90) | 3.47 (1.13) | 43.11 (2.15) | 5.52 (0.11) | 1.45 (0.03) | 49.93 (2.23) | 17.33a (0.42) |
| | 250°C | 2.05 (0.19) | 23.83 (0.70) | 70.93 (1.31) | 4.75 (0.63) | 48.87 (0.16) | 5.16 (0.02) | 1.56 (0.03) | 44.42 (0.12) | 21.01b (0.41) |
| | 275°C | 1.82 (0.52) | 33.91 (1.45) | 59.45 (1.84) | 6.04 (0.11) | 55.25 (0.22) | 4.90 (0.07) | 1.73 (0.26) | 38.13 (0.56) | 23.80c (0.55) |
| | 300°C | 3.24 (0.94) | 32.22 (2.58) | 60.97 (1.02) | 6.26 (0.67) | 54.32 (0.03) | 4.95 (0.06) | 1.76 (0.15) | 38.98 (0.18) | 23.62c (0.19) |
| Sweet sorghum bagasse | raw | 9.29 (0.00) | 20.32 (0.04) | 76.35 (0.24) | 3.28 (0.23) | 40.32 (0.25) | 5.42 (0.07) | 1.22 (0.08) | 53.06 (0.24) | 16.45a (0.30) |
| | 250°C | 5.51 (1.43) | 29.60 (2.08) | 68.36 (1.70) | 4.03 (0.37) | 53.96 (1.79) | 5.05 (0.23) | 0.94 (0.02) | 40.06 (2.01) | 20.09b (0.87) |
| | 275°C | 3.83 (0.42) | 39.68 (0.98) | 55.68 (0.29) | 4.60 (0.43) | 54.48 (3.47) | 4.58 (0.53) | 0.93 (0.10) | 40.02 (3.10) | 23.43c (1.01) |
| | 300°C | 4.37 (0.75) | 51.50 (0.07) | 45.29 (0.17) | 5.85 (0.29) | 59.30 (3.64) | 4.56 (0.18) | 0.92 (0.06) | 35.23 (2.88) | 26.88d (0.89) |

*The oxygen contents were obtained from difference, assuming sulfur content was negligible.
There was no significant difference at 5% level with the same labeled letter.

Table 5.2. The major components of liquid product (oil fraction) from sorghum torrefaction

| Oil fraction | Energy sorghum | | | Sweet sorghum bagasse | | |
|---|---|---|---|---|---|---|
| components | 250 ℃ | 275 ℃ | 300 ℃ | 250 ℃ | 275 ℃ | 300 ℃ |
| | area % | | | | | |
| ***ketones*** | *13.14* | *13.22* | *1.05* | *4.10* | *4.14* | *8.51* |
| 2,3-butanedione | 1.29 | 2.26 | 1.05 | 0.87 | 0.81 | 1.63 |
| 2-propanone, 1-hydroxy- | 2.89 | 4.82 | | 1.05 | 0.71 | 2.71 |
| 1-hydroxy-2-butanone | 5.27 | 3.25 | | | | |
| 2-propanone,1-(acetyloxy)- | 3.69 | 2.89 | | 2.18 | 2.62 | 4.17 |
| ***furans*** | *14.67* | *13.27* | *8.47* | *29.24* | *31.77* | *35.01* |
| furfural | 5.59 | 4.39 | 8.47 | 26.19 | 28.77 | 28.33 |
| 2-furanmethanol | 5.37 | 4.21 | | 3.05 | | 4.54 |
| 2-furancarboxaldehyde, 5-methyl- | | | | | 3.00 | 2.14 |
| 2-furan,tetrahydro-2-(methoxymethyl)- | | 4.67 | | | | |
| 2-furanmethanol,tetrahydro-,acetate | 3.71 | | | | | |
| ***phenol derivate*** | *16.09* | *15.62* | *45.58* | *24.20* | *26.19* | *16.20* |
| phenol | 3.92 | 3.30 | 14.50 | 1.67 | 4.39 | 2.36 |
| phenol, 4-methyl- | | | | | 1.79 | |
| phenol, 2-methoxy- | 4.79 | 4.08 | 8.49 | 5.70 | 3.50 | 3.75 |
| phenol, 4-ethyl- | 2.72 | 2.74 | 7.40 | 1.42 | 2.88 | 2.70 |
| phenol, 2-methoxy-4-methyl- | | | | 4.75 | 1.20 | |
| phenol, 4-ethyl-2-methoxy- | 1.49 | 2.11 | 4.49 | 4.34 | 3.09 | 2.18 |

| | | | | | | |
|---|---|---|---|---|---|---|
| 2-methoxy-4-vinylphenol | | | 4.31 | 1.84 | 4.66 | 2.62 |
| phenol, 2,6-dimethoxy- | 3.17 | 3.39 | 6.39 | 2.02 | 3.08 | 2.59 |
| phenol, 2-methoxy-4-(1-propenyl)- | | | | 2.46 | 1.60 | |
| ***acids*** | *38.21* | *38.72* | *25.17* | *18.09* | *13.74* | *28.94* |
| acetic acid | 38.21 | 30.12 | 12.10 | 12.48 | 11.08 | 19.87 |
| propanoic acid,2-methyl-anhydride | | | | | | 2.92 |
| n-hexadecanoic acid | | 5.19 | 8.30 | 2.25 | 2.66 | 4.07 |
| oleic acid | | 3.41 | | | | 2.08 |
| cis-vaccenic acid | | | 4.77 | 3.36 | | |
| ***others*** | *3.64* | *3.27* | *9.26* | *7.17* | *11.24* | *4.09* |
| *glucose derivate* | | | | | | |
| 1,6;2,3-dianhydro-4-O-acetyl-beta-d-gulopyranose | | | 5.46 | | 4.30 | |
| *aromatic compounds* | | | | | | |
| benzofuran,2,3-dihydro- | 3.64 | 3.27 | 3.80 | | 6.94 | 4.09 |
| *benzene derivate* | | | | | | |
| benzaldehyde,2-methyl- | | | | 3.68 | | |
| *heterocyclic compounds* | | | | | | |
| 2-(2,2-dimethylcyclopropyl) thiophene | | | | 3.49 | | |
| ***total*** | *85.75* | *84.10* | *89.53* | *82.80* | *87.08* | *92.75* |

Table 5.3. The major components of liquid product (aqueous fraction) from sorghum torrefaction

| Aqueous fraction | Energy sorghum | | | Sweet sorghum bagasse | | |
|---|---|---|---|---|---|---|
| components | 250 °C | 275 °C | 300 °C | 250 °C | 275 °C | 300 °C |
| | area % | | | | | |
| ***alcohols*** | *10.37* | *4.61* | *3.26* | *n/a* | *6.2* | *n/a* |
| 1-propanol | | | | | 2.91 | |
| 2,3-butanediol | 3.42 | 2.35 | 3.26 | | | |
| 1,2,3-propanetriol, monoacetate | 6.95 | 2.26 | | | 3.29 | |
| ***aldehydes*** | *n/a* | *n/a* | *n/a* | *2.28* | *n/a* | *1.88* |
| acetaldehyde,hydroxy- | | | | 2.28 | | |
| acetaldehyde | | | | | | 1.88 |
| ***acids*** | *39.73* | *37.22* | *51.55* | *36.33* | *55.85* | *53.08* |
| acetic acid | 39.73 | 37.22 | 51.55 | 36.33 | 55.85 | 53.08 |
| ***ethers*** | *2.58* | *2.9* | *n/a* | *n/a* | *n/a* | *n/a* |
| dimethyl ether | 2.58 | | | | | |
| acetic acid, pentyl ester | | 2.9 | | | | |
| ***ketones*** | *7.25* | *12.05* | *5.1* | *1.73* | *4.48* | *3.1* |
| 2-propanone, 1-hydroxy- | 4.52 | 8.27 | 2.39 | | 2.07 | |
| 1-hydroxy-2-butanone | 2.73 | 1.46 | 2.71 | 1.73 | 1.19 | 1.89 |
| 2,3-butanedion | | 2.32 | | | 1.22 | 1.21 |
| ***furans*** | *1.92* | *0.82* | *2.22* | *9.96* | *10.46* | *13.21* |
| furfural | | | | 5.24 | 7.78 | 10.62 |
| 2-furanmethanol | 1.92 | 0.82 | 2.22 | 1.08 | | |

| | | | | | | |
|---|---|---|---|---|---|---|
| 2-furancarboxaldehyde, 5-(hydroxymethyl)- | | | | 3.64 | 2.68 | 2.59 |
| ***amides*** | *11.42* | *4.63* | *n/a* | *3.19* | *n/a* | *6.05* |
| 1,3-butanediamine | 8.53 | | | | | |
| nitroacetamide | | 2.07 | | | | |
| 1,3-propanediamine, N-methyl- | 2.89 | 2.56 | | 3.19 | | 6.05 |
| ***heterocyclic compounds*** | *n/a* | *4.74* | *n/a* | *n/a* | *n/a* | *4.15* |
| dioxazino quinoxaline, hexahydro-3,6-bis [2-diethylaminoethyl]-10,11-diphenyl | | 4.74 | | | | |
| N-aminopyrrolidine | | | | | | 4.15 |
| ***sugar derivate*** | *n/a* | *n/a* | *n/a* | *16.81* | *n/a* | *n/a* |
| D-allose | | | | 16.81 | | |
| ***carbamidine*** | *n/a* | *n/a* | *n/a* | *n/a* | *2.72* | *n/a* |
| metformin | | | | | 2.72 | |
| ***total*** | *73.27* | *66.97* | *62.13* | *70.30* | *79.71* | *81.47* |

n/a: not detected


Fig.5.1 Physical change of torrefied sorghums from raw sorghums. (a) raw sweet sorghum bagasse, (b) torrefied sweet sorghum bagasse at 250°C, (c) torrefied sweet sorghum bagasse at 275°C, (d) torrefied sweet sorghum bagasse at 300°C; (e) raw energy sorghum, (f) torrefied energy sorghum at 250°C, (g) torrefied energy sorghum at 275°C, (h) torrefied energy sorghum at 300°C.

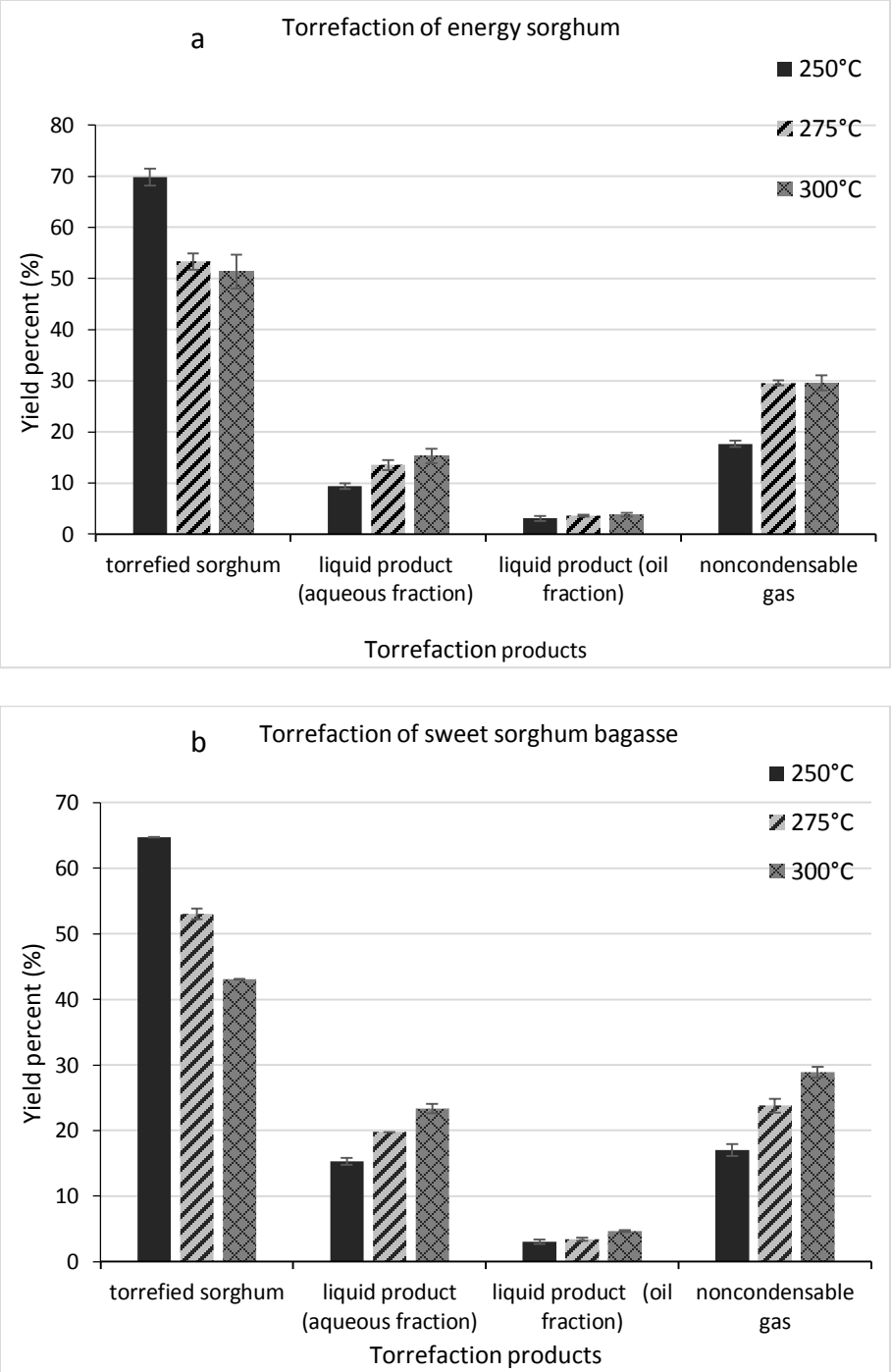


Fig.5.2 Torrefaction yields from sorghum biomass.

Note: The reaction time was 30 min for both sorghums

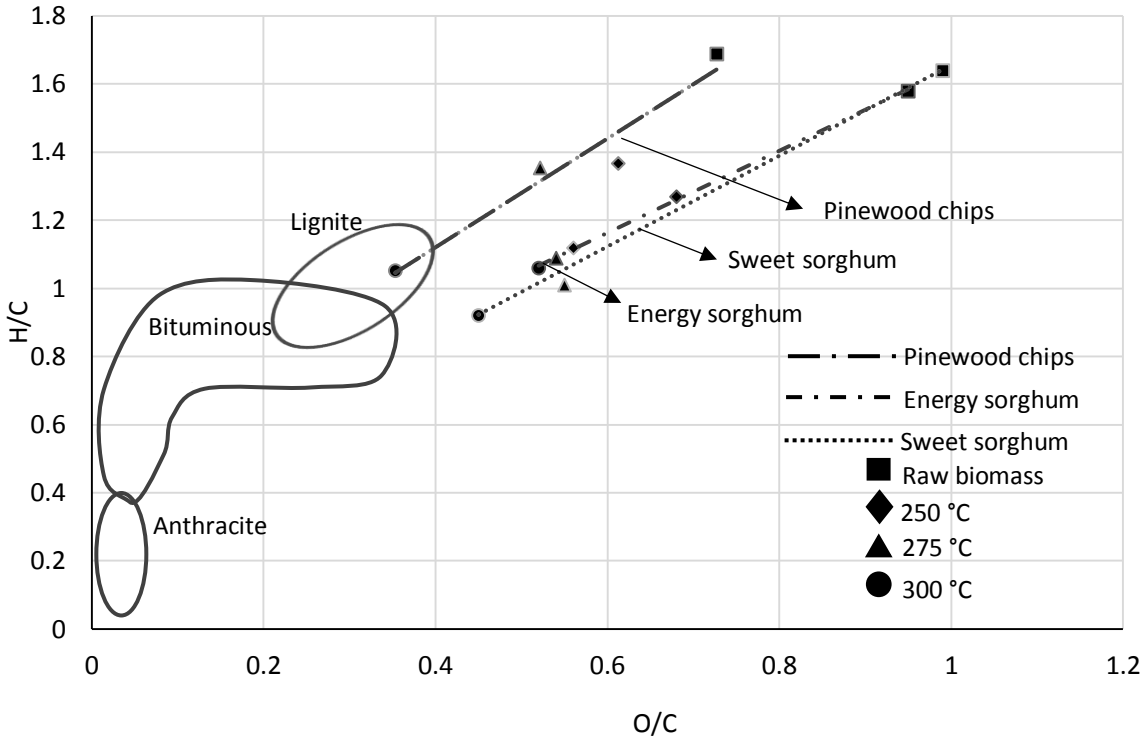


Fig.5.3 Van Krevelen Diagram for chemical composition of sorghums and wood biomass at various torrefaction temperature. (Data extracted from Phanphanich and Mani, 2011)

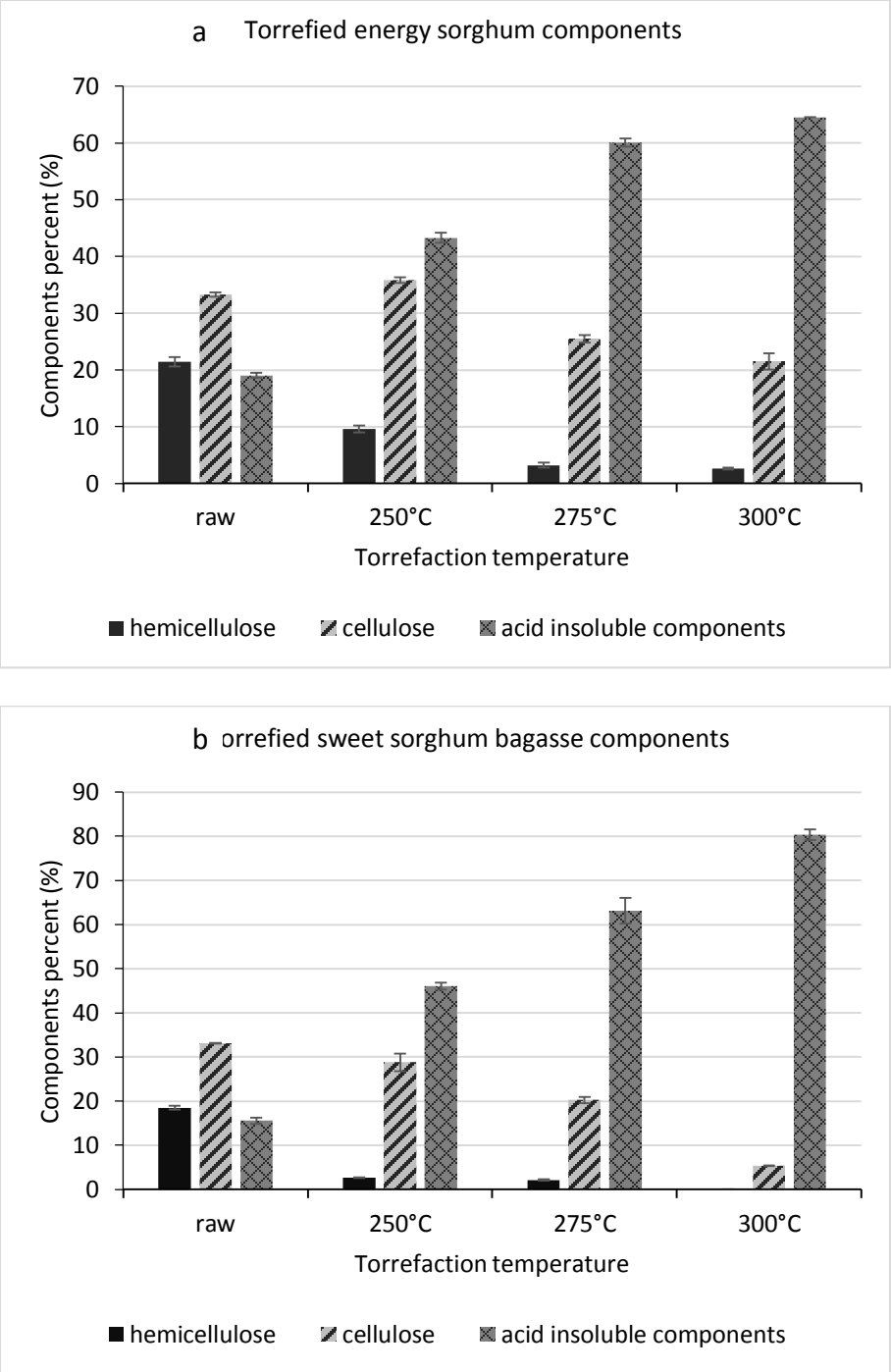


Fig.5.4 Chemical composition analysis of torrefied sorghums

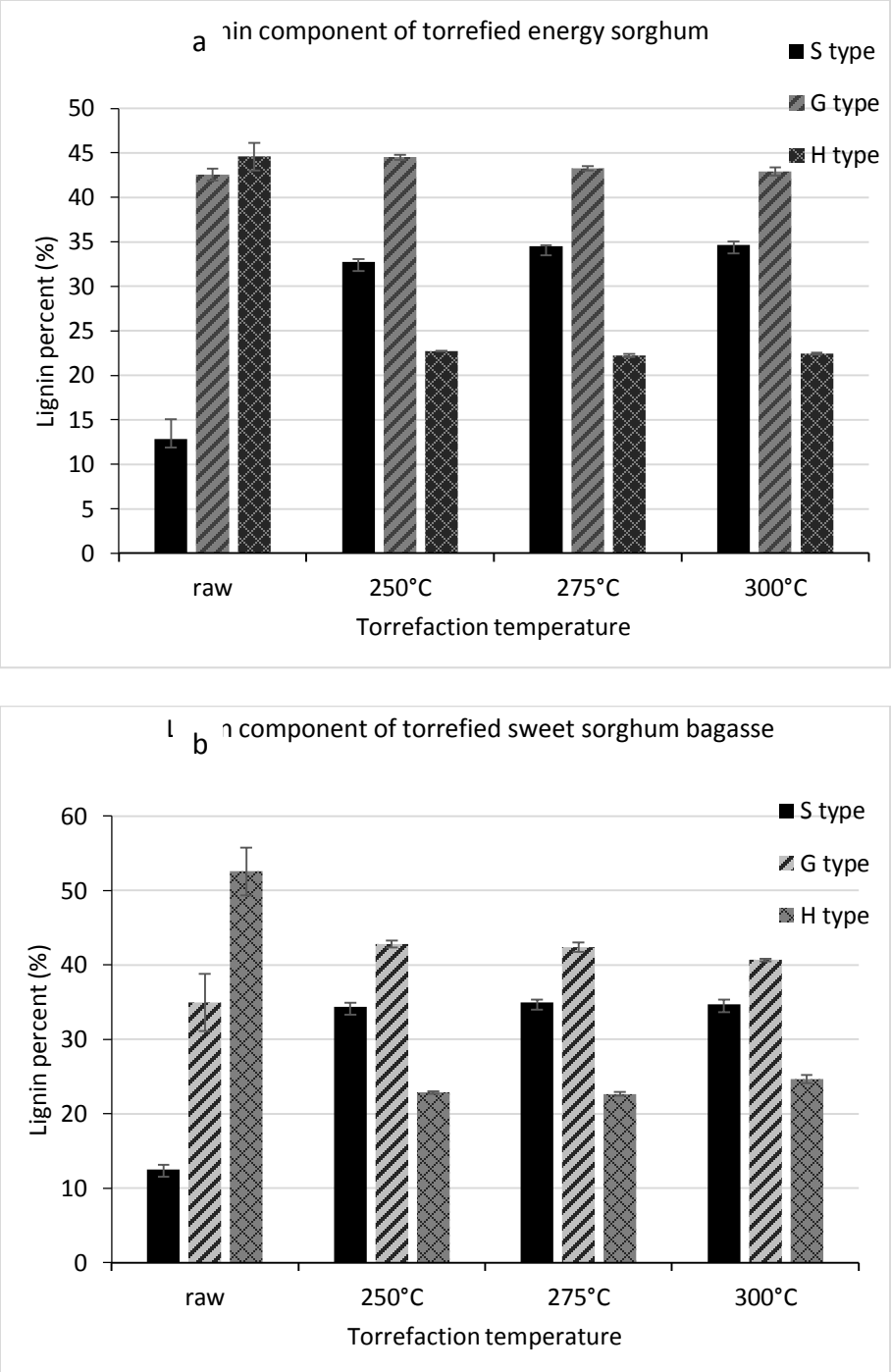


Fig.5.5 Lignin components analysis of torrefied sorghums

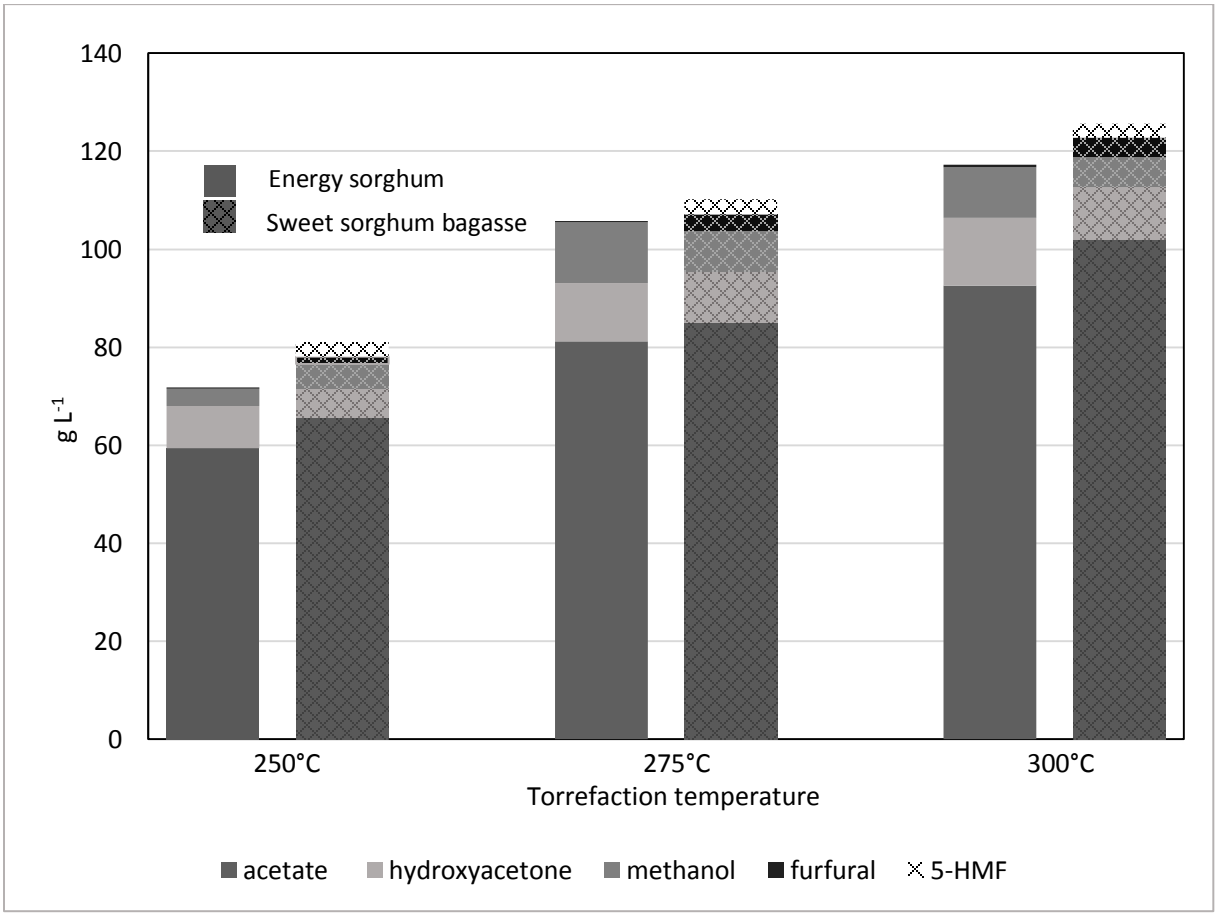


Fig.5.6 Yields of major compounds from aqueous product

## VI. Catalytic Pyro-GC/MS of Torrefied Sorghum with Reduced Red mud and Metal-modified ZSM-5 Zeolites for Aromatic Hydrocarbon Production[4]


### Abstract

Catalytic fast pyrolysis (CFP) has been comprehensively investigated for producing hydrocarbon enriched bio-oil. Zeolites, typically, HZSM-5 and metal-modified ZSM-5 displayed extraordinary catalytic properties for aromatics formation. However, the de-activity of zeolites due to coke formation was many times reported as the limitation of utilizing CFP in large scale. In this study, a coke-formation resistant, economic catalyst, red mud, was reduced and tested for fast pyrolysis through pyro-GC/MS. HZSM-5 and NiZSM-5 were both used as alternative catalysts to compare the components of pyrolytic products. Raw sorghums (sweet sorghum bagasse and energy sorghum) and three torrefied sorghums (at 250°C, 275°C and 300°C) were used as feedstock to study the impacts of torrefaction pretreatment. It was indicated 2,3-dihydro-benzofuran was the dominant compound from raw sorghums and accounted for 26.7 area %, followed by phenols and cyclic ketones. After torrefaction pretreatment, hydrocarbon area content increased approximate 9 folds; benzofurans and cyclic ketones were significantly reduced. When reduced red mud was employed as *in-situ* catalyst, hydrocarbon content reached the top of 10.2 % from torrefied sorghum at 275 °C, which was around 30 times on area % of hydrocarbons from raw sorghum. Cyclic ketones and aldehydes greatly increased with 1.73 and 1.71 times with reduced red mud; however, alcohols and benzofurans dropped 44.3 % and 47.9 % on the area. Phenols were related


[4] Yang Yue, Sudhagar Mani, To be submitted to Energy and Fuel

stable after catalytic pyrolysis with reduced red mud. The catalytic routes of pyrolytic products were also analyzed. It was displayed that red mud promoted the formation of hydrocarbons and cyclic ketones from benzofurans.

***Keywords:*** sorghum, pyro-GC-MS, catalytic fast pyrolysis, torrefation, red mud

## 6.1 Introduction

Lignocellulosic biomass is sustainably available worldwide and considered as a promising resource for fossil fuel alternation with neutral $CO_2$ emission. Fast pyrolysis has attracted increasing attention recently to achieve the conversion of lignocellulosic biomass into biofuels. The liquid fraction of fast pyrolysis product, generally named bio-oil, is a mixture of condensable chemicals from pyrolysis vapor. As the only potential renewable source of hydrocarbon fuels, bio-oil has remarkable advantages, such as negligible content of sulfur and nitrogen, wide availability of feedstock, high conversion efficiency and energy reward, large-scale exploitation and $CO_2$ neutrality (Rezaei et.al., 2014).

However, pyrolysis bio-oil contained a high content of oxygenated compounds, mainly including carboxylic acids, ketones, esters, alcohols, furans and phenols. Although the detailed compositional distribution of bio-oil varies greatly depending on the biomass feedstock, some commonly undesirable combustion properties are thereby exhibited on the basis of bio-oil components, typically the corrosiveness, viscosity and thermal instability. The former two properties challenge the current engines system, and the last one is susceptible to aging with fuel characters deterioration. Those oxygenated compounds are essentially formed through insufficient deoxygenation during thermal depolymerization and decomposition of three major lignocellulosic components: cellulose, hemicellulose and lignin. The presence of high content of above oxygenated compounds impairs the application of bio-oil directly towards drop-in fuels.

Hydrocarbon richened biofuel, derivate from pyrolysis bio-oil, is thereby promptly demanded as an alternative to transportation fuel. High content of hydrocarbons could be yielded through fast pyrolysis when combining with either upgrading process or feedstock pretreatment, such as torrefaction.

The upgrading process could be achieved through hydrodeoxygenation, esterification and catalytic reforming, among which catalytic fast pyrolysis (CFP) is extremely appealing to directly produce hydrocarbons through in-situ catalytic cracking of pyrolysis vapors intermediates (Liu et.al, 2014). Among catalysts, zeolite, especially HZSM-5 and metal modified ZSM-5 has been investigated comprehensively on rejecting oxygen from bio-oil components and producing hydrocarbons through cracking and aromatization reactions. Li et. al., reported the aromatic hydrocarbons yield from Kraft lignin reached 5.2 wt.% with HZSM-5 at the catalyst-to-lignin ratio of 20. (Li et al., 2012). Mihalcik studied the catalytic pyrolysis of various lignocellulosic biomass including hemicellulose, cellulose, lignin, oak, corn cob, corn stover, and switchgrass over five groups of zeolites (H-Mordenite, H-ZSM-5, H-Y, H-Beta, and H-Ferrierite) with pyro-GC/MS and concluded HZSM-5 was the most effective for aromatic hydrocarbons conversion from pyrolytic vapors (approximately 12 wt.%) (Mihalcik et al., 2011). Currently, researches on commercial mesoporous materials are concentrated on the effects of catalyst acidity and shape selectivity of aromatics. Foster et al. found that the concentration of acid sites inside the zeolite is critical for maximizing the aromatic yield with alkylated monoaromatics as favorable products (Foster et.al., 2012). The doping of transition metal into zeolites such as ZSM-5 is another efficient way to fine-tune the active sites, improve hydrothermal stability and increase hydrocarbon yield (Liu et.al., 2014). Iliopoulou reported nickel impregnated ZSM-5 exhibits the capability to adjust both Lewis and Brønsted acid sites. The incorporation of nickel with HZSM-5 zeolite improved oxygen

removal and aromatics selectivity (Iliopoulou et al., 2012). French investigated forty catalysts from 400 to 600 °C and found the highest hydrocarbon yield of 16 wt.%, was achieved with nickel-substituted ZSM-5 at 600 °C from aspen wood (French and Czernik, 2010). Melligan et al. found that Ni cracked large molecular phenolic compounds into light phenols from Miscanthus x giganteus with a Py-GC/MS system. (Melligan et al., 2012) Thangalazhy-Gopakumar et al. modified ZSM-5 reported an enhancement of 17.4 % (carbon yield) on aromatic yield after modified with Ni on HZSM-5 (Thangalazhy-Gopakumar et al., 2012). However, although above catalysts indicated practical and promising capability on aromatics production in laboratory, economic feasibility is a crucial hurdle for their application on commercialization. The significant coke formation during *in-situ* catalytic pyrolysis resulted in the short life of zeolite and metal modified zeolite catalysts, limited their recycle use and increase the cost of CFP (Liu et.al., 2014). Therefore, it is essential to promptly develop a new, economical, robust and efficient catalyst systems to satisfy wide-spread hydrocarbon production through CFP.

Red mud is the solid residue of bauxite industry with the production of 120 megatons/year (Karimi et al., 2014). The high alkalinity of red mud (pH>12) make it environmental hazard and currently no economic remediation approach to address this bauxite mining waste efficiently (Karimi et al., 2014). As a mineralogical complex mixture, red mud contains of multiple potentially active metal oxides such as iron oxide, aluminum oxide, titanium dioxide, magnesium oxide, calcium oxide, silicon oxide, as well as other minor compounds (Yathavan and Agblevor, 2013), among which iron oxide is the major composition and reach 12–60 wt.% depending on its place of origin (Sushil and Batra, 2011). Those metal oxides in red mud were reported to catalytically reduce oxygen content and acidity of the bio-oil through ketonization, condensation, and deoxygenation reactions (Kastner et al., 2015). Therefore, red mud has been investigated as a

potential sacrificial catalyst to replace expensive catalysts due to its very low cost and complement advantages: (i) avoid regeneration process of expensive catalyst after bio-oil upgrading; (ii) with the reduction of oxygenated compounds in bio-oil, the alkalinity of raw red mud is significantly neutralized, thus reduces its environmental deposit hazard; (III) thermal stability and was not susceptible to deactivated by coke for more than 300 hr operation. Karimi et al. studied the capability of red mud on the conversion of alkenes and ketones from carboxylic acids (Karimi et al., 2012, Karimi et al, 2014). Kastner et al. studied continuous catalytic upgrading process of pyrolysis bio-oil over red mud and reported the yield of ketones conversion reached 15-20 mol% from water extracted bio-oil (Kastner et al., 2015). Yathavan and Agblevor compared the catalytic impacts of red mud and HZSM-5 on bio-oil from pinyon – juniper woods and found red mud catalytic bio-oil had a lower viscosity, comparative yields (42-49 wt.%) and heating value (28.6-29.5 MJ/kg) with HZSM-5. The major components of red mud catalytic bio-oil were aromatics, followed by aliphatics and levoglucosan (Yathavan and Agblevor, 2013).

Torrefaction pretreatment, as promising approach to increase bio-oil quality and enhance hydrocarbon content is also comprehensively studied recently. Torrefaction is operated at moderate temperature (240-320°C) under anoxic condition with the products of terrified solid biomass, condensable liquids and non-condensable gasses from raw lignocellulose. During torrefaction, the fibrous structure and tenacity of biomass are destructed (Stelt et al., 2011); oxygen and moisture are remarkably removed from lignocellulose through carboxylation and dehydration reactions. It was reported the torrefaction pretreatment prior to pyrolysis modified the compositional structure of the biomass feedstock and altered pyrolysis behaviors, which finally decreased the contents of acetic acid, hydroxyacetone and furfural, and ameliorated the acidity and stability of bio-oil (Zheng et al., 2013). Neupane et.al., reported the yield of hydrocarbon

precursors, phenol derivate, increased 2.7 folds after torrefaction pretreatment of pinewood at 275 °C for 15 min; when under the catalysis of HZSM-5, hydrocarbon yield reached 35.3 %, 67% higher than non-torrefied pinewood (Neupane et.al., 2015). Additionally, aldehydes, typically formaldehyde and acetaldehyde are active coke precursors and easily form thermal coke during CFP; aldehydes in bio-oil were found to be remarkably removed after torrefaction (Meng et al, 2012) this greatly extended the life span of catalyst.

Most current researches on improving bio-oil quality are either focusing on catalyst screening or the impact of torrefaction pretreatment. There have been few reports to produce hydrocarbons with the combination of torrefaction pretreatment and CFP. In this study, red mud as a coking resistant, sacrificial catalysts was reduced and systematically investigated for pyrolysis hydrocarbon conversion from torrefied sorghums. HZSM-5 and NiZSM-5 were both used as controls to estimate the catalytic capability of reduced red mud on hydrocarbons. Pyro-GC/MS was applied for pyrolytic products analysis. The goals of this study were (i) to investigate the impact of red mud on bio-oil compositional distribution from torrefied biomass; (ii) attempting to understand the catalytic pyrolysis reaction pathways of torrefied biomass under reduced red mud.

## 6.2 Materials and Methods

### 6.2.1 Biomass torrefaction pretreatment and characterization analysis

Energy sorghum and sweet sorghum bagasse used in this study were obtained from Fort Valley State University, Fort Valley, Georgia, USA. Both sorghums were chopped into 10 mm to 240 mm in length and pre-dried before torrefaction pretreatment. Three torrefaction temperatures were separately employed at 250, 275 and 300 °C with holding time of 30 min for both raw sorghums at the heating rate of 1.15°C /min. Nitrogen was continuously passed through the reactor during the torrefaction to avoid ignition with the influx rate of 2 ppl. After torrefaction, the

torrefied sorghums were collected and grinded into 0.2mm. The structural hydrocarbons and lignin contents of raw and torrefied sorghums were analyzed with wet chemical analysis according to NREL standard protocol (Selig et al., 2008).

6.2.2 Catalyst preparation and characterization analysis

HZSM-5 used in this studied was prepared from by calcining commercially available zeolite $NH_4$ZSM-5 (Zeolyst International, CBV 5524 G) at 550°C for 4 h in air. Ni modified ZSM-5 was prepared with incipient wetness impregnation method from the precursor of $Ni(NO_3)_2 \cdot 6H_2O$ from Sigma-Aldrich. 28.19 g of $Ni(NO_3)_2 \cdot 6H_2O$ was weighted and mixed thoroughly with 20 ml water -ethanol solution (water: ethanol (v/v) = 9:1) until completely soluble. 108.1 g of granulated HZSM-5 was used to absorb above solution under magnetic stir of 30 min. The prepared NiZSM-5 were dried in oven at 105°C overnight and calcined in air at 500°C for 3 hr. Before CFP, the dried powders of NiZSM-5 were reduced by passing 5% $H_2$ with the balance of $N_2$ in the flow rate of 100 mL/min at 500°C for 2 h.

Red mud was obtained from Rio Tinto (Alcan, Canada) in the form of slurry. After drying at 105 °C for 20 hr, the solid red mud was crushed and sieved with the particle sizes less than 0.2mm. Before CFP, the red mud was *in-situ* reduced respectively at 300°C and 500°C with $H_2$ flow of 100 mL/min for 20 hours on Parr continuous packed bed reactor system (4871 process controller and 4875 power controller, Parr instrument company, USA).

The characterizations of HZSM-5, NiZSM-5 and reduced red mud were determined on surface area (BET method), pore volume and mesoporous size distribution (BJH method) with surface area analyzer (Quantachrome Autosorb, model 1-C, Boynton Beach, FL) by measuring $N_2$ adsorption/desorption isotherms at −196°C. The characterization of each catalyst was listed in Table 6.1

6.2.3 Quantity analysis with pyro-GC/MS

Non-catalytic and catalyst Fast pyrolysis experiments were both implemented with pyro-GC/MS to investigate the effect of catalyst on hydrocarbon conversion in bio-oil. The pyro-GC/MS was carried out on a vertical furnace Frontier lab pyrolyzer (PY-2020 iD) connecting with HP-5ms Capillary Column (30m x 0.25um x 0.25mm) (Agilent Technologies Inc) and a 6890N GC system. The GC/MS interface temperature was maintained at 280°C. The GC oven temperature program was initially set at 50 °C for 2 min; then ramped to 280 °C with the heating rate of 5 °C /min and kept constantly for 53 min. Helium was employed as the carrier gas with the flow rate of 1 ml/min and the split ratio was set at 50:1.

In a typical pyro-GC/MS experiment, approximate 2.0 mg of raw sorghums or torrefied sorghums were introduced into the pyrolysis metal sample cup. For CFP, the ratio of sorghums to catalyst was adjusted to be either 1:1 or 1:5 (w/w). The sorghum and catalyst were completely mixed before loading into the sample cup to ensure the pyrolysis vapor experienced in-situ catalysis over catalyst before transferring into GC/MS. Three replications of each sample were pyrolyzed with single-shot at 500 °C for 12 sec. The peaks were identified with NIST mass spectral library. The average area percentage and standard deviation of each peak were calculated to estimate the content of pyrolytic product. As the quantitative analysis of pyrolytic products was not able to be obtained with pyro-GC/MS, peak area % value of each compound was employed to indicate the relative contents of the identified compounds (Lu et al., 2013).

6.2.4 Statistical analysis

The compositions of pyrolytic products were measured with three replication. The average area contents of each groups from pyrolytic vapors were summarized in the figures as the results with standard deviation

## 6.3 Results and Discussions

Raw sorghums were firstly pyrolyzed and their pyrolytic products were analyzed to study the impacts of torrefaction and *in-situ* catalytic pyrolysis on aromatic hydrocarbon conversion. The amounts of pyrolytic products were reported in the form of area percentage from chromatograph. There were more than one hundred and sixty compounds identified from pyrolytic products with MS library. Approximately, top 20 compounds with largest peak areas accounted for more than 90% of total peak areas. Therefore, the compositional distribution of pyrolytic product was investigated through the analysis of top 20 compounds. These compounds were mainly categorized into 9 groups depending on their crucial functional groups: straight ketones, cyclic ketones, aldehydes, esters, alcohols, furans, phenols, benzofurans, hydrocarbons, and fatty acids. Among above groups, hydrocarbons were desirable products. Phenols and cyclic ketones were value-added chemicals. Straight ketones and aldehydes were highly oxygenated compounds and thermal instable during the storage (Iliopoulou, 2012).

### 6.3.1 Impact of torrefaction pretreatment on pyrolytic products

Torrefaction pretreatment destructed the tenacity of lignocellulosic structure, reduced O/C ratio in pyrolysis feedstock, and enhanced hydrocarbon yield in pyrolysis bio-oil (Neupane et al. 2005). After torrefaction, the contents of structural carbohydrates and lignin in biomass were significantly altered. The majority of hemicellulose and a small fraction of lignin were thermally decomposed with mild torrefaction. Cellulose started to decompose after 275 °C; while most lignin was thermal tolerance at torrefaction temperature. The contents of hemicellulose, cellulose and lignin in torrefied sorghum were regulated with three torrefaction temperatures (250, 275 and 300 °C). The components of torrefied sorghums were reported previously in table 6.2. Hemicellulose

was almost completely removed after 275 °C. No significant difference was indicated on structural carbohydrates and lignin content between torrefaction at 275 and 300 °C.

Raw sorghums and torrefied sorghums were employed as feedstock in non-catalytic pyrolysis. The compositional distributions of pyrolytic vapors from raw and torrefied sorghums were indicated in Fig.6.1 and Fig.6.2 showed the major chemicals in vapor from pyro-GC/MS graph. When raw ES was used as feedstock, 2,3-Dihydro-benzofuran was the dominant compound and accounted for 26.7 area %, followed by phenols and cyclic ketones, which respectively took up to 22.3 and 13.1 area %. 2-Methoxy-4-vinylphenol, 2-methoxy-phenol and 3-tert-butyl-4-hydroxyanisole were the major phenols products derived from lignin units thermal decomposition. These three phenols compounds took up to 70.0 % of identified phenols peak areas. 2-Hydroxy-2-cyclopenten-1-one and 2-hydroxy-3-methyl-2-cyclopenten-1-one were dominant cyclic ketones with the percentage of 57.7 % and 36.3 % of total cyclic ketones. These 2-cyclopenten-1-one ketones were converted from furans, such as furfural and tetrahydro-2-furanmethanol, which were decomposed from cellulose and hemicellulose through either levoglucosan or xylose. The hydrocarbon amount was as low as 0.34 area % in the form of cyclanes.

After torrefaction, the identified compounds in pyrolytic vapor were approximately same as those from non-torrefied samples (Fig.6.2). As regard to the amount of each group, compared to pyrolytic products from raw ES, straight ketones, cyclic ketones and benzofurans decreased nearly 100%, 31.6 % and 89.0 % after torrefaction at 275 °C. This was because the contents of structural carbohydrates, typically hemicellulose, were dramatically removed from torrefied ES after 275°C; this limited the conversion of 2,3-dihydro-benzofuran, 2-cyclopenten-1-one derivate and 1-hydroxy- 2-propanone from furfurals and tetrahydrofuran.

Aldehyde, phenols, alcohols and hydrocarbons respectively increased 48.7 %, 44.0 %, 1.03 folds and 3.48 times on area percentage from torrefied ES at 250 °C. Remarkable reduction occurred on benzofurans with 65.5 % and fatty acids with 39.2 %. No significant changes took place on the contents of straight ketones, cyclic ketones, esters and furans. When torrefied at the temperature of 275 °C and 300 °C, above trends of benzofurans, phenols and hydrocarbons amplified. Same as pyrolytic vapor from raw ES, 2,3-dihydro-benzofuran was still the only detected benzofurans, but with 10 times less on area percentage. All identified phenols were modified with methoxy group, derivate from lignin unit. 2-methoxy phenol became the dominant phenol from torrefied ES at 275 °C and 300 °C, instead of 2-methoxy-4-vinylphenol, which was obtained with largest area % from raw ES and torrefied ES at 250 °C. Hydrocarbon increased 8.97 to 9.35 times after torrefaction at 275 °C and 300 °C. Toluene, ethyl-cyclopropane and hexene were three major hydrocarbons, found with equal area percentage. Additionally, there was no significant difference on the contents of benzofurans, phenols and hydrocarbons between torrefaction temperature at 275 and 300 °C. This was resulted from approximate contents of structural carbohydrates and lignin in torrefied ES at 275 and 300 °C. Straight ketones and cyclic ketones indicated dramatically declined after torrefaction at 275 and 300 °C. After 275 °C, no straight ketones were detected; meanwhile, around 26.4 area % to 31.6 area % of cyclic ketones were reduced. Aldehydes display a similar trend of cyclic ketones with torrefaction pretreatment. This was resulted from the removal of hemicellulose during torrefaction, which suppressed the conversion of cyclic ketones and small molecular secondary products, such as butanedial and 1-hydroxy- 2-propanone, from intermediates of furans. However, the content of furan compounds indicated slight decreased at torrefaction of 250 °C, then increased around 66.0 % to 43.3 % respective after torrefaction of 275 °C and 300 °C. Another important product from furans was

alcohols. Cyclopentanol was the only found alcohol from pyrolytic vapor, the content of which was related stable after torrefaction pretreatment, with the enhancement of 1.03 to 1.42 folds from raw ES. Generally, torrefaction after 275 °C remarkably suppressed the formation of high oxygenated compounds, such as straight ketones and aldehydes, reduced the content of byproduct of benzofurans and cyclic ketones, and obviously promoted the conversion of hydrocarbons and its precursor of methoxy and alkylated phenols. Therefore, it benefits the component distribution in pyrolytic products. Meanwhile, the greatly increased alcohols were non-negligible.

6.3.2 Catalytic pyrolytic products analysis from raw sorghums

Iron and its oxidase were the main component, accounted for around 40 wt.% of red mud, mainly acted for *in-situ* catalytic effect of ES pyrolysis. There were approximate 50 wt. % of magnetite and 50 wt.% of 0-valent Fe in the reduced red mud. Comparing with HZSM-5 and NiZSM-5, the catalytic effect of reduced red mud on raw ES were indicated on Fig.6.3 and Fig.6.4. When the ratio of catalyst to biomass was 1:1, reduced red mud did not show significant difference between catalytic pyrolytic vapors and non-catalytic pyrolytic vapors on area percentages of straight ketones, aldehydes, furans, alcohols, benzofurans and phenols from raw ES. Whereas, the contents of cyclic ketones, hydrocarbon and fatty acids indicated obviously difference, the former reduced 32.7% on area %, the latter two respectively increased 1.56 times and 26.0 %. Additionally, the dominant compounds of above groups did not change when reduced red mud was employed. Compared to HZSM-5 and Ni-ZSM5 as catalysts, the desirable product of hydrocarbon with reduced red mud was far from competition, respectively 76.7 times less than HZSM-5 and 31.2 times lower than NiZSM-5. Most yielded hydrocarbons under reduced red mud were toluene and cyclanes. There was no straight ketones, aldehydes, alcohols and furans detected in pyrolytic vapor when catalyzed with HZSM-5 and Ni-ZSM5. Approximately, 10.6 area % of

cyclic ketones were identified from NiZSM-5 catalytic products, 2-cyclopenten-1-one and its methoxy modified compounds of 2-hydroxy-2-cyclopenten-1-one were the only two detected cyclic ketones with GC-MS. However, no cyclic ketones obtained from HZSM-5 catalytic products. The hydrocarbon yielded from HZSM-5 catalyzed vapor was 2.41 folds of that from NiZSM-5 catalyzed product. Toluene, p-xylene and 1-ethyl-2-methyl-benzene were major aromatics in both catalytic products, no alkylated hydrocarbons or cyclanes were detected. The hydrocarbon distribution was showed in Fig.6.5. Additionally, rather than completely converted into BTX aromatics, 17.1 area % of benzofurans and 32.5 area % of phenols remained after NiZSM-5 catalysis. This reflected the catalytic effect of HZSM-5 was stronger than Ni-ZSM5.

When the ratio of catalyst to biomass increased to 1:5, hydrocarbons content under reduced red mud, HZSM-5 and NiZSM-5 showed remarkable enhancement, respectively 3.48, 1.47 and 3.54 folds from that at the ratio of 1:1. The hydrocarbon composition was not dependent on the catalyst to biomass ratio. Under the catalysis of reduced red mud, besides hydrocarbons, phenols and benzofurans both showed enhancement of 52.0 % and 29.9 % on the area; whereas, straight ketones, aldehydes, alcohols and furans all displayed declined trends; The content of cyclic ketones kept stable with additional reduced red mud. As regard to pyrolytic products under HZSM-5 and Ni-ZSM5 with the biomass to catalyst ratio of 1:5, the most obvious change was the disappearance of cyclic ketones and phenols. Benzofurans also dropped nearly to 1%. Basically, the increased catalyst to biomass ratio promoted the conversion of hydrocarbons, and significantly declined the byproducts when raw ES were used as feedstock.

6.3.3 Pyrolytic products analysis from the combination of torrefaction and catalytic fast pyrolysis

It has been indicated both torrefaction pretreatment and reduced red mud benefited hydrocarbons conversion from raw sorghums. In this section, the impact of the combination of torrefaction and *in-situ* catalytic pyrolysis under reduced red mud were estimated.

It was indicated from Fig.6.5, when catalyzed with reduced red mud (ratio of 1:1), the pyrolytic products from torrefied ES at 250 ℃ showed similar compounds as non-catalytic pyrolytic products. The effect of reduced red mud was to regulate the content of each compound. For example, the straight ketones, cyclic ketones and aldehydes were important products from furans; the area contents of above group compounds were greatly increased with 1.73, 1.71 and 2.08 times. However, other products of alcohols and benzofurans from furans dropped 44.3 % and 47.9 % on the area. Phenols were related stable after catalytic pyrolysis with reduced red mud, however, there was no hydrocarbon detected when reduced red mud was employed. Fatty acids were found increased 64.8 %, probably reduced red mud could promote the formation of fatty acids from residual lipids in torrefied ES. When HZSM-5 was applied, it was obviously observed that all compounds in the groups of straight ketones, cyclic ketones, aldehydes, alcohols, furans and fatty acids were converted into hydrocarbons. Benzofurans and phenols area contents were decreased 28.4% and 71.7%, whereas, hydrocarbon area content increased 54.77 folds compared non-catalytic products from torrefied ES at 250 ℃. NiZSM-5 showed similar trends on above compounds but with less catalytic capability than HZSM-5. This could be confirmed that still 2.58% of cyclic ketones were remaining in the pyrolytic product.

When torrefied ES at 275℃ and 300 ℃ were used as feedstocks, the majority of catalytic pyrolytic products were identified the same as those from torrefied ES at 250℃; such as butanedial

of aldehydes, 2-cyclopenten-1-one and 2-hydroxy-2-cyclopenten-1-one of cyclic ketones, 2-methoxy-phenol, 2-methoxy-4-vinylphenol and 2,6-dimethoxy-phenol of phenols, n-Hexadecanoic acid of fatty acids. When reduced red mud was used as catalyst, the change of compounds in catalytic vapors from torrefied ES at 275℃ and 300 ℃ exactly followed that same trend of those compounds from torrefied ES at 250 ℃. However, compared to products from torrefied ES at 250 ℃, the hydrocarbon area content reached the top of 10.2 % from torrefied ES at 275 ℃, then decreased a little to 8.6 % from torrefied ES at 300 ℃. Another most impacts of reduced red mud on catalytic pyrolysis of torrefied ES was the enhancement of cyclic ketones and the decline of methoxy phenols. Actually, the cyclic ketone and methoxy phenols were the dominant components from catalytic vapors of torrefied ES, respectively from cellulose and lignin thermal decomposition. It was also observed the area content of cyclic ketones and phenols were related stable from torrefied ES at various temperature, respectively around 23.3 area % and 31.4 area %. The reduced 29.5% of phenols from non-catalytic pyrolytic products was much more than the enhancement of 10.2 % on hydrocarbon with reduced red mud. This indicated a possible pathway that cyclic ketones could be converted from methoxy phenols. It was also found area contents of alcohols dropped with the torrefaction severity, however, its precursors of furans, such as 2-propyl-tetrahydrofuran and tetrahydro-2-furanmethanol, increased 2.92 folds from 275 ℃ torrefied ES and then dropped 20.3 % from 300 ℃ torrefied ES. Mainly decomposed from cellulose, furans content increased resulting from the suppression of benzofuran and alcohols, the former was not able to detect from 275 ℃ torrefied ES. Compared to that from 250℃ torrefied ES, fatty acids area content decreased 26.9 % from 275 ℃ torrefied ES, then increased 78.8% from 300℃ torrefied ES. It was deduced rather than lipids from torrefied ES, the fatty acids, especially n-hexadecanoic acid were formed from other routes, however, more study was required

to testify this possible pathway. Generally, torrefaction at 275 ℃ was illustrated most effectively on hydrocarbon conversion. Meanwhile, the other two major components in pyrolytic products were 2-cyclopenten-1-one derivate and methoxy phenols, which were potentially used as value-added compounds, and increased the value of red mud as catalyst. When the ratio of biomass to catalyst was 1:5, the only difference was a remarkable enhancement on 2-methoxy-phenol, which reached nearly 50 area %, however, no obvious change on hydrocarbons. Thereby, there was no necessary to apply the ratio of 1:5 for hydrocarbon conversion.

Compared to reduced red mud, HZSM-5 and Ni-ZSM5 showed dramatically increased on hydrocarbon conversion with the area % of 93.0 and 97.0 area %. Only aromatics were identified, with the same dominant compounds of toluene, p-xylene and 1-ethyl-2-methyl-benzene from torrefied ES at 275℃ and 300 ℃. It was also observed around 2.0 area % of pyrolytic product was occupied by benzofurans from torrefied ES at 275℃ with HZSM-5 and Ni-ZSM5. The compositional distribution of pyrolytic products with reduced red mud, HZSM-5 and NiZSM-5 from torrefied ES was indicated in Fig. 6.6.

## 6.4. Conclusions

Catalytic pyrolysis is a promotion approach to convert lignocellulosic biomass into bio-oil. Current research advocated the feasibility of up-scale bio-oil production by investigating various pretreatment approaches and searching appropriate catalyst. It has indicated in this study that the product of aromatic hydrocarbons was both improved by torrefaction pretreatment and reduced red mud. Torrefaction increased the production of hydrocarbon through altering the composition of lignocellulose feedstock, which ultimately accumulated lignin derivate and promoted the formation of hydrocarbon through phenols. Reduced red mud was testified with moderate catalytic effect on hydrocarbon production, the area content of hydrocarbon reached 11 %, accompanying

with main pyrolytic products of cyclic ketones. It was indicated the presence of reduced red mud significantly promoted the formation of cyclic ketones from phenols. The mechanism of this reaction involved the magnetite and 0-valent of iron. The application of red mud on catalytic pyrolysis aimed for producing multiple value-added compounds, especially 2-Cyclopenten-1-one and 2-methoxy-phenol, rather than aromatics alone. The proposed catalytic pyrolytic pathway from lignocellulosic biomass was showed in Fig. 6.7.

References

Foster, A. J., Jae, J., Cheng, Y.T., Huber, G.W. and Lobo, R. F. Optimizing the aromatic yield and distribution from catalytic fast pyrolysis of biomass over ZSM-5. Appl. Catal., A, 2012, 423–424, 154–161.

French, R. and Czernik, S. Catalytic pyrolysis of biomass for biofuels production, Fuel Processing Technology, 2010, 91, 25–32

Iliopoulou, E.F., Stefanidis, S.D., Kalogiannis, K.G., Delimitis, A., Lappas, A.A., Triantafyllidis, K.S. Catalytic upgrading of biomass pyrolysis vapors using transition metal-modified ZSM-5 zeolite." Applied Catalysis B: Environmental 2012, 127: 281-290.

Karimi, E., et al. Synergistic co-processing of an acidic hardwood derived pyrolysis bio-oil with alkaline Red Mud bauxite mining waste as a sacrificial upgrading catalyst. Applied Catalysis B: Environmental. 2014. 145: 187-196.

Karimi, E., Tiexeria, I. F., Ribeiro, L. P., Gomez, A., Lago, R. M., Penner, G., Schlaf, M. Ketonization and deoxygenation of alkanoic acids and conversion of levulinic acid to hydrocarbons using a Red Mud bauxite mining waste as the catalyst. Catalysis Today. 2012. (190), 73-88.

Kastner, J. R., Hilten, R., Weber, J. W., McFarlane, A. R., Hargreaves, J. S. J., & Batra, V. S. Continuous catalytic upgrading of fast pyrolysis oil using iron oxides in red mud. RSC Advances, 2015, 5, 29375-29385.

Liu, C., Wang, H., Karim, A.M. , Sun, J., Wang, Y. Catalytic fast pyrolysis of lignocellulosic biomass. Chemical Society Reviews 2014, 43(22): 7594-7623.

Melligan, F., Hayes, M. H. B., Kwapinski, W. and Leahy, J. J. Hydro-Pyrolysis of Biomass and Online Catalytic Vapor Upgrading with Ni-ZSM-5 and Ni-MCM-41. Energy Fuels, 2012, 26, 6080–6090.

Lu, Q., Zhang, Z., Yang, X., Dong, C., Zhu, X. Catalytic fast pyrolysis of biomass impregnated with $K_3PO_4$ to produce phenolic compounds: Analytical Py-GC/MS study. Journal of Analytical and Applied Pyrolysis 2013, 104: 139-145.

Meng, J., Park, J., Tilotta, D., Park, S. The effect of torrefaction on the chemistry of fast-pyrolysis bio-oil. Bioresource Technology. 2012. 111: 439-446.

Neupane, S., Adhikari, S., Wang, Z., Ragauskas, A. J. and Pu, Y. Effect of torrefaction on biomass structure and hydrocarbon production from fast pyrolysis. Green Chemistry. 2015, 17(4): 2406-2417.

Rezaei, P. S., Shafaghat, H., Daud, W.M.A.W. Production of green aromatics and olefins by catalytic cracking of oxygenate compounds derived from biomass pyrolysis: A review. Applied Catalysis A: General 2014. 469: 490-511.

Selig, M., Weiss, N., Ji, Y., 2008. In: Laboratory Analytical Procedure No. TP-510-42629. National Renewable Energy Laboratory, Golden, CO.

Sushil, S. and Batra, V. S.J. Characterization of Indian red mud for catalytic application. Solid Waste Technol. Manage. 2011,37, 188–196.

Thangalazhy-Gopakumar, S., Adhikari, S. and Gupta, R. B. Catalytic pyrolysis of biomass over H+ ZSM-5 under hydrogen pressure. Energy Fuels, 2012, 26, 5300–5306.

Yathavan, B. K. and F. A. Agblevor. Catalytic Pyrolysis of Pinyon–Juniper Using Red Mud and HZSM-5. Energy & Fuels 2013, 27(11): 6858-6865.

Zheng, A., Zhao, Z., Chang, S., Huang, Z., Wang, X., He, F., Li, H. Effect of torrefaction on structure and fast pyrolysis behavior of corncobs. Bioresource Technology. 2013, 128: 370-377.

Table 6.1. Characterizations of pyrolysis catalysts

| Catalyst | surface area [$m^2/g$] | average pore radius [Å] | pore volume [$cm^3/g$] |
|---|---|---|---|
| HZSM-5 | 345 | 10.8 | 0.19 |
| NiZSM-5 | 355.9 | 16.98 | 0.1511 |
| Reduced red mud at 300°C | 30.7 | 31.26 | 0.024 |
| Reduced red mud at 500°C | 22.76 | 11.48 | 0.0065 |

Surface area, pore size distribution, and pore volume determined by BET/BJH

Table 6.2. The components of torrefied sorghums

| Biomass | Components content [wt.%] | | |
|---|---|---|---|
| | hemicellulose | cellulose | Acid insoluble compounds (manly lignin) |
| | | Energy sorghum | |
| Raw | 21.44[a] | 33.24[a] | 19.04[a] |
| Torrefied at 250 °C | 9.58[b] | 35.82[a] | 43.29[b] |
| Torrefied at 275 °C | 3.19[c] | 25.52[b] | 60.10[c] |
| Torrefied at 300 °C | 2.64[c] | 21.50[b] | 64.50[c] |
| | | Sweet sorghum bagasse | |
| Raw | 18.50[a] | 33.15[a] | 15.56[a] |
| Torrefied at 250 °C | 2.65[b] | 28.79[a] | 46.10[b] |
| Torrefied at 275 °C | 2.14[b] | 20.26[b] | 63.15[c] |
| Torrefied at 300 °C | 0[b] | 5.37[c] | 80.34[d] |

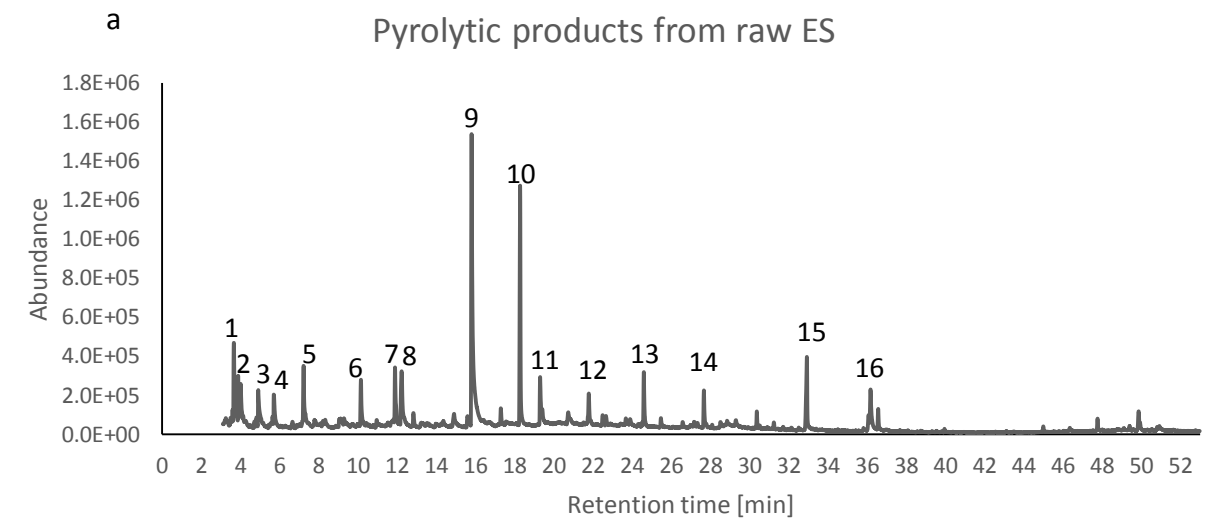


(1) 1-hydroxy-2-propanone, (2) Butanedial, (3) furfural, (4) 1-(acetyloxy)-2-propanone, (5) 2-hydroxy-2-cyclopenten-1-one, (6) 2-hydroxy-3-methyl-2-cyclopenten-1-one, (7) 2-methoxy-phenol, (8) cyclopentanol, (9) 2,3-dihydro-benzofuran, (10) 2-methoxy-4-vinylphenol, (11) 2,6-dimethoxy-phenol, (12) 2-methoxy-4-(1-propenyl)-Phenol, (13) 3-tert-butyl-4-hydroxyanisole, (14) 2,6-dimethoxy-4-(2-propenyl)-phenol, (15) n-hexadecanoic acid, (16) cis-Vaccenic acid

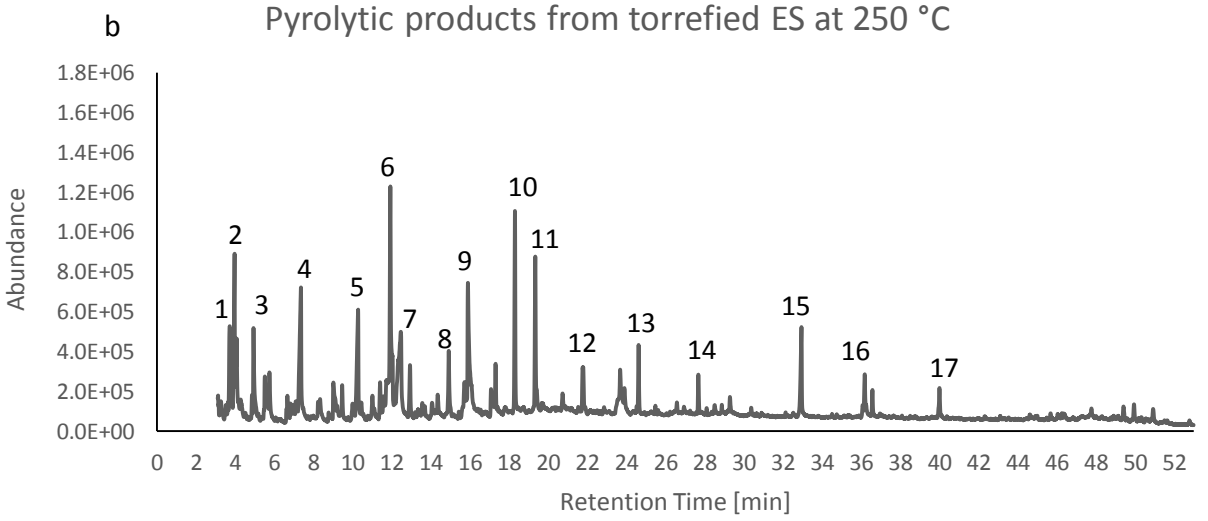


(1) 1-hydroxy-2-propanone, (2) Butanedial, (3) furfural, (4) 2-hydroxy-2-cyclopenten-1-one, (5) 2-hydroxy-3-methyl-2-cyclopenten-1-one, (6) 2-methoxy phenol, (7) cyclopentanol, (8) 2-methoxy-4-methyl-phenol, (9) 2,3-dihydro-benzofuran, (10) 2-methoxy-4-vinylphenol, (11) 2,6-dimethoxy-phenol, (12) 2-methoxy-4-(1-propenyl)-Phenol, (13) 3-tert-butyl-4-hydroxyanisole, (14) 2,6-dimethoxy-4-(2-propenyl)-phenol, (15) n-hexadecanoic acid, (16) cis-Vaccenic acid, (17) (Z)-9-Octadecenamide

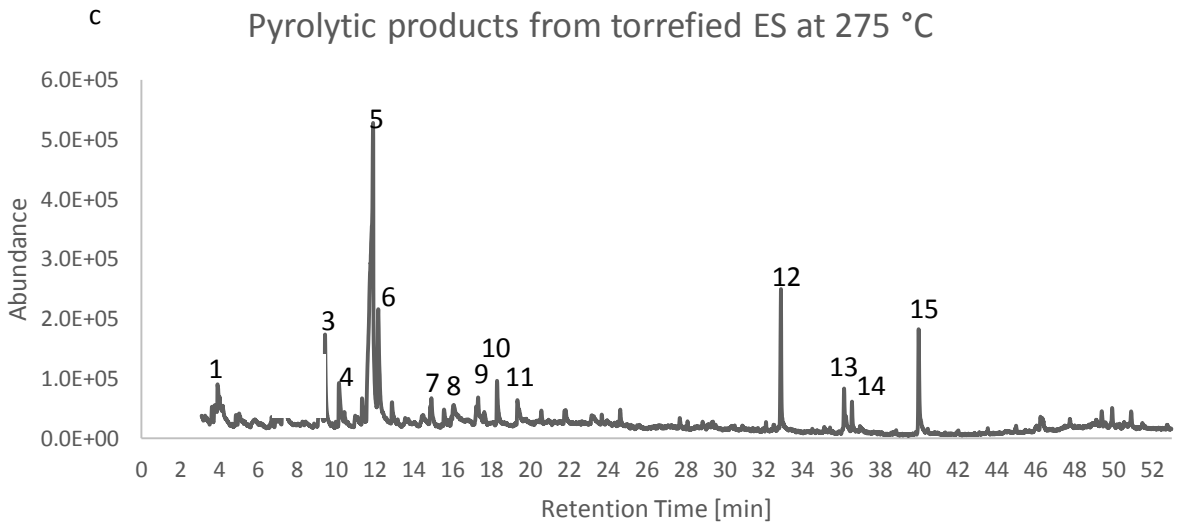


(1)Butanedial, (2) 2-hydroxy-2-cyclopenten-1-one, (3) 2-propyl-tetrahydrofuran, (4) 2-hydroxy-3-methyl-2-cyclopenten-1-one, (5) 2-methoxy phenol, (6) cyclopentanol, (7) 2-methoxy-4-methyl-phenol, (8) 2,3-dihydro-benzofuran, (9) 4-ethyl-2-methoxyphenol, (10) 2-methoxy-4-vinylphenol, (11) 2,6-dimethoxy-phenol, (12) n-hexadecanoic acid, (13) cis-Vaccenic acid, (14) octadecanoic acid, (15) (Z)-9-Octadecenamide

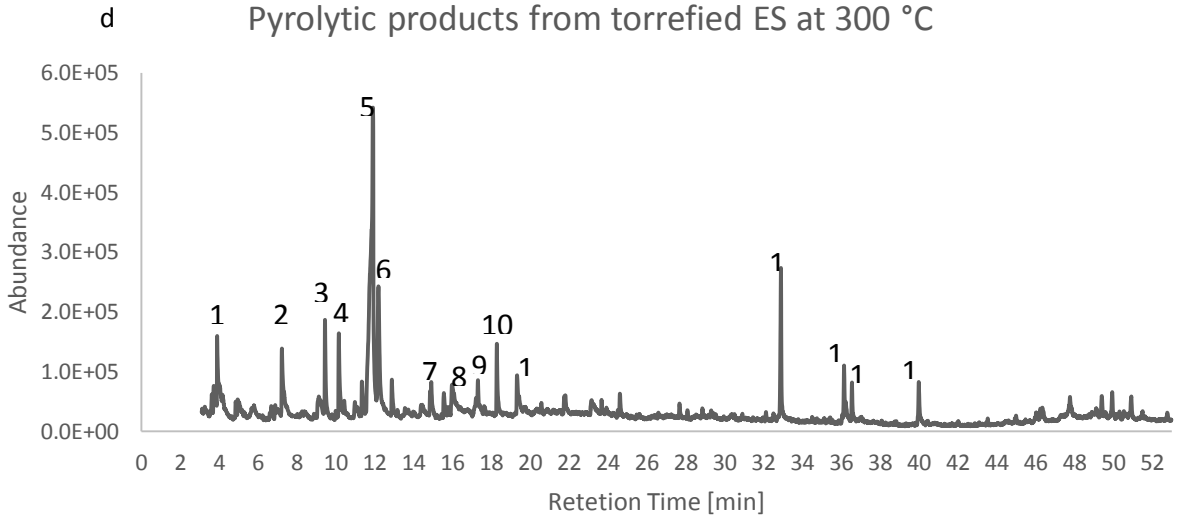


(1)Butanedial, (2) 2-hydroxy-2-cyclopenten-1-one, (3) 2-propyl-tetrahydrofuran, (4) 2-hydroxy-3-methyl-2-cyclopenten-1-one, (5) 2-methoxy phenol, (6) cyclopentanol, (7) 2-methoxy-4-methyl-phenol, (8) 2,3-dihydro-benzofuran, (9) 4-ethyl-2-methoxy-phenol, (10) 2-methoxy-4-vinylphenol, (11) 2,6-dimethoxy-phenol, (12) n-hexadecanoic acid, (13) cis-Vaccenic acid, (14) octadecanoic acid, (15) (Z)-9-Octadecenamide

Fig.6.1 Main compounds from pyrolytic vapors from raw and torrefied energy sorghum

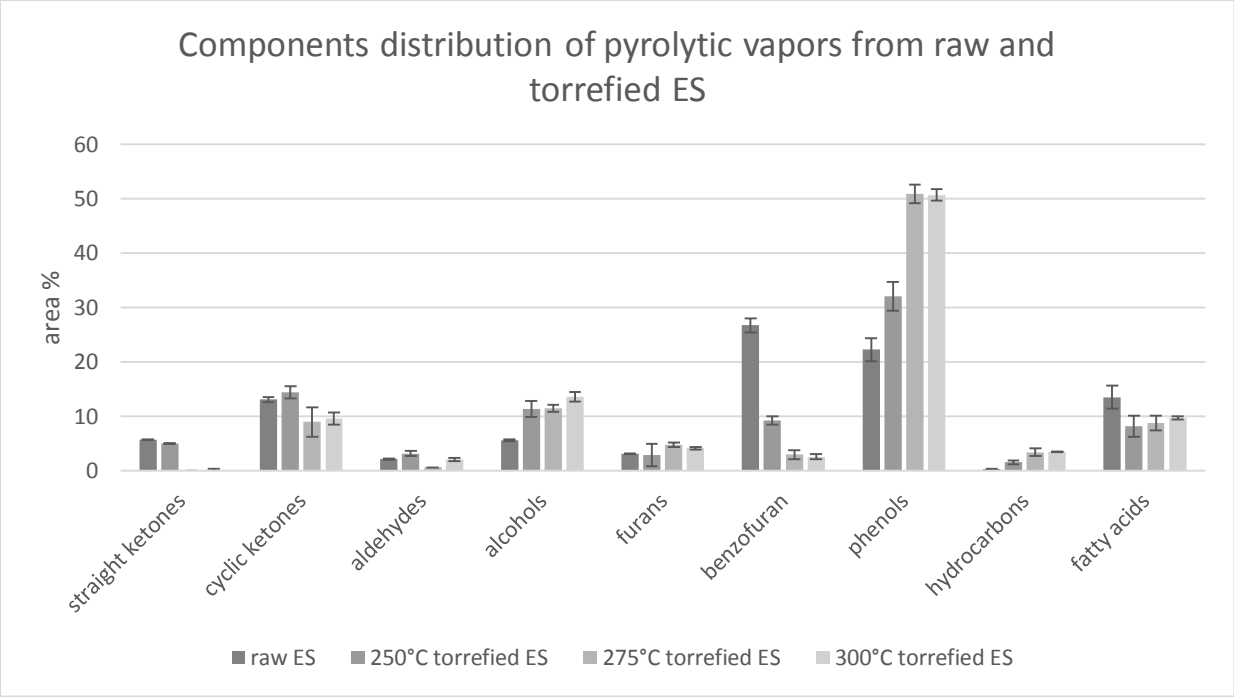


Fig.6.2 The components distribution of pyrolytic vapors from raw and torrefied ES

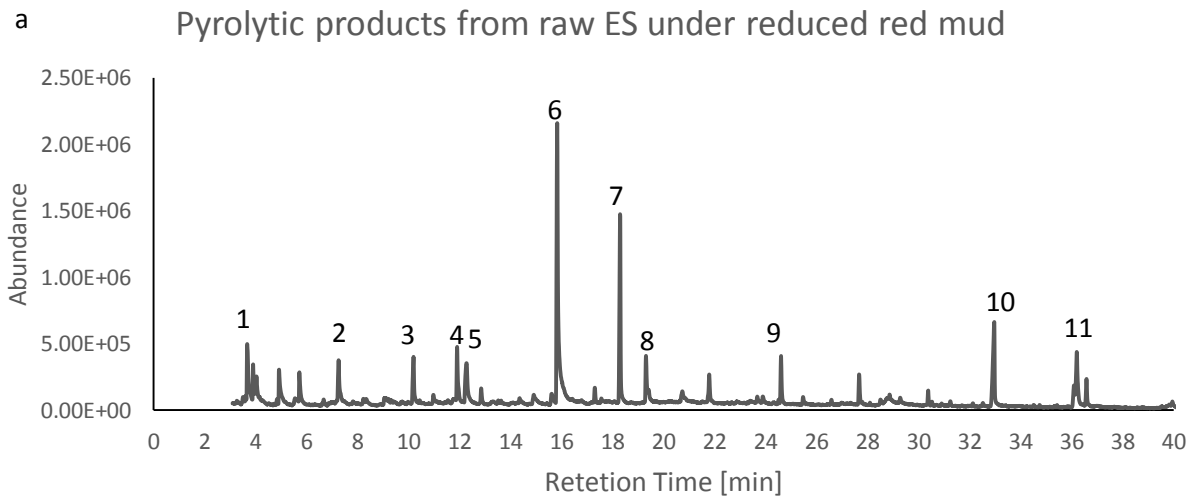


(1) 1-hydroxy-2-butanone, (2) 2-hydroxy-2-cyclopenten-1-one, (3) 2-hydroxy-3-methyl-2-cyclopenten-1-one, (4) 2-methoxy-phenol, (5) cyclopentanol, (6) 2,3-dihydro-benzofuran, (7) 2-methoxy-4-vinylphenol, (8) 2,6-dimethoxy-phenol, (9) 3-tert-butyl-4- hydroxyanisole, (10) n-hexadecanoic acid, (11) 6-Octadecenoic acid

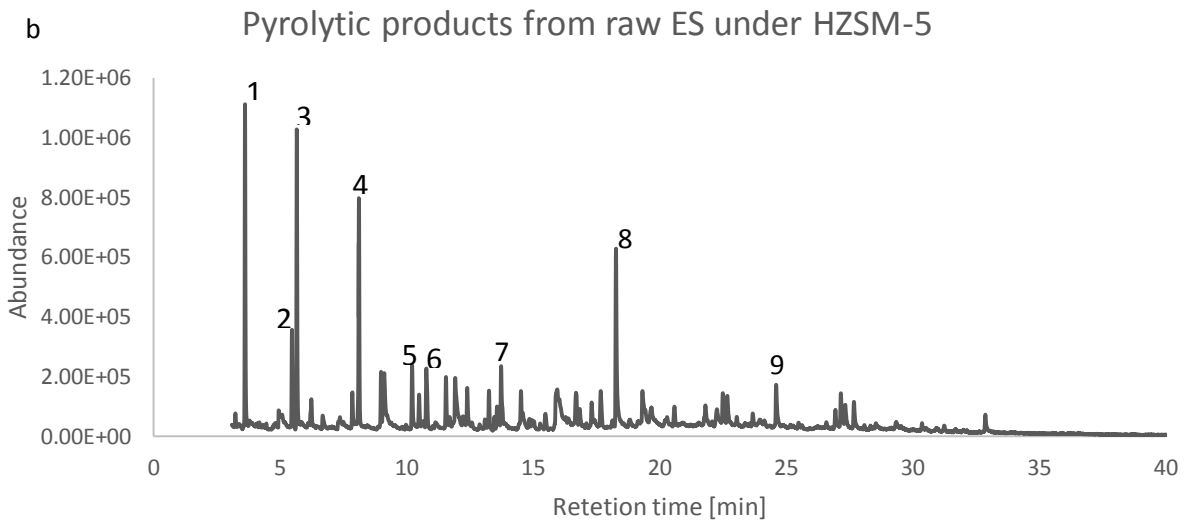


(1) toluene, (2) ethylbenzene, (3)p-xylene, (4) 1-ethyl-2-methyl-benzene, (5) benzofuran, (6) 2-methoxy-phenol, (7) 2,3-dihydro-benzofuran, (8) 2-methoxy-4-vinylphenol, (9) 2,4-bis(1,1-dimethylethyl)-phenol

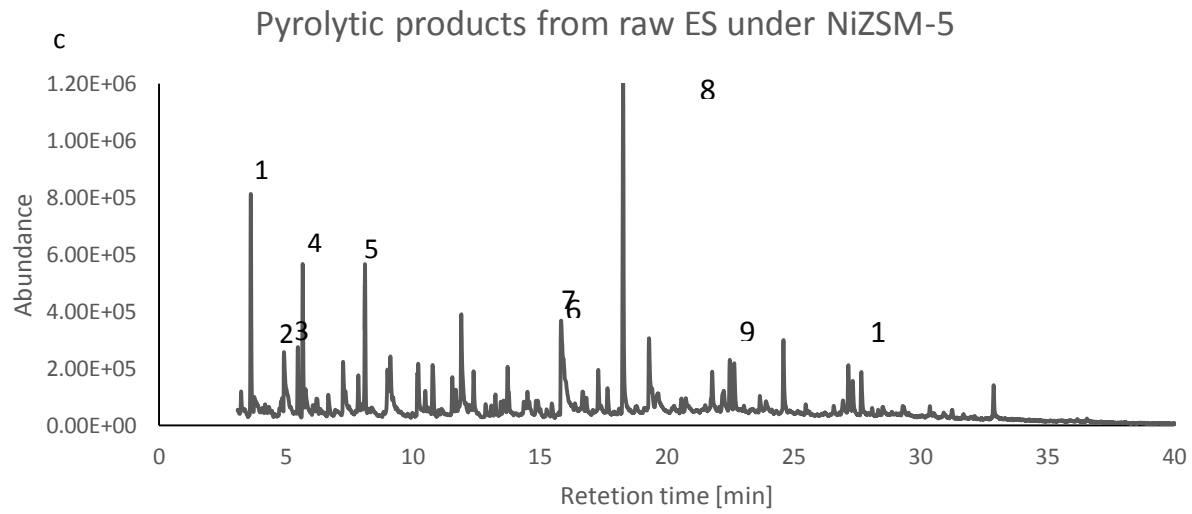


(1) toluene, (2) 2-Cyclopenten-1-one, (3) ethylbenzene, (4) p-xylene, (5) 1-ethyl-2-methyl-benzene, (6) 2-methoxy-phenol, (7) 2,3-dihydro-benzofuran, (8) 2-Methoxy-4-vinylphenol, (9) 2,6-dimethoxy-phenol, (10) 3-tert-butyl-4-hydroxyanisole

Fig.6.3 Main compounds from catalytic pyrolytic vapors from raw energy sorghum

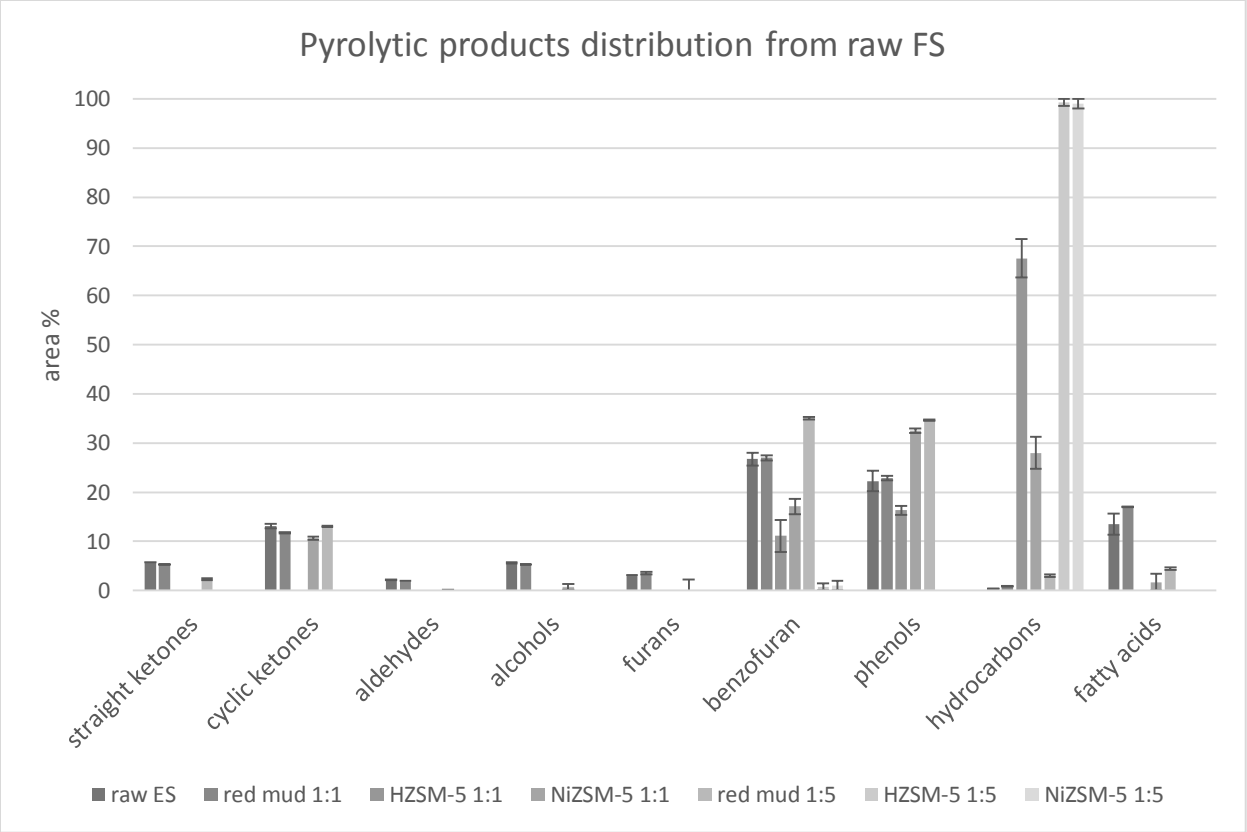


Fig.6.4 The components distribution of catalytic pyrolytic products from raw ES

a

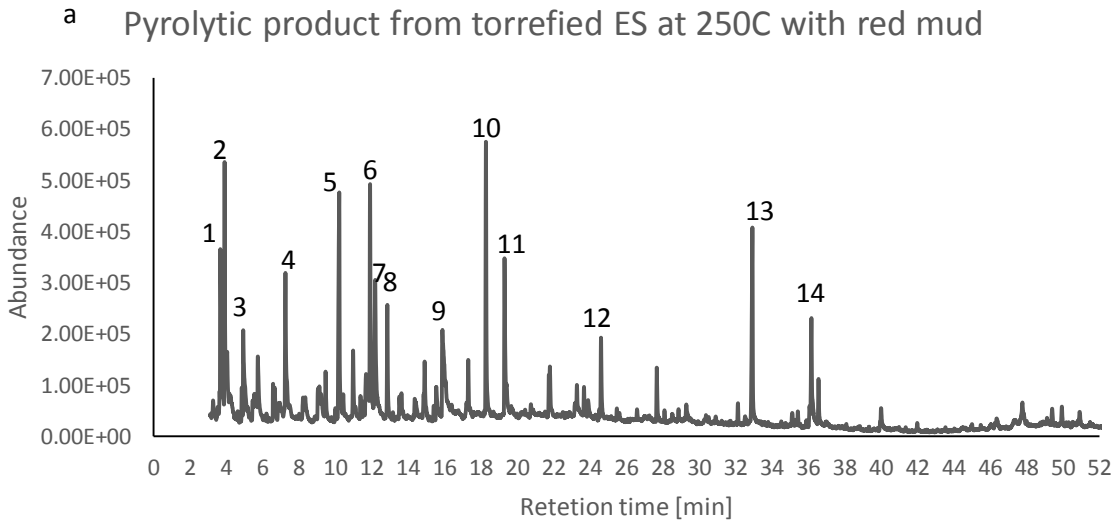


(1) 1-hydroxy-2-butanone, (2) butanedial, (3) 2-cyclopenten-1-one, (4) 2-hydroxy-2-cyclopenten-1-one, (5) 3-methyl-1,2-cyclopentanedione, (6) 2-methoxy-phenol, (7) cyclopentanol, (8) 3-ethyl-2-hydroxy-2-cyclopenten-1-one, (9) 2,3-dihydro-benzofuran, (10) 2-methoxy-4-vinylphenol, (11) 2,6-dimethoxy-phenol, (12) 3-tert-butyl-4-hydroxyanisole, (13) n-Hexadecanoic acid, (14) cis-Vaccenic acid

b

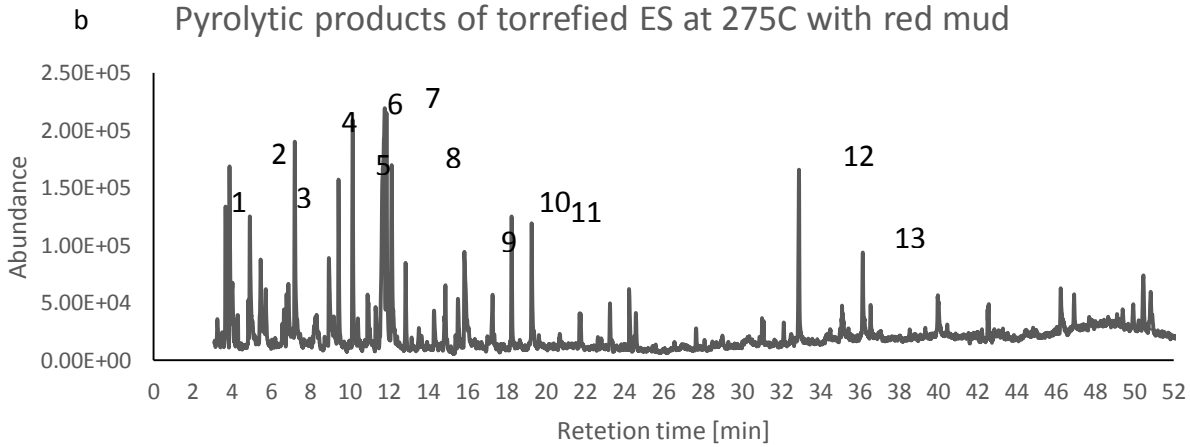


(1)toluene, (2) butanedial, (3) 2-cyclopenten-1-one, (4) 2-hydroxy-2-cyclopenten-1-one, (5) tetrahydro-2-furanmethanol, (6) 2-hydroxy-3-methyl-2-cyclopenten-1-one, (7) 2-methoxy-phenol, (8) cyclopentanol, (9) 2-methoxy-4-methyl-phenol, (10) 2-methoxy-4-vinylphenol, (11) 2,6-dimethoxy-phenol, (12) n-Hexadecanoic acid, (13) Oleic Acid

c

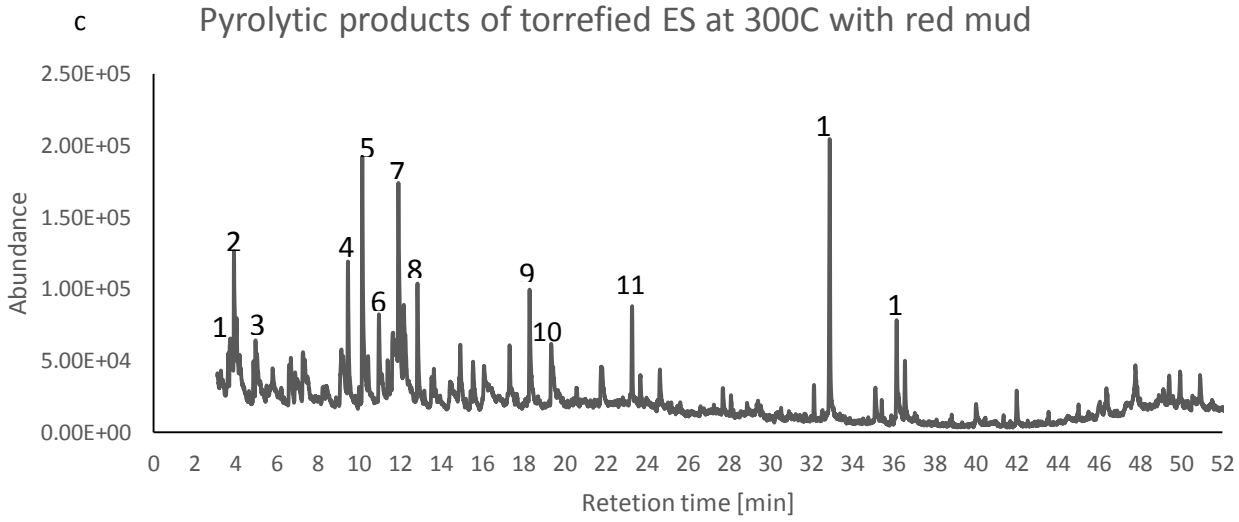


(1) toluene, (2) butanedial, (3) 2-cyclopenten-1-one, (4) tetrahydro-2-furanmethanol, (5) 2-hydroxy-3-methyl-2-cyclopenten-1-one, (6) 1,2,3-trimethylbenzene, (7) 2-methoxy-phenol, (8) 3-ethyl-2-hydroxy-2-cyclopenten-1-one, (9) 2-methoxy-4-vinylphenol, (10) 2,6-dimethoxy-phenol, (11) 2,4-bis(1,1-dimethylethyl)-phenol, (12) n-Hexadecanoic acid, (13) Octadecanoic acid

d

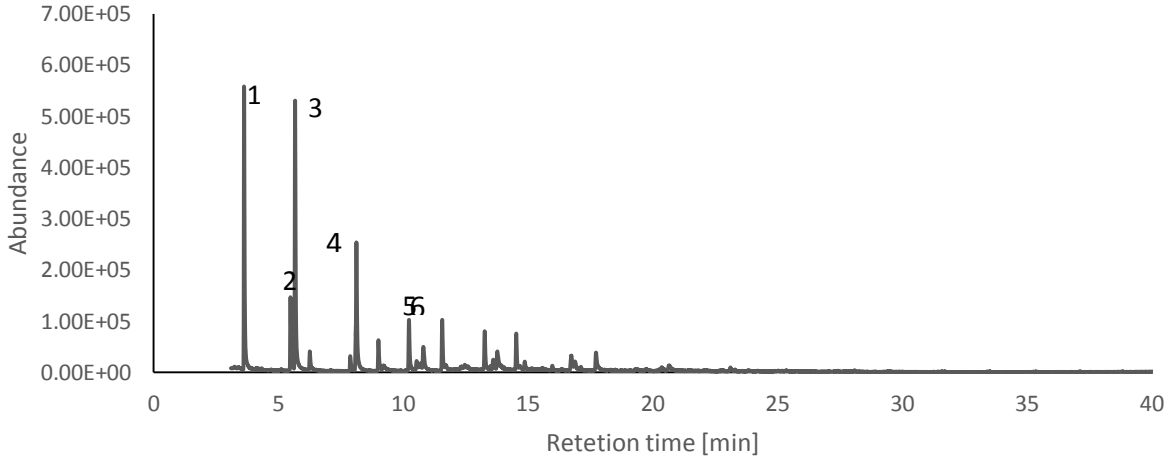


(1) toluene, (2) ethylbenzene, (3)p-xylene, (4) 1-ethyl-2-methyl-benzene, (5) 1-methyl-3-propyl- Benzene, (6) 2-methyl-2-propenyl-benzene,

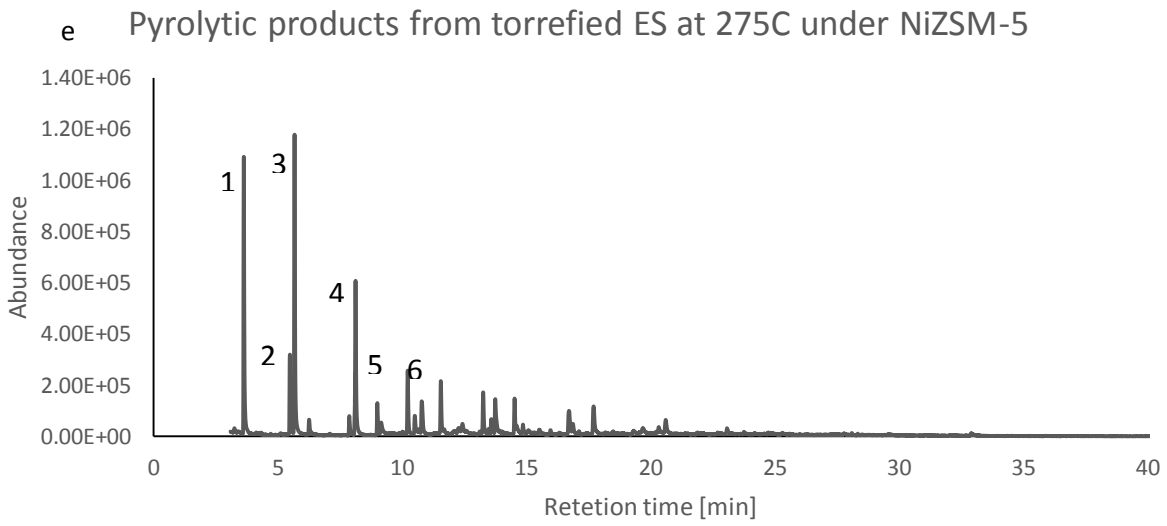


(1) toluene, (2) ethylbenzene, (3) p-xylene, (4) 1-ethyl-2-methyl-benzene, (5) 1-methyl-4-propyl-benzene, (6) 2-ethenyl-1,3-dimethyl-benzene

Fig.6.5 Main compounds from catalytic pyrolytic vapors from torrefied ES

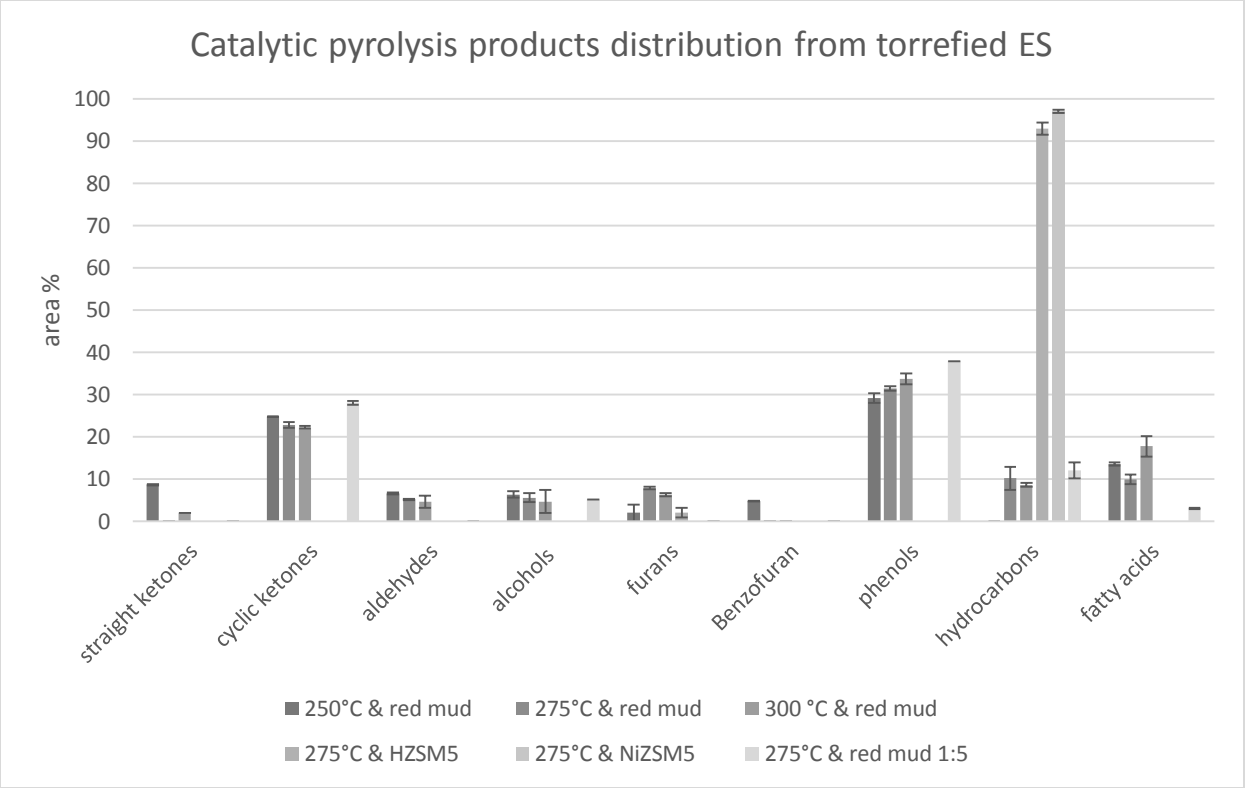


Fig.6.6 The components distribution of catalytic pyrolytic products from torrefied ES

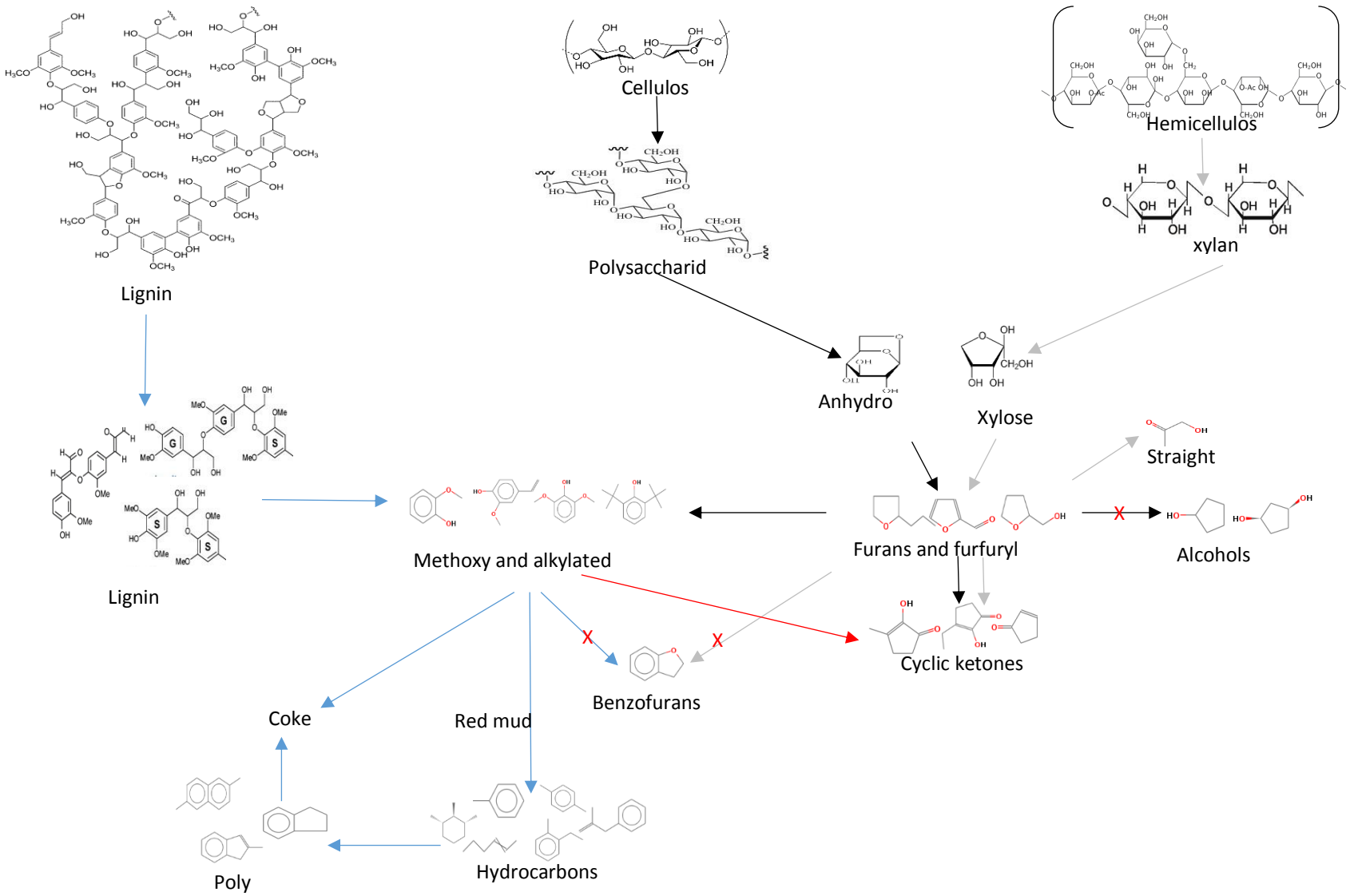


Fig.6.7 Catalytic pyrolysis reaction pathways of lignocellulose with red mud from torrefied sorghum. Grey line is the pyrolytic pathway of hemicellulose, black is the dominant pathway of cellulose pyrolysis, blue refers to lignin, red indicated the promotion or inhibition effects of red mud.

## VII. Compositional Analysis of Catalytic Pyrolysis Bio-oil from Torrefied Sorghum[5]

**Abstract**

Improving hydrocarbons content of bio-oil with pretreatment and economic, coke resistant catalyst was crucial for catalytic fast pyrolysis. In this study, both impacts of torrefaction pretreatment and red mud catalyst were investigated on hydrocarbon conversion. Torrefaction increased hydrocarbons content of 1.68 folds in oil fraction, in which, the dominant component was phenol type compounds. Red mud alone, mainly promoted the formation of cyclic ketones, with slight enhancement on hydrocarbon conversion. The combination of torrefaction pretreatment and red mud showed synthetic effect on hydrocarbon conversion, with 16.6 wt. % in the oil fraction, 10.5 times of that from direct pyrolysis. The bio-oil yield from torrefied energy sorghum was 16.1 wt. % after catalytic pyrolysis, with the oil fraction of 57.2 wt.%. Compositional analysis on aqueous fraction indicated carboxylic acids concentration were almost negligible, approximate one hundredth of that from direct non-catalytic pyrolysis.

***Keywords***: pyrolysis, bio-oil, fluidized bed reactor, red mud, torrefaction, hydrocarbon

### 7.1 Introduction

Fossil fuels, supporting around 85% of global energy supplies, has been shown a rapidly dwindling reservation. Additionally, the utilization of fossil fuels associates with negative environmental impact, such as excess greenhouse gas emission. It was reported 98% of carbon emission into the atmosphere was introduced by fossil fuel combustion, let alone deleterious

[5] Yang Yue, Sudhagar Mani To be submitted to BioEnergy Research

nitrogen oxides and sulfur oxides gasses and particle pollutions. Carbon dioxide is the major fraction of greenhouse gas; raising from 29.0 billion metric tons in 2006 to 33.1 billion metric tons in 2015 and excepting to be 40.4 billion metric tons in 2030. The transportation sector is responsible for about 25% of worldwide $CO_2$ emissions and it will increase to nearly 50% of the total emissions by 2030 (http://planetforlife.com/). Therefore, developing an alternative to fossil fuel is promptly demanded and widely studied within last decades. Biofuels as a renewable energy, displays net carbon emission and is regarded as an excellent drop-in fuel for transportation.

Fast pyrolysis is an attractive thermal chemical technology to convert various biomasses into biofuels. It is conducted at high temperature (500-600°C) in the absence of oxygen under atmosphere. The products of fast pyrolysis are consequently obtained with catalytic vapor condensation. Char is firstly collected from residues, followed by bio-oil, which mainly contains water, carboxylic acids, alcohols, ketones, phenols and furans derivate. Non-condensable gasses (NCG), such as CO and CO2, formed through decarboxylation reaction of structural carbohydrates and lignin, is exhausted into the atmosphere (Carpenter et al., 2014). The target of bio-oil contains highly oxygenated compounds, which significantly damages the quality of bio-oil. Catalytic cracking has shown extremely appealing on improving bio-oil quality by deoxygenating the oxygen from oxygenated compounds into water. The majority of pyrolytic vapors are catalytically converted into hydrocarbons, with much more desirable prosperities on energy density, acidity, corrosiveness, viscosity and thermal stability for engine combustion.

Most commonly *in-situ* used catalyst for catalyst fast pyrolysis (CFP) is derivate from microporous materials, such as zeolite for its excellent activity sites, shape selectivity and thermal stability for hydrocarbons production. Mihalcik studied the catalytic effects of five groups of zeolites (H-Mordenite, H-ZSM-5, H-Y, H-Beta, and H-Ferrierite) on lignocellulosic biomass

pyrolysis with pyro-GC/MS and concluded HZSM-5 was the most effective for hydrocarbons conversion with the yield of 12 wt.% (Mihalcik et al., 2011). However, the cost of ZSM-5 is the limitation of its economic feasibility on industrial scale. Additionally, the coke formation during *in-situ* catalytic pyrolysis resulted in the short life of HZSM-5 and increase the cost of CFP (Liu et.al., 2014).

Red mud is the solid residue of bauxite industry with affluent availability (Karimi et al., 2014) and its majority faction of iron oxide, (Yathavan and Agblevor, 2013), show catalytic capability on reducing oxygen content and acidity of the bio-oil through ketonization, condensation, and deoxygenation reactions (Kastner et al., 2015). Therefore, red mud is attractive as a sacrificial catalyst to replace expensive catalysts for its low cost and complement thermal stability. It was reported red mud could sustain more than 300 hr pyrolysis before deactivate. Yathavan and Agblevor compared the catalytic impacts of red mud and HZSM-5 on bio-oil from pinyon – juniper woods and found red mud catalytic bio-oil had a lower viscosity, comparative yields (42-49 wt.%) and heating value (28.6-29.5 MJ/kg) with HZSM-5. The major components of red mud catalytic bio-oil were aromatics, followed by aliphatics and levoglucosan (Yathavan and Agblevor, 2013).

Torrefaction pretreatment is as promising approach to reduce oxygen content from biomass through the decomposition, carboxylation and dehydration reactions of hemicellulose and partial lignin and cellulose. It was reported the torrefaction pretreatment prior to pyrolysis altered pyrolysis behaviors, which finally decreased the contents of acetic acid, hydroxyacetone and furfural, and ameliorated the acidity and stability of bio-oil (Zheng et al., 2013). Neupane et.al., reported the yield of hydrocarbon precursors, phenol derivate, increased 2.7 folds after torrefaction pretreatment of pinewood at 275 °C for 15 min (Neupane et.al., 2015). Additionally, pyrolysis

coke precursors such as formaldehyde and acetaldehyde are found to be remarkably removed after torrefaction (Meng et al, 2012). Therefore, torrefaction pretreatment benefits pyrolysis process by increasing hydrocarbon content and extending catalyst life.

There were several reports on investigating red mud catalytic performance and on estimating the effects of torrefaction pretreatment prior to CFP. However, no study related to hydrocarbons production has been reported with the application of both red mud and torrefaction. In this study, the combination of torrefaction pretreatment and red mud CFP was conducted, with the purpose of studying their synthetic performances on hydrocarbon conversion. The yields and compounds in bio-oil were typically analyzed and the possible reaction pathways were studied.

## 7.2 Materials and Methods

Energy sorghum used as the feedstock in this study was obtained from Fort Valley State University, Fort Valley, Georgia, USA. The energy sorghum was planted at 32° 30' N and 83° 52' W, with elevation of 155 m above mean sea level. The soil was classified as Orangeburg loamy fine sand (fine loamy, kaolinitic, themic Typic Kandiudults), with 2 to 5% slope (USDA, NCRS, 2015). The used energy sorghum was first field dried and subsequently open air dried in shade before experiment and analysis. When received, energy sorghums has the length distribution of 10 mm to 240 mm and was grinded into 1/16 inch with hammer mill before torrefaction pretreatment and pyrolysis. The compositional prosperity of energy sorghum was determined after size reduction, which was indicated in table 7.1.

Solvents of dichloromethane (DCM), acetone, methanol and toluene used for bio-oil extraction in this study were purchased from Sigma-Aldrich with chemical pure. Red mud slurry was obtained from Rio Tinto (Alcan, Canada). The slurry of red mud was dried in oven at 105 °C for 20 hours, and then crushed. The particle sizes between 600 and 800 μm was screened and used

for CFP. Deionized water used in the experiments was prepared by our lab. Nitrogen used for torrefaction and pyrolysis were purchased from Airgas.

The process of torrefaction was implemented at 275 ℃ with the holding time of 30 min. The yield of torrefied energy sorghum was 53.3 wt.%. The characterizations of torrefied energy sorghum were measured and also listed in table 7.1. The torrefaction process was described in details in the section of sorghum biomass torrefaction.

7.2.1 Pyrolysis with fluidized bed reactor

Fluidized bed reactor was developed and utilized for energy sorghum pyrolysis and CFP. The picture of fluidized bed reactor was indicated in Fig.7.1. The feedstock (raw or torrefied energy sorghum) was loaded into a volumetric auger feeder with the feeding rate of approximately 400 g/hr. The feedstock was fed into the reaction zone at 500 ℃, which was designed 61cm length by 4.75 cm inner diameter. Nitrogen was used as carrier gas with the flowrate of 8 ppl. Around 250 g of sand (red mud if CFP) was used as heat carrier, which was located at below the reaction zone and preheated to 500 ℃. A split nitrogen blew up sand or red mud particles and mixed it with feedstock at reaction area. Within seconds, the pyrolytic products were carried through two sequential cyclones, where char was separated and collected. The pyrolytic vapors were condensed through three condensers, respectively cooled with water at room temperature, air at room temperature and salted ice-bath at -5 ℃. The compounds in pyrolytic condensable gas were collected consequentially according to their boiling points. The bio-oil was the liquid product in all condensers. The non-condensable gas was exhausted. The biomass continuously fed into the reactor for an hour. The weight of feedstock was measured before and after pyrolysis.

### 7.2.2 Pyrolysis products separation

After pyrolysis (CFP), the weight of bio-oil was calculated according to the weight difference of above three condensers before and after the pyrolysis. Same amount of DCM solvent was added into the condensers to solve and collect bio-oil. The obtained bio-oil contained oil fraction and aqueous fraction. To separate oil fraction and aqueous fraction, the harvested bio-oil was transferring into a separator funnel. After standing for an hour, the oil fraction was completely extracted with DCM and decanted off from the bottom of the separator funnel. The majority of nonpolar compounds existed in the oil fraction. The polar chemicals were mainly solved into water and weighted after collection. The weight of oil fraction was obtained from the difference of bio-oil and aqueous fraction. Both oil fraction and aqueous fraction were stored in refrigerator before analysis.

### 7.2.3 Analysis of pyrolysis liquid product

The compositions of oil fraction from bio-oil were analyzed with GC-MS using HP-5ms Capillary Column (30m x 0.25um x 0.25mm). The oven temperature program was initially set to 40 ℃ for 4 min; then increased to 275 ℃ with the heating rate of 5 ℃ /min and hold constantly for 5 min. The Mass Spec interface was set at 280 ℃. The inlet temperature was 260 ℃. Helium was used as carrier gas with the flow rate of 0.8 mL/min and the split ratio of 50:1. DCM was used as solvent to mix the internal standard of 1-hexanol and oil fraction. The concentration of internal standard was 1.04 g/L. Major compounds identified with GC-MS from oil fraction were quantitatively analyzed if necessary. Neat compounds of toluene, trimethyl benzene, pentadecane, 2-methoxy phenol and 2-cyclopenten-1-one were respectively used to estimate the mass percentage of aromatic hydrocarbons, benzenes, alkanes, phenols and cyclic ketones. For oil fraction compositional analysis, the standard stock solution was prepared immediately before GC-

MS operation by adding 10 µl 1-hexanol into 800 µl DCM. After vortex, 35 µl standard stock solution was mixed with 302 µl oil fraction sample. 1 µl mixed sample solution was injected into GC-MS after filtration with 0.45 µm filter. The solvent delay was setup for 3 min for DCM. The compositions were identified by matching fragmentation patterns with NIST mass spectral library.

The concentrations of major compounds in aqueous fraction were measured with HPLC using Coragel 94 column. The oven temperature was 60°C and 4 mN sulfuric acid was used for mobile phase. The flow rate was constant at 0.6 ml/min. The sample volume injected was 5 µl.

## 7.3 Results and Discussion

### 7.3.1 Yield analysis of pyrolysis products

The yields of pyrolysis products were indicated in Fig.7.2. NCG was the dominant product from all designed pyrolysis reactions with the yields ranging from 41.9 wt. % to 48.4 wt. %. Among which, red mud catalyzed pyrolysis showed higher NCG yields than non-catalytic reactions because of the formation of $CO_2$ and CO from decarboxylation and decarbonylation reaction promoted by catalyst (Liu et al., 2014). The yields of chars were enhanced around 70 to 90 % with torrefied energy sorghum from raw energy sorghum. This was resulted from the more lignin content available after torrefaction pretreatment, which decomposed intermediates of phenol derivate were more apt to repolymerized.

It was showed the bio-oil yield from raw energy sorghum was 33.3wt. %, lower than corn stover of 52.7% (Fahmi et al., 2007) and corn cob of 56.2 % (Schell and Harwood, 1994); but competitive with switchgrass of 34.3 (Raveendran et al., 1995). This difference on yields was considered to be resulted from biomass feedstock and pyrolysis conditions. After extraction, the oil fraction approximately shared equally with aqueous fraction from bio-oil (Fig.7.3). The aqueous fraction was mainly composed of water, with a small amount of polar organics; the former

was from biomass moisture and dehydration; while the later, such as carboxylic acids and alcohols, was from the thermal decomposition.

Both applications of catalyst and torrefaction pretreatment decreased the yields of bio-oil. When red mud was used as catalyst for energy sorghum pyrolysis, the hydrocracking reaction occurred with the thermal decomposition of feedstock. The heavier organics from the secondary re-polymerization reaction were cracked into small molecular compounds. Simultaneously, highly oxygenated compounds from pyrolytic vapor were deoxygenated with the formation of water and NCGs. Therefore, the bio-oil yield decreased from 33.3wt. % to 26.5 wt. %, with 20.4 % decrease. The oil fraction was 8.2 wt. % from raw energy sorghum, lower than that of 17.4 wt. % from non-catalytic pyrolysis. Compared with most commonly used catalyst of HZSM-5, this oil fraction was between Williams's reports of 4.4% from rice rusk (Williams and Nugranad, 2000) and Zhang's report of 13.7% from corncob (Zhang et al., 2009). This potentially implied milder hydrocrack reaction occurred with less hydrocarbon converted. Meanwhile, the percentage of aqueous fraction in bio-oil increased 45% because of the hydrodeoxygenation.

When torrefied energy sorghum was used as feedstock, the bio-oil yield decreased 30.4%. This was resulted from the compositional change of feedstock after torrefaction. During torrefaction, devolatilization, carbonization reactions and carboxylation and dehydration of decomposed smaller molecular compounds consequentially occurred. Hemicellulose and partial thermal non-resistant lignin were decomposed and their major decomposed products, as well as moisture, were removed in the form of vapors. The torrefied biomass was mainly composed of lignin and cellulose, with negligible moisture content. The declining percentage of bio-oil was approaching to Zheng's report of 31.2% from torrefied corncobs (Zheng et al., 2013), in the range of Meng's report of 50.2% decline from Loblolly pine (Meng et al., 2012) and Boateng's report of

9.2 % from Switchgrass (Boateng et al.,2013) after torrefaction. The oil fraction in bio-oil accounted for more than 60%, due to moisture removed during torrefaction.

When both red mud and torrefaction pretreatment were applied, the bio-oil yield was reduced to 16.1 wt.%, among which 57.2 % was oil fraction, which finally accounted for 9.2 wt. % from torrefied energy sorghum. If calculated from the raw energy sorghum, the mass flowrate was indicated in Fig.7.4, which indicated the oil fraction converted from raw energy was only 4.9 % after torrefaction pretreatment and CFP. This oil fraction yield was competitive to Hilten's reports of 4.2 wt. % from raw pine wood, in which study, torrefaction pretreatment at 275 °C was also applied before catalytic fast pyrolysis with HZSM-5 (Hilten et al., 2013). A further optimization on catalytic pyrolysis operation was advocated to improve the oil fraction yield.

7.3.2 Compositional analysis of aqueous fraction

The aqueous fraction was extracted from bio-oil with polar compounds formed through pyrolysis reactions. Definitely, water was the dominant composition, which accounted for more than 90 wt. % of the aqueous fraction. Other major compounds in aqueous fraction were analyzed with HPLC (Fig.7.5). Carboxylic acids, such as formic acid and acetic acid, were the main compounds, which concentrations separately reached 40.9 g/L and 28.4 g/L after pyrolysis from raw energy sorghum. Torrefaction pretreatment significantly reduced the yields of formic acid and acetic acid, which respectively decreased 85% and 67% from raw energy sorghum. This was because hemicellulose in raw energy sorghum was almost completed decomposed, which was the main resource of carboxylic acids through pyrolysis. A more remarkable reduction of carboxylic acids was observed after catalytic pyrolysis with red mud. The concentrations of formic acid and acetic acid respectively reduced 99% and 83% from raw energy sorghum with non-catalytic pyrolysis. It was indicated that red mud promoted the conversion of carboxylic acids into other

compounds, which was also reported by Kastner that ketones were the main products from the decarboxylation reaction of carboxylic acids under red mud (Kastner er al., 2015). When the combination of torrefaction pretreatment and red mud were both applied, there was no formic acid identified with HPLC and the concentration of acetic acid was as low as 0.7 g/L. The more reduction on acetic acids than formic acid implied the red mud favored smaller molecular for decarboxylation, probably because of the average core size of red mud.

Besides carboxylic acids, methanol was also an important component, which concentration was 7.3 g/L in aqueous phase of raw energy sorghum pyrolysis. Both torrefaction and red mud decreased methanol concentration with respectively 29.7% and 70.6%. The methanol was formed from hemicellulose and lignin pyrolysis, and could be served as a precursor for hydrocarbons conversion with hydrocracking. (Liu et al., 2014). Acetone, as one of the most important small carbonyl compounds, has the yield of 1.9 g/L from aqueous fraction of raw energy sorghum pyrolysis. Acetone was formed from cellulose direct decomposition, and the ketonization of acetic acid, with co-products of $CO_2$ and $H_2O$. (Liu et al., 2014). However, after either torrefaction pretreatment and catalytic pyrolysis, the yield of acetone was not able to be measured with HPLC. Additionally, the levoglucosan concentration was negligible at 0.73g/L from raw energy sorghum pyrolysis, either torrefaction pretreatment or catalysis with red mud led the levoglucosan concentration undetected. Meanwhile, no the concentration of furfural was unable to determine from aqueous fraction of any pyrolysis process.

### 7.3.3 Compositional analysis of oil fraction

The compositions of oil fractions were determined with GC-MS. Table 7.2 indicated the distributions of major components of oil fractions. It was indicated straight ketone of 1-hydroxy-2-propanone was the dominant compounds with the content of 27.76 wt. % of oil fraction, only

detected from raw energy sorghum after non-catalytic pyrolysis. 1-hydroxy-2-propanone was mainly formed from hemicellulose, torrefaction pretreatment prevented the formation of straight ketones by removing hemicellulose. Red mud also showed similar inhibition by block the conversion of 1-hydroxy-2-propanone from furans. Phenols and alcohols were other main components in non-catalytic pyrolysis oil fraction from raw energy sorghum. 1-Propanol, 2-methyl- was the only identified alcohol accounted for 19.90 wt. %. The alcohol was formed from both cellulose and hemicellulose decomposition. The torrefaction pretreatment removed hemicellulose and partial cellulose, which reduced the formation of alcohol intermediate compounds of furans and furfural alcohols, and resulted in a dramatical decrease of 52.5% from torrefied energy sorghum. Lignin content was concentrated by 2.2 folds after torrefaction pretreatment, which units were the main resource of phenols. Torrefaction increased the phenols content from 24.16 wt.% to 72.37 wt.%, higher than Neupane's report of 2.7 times (Neupane et al., 2015). Benzofurans were also only identified from non-catalytic pyrolysis oil fraction, which was also derivate from furan intermediates, with the content decline 71% after torrefaction. Meanwhile, the hydrocarbons content after torrefaction reached 4.42 wt. %, increased 1.68 times from raw energy sorghum. This certified the torrefaction pretreatment benefited pyrolysis bio-oil quality. Additionally, aldehyde of hydroxyacetaldehyde, was only detected from raw energy sorghum with non-catalytic pyrolysis.

When red mud was applied as catalyst for raw energy sorghum catalytic pyrolysis, the most remarkable change was the enhancement of cyclic ketones accompanying with the decline of straight ketones, alcohols and benzofurans. The cyclic ketones content reached 59.28 wt. %, increased 3.87 folds from non-catalytic pyrolysis, becoming the dominant component. When torrefied energy sorghum was employed as the feedstock, a similar trend was also observed with

4.61 folds enhancement on cyclic ketones content after catalysis with red mud. The increased cyclic ketones were formed from both cellulose and hemicellulose through furans. It was inferred red mud inhibited the formation of straight ketones, alcohols and benzofurans, and promote the ketonization of furans with the oxidized iron in the form of hematite, which blocked the hydrogenation reaction of furans into alcohols and defragment reaction of furans into straight ketones. Furans of 2-propyl-tetrahydrofuran, 2,4-dimethyl-furan were detected with the slight contents.

Another important impact of red mud was the improvement on hydrocarbon formation from phenols. With red mud, the hydrocarbon content reached 16.60 wt. % from torrefied energy sorghum, 10.05 times of that from raw energy sorghum with non-catalytic pyrolysis. However, considering the mass loss of around 47% during torrefaction, the hydrocarbon yield was only approximate 0.78 wt. % of raw energy sorghum. This hydrocarbon yield was much lower than that obtained with HZSM-5 catalytic pyrolysis, which ranging from 13.7 % (Zhang et al., 2009) from corncob to 33.6% (Agblevor et al., 2010) from poplar wood. Therefore, red mud was not considered as a desirable catalyst, in spite of its economic cost. The catalytic pyrolysis pathways of lignocellulose were indicated in Fig.7.6

## 7.4 Conclusions

The impacts of torrefaction pretreatment and red mud catalyst on pyrolysis bio-oil were investigated in this study. It was showed that torrefaction pretreatment increased the hydrocarbon yield of 1.88 times at the cost of 47 wt.% biomass loss, which finally increased 24% of hydrocarbon yield. Red mud mainly promoted the formation of cyclic ketones from alcohols and benzofurans. When combined with torrefaction pretreatment, red mud also significantly improved the hydrocarbon content of 10.9 folds from raw energy sorghum. However, when used alone, this

improvement on hydrocarbon conversion was not so obvious. An optimization on red mud reduction pretreatment and catalyst characterization might ameliorate its catalytic capability.

References

Carpenter, D., Westover, T.L.,Czernik, S. and Jablonski, W.. Biomass feedstocks for renewable fuel production: a review of the impacts of feedstock and pretreatment on the yield and product distribution of fast pyrolysis bio-oils and vapors. Green Chemistry. 2014. 16,384-406.

Liu, C., Wang, H., Karim, A.M., Sun, J., Wang, Y. Catalytic fast pyrolysis of lignocellulosic biomass. Chemical Society Reviews. 2014, 43(22): 7594-7623

Yathavan, B.K. and Agblevor, F.A. Catalytic Pyrolysis of Pinyon–Juniper Using Red Mud and HZSM-5." Energy & Fuels.2013. 27(11): 6858-6865.

Meng, J., Park, J., Tilotta, D., Park, S. The effect of torrefaction on the chemistry of fast-pyrolysis bio-oil. Bioresource Technology. 2012. 111: 439-446.

Neupane, S., Adhikari, S., Wang, Z., Ragauskas, A. J. and Pu, Y. Effect of torrefaction on biomass structure and hydrocarbon production from fast pyrolysis. Green Chemistry. 2015, 17(4): 2406-2417.

Kastner, J. R., Hilten, R., Weber, J. W., McFarlane, A. R., Hargreaves, J. S. J., & Batra, V. S. Continuous catalytic upgrading of fast pyrolysis oil using iron oxides in red mud. RSC Advances, 2015, 5, 29375-29385.

Karimi, E., et al. Synergistic co-processing of an acidic hardwood derived pyrolysis bio-oil with alkaline Red Mud bauxite mining waste as a sacrificial upgrading catalyst. Applied Catalysis B: Environmental. 2014, 145: 187-196.

US Department of Agriculture (USDA), Natural Resources Conservation Service (NCRS). Custom Soil Resource Report. Accessed on 3/ 2/2015.

Fahmi, R., Bridgwater, A.V., Darvell, L. I., Jones, J. M., Yates, N., Thain, S. and Donnison I. S. The effect of alkali metals on combustion and pyrolysis of Lolium and Festuca grasses, switchgrass and willow. Fuel. 2007. 86, 1560 – 1569.

Schell, D. J., Harwood, C. Milling of lignocellulosic biomass: results of pilot-scale testing. Applied Biochemistry and Biotechnology. 1994. 45, 159 – 168.

Raveendran, K., Ganesh, A. and Khilar, K.C. Influence of mineral matter on biomass pyrolysis characteristics. Fuel. 1995. 74, 1812–1822

Zheng, A. , Zhao, Z., Chang, S., Huang, Z. , X. Wang, F. He, and H. Li. Effect of torrefaction on structure and fast pyrolysis behavior of corncobs. Bioresource Technology. 2013. 128, 370-377

Boateng, A.A. and Mullen, C.A. Fast pyrolysis of biomass thermally pretreated by torrefaction. Journal of Analytical and Applied Pyrolysis. 2013. 100, 95–102

Williams, P. T. and Nugranad, N. Comparison of products from the pyrolysis and catalyticpyrolysis of rice husks. Energy, 2000, 25, 493–513.

Zhang, H., Xiao, R., Huang, H. and Xiao, G. Comparison of non-catalytic and catalytic fast pyrolysis of corncob in a fluidzed bed reactor. Bioresour. Technol., 2009, 100, 1428–1434.

Hilten, R.N., Speir, R.A., Kastner, J.R., Mani, S., Das, K. C. Effect of Torrefaction on Bio-oil Upgrading over HZSM-5. Part 1: Product Yield, Product Quality, and Catalyst Effectiveness for Benzene, Toluene, Ethylbenzene, and Xylene Production. Energy Fuels. 2013, 27, 830-843

Kastner, J.R., Hilten, R.N., Weber, J., McFarlane, A.R., Hargreaves, J. S. J. and Batra, V.S. Continuous catalytic upgrading of fast pyrolysis oil using iron oxides in red mud. RSC Adv., 2015, 5, 29375-29385

Agblevor, F. A., Beis, S., Mante, O. and Abdoulmoumine, N. Ind. Eng. Fractional Catalytic Pyrolysis of Hybrid Poplar Wood. Chem. Res., 2010, 49, 3533–3538.

Table 7.1. The components of torrefied sorghums

| Biomass | Components content [wt.%] | | |
|---|---|---|---|
| | hemicellulose | cellulose | acid insoluble compounds (manly lignin) |
| Energy sorghum | | | |
| Raw | 21.44[a] | 33.24[a] | 19.04[a] |
| Torrefied at 275 °C | 3.19[b] | 25.52[b] | 60.10[b] |

The different letter on superscript indicated significant difference at $p<0.05$.

Table 7.2 The major compounds distribution in oil fractions

| Compounds | pyrolysis | catalytic pyrolysis | Pyrolysis with torrefaction pretreatment | catalytic pyrolysis with torrefaction pretreatment |
|---|---|---|---|---|
| | Mass % | | | |
| ***Straight ketones*** | ***27.76*** | | | |
| 2-Propanone, 1-hydroxy- | 27.76 | | | |
| ***Cyclic ketones*** | ***12.16*** | ***59.28*** | ***6.46*** | ***36.25*** |
| 2-Cyclopenten-1-one | | 10.40 | | |
| 2-Cyclopenten-1-one,2-methyl- | | 4.08 | | |
| 2-Cyclopenten-1-one, 3-methyl- | | 16.97 | | |
| 2-Cyclopenten-1-one, 2,3-dimethyl- | | 17.94 | | 11.51 |
| 2-Cyclopenten-1-one, 2,3,4-trimethyl- | | | | 11.18 |
| 2-Cyclopenten-1-one, 2,3,4,5-tetramethyl- | | | | 8.79 |
| 2-Cyclopenten-1-one, 2-hydroxy-3-methyl- | 12.16 | | 6.46 | |
| 2-Cyclopenten-1-one, 5-hydroxy-2,3-dimethyl- | | 6.54 | | |
| Other cyclic ketones | | 3.35 | | 4.77 |
| ***Alcohols*** | ***19.90*** | | ***9.45*** | |
| 1-Propanol, 2-methyl- | 19.90 | | 9.45 | |
| ***Furans*** | | ***2.50*** | | ***7.87*** |
| Furan, 2,4-dimethyl- | | 2.50 | | |
| Tetrahydrofuran, 2-propyl- | | | | 7.87 |

| | | | | |
|---|---|---|---|---|
| ***Benzofurans*** | ***10.31*** | | ***2.98*** | |
| Benzofuran, 2,3-dihydro- | 10.31 | | 2.98 | |
| ***Phenols*** | ***24.16*** | ***32.37*** | ***72.37*** | ***36.04*** |
| Phenol | 4.71 | 23.12 | 23.47 | 3.29 |
| Phenol, 2-methyl- | | 5.03 | 6.94 | |
| Phenol, 4-methyl- | 5.92 | 4.22 | 16.99 | |
| Phenol, 4-ethyl- | 9.68 | | 8.86 | |
| Phenol, 2,4-dimethyl- | | | 5.21 | 3.53 |
| Phenol, 2,3,6-trimethyl- | | | | 12.52 |
| Phenol, 2-ethyl-6-methyl- | | | 8.18 | 4.26 |
| 4-Hydroxy-3-methylacetophenone | | | | 6.79 |
| Others phenols | 3.86 | | 2.73 | 5.64 |
| ***Hydrocarbons*** | ***1.65*** | ***1.87*** | ***4.42*** | ***16.60*** |
| Benzene | | | | 1.22 |
| Toluene | | | 0.96 | 2.44 |
| o-Xylene | | | 0.93 | |
| 2-Hexene, (Z)- | | 1.15 | | |
| Benzene, 1-ethenyl-3-ethyl- | | | | 3.27 |
| Benzene, (1-ethyl-1-propenyl)- | | | | 2.17 |
| 1H-Indene, 2,3-dimethyl- | | | | 2.06 |
| 1-Pentadecene | 0.50 | 0.72 | 0.70 | |
| 1-Hexadecene | 0.59 | | 0.93 | |
| other hydrocarbons | 0.56 | | 0.90 | 5.44 |
| ***Fatty acids*** | ***4.06*** | ***3.98*** | ***4.32*** | ***3.23*** |
| n-Hexadecanoic acid | 2.50 | 3.98 | 4.32 | 3.23 |
| 6-Octadecenoic acid | 1.56 | | | |


Fig.7.1 Picture of fluidized bed reactor for pyrolysis reaction

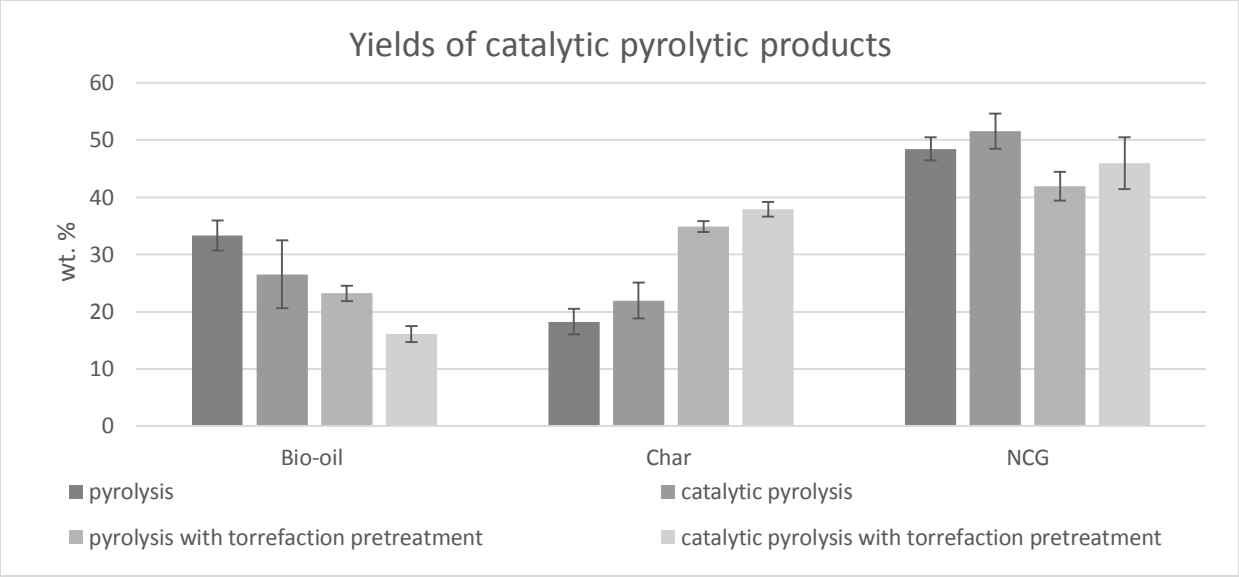


Fig.7.2 Yields of catalytic pyrolysis products from energy sorghum

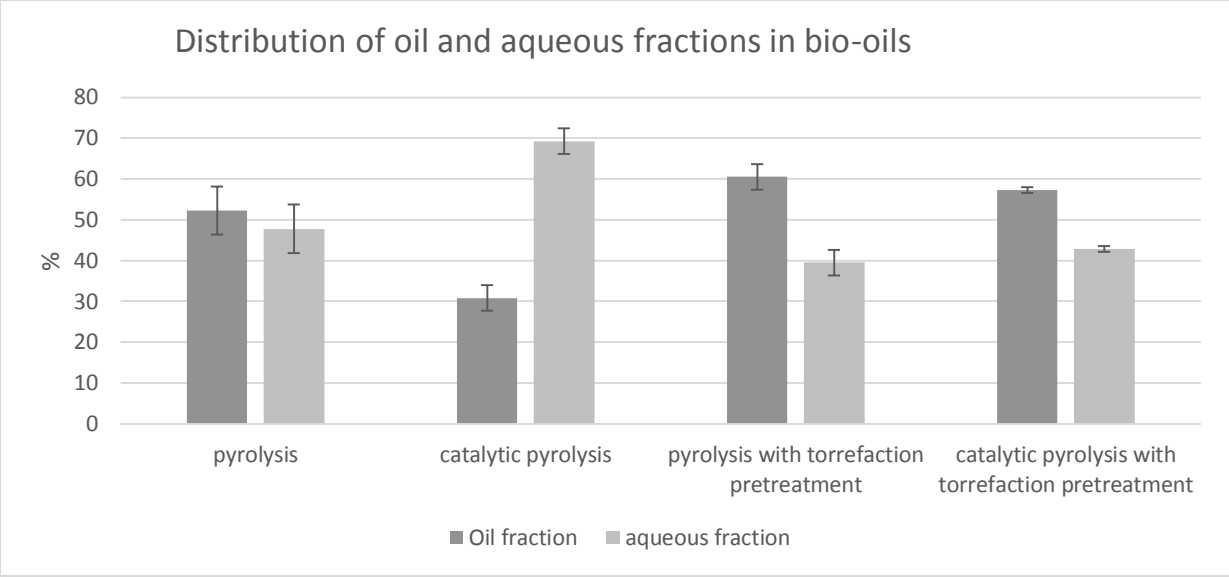


Fig.7.3 Distribution of oil and aqueous fractions in bio-oils

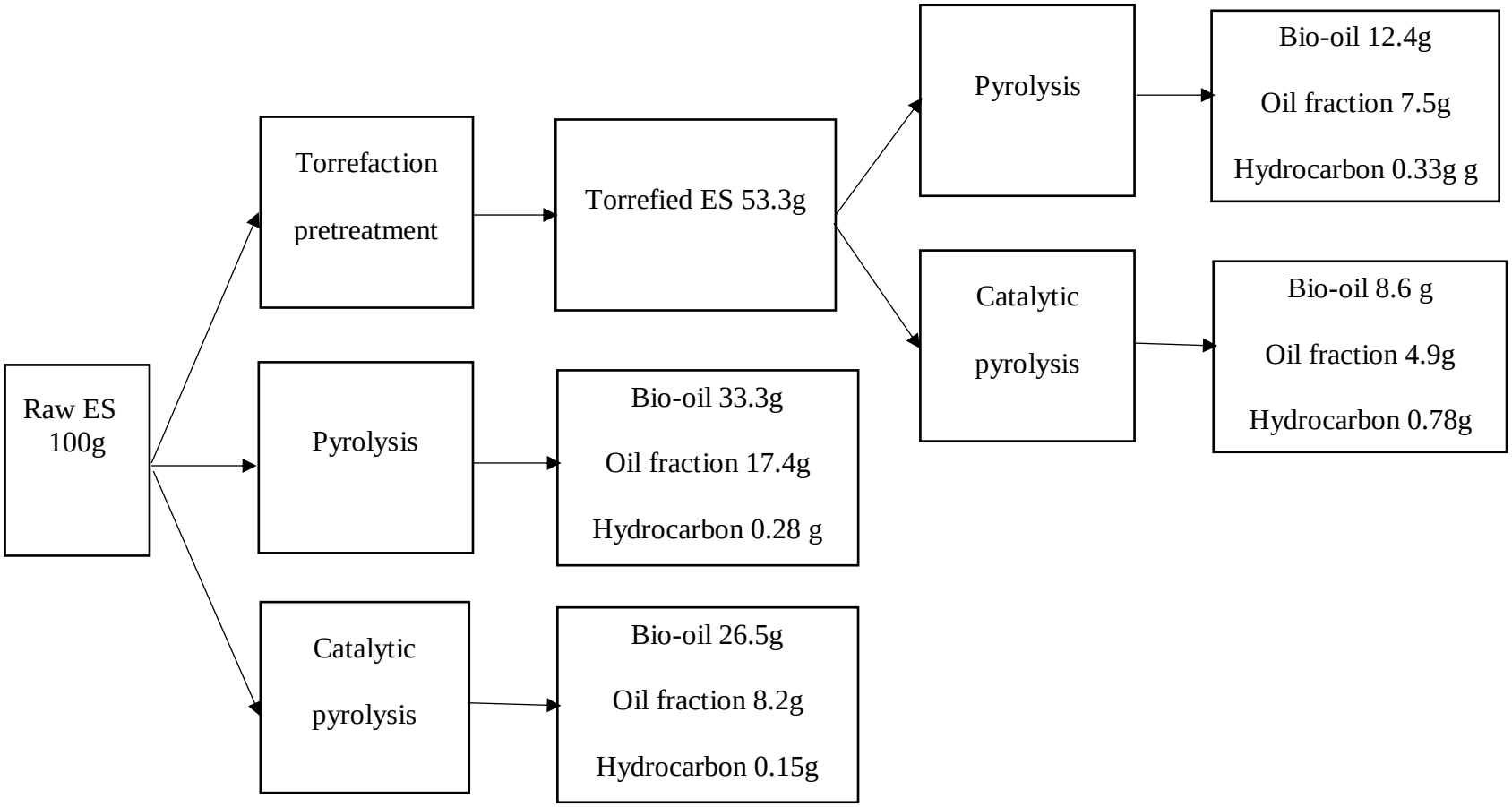


Fig.7.4 Mass flowrate diagram of bio-oil from raw energy sorghum (ES)

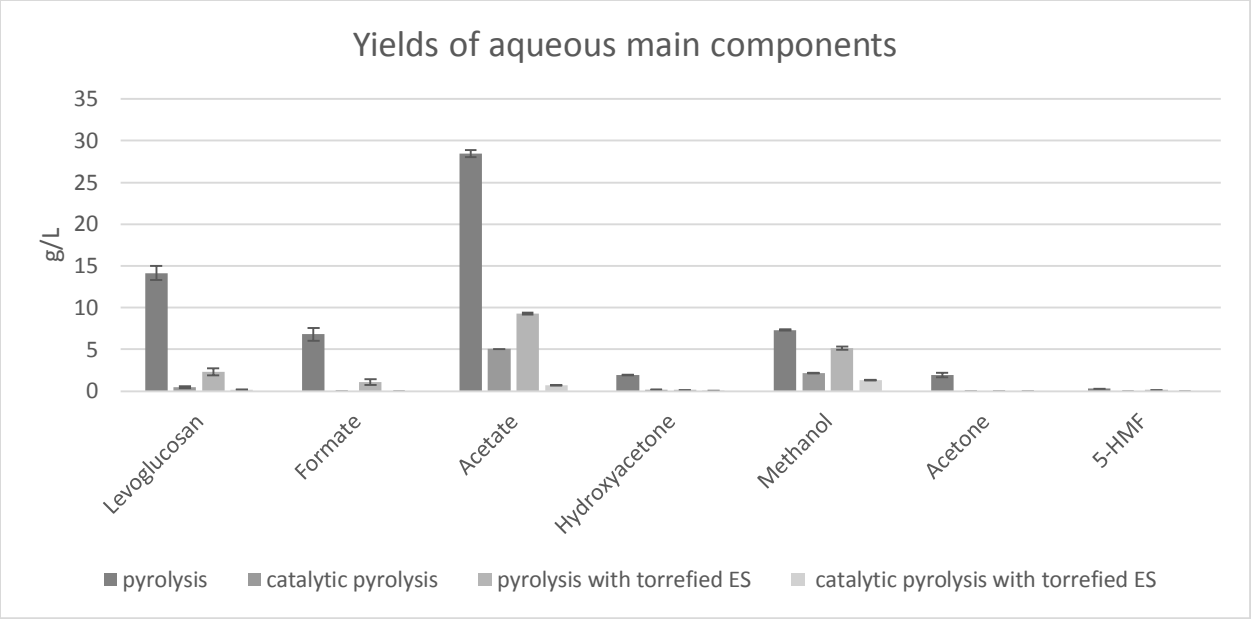


Fig.7.5 Yields of aqueous main compounds in bio-oils

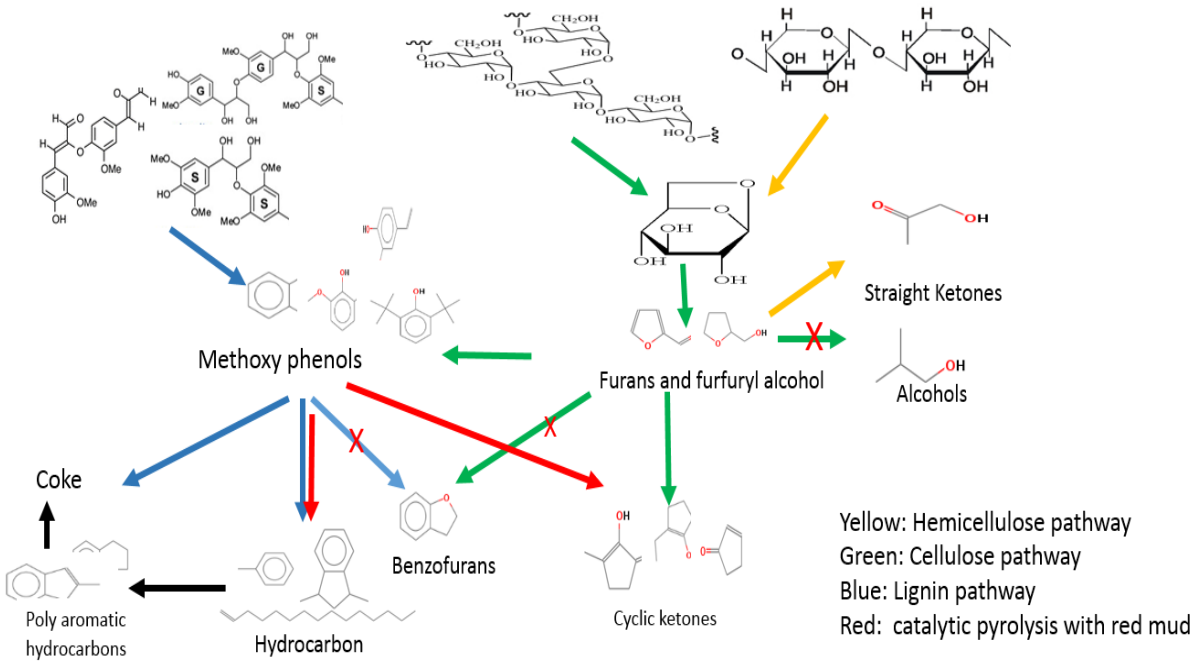


Fig.7.6 Pathways of lignocelluose catalytic pyrolysis with red mud

## VIII. Techno-economic Analysis of Torrefaction-CFP and Two-stage HTL Technologies[6]


### Abstract

During last decade, with more attention, pyrolysis and hydrothermal liquefaction (HTL) have been widely reported for the biofuel production with lab or pilot scale. In this study, based on pyrolysis and HTL process, thermal pretreatments were combined and two developed thermal conversion technologies were designed: torrefaction-CFP and two-stage HTL. Techno-economic analysis was conducted to evaluate their economic feasibility to produce upgraded biofuel with the capability of daily 2000 dry ton sorghum biomass. The annual production rate of final biofuel product was respectively 28.74 million gallon gasoline-equivalent (GGE) for torrefaction-CFP and 72.15 M gge for two-stage HTL, with minimum fuel selling price (MFSP) of 6.68 and 3.19 $/gge. The overall energy efficiency were respectively 9.1% and 20.1% for torrefaction-CFP and two-stage HTL. Total install equipment cost (TIEC) was identified as the most significant parameter impacting MFSPs. Two-stage HTL indicated remarkable advantages on economic feasibility for two main reasons: (i) co-product of C5 and C6 sugars in two-stage HTL technology offset 13% of final biofuel cost; (ii) the undesirable yield of bio-oil from CFP with red mud significantly damaged the biomass utilization efficiency.



***Keywords:*** techno-economic analysis, hydrothermal liquefaction, catalytic fast pyrolysis, upgraded biofuels


[6] Yang Yue and Sudhagar Mani. To be submitted to Biomass & Bioenergy

## 8.1 Introduction

Pyrolysis and hydrothermal liquefaction (HTL) were two promising thermal chemical technologies to convert biofuel from various lignocellulosic biomasses and widely studied on bench scale. Pyrolysis was operated at high temperature of 500-600°C in the absence of oxygen under atmosphere. HTL was conducted with moderate temperature of 280-370 °C and high pressure of 10-25 Mpa with the presence of subcritical water as solvent. The most notable difference between pyrolysis and HTL was the use of solvent, which reflected moisture content of feedstock. The product of either pyrolysis (bio-oil) or HTL (biocrude) was not adaptable as drop-in biofuel until upgrading. Hydrotreating and hydrocracking were commonly applied upgrading approaches to remove oxygen from highly oxygenated oil compounds. The physiochemical properties of upgraded biofuels, such as acidity, thermal stable and energy density were improved and approached to gasoline and diesel fuel.

Pretreatment prior to pyrolysis has widely been acknowledged to improve the hydrocarbon content in bio-oil and ameliorate the acidity and thermal stable of bio-oil. Torrefaction is a mild thermal pretreatment operated at moderate temperature (240-320°C) under anoxic condition with the products of terrified solid biomass, condensable liquids and non-condensable gasses. It was reported torrefaction increased hydrocarbon yield and reduced carboxylic acids content during pyrolysis. Neupane et.al., reported the yield of hydrocarbon precursors, phenol derivate, increased 2.7 folds after torrefaction pretreatment of pinewood at 275 °C for 15 min; when under the catalysis of HZSM-5, hydrocarbon yield reached 35.3 %, 67% higher than non-torrefied pinewood (Neupane et.al., 2015).

Cellulose, hemicellulose and lignin are the major components of lignocellulosic biomass and displayed significantly different performance during HTL. Hemicellulose constituted around

20-40 wt. %; however, it only contributed to 5.3 wt. % of biocrude, and the majority products were aqueous components (42 wt. %), among which, carboxylic acids accounted for 45% (Yoshida and Saka, 2006). Additionally, cross reactions occurred between the furfural derivate compounds decomposed from hemicellulose and phenol-type intermediates from lignin, and formed solid residues through repolymerization (Liu et. al., 2013). This further damaged the biocrude yield and increased the difficulty of hydrotreating process. Therefore, it was proposed that hemicellulose is a less efficient feedstock for HTL biocrude conversion (Pinkowska et.al., 2011) and more adaptable for producing other value-added product.

From above analysis, it was proposed to design two discrete technologies for biofuels production. One was the combination of torrefaction and catalytic fast pyrolysis; the other was the combination of mild temperature HTL (1$^{st}$ stage HTL) and severe temperature HTL (2$^{nd}$ stage HTL). The 1$^{st}$ stage HTL aimed to convert as much as hemicellulose into co-product of C5 and C6 sugars; while the 2$^{nd}$ stage HTL aimed to convert lignin and cellulose into biocrude. The bench-scale conversions with above two technologies were both successfully conducted. The practical performance with industrial scale was prompt to be studied from the techno-economic analysis.

Techno-economic analysis has been conducted by researches to estimate the economic feasibility of biofuels production from both pyrolysis and HTL processes. For pyrolysis analysis, Shemfe investigated the impact of electric power generation on bio-oil production and concluded the minimum fuel selling price (MFSP) of $8.29/gge with the plant capacity of 72 MT/day from pinewood (Shemfe et al., 2005). In Shemfe's research, an integrating power generation equipment was applied to minimize the power supply. Char and non-condensable gas from pyrolysis were used for combustion to generate power. Kinetics of pyrolysis and hydrotreating reaction from various components were firstly utilized in the simulation with Aspen plus, which promoted the

accuracy of the reactor in the simulation. It was also reported the overall energy efficiency achieved 62% with catalytic hydrotreating gasification, which was higher than most reports. However, because of the high cost of pinewood in British, approximate $120/ton, the final MFSP was uncompetitive to that from NREL in States. NREL provided two reports on TEA of pyrolysis; one was aiming to estimate the influence of hydrogen plant on MFSP (NREL 2011a); the other was to combine the processes of pyrolysis and hydroprocessing (hydrotreating and hydrocracking) (NREL 2011b). Both analyses applied the plant capacity of 2000 dry ton pinewood per day. Form the former report, it was drawn that hydrogen plant increased the cost of MFSP from $2.11/gal to $3.09/gal. From the latter report, the MFSP was found approximately $3.39/gge, with the product of gasoline and diesel. Onarheim studied different biomass feedstocks (Onarheim et.al., 2015) with plant capacity of 0.5 ton/day and found forest residual was more appropriate for bio-oil production with the MFSP of $2.2/gge, which was lower than pinewood of 3.1$/gge. In Onarheim's research, CHP (combined heat and power) process was utilized with fluidized bed boiler to generate electricity. However, hydrotreating process was not considered and crude bio-oil was the final product. Brown investigated bio-oil production from Kior with plant capacity of 2000 ton/day. The minimum fuel selling price (MFSP) was reported as $4/gge. This price was lower than cellulosic ethanol; gasification and Fischer–Tropsch synthesis (Brown et al., 2013).

HTL was obtained wide attention for biofuel production within decades. No commercialization of HTL has ever been reported in the States. Lack of reliable data on industrial scale was the main limitation of techno-economic analysis on HTL. The two available techno-economic reports were from NREL and PNNL, conducted in 2014 and 2013. In NREL's report. algae were applied as the feedstock with the plant capacity of 1034 ton/day. The MFSP was 4.49 $/gge, which included HTL and upgrading processes, algae culture, harvest and pretreatment as

well as nutrition (nitrogen) recycle. Catalytic hydrothermal gasification was also applied; in which process, the organics in HTL aqueous fraction was gasified into $CO_2$ and $CH_4$, which was used as the feedstock for $H_2$ generation. The carbon conversion efficiency of the final product from algae was 65%. The cost of algae was the limitation of MFSP, which was 430 $/ton. (NREL, 2014). PNNL employed pinewood for biofuel production with the feedstock price of 70 $/ton. The plant capacity was also designed to be 2000 ton/day. The reported MFSP of 4.44 $/gge was slightly decreased from NREL's report (Jones et al., 2013). This undesirable progress was mainly caused by the carbon conversion efficiency, which was 35% from pinewood with 46.2% lower than that from algae.

Currently, there was no report of techno-economic analysis to estimate the economic feasibility of the combination of multiple thermal chemical conversion processes on biofuel production. Additionally, no reports related to comparing MFSPs from different thermal chemical technologies. In this study, energy sorghum and sweet sorghum bagasse were respectively employed as feedstock for biofuel production through torrefaction-CFP conversion and two-stage HTL conversion. The remarkable difference on moisture content between above two sorghum biomasses determined the conversion technology. The producing processes, energy efficiencies, investment compositions and impacts of key parameters of two technologies were aimed to be analyzed and compared. A plant with 2000 dry ton per day of sorghum biomass feedstock was designed to evaluate above factors. The data used in this study was obtained from experiments and literature. The purpose of this study was to provide a preliminary assessment on above two conversion technologies with estimating potential key parameter for economic improvement.

## 8.2 Materials and Methods

To conduct TEA on economic feasibility of upgraded bio-oil production, it is necessary to define the process battery and unit operation first. In the torrefaction-CFP study, industrial scale of torrefaction (A100) was the operated after pretreatment as the beginning of TEA process, followed by grinding, CFP (A200), hydrotreating (A300) and distillation (A400). The off gasses from torrefaction, CFP and hydrotreating as well as the char from CFP were utilized for combustion to generate power (A500). The biomass of energy sorghum was purchased with the cost of 73.89 $/ton (Amosson et al., 2011), which included the cost of logistics and storage. Red mud was employed as an economic, sacrificed and coke formation resistant catalyst used in CFP, which, rather than be regenerated and reused, would be disposed after 300 hr. Hydrotreating was designed to remove oxygen from bio-oil with hydrogen as reduction donor. The hydrogen used for hydrotreating was designed to be purchased rather than generated in plant. It was indicated the purchased hydrogen could reduce the MFSP from to $3.09/gal to $2.11/gal with the plant capability of 2000 metric ton per day from NREL report (Wright et al., 2010). The distillation process was designed to separate gasoline (naphtha) from diesel. Finally, the target products of gasoline and diesel were separately collected and transferred into barrels after distillation.

As to two-stage HTL study, sweet sorghum bagasse was applied as the feedstock for upgraded biocrude production with the price of 44.0 $/ton (Gubicza et al., 2016). The plant capacity was also designed as 2000 dry ton per day. However, as the remarkablely difference on moisture content and the prosperity of HTL, the pretreatment approach of size reduction on sweet sorghum bagasse was quite distinguished from above. The bagasse was crushed and milled; the slurry was pumped into with 1$^{st}$ stage HTL reactor compressed air. 1$^{st}$ stage HTL was conducted with the aim of hydrolyzing as much hemicellulose as possible into C5 sugar stream at mild

reaction severity, which prevented the decomposition of lignin and majority of cellulose. The solid residues from 1st stage HTL were dried and used as the feedstock of 2nd stage to prepare high-quality biocrude with the catalysis of 0.94M $K_2CO_3$. After 2nd stage HTL, the biocrude was hydrotreated and distilled. These operating processes and parameters were similar as those described in torrefaction-CFP. The final product was also gasoline (naphtha) and diesel. However, there was a negligible amount of char produced, the off gas from 2nd stage HTL and hydrotreating were the main fuel for combustion to generate power.

The nth plant design was assumed for above techno-economic analysis. The operation conditions of torrefaction, catalytic fast pyrolysis (CFP) and two-stage HTL used in this assessment were mainly based on experimental results with bench and pilot plant scales. The designed specifications and yields of other processes such as hydrotreating, distillation and combustion were obtained from literature. The energy consumption and power generation were modified from reports depending on plant capacity and operation process.

8.2.1 Process overview

A simplified diagram of torrefaction-CFP and two-stage HTL were indicated in Fig.8.1. In this scheme, there were both three key unit operations in torrefaction-CFP (torrefaction, CFP, and hydrotreating) and two-stage HTL (1st stage HTL, 2nd stage HTL and hydrotreating) processes, which were respectively described in detailed below from section 2.1.1 to 2.1.6.

Besides above core operations, distillation and combustion processes in both above technologies showed great similarity. For distillation, two splitters (naphtha and diesel splitters) were mainly applied to separate gasoline and diesel sequentially after removing of the light gas components from debutanizer column (<70 °C). The upgraded bio-oil from hydrotreating was reheated into vapors and firstly went through a naphtha distillation tower from the bottom at 130

℃ at 25 psi. Those hydrocarbons within the gasoline boiling point were collected from the top at the temperature between 70 and 130 °C. The bottom product, which boiling point was higher than 130 °C, was then sent to diesel distillation tower. The temperature distribution of diesel splitter was designed in the range of 130 -220 ℃ at 15 psi. Similarly, the diesel fraction was collected from the top and the remaining negligible bottom product was considered as heavier oil. To improve the distillation efficiency, reflux drum and reboiler were used on both splitters.

Combustion process was designed to generate power to maintain the operation of torrefaction-CFP and two-stage HTL processes. For torrefaction-CFP process, vapors from torrefaction, NCG and char from pyrolysis and off gas from hydrotreating were used as the fuel. For two-stage HTL, off gas from 2$^{nd}$ stage HTL and from hydrotreating were used for combustion. Those gas fuels, containing organics and combustible gas, such as CO, were filtered before feeding into the combustor. The ash from char (HHV of 27.5 MJ/kg (Rover, 2008)) combustion was collected with cyclones at a disposal cost of $16.4/metric ton (NREL,1994).

8.2.1.1 Torrefaction

After harvest, energy sorghum was located in field for natural dry until delivery in bale with the moisture content of 7.8 wt.%. Sizing reduction was required to reduce the energy sorghum from initial height of 1.5~2 m to less than 240 mm with chopping before torrefaction. This chopping process increased around $11/MT of biomass on electricity consumption (Sokhansanj, 2006). The chipped energy sorghum was fed into a rotary dryer with hopper at the temperature of 90-110 °C. The dried energy sorghum and moisture gas was separated from a combined surge bin and cyclone. After dryness pretreatment, the physical free moisture was considered to be completely removed. The dried energy sorghum were fed into the belt conveyer torrefier immediately from surge bin. The feeding rate of torrefaction was 2000 metric ton per day at the

temperature of 275°C. After 30 min, the solid product of torrefied energy sorghum was collected into a product bin from cyclone. The byproduct of gas stream, which included moisture, condensable fraction and off-gas (mainly $CO_2$), were blew through a gas filter for combustion. The terrified energy sorghum was conveyed for further grinding with hammer mill to 1.6 mm before CFP. This small particle size improved the heat transfer and thermal decomposition during pyrolysis. The energy consumption was around 50 kwh/ton for grinding torrefied biomass (BioMatNet FAIR-CT96-3203, 2004).

8.2.1.2 Catalytic fast pyrolysis

Those grinded energy sorghum was fed into a circulating fluidized-bed-type (CFB) pyrolyzer for fast pyrolysis with auger and hopper. The pyrolysis temperature was set at 500°C with the residence time of less than 2 sec. The feeding rate was adjusted with auger to maintain the ratio of catalyst to biomass was 1:1 in the reaction zone of CFB. The catalyst of red mud was employed as heat carrier with particle size of 600-800μm, which was blew up and mixed with the feedstock of torrefied energy sorghum. Red mud was employed as a sacrificed catalyst, the process of regeneration not designed; and it would be disposed after 300 hr. The char and pyrolytic vapor were separated through cyclones. Bio-oil was sequentially collected through a series of condensers. The oil fraction was separated from aqueous effluent through a flash vessel and sent to hydrotreating process for upgrading. The char was used as one of the fuel of power generation through combustion. The majority NCG was used to fluidize the pyrolysis bed through a NCG compressor; the remaining was used for power generation.

8.2.1.3 Hydrotreating of bio-oil

To achieve the goal of producing transport fuel, oxygenated compounds in collected oil fraction was mandatory to be deoxygenated through hydroprocessing. Hydroteating was designed

to achieve the conversion of hydrocarbons from various highly oxygenated components of oil fraction. During this process, hydrogen was purchased and provided a reduction reagent. Single stage of hydrotreating was reported to cause tar-like product (Elliott, 2012). Additionally, the catalyst was poisoned during the hydrodeoxygenation and indicated thermally unstable property. The current TEA reports of pyrolysis-hydrotreating focus on multiple stage hydrotreating with increased processing severity to prevent catalyst coking. The mild stage hydrotreating was designed to reduce the amount of oxygenated compounds with less hydrogen consumption; the severe stage hydrotreating was designed to complete the conversion of hydrocarbons. At the 1st stage, the temperature of 200 °C was employed in a fluidized bed reactor with the pressure of 1700 psi, followed by a 2nd stage of 400 °C (Thilakaratne,2014).

After heating, the oil fraction was pumped to high pressure stabilizer and mixed with hydrogen. The 1st stage and 2nd stage hydrotreating were sequentially operated. The output was cooled with water at room temperature and separated into three phases of upgraded hydrocarbon richen oil, aqueous phase, and off -gases through flash chambers. The aqueous phase was treated as water waste. The hydrogen in gas byproduct was separated with PSA and the rest was either used for blowing the red mud at CFB through a NCG compressor or applied for combustion.

8.2.1.4 1st stage HTL

The harvest sweet sorghum was firstly extracted for syrups on farm and the remaining bagasse was considered as an economic lignocellulose resource. The received sweet sorghum bagasse contained a great amount of moisture of around 80 wt. %, which made this biomass appropriate for HTL. Similarly as the pretreatment of torrefaction-CFP process, size reduction was required to minimize the particle of sweet sorghum bagasse into 5 mm through crusher and hammer mill before 1st stage HTL. Water as the HTL solvent was added and mixed with grinded

sweet sorghum bagasse at the water to dry biomass ratio of 10:1 (w/w). After preheated to desired temperature of 170 °C, the slurry was pumped to the 1st HTL reactor system. CSTR was used as the reaction vessel of 1st stage HTL at the pressure of 300 psi with the holding time of 90 min. During 1st stage HTL, hemicellulose and partial cellulose from sweet sorghum bagasse were hydrolyzed into C5 and C6 sugar streams; while, lignin and crystallization cellulose were thermal stable. After the reaction, the product effluent of mixture of gas, subcritical water and solid residues were used as heat resource to exchange the heat with the feedstock slurry of 2nd stage HTL. The cooled 1st stage HTL products were fed into a flash drum to release the pressure to atmosphere; meanwhile, the gas byproduct of $CO_2$ was separated from solid and liquid product. This gas byproduct could recycle with air to pressure the 1st stage HTL after air compressor. The liquid and solid products were separated with a rotary filter. Co-product of C5 and C6 sugars were harvested to reduce the MFSP of final biofuels. The solid was collected from the filter cake, dried and loosen before using as feedstock of 2nd stage HTL.

8.2.1.5 2nd stage HTL

The dried solid product of 1st stage HTL was mainly composed of lignin (46 wt. %) and cellulose (43 wt. %). Similarly as 1st stage HTL, additional water was added as solvent with the ratio of feedstock to water of 1:10. 0.94M $K_2CO_3$ was applied as alkaline catalyst to improve the yield of biocrude during 2nd stage HTL. The slurry was preheated and pumped into 2nd stage HTL vessel at the temperature of 350 °C, with the $N_2$ pressure of 500 psi. The holding time was designed to be 30 min. During the reaction, hydrolysis, defragment and repolymerization reactions were sequentially occurred, with the product of off gas, oil fraction and aqueous phase. This mixture was separated with flash drum, which process was described in section 2.1.3. The inert $N_2$ in off gas was collected with PSA for recycle use. The oil fraction was fed into hydrotreating process.

8.2.1.6 Hydrotreating of biocrude

On the basis of our experiment results, it was indicated that negligible heavier oil fraction existing in biocrude. Actually, after one step hydrotreating process, the hydrocarbons content in upgraded biocrude accounted for more than 95 wt. %. Therefore, one step hydrotreating with severe condition was considered sufficient for hydrocarbon conversion at the temperature of 400 °C with the pressure of 1700 psi. The process of biocrude hydrotreating quite similar as that of torrefaction-CFP, which was described in section 8.2.1.3

8.2.2 Economic Analysis.

Two strategies were designed based on the previous experimental analysis of torrefaction and CFP and two-stage HTL to producing hydrocarbon biofuels with the final products of gasoline and diesel. The $n^{th}$ plant was assumed in this study. The estimation of capital costs of standard equipment, which included distillation columns, flash tanks, pumps, compressors, and heat exchangers was modified based on the previous reports. The capital cost of non-standard equipment was estimated by adjusting the scales of literature equipment, such as belt conveyer torrefier, circulating fluidized-bed-type pyrolyzer, HTL CSTR systems and hydrotreating reactors with the following equation:

$$\text{current equipment cost} = \text{base equipment cost} \times \left(\frac{current\ year\ index}{quote\ year\ index}\right) \times \left(\frac{capacity\ of\ new\ equipment}{capacity\ of\ base\ equipment}\right)^{n}$$

where, n is the scaling factor, ranging from 0.6 to 0.8

The installation cost was calculated by multiplying installation factors, which varied individually according to equipment. The total direct cost was obtained from the summary of

installed equipment cost, building cost, piping cost and site development. The fixed capital investment was calculated by direct cost, plus indirect cost, which was respectively assumed 128% of total direct cost (Peters et al., 2003). The working capital and land cost were respectively assumed to be 15% of fixed capital investment and 8% of total direct cost. The total project investment was calculated by adding fixed capital investment, working capital and land cost. Operating cost included variable and fixed operating costs. The former mainly contained feedstocks, chemicals, fuels, water, and electricity, which was calculated based on the mass flowrate and energy requirement. The latter was composed of the overhead, maintenance, insurance and tax and labor cost. Among above items, the maintenance, and insurance and tax were respectively supposed to be 3% and 0.7% of the fixed capital investment (Jones et al.,, 2014 a); the overhead cost was assumed to be 90% of labor cost, which was around 4.06 $MM obtained from the data of Bureau of Labor Statistics reported by NREL (NREL, 2011c)

Minimum fuel selling price (MFSP) was used to estimate the final product cost, which makes the net present value of the process equal to zero, with a discounted cash flow rate of 10% over plant life of 20 years at the stream factor of 0.9. The MFSP was provided in the unit of gallon gasoline-equivalent ($/GGE) to compared the final product of gasoline and diesel from energy sorghum with generic commercial gasoline. The MFSP was calculated by the following formula:

$$\text{MFSP}\ \left({}^{\$}/_{\text{gge}}\right) = {}^{MFSP\ of\ final\ product\ from\ energy\ sorghum \times\ HHV\ of\ gasoline}/_{HHV\ of\ final\ product}$$

8.3 Results and Discussions

8.3.1 Processing Analysis

The yields of torrefaction, CFP, 1st stage HTL, 2nd stage HTL and hydrotreating of HTL processes were obtained from experimental results; the yields of hydrotreating of torrefaction-CFP

was cited from Thilakaratne's report (Thilakaratne et.al., 2014). For torrefaction-CFP technology investigation, the torrefied energy sorghum yield was 53.3 wt. %, which equaled to 1066 dry ton/day of feedstock for CFP. After CFP, only 16.1wt. % of torrefied energy sorghum was converted into bio-oil under the catalysis of red mud, which mainly promoted the formation of cyclic ketones from phenols. The water fraction in bio-oil was measured to be 42.8 wt. %. The NCG were the main byproduct with the yield of 46.0 wt. %. For hydrotreating process after CFP, unfortunately, no detailed data was reported related to red mud catalytic bio-oil. The yield of hydrotreating was referred to the reports from Thilakaratne (Thilakaratne,2014), as the bio-oil produced from Thilakaratne's report was obtained from mild CFP. Hydrotreating processing converted 78 wt. % of oil fraction from CFP into hydrocarbons with the theoretical $H_2$ consumption of 2.7 wt. % (Thilakaratne,2014). The off gas from hydrotreating was 15.3 ton/day for power generation. After distillation, the productions of gasoline and diesel were respectively 65.3 ton/day and 11.5 ton/day, the final fuel product yield was 3.84 % based on the plant capacity of 2000 ton energy sorghum per day. This yield is much lower than the reports of 17.7% from Thilakaratne's report (Thilakaratne et.al., 2014)， 33.3% from Shemfe's report (Shemfe et.al., 2015) and 34.8 % from NREL report (Jones et al., 2013) . This low fuel yield was because the mass loss during torrefaction and low bio-oil yield during CFP. Meanwhile, totally approximate 1439.7 tons of off gas and 388.8 tons of chars were used for combustion to generate power per day. Additionally, 79.5 tons of aqueous fractions from pyrolysis and hydrotreating were effluent.

As to the two-stage HTL technology, 56.6 wt.% of feedstock was hydrolyzed into the C5 and C6 sugars co-product of 544 ton/day as well as $CO_2$ off gas of 66 ton per day. The solid residues of 868 ton from 1$^{st}$ stage HTL was further converted into 306 ton biocrude per day with the yield of 35.4 wt.%. The yields of off gas and aqueous byproducts were respectively 36.9 and 25.2 wt.

%. After hydrotreating process, 81.0 wt. % of biocrude was converted into upgraded biocrude with more than 95 wt.% of hydrocarbons at the consumption of 3.3 wt. % $H_2$ (Zhu et.al 2014). The total obtained hydrocarbons was 236 ton per day, among which, approximate 95% was collected with naptha splitter, and 5% were collect with diesel splitter. The yield of heavier oil after hydrotreating processing was negligible. The total conversion efficiency of final fuel was 12.4 wt. % from initial sweet sorghum bagasse with the plant capacity of 2000 ton feedstock per day. This biofuel yield was lower than Zhu's reported of 19.4 wt.% from pinewood (Zhu et.al., 2014) and NREL's reports of 45.4% from algae *Nannochloropsis* and 28.5 from algae *Chlorella*. This was resulted from the 56.6 % of biomass was hydrolyzed during 1$^{st}$ stage HTL for co-product of C5 and C6 sugars, which had the conversion efficiency of 27.2 wt.% from initial sweet sorghum bagasse. Additionally, the biomass of algae contained more lipids, which contributed more biocrude than lignocellulose. The mass balance and main characterization of feedstock were respectively listed in table 8.1 and table 8.2 for both torrefaction-CFP and two stage HTL technologies.

Compared to torrefaction-CFP technology, the yield of deoxygenated oil (hydrocarbons) from two-stage HTL indicated 2.07 folds higher. This was because red mud was not a highly efficient catalyst for bio-oil yield, in spite of economic cost. Actually, most byproducts from torrefaction-CFP processes were used for power generation, which indicated torrefaction-CFP required much less cost on variable operating. This might be served as a setoff of the low bio-oi yield on MFSP. This will be discussed in following sections.

### 8.3.2 Energy Efficiency Analysis

For biofuel energy analysis, the energy input included the energy in the feedstock and the energy provided from electricity, where energy in the feedstock was calculated based on the higher

heating values (HHVs) and flowrate. The energy output was obtained from the HHVs of final fuel products.

For torrefaction-CFP technology, the energy from energy sorghum was 401.2 Mwe. The electricity consumptions for torrefaction, CFP, hydrotreating and distillation and combustion were respectively 21.5 Mwe (calculated), 6.16 Mwe (Solantausta et al., 2003; Ringer et.al., 2006; Beckman et al., 1990; Bridgewater et al., 2002), 1.48 Mwe (Shemfe et al., 2015) and -3.55Mwe (Shemfe et al., 2015). The energy efficiencies of producing torrefied energy sorghum, bio-oil and final biofuel product were respectively 69.8%, 8.2% and 9.1% on the basis of total energy input. The higher efficiency of upgraded bio-oil indicated higher hydrodeoxygenation conversion efficiency during hydrotreating with hydrogen.

For two-stage HTL technology, similarly, the energy input from sweet sorghum bagasse was 377.3 Mwe. The electricity consumptions for 1$^{st}$ stage HTL was 148.11 Mwe (calculated) and 12.76 Mwe for the summary of 2$^{nd}$ stage HTL, hydrotreating, distillation and combustion (Jones et al., 2014). Meanwhile, the consumed hydrogen provided 16.57 Mwe into the final biofuel product during hydrotreating. The energy efficiencies of producing 1$^{st}$ stage HTL solid product, final biofuel product were respectively 33.3%, and 20.1% on the basis of total energy input. It was indicated the over energy efficiencies of converting sorghums into upgraded biofuel through two-stage HTL technology was 2.2 times of that through torrefaction-CFP technology. However, both above overall energy efficiencies were much lower than Shemfe's report of 62% (Shemfe et al., 2015) and cellulosic ethanol of 45% (Humbird et.al., 2011). This was mainly resulted from biomass reduction during the treatments before either CFP or 2$^{nd}$ stage HTL.

### 8.3.3 Economic Analysis

The fixed capital investment (FCI) for 2000 ton per day energy sorghum conversion into hydrocarbons was respectively 731.9 $MM for torrefaction-CFP and 880.0 $MM for two-stage HTL, among which indirect cost were assumed 128% of direct cost. Total installed equipment cost were respectively 270.9 $MM and 325.7 $MM for torrefaction-CFP and two-stage HTL technologies. The dominant cost laid on the CFP system and HTL system, which accounted for 90.1% and 75.7%. The distribution of each unit operation on FCI was analyzed in Fig.8.2. The working capital and land cost were separately calculated as 15% and 8% of FCI. The total project investment (TPI) was the summarization of FIC, working capital and land cost; and estimated 867.4 $MM for torrefaction-CFP and 1042.9 $MM for two-stage HTL. The operating cost included fixed operating cost and variable operating cost. The former contained labor cost, overhead, maintenance, insurance and taxes. The labor cost were adjusted from NREL report based on the labor indices from Bureau of Labor Statistics (Jones et al., 2014). The overhead was assumed to be 90% of labor cost; while maintenance and insurance and taxes were obtained as 3% and 0.7% of FCI. The total fixed operating cost were calculated to be 34.79 $MM/year for torrefaction-CFP and 37.16 $MM/year for two-stage HTL. As to the variable operating cost, the cost of feedstock of 48.8 $MM/year on energy sorghum was the dominant fraction in torrefaction-CFP, accounting for 66.5%. The crucial fraction of two-stage HTL variable operating cost was electricity consumption of 87.8 $MM/year because of heating water during two HTL processes; however, the co-product of C5 and C6 sugars could offset 75.4 $MM/year on variable operating cost. The total operating cost was 110.5 $MM annually for torrefaction-CFP and 96.3 $MM for two-stage HTL. With the assumption of income tax rate, stream factor, discount rate and life span were respectively 35%, 90%, 10% and 20 years, the MFSP could be obtained when net present

value was set to be zero. The MFSP of torrefaction-CFP biofuels was 6.68 $/gge, and MSFP of two-stage HTL biofuels was 3.19 $/gge. This remarkable difference was resulted from (i) low bio-oil yield from CFP with red mud; (2) co-products of C5 and C6 sugars offset the cost. However, the above estimated MFSPs of torrefaction-CFP biofuels and two-stage HTL biofuels were respectively 19.4% and 61.5% lower than that from Shemfe's report of 8.29 $/gge (Shemfe et.al., 2015), which study applied the pinewood as the feedstock with an expensive price of 120 $/ton in Britain (70 $/ton in the States). The MFSP of two-stage HTL biofuels was competitive with NREL's report of 3.39 $/gge (NREL, 2011b), but higher than Onarheim's reports of 2.20 -3.09 $/gge (Onarheim et. al., 2015). However, no hydrotreating process was operated in Onarheim's reports. The contribution and key assumptions of each cost on MFSP summarized in table 8.3.

8.3.4 Sensitivity analysis

Sensitivity analysis was studied to estimate the impacts of crucial economic and operating parameters on the MFSPs of final biofuels through above two technologies. In this study, it was specially aimed to reduce the up-scale uncertainty on operating parameters and results, some of which were obtained from small-scale processes, such as torrefaction, CFP, HTL and hydrotreating.

Based on above economic analysis, it was indicated the price of energy sorghum, bio-oil yield from CFP process and total installed equipment cost were significant impacts on MFSP; while for the technology of two-stage HTL, the significant impacts involved the price of sweet sorghum bagasse, C5 and C6 sugar yield from 1$^{st}$ stage HTL, biocrude yield from 2$^{nd}$ stage HTL and total installed equipment cost. An alternative configuration of positive and negative 20% of above significant factors were investigated. The results of sensitivity analysis were indicated in Fig.8.3.

It was indicated that total installed equipment cost was the most crucial factor on both torrefaction-CFP and two-stage HTL technologies. The ±20% change of total installed equipment cost respectively resulted in around 9.1 % and 15.1% of change on final product cost from torrefaction-CFP and two-stage HTL. This implied the cost of equipment was the main limitation of MFSP reduction. For torrefaction-CFP, the bio-oil yield from CFP only contributed from +0.69% to -0.28% change on final production cost. This was deducted that the initial bio-oil yield was too low and ±20% could not change much on bio-oil production. Actually, 20% change on bio-oil yield only altered 19.6 ton/day of bio-oil production, which equaled to 0.98% of feedstock. However, equal percentage of vibration on bio-oil yield led into an unbalanced change on MFSP, which indicated bio-oil yield was the most promising parameters to improve MFSP. For two-stage HTL, the MFSP was also strongly dependent on C5 and C6 sugar yield. This co-product from 1st stage HTL lowered the value of MFSP with 5.9% from the baseline cost.

## 8.4 Conclusions

The analysis showed with the technologies of torrefaction-CFP and two-stage HTL, the yields of final fuel products were respectively 9.21 and 29.8 gal per ton sorghum biomass. Meanwhile, approximately, 272 kg C5 and C6 sugar co-products were produced from unit ton of sweet sorghum bagasse through two-stage HTL technology, which offset 13% of final biofuel cost. The MFSPs of torrefaction-CFP and two-stage HTL were respectively 6.68 $/gge and 3.19 $/gge. The energy conversion efficiencies were 9.1% of torrefaction-CFP and 20.1 of two-stage HTL. It was obviously indicated, both from economic feasibility and energy efficiency, the two-stage HTL technology dramatically outstripped torrefaction-CFP. Total installed equipment cost was identified as the key parameter with most significant impact on MFSP, which led to ±9.1% on MFSP of torrefaction-CFP and ±15.1% of two-stage HTL. However, the low yield of bio-oil was

the limitation of MFSP of torrefaction-CFP. An improvement on CFP process was suggested to optimize the economic feasibility of torrefaction-CFP technology.

References

Amosson, S., Girase, J., Bean, B., Rooney, W. and Becker, J. Economic Analysis of Biomass Sorghum for Biofuels Production in the Texas High Plains. Agrilife research. 2011.

Biomass to Ethanol Process Evaluation. Subcontract report. Prepared by Chem Systems, Tarrytown, NY. Golden, CO: National Renewable Energy Laboratory, 1994.

Douglas, E., Hart, T., Neuenschwander, G., Rotness, L., Olarte, M., Zacher, A., Solantausta, Y. Catalytic hydroprocessing of fast pyrolysis bio-oil from pine sawdust. Energy Fuels, 2012, 26(6): 3891–3896.

Gubicza, K., Nieves, I.U., Sagues, W.J., Barta, Z., Shanmugam, K.T., Ingram, L.O. Techno-economic analysis of ethanol production from sugarcane bagasse using a Liquefaction plus Simultaneous Saccharification and co-Fermentation process. Bioresource Technology 2016, 208: 42-48

NREL, in DCFROR based spreadsheet for calculating minimum fuel selling price, National Renewable Energy Laboratory, USA, 2011c

Humbird, D., Davis, R., Tao, L., Kinchin, C., Hsu, D., Aden, A., Schoen, P., Lukas, J., Olthof, Worley, B., Sexton, M.D. and Dudgeon, D. Process Design and Economics for Biochemical Conversion of Lignocellulosic Biomass to Ethanol, Report NREL/TP-5100-47764, National Renewable Energy Laboratory, USA, 2011.

Jones, S., Davis, R., Zhu, Y., Kinchin, C., Anderson, D., Hallen, R., Elliott, D., Schmidt, A., Albrecht, K., Hart, T., Butcher, M., Drennan, C., Snowden-Swan, L. Process Design and Economics for the Conversion of Algal Biomass to Hydrocarbons: Whole Algae Hydrothermal Liquefaction and Upgrading. 2014 a, NREL report.

Jones, S., Tan, E., Jacobson, J., Meyer, P., Dutta, A., Cafferty, K., Snowden-Swan, L., Padmaperuma, A. Process Design and Economics for the Conversion of Lignocellulosic Biomass to Hydrocarbon Fuels. 2013. PNNL report

Liu, H., Li, M., Yang, S., Sun, R. Understanding the Mechanism of Cypress Liquefaction in Hot-Compressed Water through Characterization of Solid Residues. Energies. 2013. 6, 1590-1603.

Onarheim, K., Lehto, J., and Solantausta, Y. Technoeconomic Assessment of a Fast Pyrolysis Bio-oil Production Process Integrated to a Fluidized Bed Boiler. Energy Fuels, 2015, 29 (9), 5885–5893

Peters, M., Timmerhaus, K. Plant Design and Economics for Chemical Engineers, New York McGraw-Hill Chemical engineering

Pinkowska H, Wolak P, Z1ocinska A. Hydrothermal decomposition of xylan as a model substance for plant biomass waste -Hydrothermolysis in subcritical water. Biomass Bioenergy. 2011, 35, 3902-3912

Rover, M. Pyrolysis bio-oil and char analysis sample #2006 – 27. Wright, M., ed. Ames, IA: Iowa State University, 2008

Scaling-Up and Operation of a Flash-Pyrolysis System for Bio-Oil Production and Applications on Basis of the Rotating Cone Technology. BioMatNet FAIR-CT96-3203 [cited 2004; available from: http://www.biomatnet.org/secure/Fair/S538.htm].

Shemfe, M.B., Gu, S., Ranganathan,P. Techno-economic performance analysis of biofuel production and miniature electric power generation from biomass fast pyrolysis and bio-oil upgrading. Fuel 2015, 143: 361-372.

Sokhansanj, S., Kumar, A., Turhollow, A. Development and Implementation of Integrated Biomass Supply Analysis and Logistics Model (IBSAL). Biomass and Bioenergy; 2006, 30(10), 838-847.

Thilakaratne, R., Brown, T., Li, Y., Hu, G., Brown, R. Mild catalytic pyrolysis of biomass for production of transportation fuels: a techno-economic analysis. Green Chem., 2014, 16 , 627–636

Wright, M.M., Satrio, J.A., Brown, R.C., Daugaard, D. E. and Hsu, D.D. Techno-Economic Analysis of Biomass Fast Pyrolysis to Transportation Fuels. 2010. NREL report

Yoshida, K., Saka, S. Organic acid production from Japanese beech by supercritical water treatment. In: The 2nd Joint International Conference on Sustainable Energy and Environment. C-032, Thailand; 2006. p. 1–6, 22.02.2010.

Zhu, Y., Biddy, M.J., Jones, S.B., Elliott, D.C., Schmidt, A.J. Techno-economic analysis of liquid fuel production from woody biomass via hydrothermal liquefaction (HTL) and upgrading. Applied Energy 2014,129:384–394.

Table 8.1. Flowrate of torrefaction-CFP process and two-stage HTL process

| Process | products | Yield, [%] | Mass flowrate, [ton/day] |
|---|---|---|---|
| Torrefaction-CFP | | | |
| Energy sorghum | | | 2000 |
| Torrefaction | Torrefied sorghum | 53.3 | 1066 |
| | Torrefied NCG | 17.1 | 342 |
| | Torrefied CG | 29.6 | 592 |
| CFP | Bio-oil | 16.1 | 172 |
| | Oil fraction | 57.2 | 98 |
| | Aqueous fraction | 42.8 | 74 |
| | Char | 37.9 | 404 |
| | Pyrolysis NCG | 46.0 | 490 |
| Hydrotreating | Hydrocarbons | 78.2 | 77 |
| | Off gas | 15.6 | 15 |
| | Aqueous fraction | 6.2 | 6 |
| Distillation | Naptha | 85.0 | 65 |
| | Diesel | 15.0 | 12 |
| Two-stage HTL | | | |
| Sweet sorghum bagasse | | | 2000 |

| | | | |
|---|---|---|---|
| 1st stage HTL | Solid residual product | 43.4 | 868 |
| | Liquid product | 53.6 | 1072 |
| | Co-product | 27.2 | 544 |
| | Off gas | 0.03 | 6 |
| 2nd stage HTL | Biocrude | 35.3 | 306.4 |
| | Aqueous fraction | 25.8 | 224 |
| | Off gas | 38.7 | 336 |
| Hydrotreating | Hydrocarbons | 81.0 | 248 |
| | Off gas | 11.2 | 34 |
| | Aqueous fraction | 7.8 | 24 |
| Distillation | Naptha | 95.0 | 235.6 |
| | Diesel | 5.0 | 12.4 |

Table 8.2. Main characterizations of feedstocks

| Biomass | Moisture (%) | Fixed Carbon (%) | Volatiles Dry (%) | Ash Dry (%) | C (wt.%) | H (wt.%) | N (wt.%) | O* (wt.%) | HHV (MJ $kg^{-1}$) |
|---|---|---|---|---|---|---|---|---|---|
| Energy sorghum | 7.83 (0.24) | 17.01 (0.63) | 79.39 (1.90) | 3.47 (1.13) | 43.11 (2.15) | 5.52 (0.11) | 1.45 (0.03) | 49.93 (2.23) | 17.33 (0.42) |
| Sweet sorghum bagasse (dried) | 7.36 (0.03) | 18.38 (0.12) | 77.03 (0.12) | 4.59 (0.03) | 41.30 (0.11) | 5.39 (0.04) | 1.32 (0.14) | 51.98 (0.21) | 16.30 (0.25) |

Table 8.3. Key parameters and assumptions of economic analysis

| Parameters | | | Torrefaction-CFP |
|---|---|---|---|
| Items | | ratio | $MM |
| Total project investment (TPI) | | | 867.40 |
| Fixed capital investment (FIC) | | | 731.93 |
| Direct cost | | | 321.02 |
| Total installed equipment cost (TIEC) | | | 270.90 |
| Building cost | | 4% TIEC | 10.83 |
| Additional pipes cost | | 4.5% TIEC | 12.19 |
| Site development cost | | 10% TIEC | 27.09 |
| Indirect cost | | 128% direct cost | 410.91 |
| Working capital | | 15% FCI | 109.79 |
| Land cost | | 8% FCI | 25.68 |
| | | | $MM/year |
| Operating cost | | | 110.50 |
| Variable operation cost | | | 75.70 |
| | price | unit | |
| Energy sorghum | 73.89 | $/ton | 48.76 |
| CFP catalyst (red mud) | 164 | $/ton | 8.66 |
| Hydrotreatment | | | |
| Catalyst | 15.5 | $/lb | 1.02 |
| Electricity | 0.0689 | $/kwh | 14.90 |
| Hydrogen | 2.7 | $/kg | 2.36 |
| Fixed operating cost | | | 34.79 |
| Labor cost | | | 4.05 |
| Overhead | | 95% working capital | 3.65 |
| Maintenance | | 3% FCI | 21.96 |
| Insurance and taxes | | 0.7% FCI | 5.12 |
| Discount rate | | 10% | |
| Life span | | 20 years | |
| ROI | | 101.88 $MM | |
| Income tax rate(TR) | | 35% | |
| MFSP | | 6.68 $/gge | |

(a) torrefaction-CFP

| Parameters | | | Two-stage HTL |
|---|---|---|---|
| Items | | ratio | $MM |
| Total project investment (TPI) | | | 1042.88 |
| Fixed capital investment (FIC) | | | 880.00 |
| Direct cost | | | 385.96 |
| Total installed equipment cost (TIEC) | | | 325.71 |
| Building cost | | 4% TIEC | 13.03 |
| Additional pipes cost | | 4.5% TIEC | 14.66 |
| Site development cost | | 10% TIEC | 32.57 |
| Indirect cost | | 128% direct cost | 494.03 |
| Working capital | | 15% FCI | 132.00 |
| Land cost | | 8% FCI | 30.88 |
| | | | $MM/year |
| Operating cost | | | 96.33 |
| Variable operation cost | | | 59.17 |
| | price | unit | |
| Sweet sorghum | | | 29.04 |
| bagasse | 44 | $/ton | |
| Co-product credit | -420 | $/ton | -75.40 |
| 2nd stage HTL | | | 11.89 |
| catalyst | 40.15 | $/kg | |
| Electricity | 0.0689 | $/kwh | 87.79 |
| water | 0.22 | $/ton | 1.50 |
| Hydrotreatment | | | |
| Catalyst | 15.5 | $/lb | 1.02 |
| Hydrogen | 2.7 | $/kg | 3.33 |
| Fixed operating cost | | | 37.16 |
| Labor cost | | | 2.36 |
| Overhead | 95% working capital | | 2.24 |
| Maintenance | 3% FCI | | 26.40 |
| Insurance and taxes | 0.7% FCI | | 6.16 |
| Discount rate | 10% | | |
| Life span | 20 years | | |
| ROI | 102.52 $MM | | |
| Income tax rate(TR) | 35% | | |
| MFSP | 3.19 $/gge | | |

(b) two-stage HTL

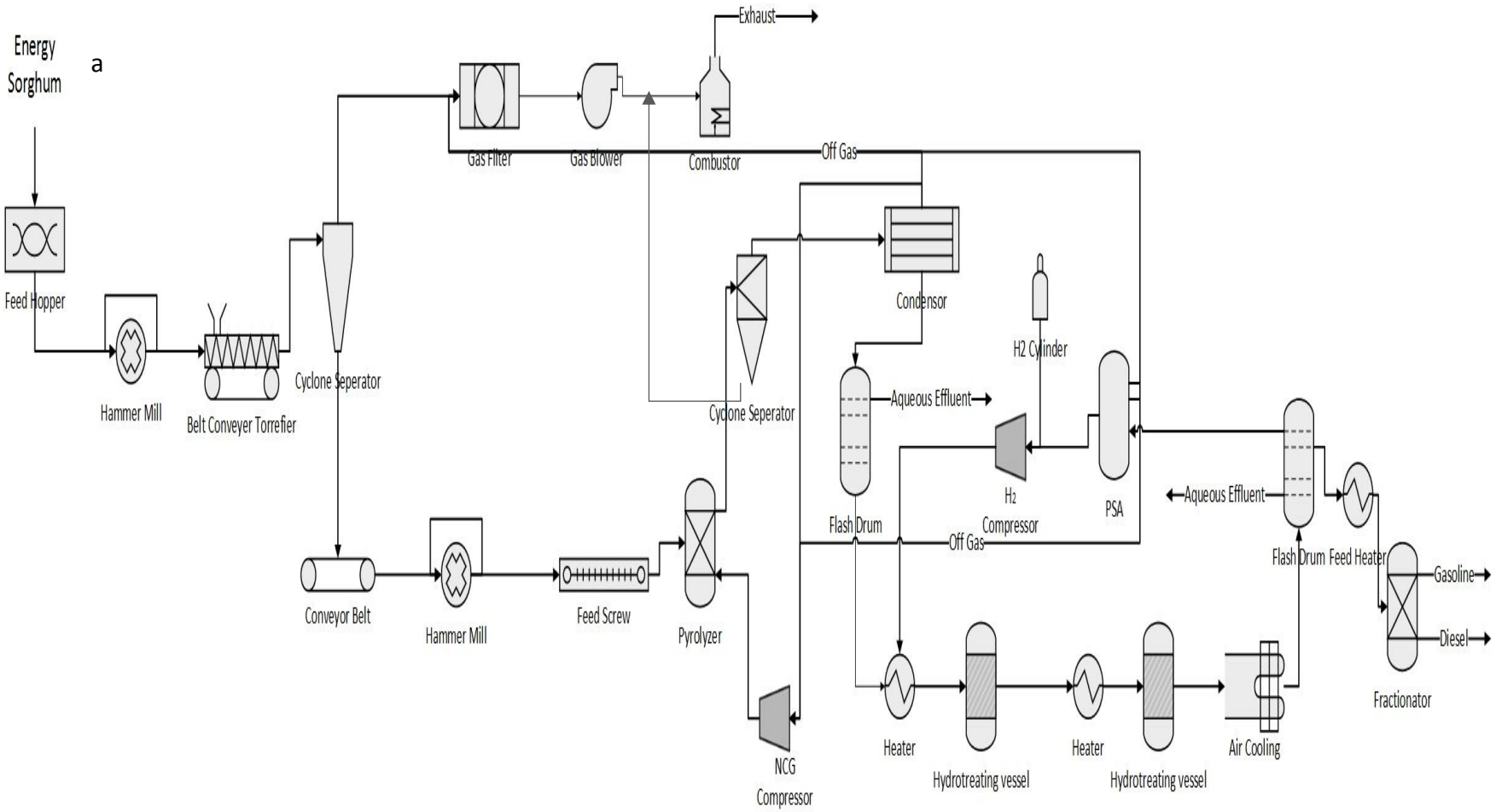
Energy Sorghum
a
Exhaust
Gas Filter
Gas Blower
Combustor
Off Gas
Feed Hopper
Hammer Mill
Belt Conveyer Torrefier
Cyclone Seperator
Cyclone Seperator
Condensor
H2 Cylinder
Aqueous Effluent
Flash Drum
H2 Compressor
PSA
Off Gas
Aqueous Effluent
Flash Drum
Feed Heater
Gasoline
Diesel
Fractionator
Conveyor Belt
Hammer Mill
Feed Screw
Pyrolyzer
NCG Compressor
Heater
Hydrotreating vessel
Heater
Hydrotreating vessel
Air Cooling

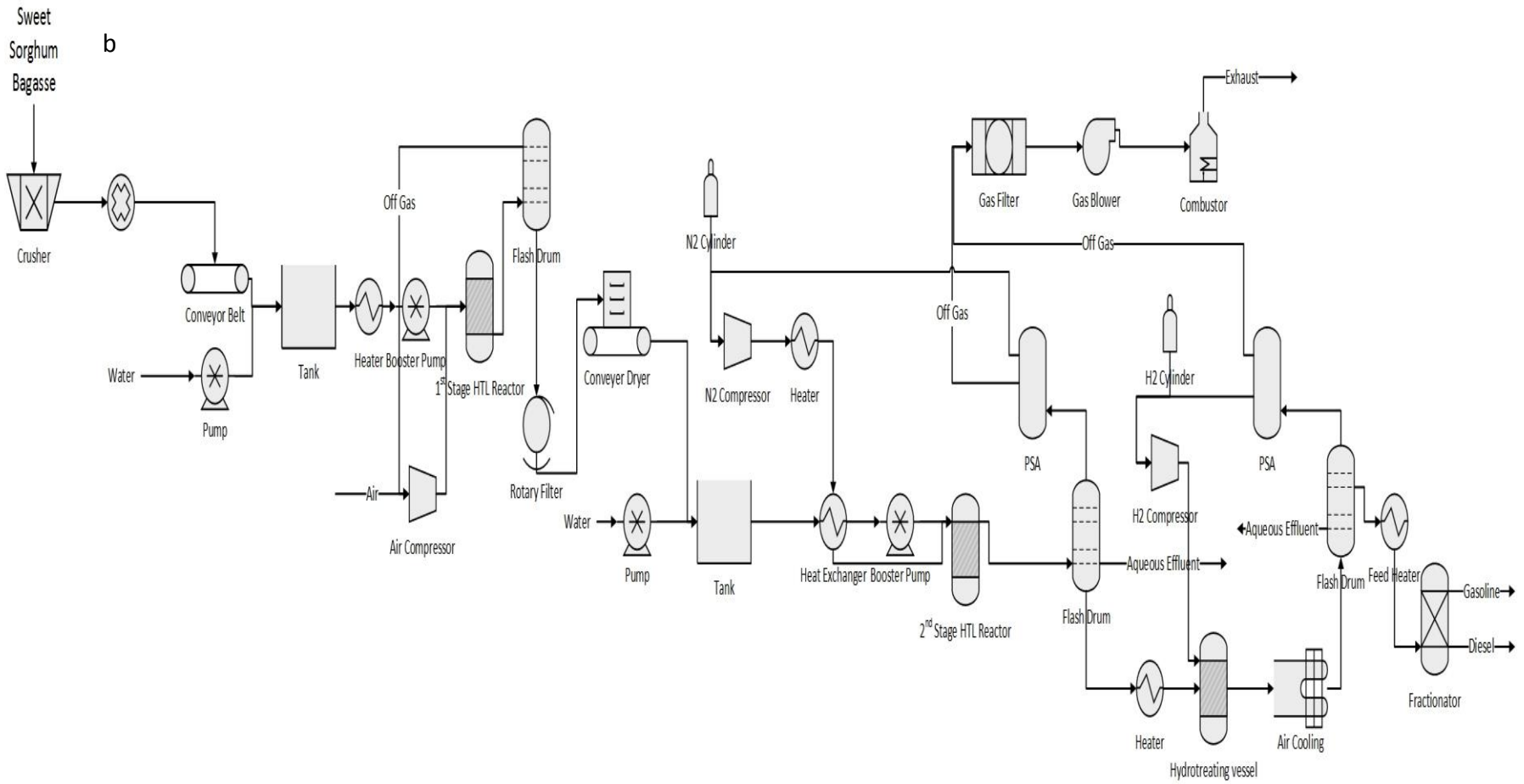


Fig.8.1. Simplified diagram of torrefaction-CFP (a) and two-stage HTL (b) processes with plant scale

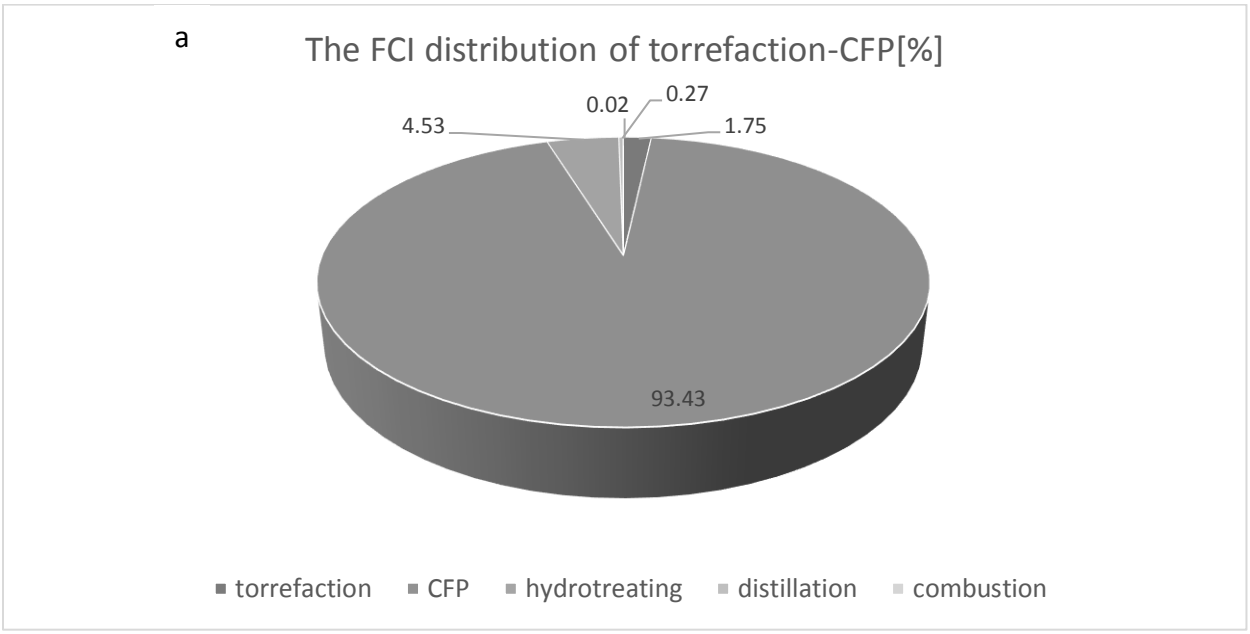


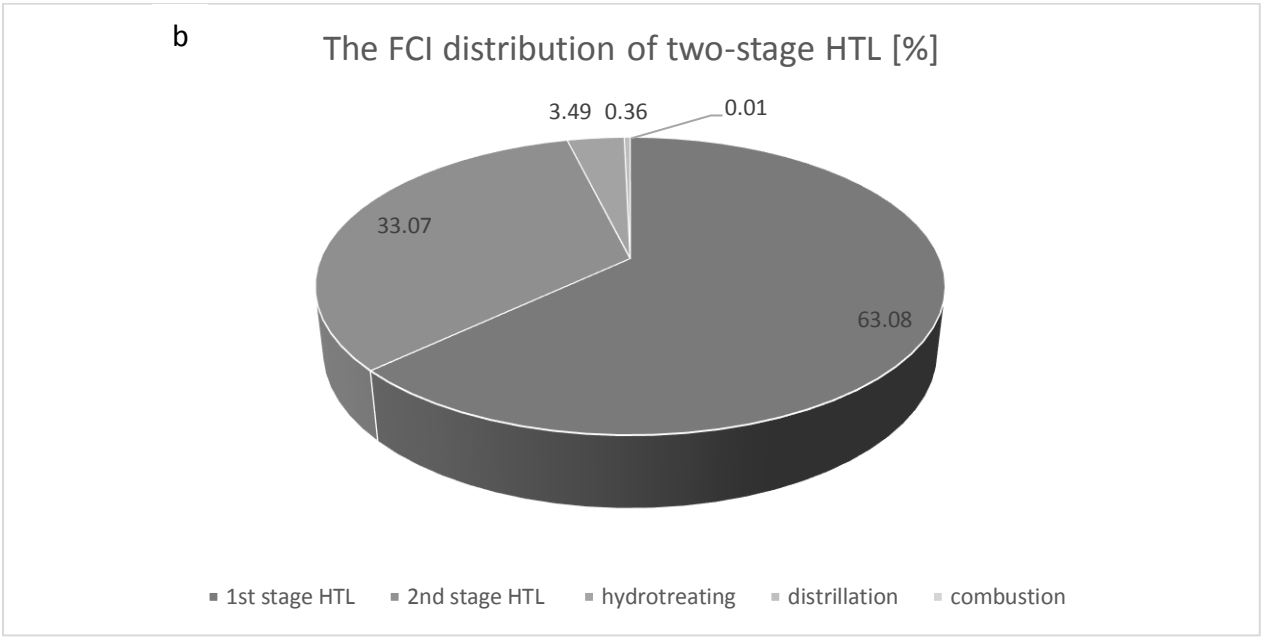


Fig.8.2. FIC distribution of (a) torrefaction-CFP and (b) two-stage HTL processes

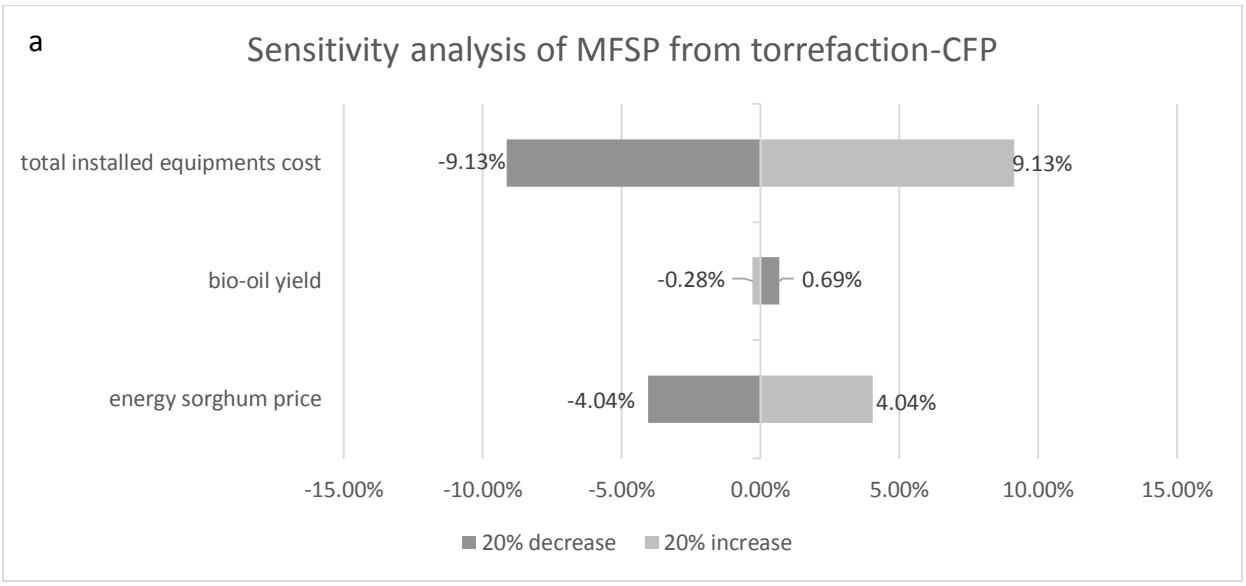


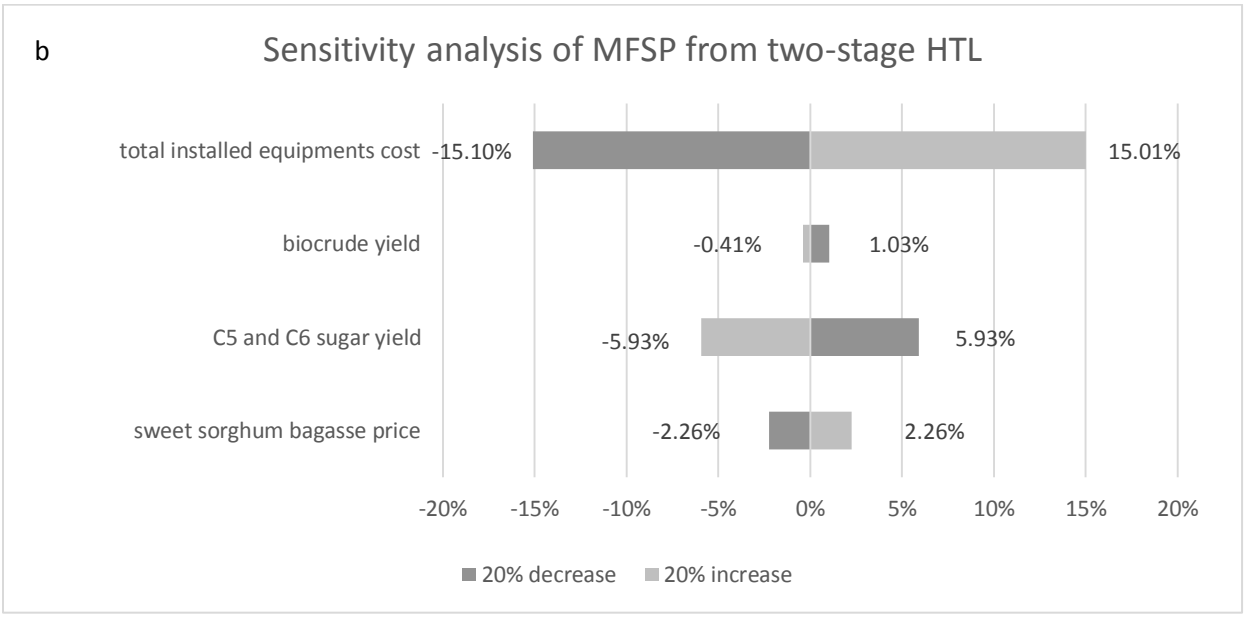


Fig.8.3 Sensitivity analysis of MFSP (a) torrefaction-CFP, (b) two-stage HTL

# IX. Conclusions and Recommendations

## Conclusions

In this study, sweet sorghum bagasse after sugar extraction was subjected to two-stage hydrothermal liquefaction technology along with hydrodeoxygenation to produce sugar-rich intermediates and hydrocarbon rich oil fractions. In the two-stage HTL process, the hydrocarbon yield reached to 11.9 %, nearly 2.0 folds of that compared with conventional HTL. The first stage HTL process was optimized to produce sugar rich intermediates with the yield of 27 wt. % from unit sorghum feedstock. This result confirmed that the C5 sugar mixtures derived from hemicellulose hydrolysis can be used to produce value-added chemicals rather than to produce biocrude oil.

When energy sorghum was subjected to torrefaction pretreatment prior to catalytic fast pyrolysis using red mud, the bio-oil quality was improved by increasing the hydrocarbon yield 1.8 folds more than that of conventional fast pyrolysis. Torrefaction pretreatment was demonstrated to accumulate high lignin derivate, therefore, promoted the formation of hydrocarbon through phenols by 2.2 folds. It was also indicated the use of reduced red mud during *in-situ* CFP significantly promoted the formation of cyclic ketones of 5 wt. % from raw sorghum and moderately enhanced hydrocarbon yield of 0.78 wt. % from torrefied sorghum.

TEA indicated the final biofuel product yields through torrefaction-CFP and two-stage HTL were respectively 9.21 and 29.8 gal per ton dried sorghum biomass, with their MFSPs of 6.68 $/gge and 3.19 $/gge respectively. The higher hydrocarbon yield though two-stage HTL was one significant reason that made less expensive MFSP; another reason was resulted from C5 and C6

sugars co-product credit, which offset 13% of MFSP. Therefore, two-stage HTL displayed higher economic feasibility.

Recommendations

This study illustrated the pretreatment and hydroprocessing (hydrodeoxygenation of two stage HTL process and hydrocracking of torrefaction-CFP process) benefited hydrocarbon production. Although the expected objectives have been achieved, more researches could be conducted in future on each process:

For torrefaction-CFP process

(i) Various valuable co-products were obtained from liquid products after torrefaction pretreatment. In the oil fraction, phenolic type chemicals and furan derivate were the major components, accounted up to 58 wt %. In the aqueous fraction, the yield of acetic acid could reached 102 g/L. These compounds could be further upgraded into high-value platform chemicals, but rational design and appropriate conversion route were required for future study.

(ii) An optimization on red mud characterization, typically the average pore size could ameliorate its catalytic capability, which might make red mud more adaptable for bio-oil yield and hydrocarbon conversion efficiency.

(iii) The recycle utilization of used red mud was also suggested for investigate to the life span of red mud during CFP

For two-stage HTL process:

(i) The homogenous catalyst ($K_2CO_3$) used in HTL was almost impossible to be recovered from aqueous fraction. This dramatically increased the cost of HTL process, seeking for an appropriate heterologous catalyst for HTL was promptly demanded.

(ii) The hydrocarbon yield through HDO was significantly depended on hydrogen concentration in solution. Batch reactor limited hydrogen mass transfer because of its configuration. It was

also considered not adaptable for industrial scale. CSTR was strongly encouraged to be implemented instead of batch reactor in future study.

(iii) Similarly as the third recommendation of torrefaction-CFP process, the study on recycling used Ru/C in HDO was also suggested

(iv) Ru/C was an expensive catalyst and not easy to be regenerated after deactivation by coke, an economic catalyst was demanded as an alternative of Ru/C for HDO.

# X. Appendices

Table A1. Ultimate analysis of solid products

| WSH | | | | | | 2nd SH | WSHH | TSHH |
|---|---|---|---|---|---|---|---|---|
| Catalyst | | 0.94M $K_2CO_3$ | | | Non-catalyst | 0.94 M $K_2CO_3$ | 5 % Ru/C | 5 % Ru/C |
| Gas inlet** | | He | | $H_2$ | He | He | $H_2$ | $H_2$ |
| Time /min | 15 | 30 | 60 | 60 | 30 | 30 | 240 | 240 |
| C [wt.%] | 42.23 (0.26) | 31.60 (0.50) | 37.59 (0.55) | 36.91 (0.35) | 69.43 (1.19) | 59.34 (1.65) | 73.89* (1.28) | 73.78* (0.57) |
| H [wt.%] | 3.90 (0.03) | 3.09 (0.09) | 3.73 (0.04) | 3.48 (0.02) | 4.71 (0.13) | 4.70 (0.28) | 2.01* (0.33) | 2.34* (0.10) |
| N [wt.%] | 1.16 (0.04) | 0.99 (0.15) | 0.97 (0.17) | 1.09 (0.10) | 1.92 (0.23) | 0.63 (0.05) | 0.99* (0.04) | 0.55* (0.02) |
| O [wt.%] | 52.70 (1.32) | 64.32 (0.58) | 57.71 (0.45) | 58.52 (0.27) | 23.94 (1.41) | 35.33 (1.96) | 23.11* (1.37) | 23.33* (0.67) |
| O/C | 0.94 | 1.53 | 1.15 | 1.19 | 0.26 | 0.45 | 0.23* | 0.24* |
| H/C | 1.11 | 1.17 | 1.19 | 1.13 | 0.81 | 0.95 | 0.44* | 0.51* |

* The elemental content of solid residues included Ru/C when measured or calculated

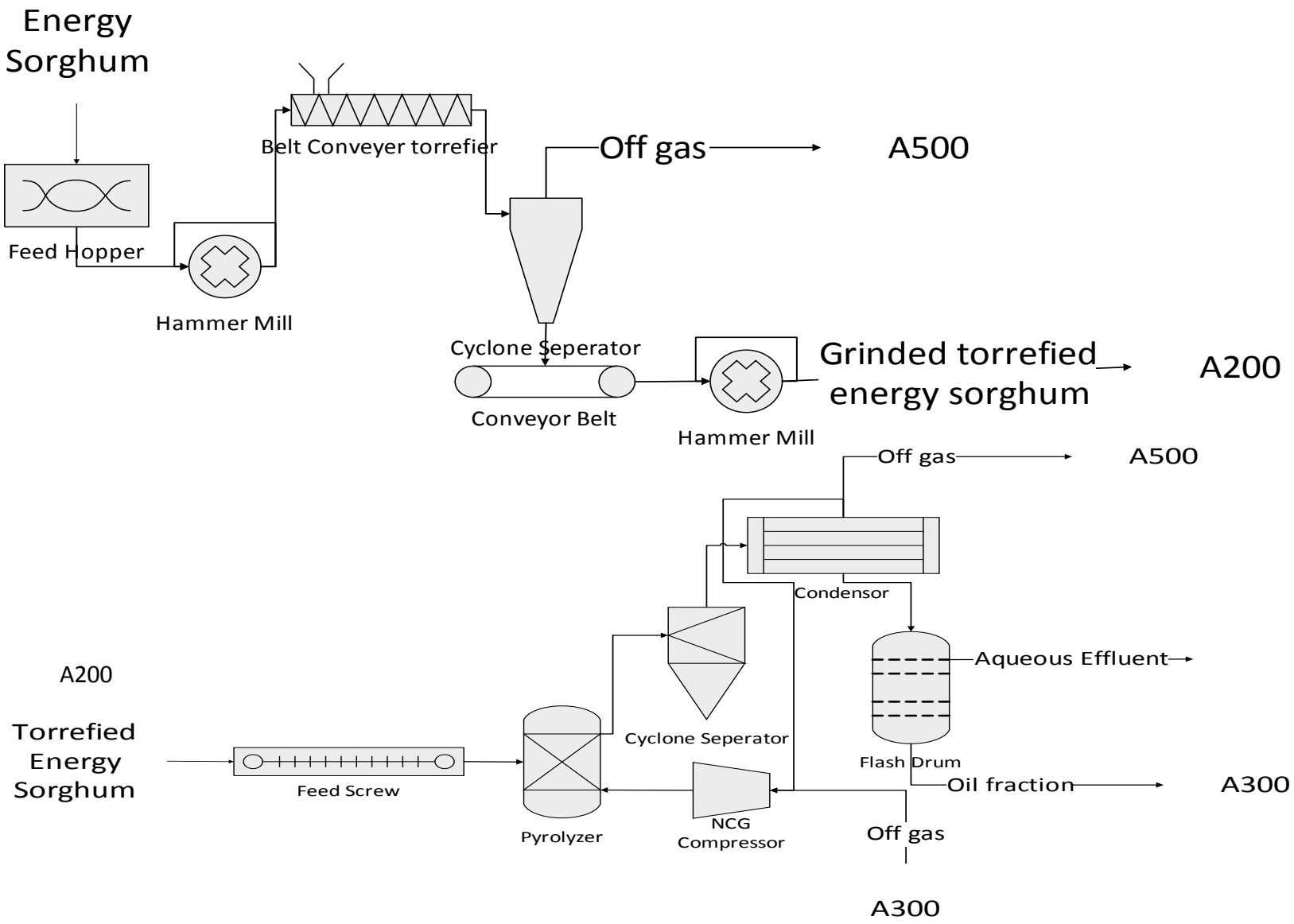
Energy Sorghum
Feed Hopper
Hammer Mill
Belt Conveyer torrefier
Off gas
A500
Cyclone Seperator
Conveyor Belt
Hammer Mill
Grinded torrefied energy sorghum
A200
Off gas
A500
Condensor
Aqueous Effluent
A200
Torrefied Energy Sorghum
Feed Screw
Pyrolyzer
Cyclone Seperator
NCG Compressor
Flash Drum
Oil fraction
A300
Off gas
A300

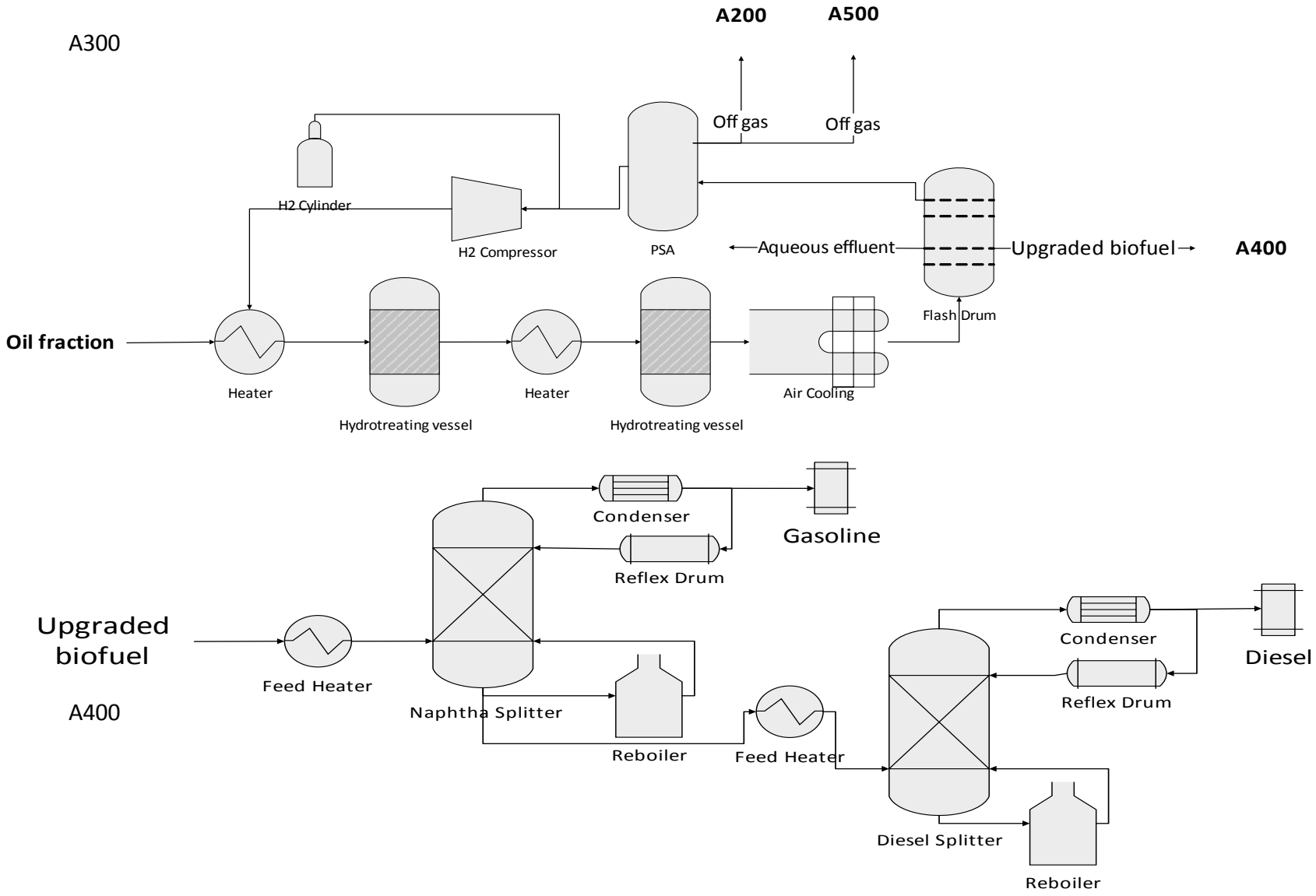
A300
A200
A500
Off gas
Off gas
H2 Cylinder
H2 Compressor
PSA
Aqueous effluent
Upgraded biofuel
A400
Flash Drum
Oil fraction
Heater
Hydrotreating vessel
Heater
Hydrotreating vessel
Air Cooling
Condenser
Gasoline
Reflex Drum
Upgraded biofuel
A400
Feed Heater
Naphtha Splitter
Reboiler
Feed Heater
Condenser
Diesel
Reflex Drum
Diesel Splitter
Reboiler

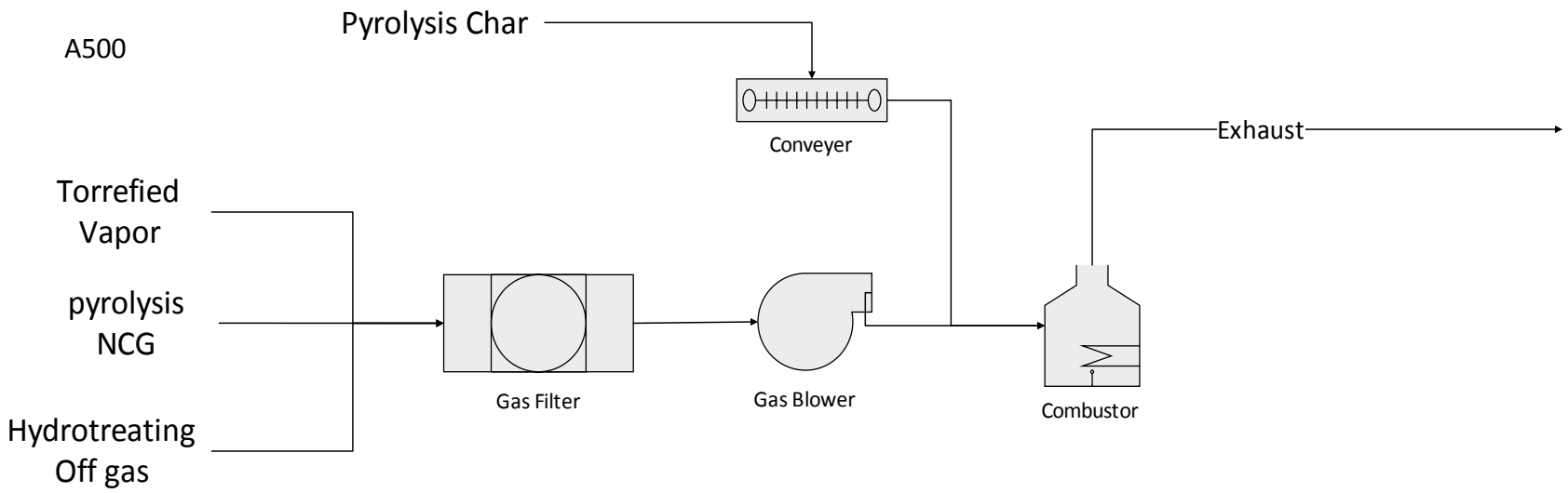


Fig. A1 Diagram of unit process of torrefaction- CFP. A100: pretreatment and torrefaction; A200: CFP; A300: hydrotreating; A400: distillation; A500: combustion

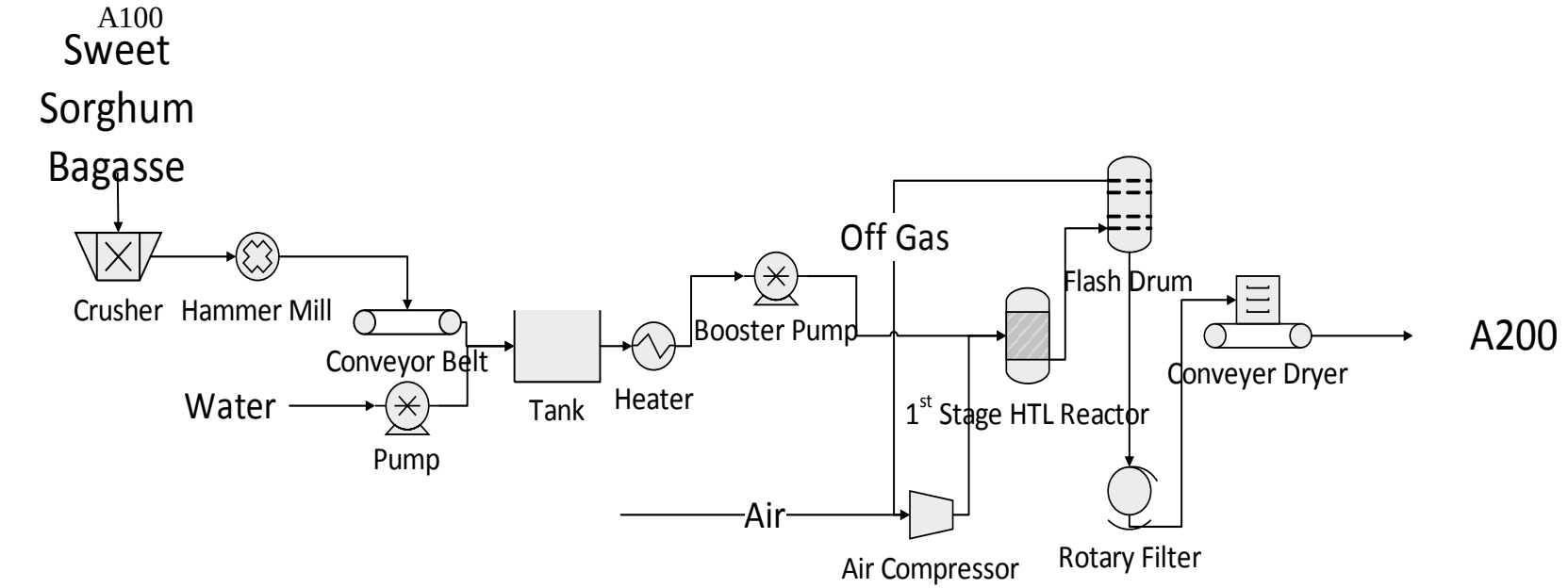
A100
Sweet
Sorghum
Bagasse
Crusher
Hammer Mill
Conveyor Belt
Water
Pump
Tank
Heater
Booster Pump
Off Gas
Flash Drum
1st Stage HTL Reactor
Air
Air Compressor
Rotary Filter
Conveyer Dryer
A200

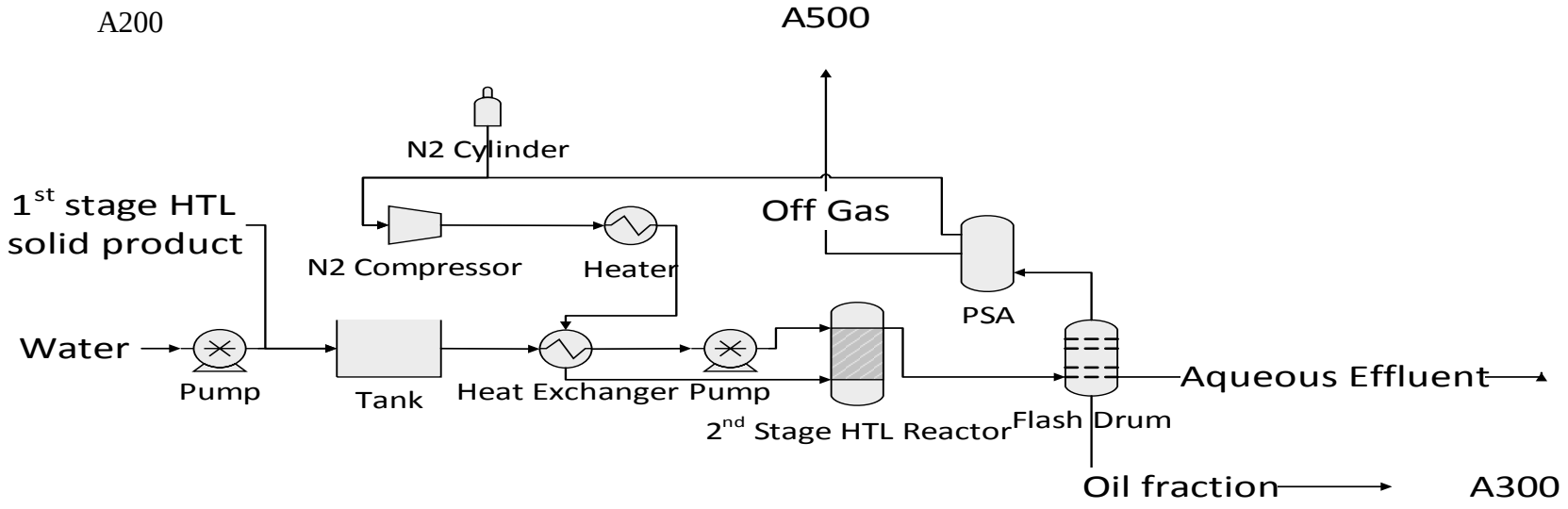
A200
A500
N2 Cylinder
1st stage HTL
solid product
N2 Compressor
Heater
Off Gas
PSA
Water
Pump
Tank
Heat Exchanger
Pump
2nd Stage HTL Reactor
Flash Drum
Aqueous Effluent
Oil fraction
A300

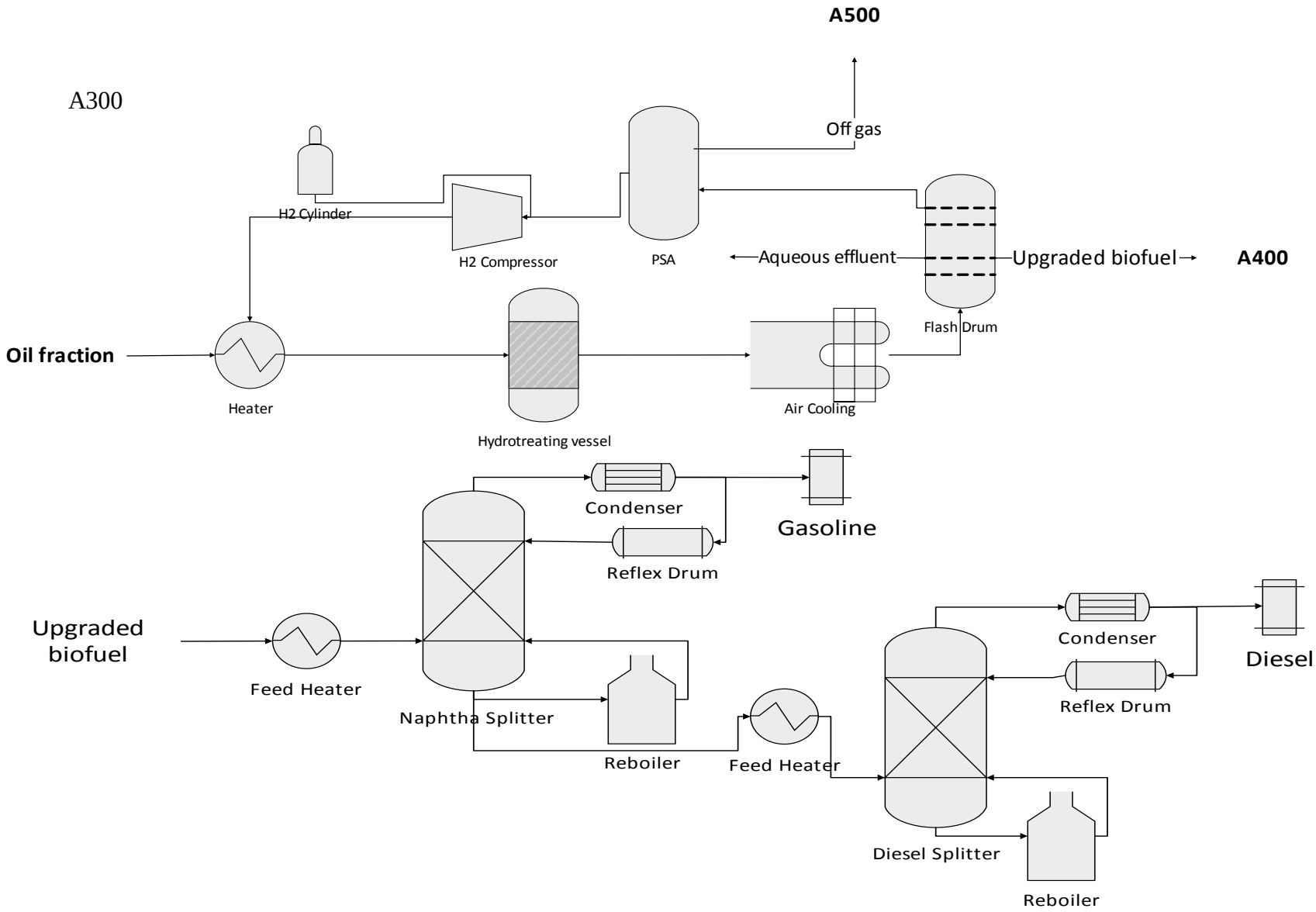
A500
A300
Off gas
H2 Cylinder
H2 Compressor
PSA
Aqueous effluent
Upgraded biofuel
A400
Flash Drum
Oil fraction
Heater
Hydrotreating vessel
Air Cooling
Condenser
Gasoline
Reflex Drum
Upgraded biofuel
Feed Heater
Naphtha Splitter
Reboiler
Feed Heater
Condenser
Diesel
Reflex Drum
Diesel Splitter
Reboiler

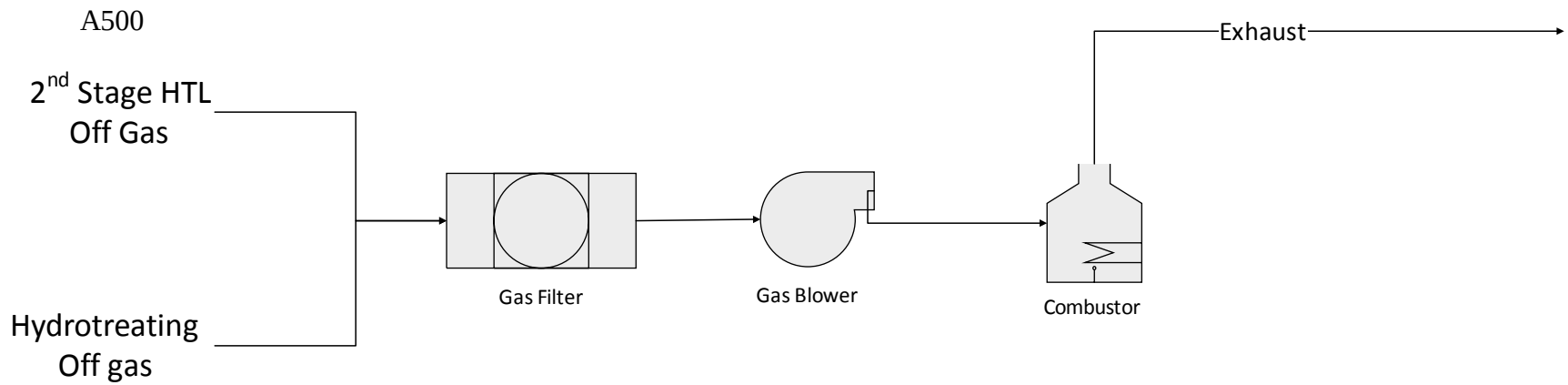


Fig. A2 Diagram of unit process of two-stage HTL. A100: pretreatment and1st stage HTL; A200:2nd stage HTL; A300: hydrotreating; A400: distillation; A500: combustion